DETERMINATION AND DYNAMIC COMPENSATION OF FICTITIOUS POWER IN ELECTRIC POWER SYSTEMS

by

JOHAN HEINRICH RICHTER ENSLIN

THESIS

submitted in partial fulfilment of the requirements for the degree

DOCTOR IN ENGINEERING

in

ELECTRICAL AND ELECTRONIC ENGINEERING

in the

FACULTY OF ENGINEERING

at the

RAND AFRIKAANS UNIVERSITY

SUPERVISOR: PROF. J.D. VAN WYK
CO-SUPERVISOR: PROF. DR.-ING. H.-CH. SKUDELNY

JUNE 1988

ACKNOWLEDGMENTS

Prof J D Van Wyk vir sy vorming oor baie jare, entoesiasme wat hy kweek in hierdie vakgebied en navorsing in die algemeen. 'n Man waarsonder hierdie studie nie moontlik sou gewees het nie.

Prof N Wessels vir sy goeie gesindheid, geleenthede wat deur hom geskep is en onbaatsugtige leiding tydens hierdie studie.

Mein besondere Dank gilt Herrn Prof Dr.-Ing. H.-Ch. Skudelny, Institutsdirektor am Institut für Stromrichtertechnik und elektrische Antriebe der RWTH Aachen, für die interessanten Diskussion, Korreferates und Anregungen zu der Arbeit.

Opregte dank aan al my voor- en nagraadse studente.

Aan Elsabé vir haar ondersteuning gedurende die afgelope tyd en ook in die toekoms.

The external examiners, Prof R Kitai, Prof C Landy and Prof M Case for their efforts and the interesting discussions.

Die Skepper vir insig, krag en ondersteuning.

"A moment's insight is sometimes worth a life's experience", in The Professor at the Breakfast Table, ch. 10, Oliver Wendell Holmes 1809-1894.

OPGEDRA AAN DIE NIEULIGTERS VAN SUID-AFRIKA

ABSTRACT

This thesis contains an investigation into distortion in electric power networks. Fictitious power, the component of power which does not contribute to net energy transfer through the network, is determined and compensated for by means of adequate compensation systems. This study comprises the accurate definition, analysis, characterization, measurement and compensation of fictitious power in power networks. A generalized time domain definition of electric power, using only correlation techniques, is proposed for the analysis, based on distortion categorization and characterization in terms of the proposed power components, effective measurement and compensation of fictitious power. This definition is generally valid, even when the generating function and the loading function, one of them being the voltage and the other the current, are non-sinusoidal or aperiodic.

The analysis techniques are based on an equivalent circuit diagram representing the power phenomena of the load and the energy attributes of the total energy network. This leads to the proposal of a new equivalent network parameter, disceptance, which describes the uncorrelation between the generating and loading functions, normally resulting from the non-linear properties of the load. Frequency domain analysis is proposed to be performed using the power cross-spectral density function. The power components have been measured using a digital correlation algorithm on a personal computer with system interfacing capabilities. Real-time measurements of power components seems possible when the statistical network properties are used in adaptive signal processing techniques, implemented with dedicated digital signal processing microprocessors. High speed correlation calculations, from measured generating and loading functions, are proposed to be implemented with optics, acoustic waves or dedicated signal processing microprocessors.

A new philosophy for the compensation of fictitious power in contaminated power networks, is derived. The principle of the compensation philosophy is to make collective use of different compensation systems, each compensating a different component of fictitious power based on its dynamic system response. These different fictitious power components are derived from the proposed power definition. The loading function is decomposed into several orthogonal components which form the control inputs for these power electronic, fictitious power compensation systems.

CONTENTS

CHAPTER 2

CLASSIFICATION, SOURCES, PENETRATION AND EFFECTS OF DISTORTION IN ELECTRIC POWER SYSTEMS

CHAPTER 3

PROPOSED GENERALIZED DEFINITION OF POWER IN ELECTRIC POWER SYSTEMS

CHAPTER 4

MEASUREMENT OF ELECTRIC POWER USING THE PROPOSED DEFINITION

CHAPTER 5

PHILOSOPHY FOR FICTITIOUS POWER COMPENSATION USING ADAPTIVE SIGNAL PROCESSING TECHNIQUES

CHAPTER 6

STRUCTURE, DEVELOPMENT AND CONTROL OF DYNAMIC POWER FILTERS

CHAPTER 7

SUMMARY OF THE CONCLUSIONS FROM THIS THESIS

REFERENCES

APPENDICES

APPENDIX A : MATHEMATICAL ANALYSIS AND MANIPULATIONS

LIST OF FIGURES

ALPHABETIC LIST OF SYMBOLS AND ABBREVIATIONS

CONVENTIONS:

1. An overscore symbolizes the average of a function: $\overline{i_a . i_f}$ implies the time average of the instantaneous product of $i_a(t)$ and $i_f(t)$.
2. The symbol | | means the magnitude, norm or modulus of the time function contained within.
3. Throughout the text small characters are used for instantaneous values.
4. Throughout the text capital characters are used for effective or average values.
5. Bold characters symbolize phasors, vectors, quaternions, tensors or matrices. The appropriate symbol will clearly be shown in the text.
6. Amplitudes or maximum values are shown with a preceded control character, for example ^U implies amplitude of a voltage signal.
7. The symbol Re[ ] reads the "real part of", and Im[ ] the "imaginary part of".
8. The symbol arg( ) means the phase angle of the complex quantity contained within.
9. The symbol E{ } means the expected value of the random variable enclosed within.
10. The symbol Var[ ] means the variance of the random variable enclosed within.
11. The symbol Max[ ] means the maximum value of the function enclosed within.
12. The use of an asterisk as superscript denotes complex or quaternion conjugate values.
13. The inverse of a square matrix $\mathbf{A}$ is denoted by $\mathbf{A}^{-1}$. The tranpose of a vector $\mathbf{x}$ is denoted by $\mathbf{x}^T$.

SYMBOLS:

$\mathbf{A}$	≡	Kalman dynamic parameter gain matrix
$a_{g,b}$	≡	Kalman algorithm weighted gains
B	≡	Equivalent susceptance [Siemens]
$\mathbf{c}$	≡	Measurement gain vector of G and B (c_g and c_b)
D	≡	Deactive power [VA]
D_N	≡	Nowomiejski distortion power [VA]
dT	≡	Measurement time window [s]
$\mathbf{E}$	≡	Electric field intensity vector [$V.m^{-1}$]
F	≡	Fictitious power [VA]
f	≡	Frequency [Hz]
F_i	≡	Fourier transform of current [A]
F_u	≡	Fourier transform of voltage [V]
G	≡	Equivalent conductance [Siemens]
$\mathbf{G}$	≡	Kalman gain matrix
G_l	≡	Equivalent converter loss conductance [Siemens]
$\mathbf{H}$	≡	Magnetic field intensity vector [$A.m^{-1}$]
H{u}	≡	Hilbert transform of a voltage signal [V]
I	≡	Effective current [A]
I_a	≡	Active current [A]
I_{al}	≡	Active current from DPF losses [A]
I_{as}	≡	Active current signal [A]
I_c	≡	Dynamic Power Filter (DPF) compensation current [A]
I_{cf}	≡	Filtered DPF current [A]
I_d	≡	Deactive current; Distortion current [A]
I_{ds}	≡	Deactive current signal [A]
I_f	≡	Fictitious current [A]
I_{fs}	≡	Fictitious current signal [A]
I_L	≡	Inductor current [A]
I_r	≡	Reactive current [A]
I_{rs}	≡	Reactive current signal [A]
I_v	≡	Depenbrock conversion current [A]
I_w	≡	Depenbrock rest current [A]
K	≡	Equivalent disceptance [Siemens]
N	≡	Number of digital samples
P	≡	Active power [W]
p	≡	Instantaneous power [VA]
$\mathbf{P}$	≡	Instantaneous Poynting vector [W/m^2]
$\mathbf{P}$	≡	Mean-square error vector
$\mathbf{P}_c$	≡	Complex form of the Poynting vector [W/m^2]
P_k	≡	k-th Harmonic active power [W/Hz]
P_0	≡	Oberdorfer throughput power [VA]
q	≡	Akagi instantaneous imaginary power [VA]
$\mathbf{Q}$	≡	Covariance of the process noise
$\mathbf{q}$	≡	Quaternion
Q	≡	Reactive power [VA]
Q_B	≡	Budeanu reactive power [VAR]

Q_f ≡ Fundamental reactive power [VA]
Q_k ≡ k-th Harmonic reactive power [VA/Hz]
Q_N ≡ Nowomiejski reactive power [VA]
Q_r ≡ Residual reactive power [VA]
R_{ii} ≡ Current autocorrelation [V^2]
R_{ui} ≡ Voltage-current cross-correlation [VA]
R_{uu} ≡ Voltage autocorrelation [V^2]
$\mathbf{R}, \Sigma_{vv}$ ≡ Covariance of the measurement noise matrix
$\mathbf{S}$ ≡ Complex power [VA]
s ≡ Induction machine rotor slip
S ≡ Loading / Apparent power [VA]
s ≡ Surface of a volume v [m^2]
S_c ≡ Capacitor power rating [VA]
s_n ≡ Induction machine rotor slip at harmonic frequencies
S_0 ≡ Oberdorfer return power [VA]
$\mathbf{Sq}$ ≡ Quaternion power [VA]
Sq ≡ Scalar of a quaternion
S_s ≡ Short circuit capacity [VA]
S_{ui} ≡ Power cross-spectral density [W/Hz]
T ≡ Fundamental period of sinusoidal waveforms [s]
T ≡ Torque on an electric machine axis [N.m]
U ≡ Effective voltage [V]
U_g ≡ Depenbrock fundamental voltage [V]
U_m ≡ Modulation portion of the voltage (Depenbrock) [V]
U_n ≡ Harmonic voltage [V]
U_T ≡ Periodic portion of the voltage (Depenbrock) [V]
v ≡ Volume through which energy is transformed [m^3]
$\mathbf{v}$ ≡ Measurement noise vector of G and B (v_g and v_b)
Vq ≡ Vector of a quaternion
w ≡ Angular frequency [rad. s^{-1}]
$\mathbf{w}$ ≡ Process noise vector of G and B (w_g and w_b)
Y ≡ Equivalent admittance [Siemens]
$\hat{R}_{1ui}$ ≡ Peak value of fundamental U-I cross-correlation [VA]
$\hat{R}_{ui}$ ≡ Peak value of U-I cross-correlation [VA]
$\hat{\mathbf{x}}$ ≡ Estimated values of G and B in vector form
α ≡ Power electronic converter fire angle [°]
α ≡ Voltage phase angle displacement [rad]
α-β ≡ Orthogonal co-ordinates (Akagi)
β ≡ Current phase angle displacement [rad]
Γ ≡ Power factor
Γ_d ≡ Uncorrelation or distortion factor
Γ_o ≡ SAW signal wavelength [m]
Γ_r ≡ Displacement factor
Σ_m, σ_v ≡ Mean-square error
τ ≡ Correlation time shift variable [s]
τ ≡ Filter constant [s]
Φ_n ≡ Cross-spectral density phase shift [rad]
θ ≡ Phase angle between sinusoidal waveforms [rad]

ϕ_n ≡ Frequency transform phase shift of n-harmonic [rad]
ϵ ≡ Error signal
$\hat{}\tau$ ≡ Correlation shift variable at $\hat{}R_{ui}(\tau)$ [s]

ABBREVIATIONS:

AC :- Alternating Current.
CPC :- Common Point of Coupling in a power network.
DC :- Direct Current.
DPF :- Dynamic Power Filter.
DSP :- Digital Signal Processing.
FFT :- Fast Fourier Transform.
FIR :- Finite Impulse Response filter.
HF :- High Frequency.
HPF :- Harmonic Power Filters.
IDT :- SAW Interdigital Transducers.
IIR :- Infinite Impulse Response filter.
LPF :- Low Pass Filter.
PEC :- Power Electronic Converter.
PFC :- Power Factor Correction Capacitor banks.
PWM :- Pulse Width Modulation.
RCG :- Reference Current Generation system for DPF.
SAW :- Surface Acoustic Waves.
SMC :- Synchronous Machine Condenser.
TCR :- Thyristor Controlled Reactive Source.

CHAPTER 1

GENERALIZED PROBLEM ASSOCIATED WITH NON-SINUSOIDAL QUANTITIES AND DEFINITIONS IN POWER SYSTEMS

1.1 INTRODUCTION

The quality of electric power in an age with continuous breakthroughs in superfast optical computers, ceramic high temperature superconductors, expert system applications and other technologies from the eighties, seems to be an insignificant matter. Energy, however, in all its forms, is the prerequisite for all these technologies and is, as a matter of fact, absolutely necessary for human existence at large. These mentioned technologies can however be harnessed, with many advantages, to contribute to setting better standards and obtaining a higher quality of electric power at a moderate cost, which seems to be the everlasting problem in all communities.

In developed communities the power supply is, in the majority of cases, very strong, with small equivalent reactance, which contributes to the fact that the quality of the power supply in these communities is very high. In developing communities on the other hand, long distribution power lines, low load factors and remote loads of a nature that generates distortion, tend to lead to power systems which have much more distortion. This has detrimental effects for both the supplier and user of electrical energy.

The problem of power system distortion in general is not new. Power system utilities recognized the importance of distorted waveforms of currents and voltages, i.e. departing from a sinusoidal waveform, since the 1920's [A12-14,147,148]. Electrical alternating power was originally defined on a basis of the period of sinusoidal voltage and current signals. Active power

was defined as the time average of the instantaneous power comprising the instantaneous product of voltage and current signals. Originally reactive power was undefined even for sinusoidal waveforms. The difference between apparent power and active power was described by Buchholz in the early 1920's [A12]. Before this the manufacturers of electrical equipment were to be blamed if the apparent power in their devices did not match the active power output.

It was, however, the increased use of power electronic control systems, arc-furnaces, HVDC transmission systems, fluorescent lighting and other waveform distorting apparatus, as well as the ever-present magnetic saturation in equipment, which emphasized the problems associated with a distorted power supply in all the major power systems throughout the world [H16, A148]. These non-linear loads inject characteristic and uncharacteristic distortion into power utility networks. High-frequency harmonics have secondary effects on computer systems, communication networks and control systems, and in general cause electromagnetic interference in sensitive systems.

Since the early years of distortion characterization and analysis, Fourier analysis of periodic waveforms [H15] was adopted to define, characterize and compensate for these distortion effects in power systems. Until recently it was also the only internationally accepted method to design compensation systems for these contaminated power systems [H10]. In the early 1930's the idea of reactive power measurements in the time domain was first introduced by Fryze [A69].

It was, however, only in the 1960's, when this approach was developed further by Depenbrock [D1, A31,32], that the full consequences of this method were realized and recently this method to define and characterize distortion in power systems was recommended by the International Electrotechnical Commission [H10].

Today, even with the above-mentioned schools of thought, the generalized theory of power is still a major shortcoming in power engineering. Some work, to establish a generally accepted

definition and characterization method, has already been done by Nowomiejski [A108,109], Emanuel [A42-44,47], Shepherd and Zakikhani [A122,123], Kusters and Moore [A93], Depenbrock [A35], Sharon [A121], Page [A113], Fischer [A64-67] and Czarnecki [A23-27]. There is still much to be said on this matter relating to the characterization approach which should pose attributes which relate to the power phenomena of the circuit and provide information on the design of fictitious power compensation systems. Furthermore information on the detrimental effects of distortion on power systems and on electrical equipment is of cardinal importance, which should also be obtained from this characterizing approach.

The work in this thesis should be seen against the background of these above-mentioned considerations. The sources of distortion, found in electric power systems, as well as their effects and penetration into the power system are considered. Distortion characterization approaches are critically reviewed and a new approach towards the measurement, analysis and control of fictitious power is developed. This approach is backed up with results from simulated power waveforms and actual measurements in practical power control systems and tested in the control of fictitious power, with the aid of a passive dynamic power filter.

Throughout this work the term electric power is used in a collective sense for all the concepts of power. To avoid possible misinterpretations and misconceptions, all the different "components" of electric power, i.e. active power, fictitious power, etc., will be called by their full names.

Distortion in power systems is seen collectively as all the possible causes of power system pollution. Thus in any power system a power loading of the network higher than the net useful or required energy transfer rate, implies the presence of power distortion. Thus time-shifted reactive power, which is caused by reactive elements, harmonics and modulation of voltage and current waveforms, voltage spikes, etc., are all accounted for under the broad term of power system distortion.

In contrast to inconsistent practices of other authors in the past [H16, A127,128], the unit of electric power will be given unambiguously as volt-ampere [VA] throughout this work. This unit of electric power is equivalent to joules per second or watts only where a reference is made to active power, which relates to the average rate of energy transfer.

Because both the causes and consequences of power quality problems are so diverse, they are not likely to be amenable to a single solution. Rather, a broad spectrum of co-operative efforts amongst power supply utilities, electric products manufacturers, organizations that produce distortion standards and the individual energy consumers will be needed. This chapter will give a synopsis and perspective of constraints placed on these above-mentioned parties.

The fundamental definitions of power, which are used in most of the distortion analysis and synthesis techniques, are critically reviewed on the basis of establishing proper fictitious power (the power component not associated with net energy transfer) control and measurement criteria for power systems with non-sinusoidal and, in general, aperiodic currents and voltages. The definition, analysis and synthesis of distortion in power systems, in the frequency and time domain, have been addressed by a number of authors. Some of the more important approaches are shown in the following references: A13-15,20-27,31-35,42-49,60-67,88,108-117,126, D1,3, and D8. Some authors have shown that the analysed "components" of power are not precisely and unambiguously defined under all conditions and can therefore not always be used for controlling fictitious power compensation systems, as this yields inconsistent results under dynamic conditions [A25-27,42,49,50].

This study can be divided into four major categories:

(a) the generalized definition of power under non-sinusoidal conditions;

(b) the effective measurement of power in contaminated power networks;

(c) the analysis and characterization of distortion in power networks;

(d) the effective compensation of distortion in contaminated power networks.

1.2 CONSTRAINTS PLACED ON POWER UTILITIES

Power supply utilities are primarily concerned with the supply of high quality uninterruptable electric power at a moderate cost to consumers with a moderate diversity. This goal is adversely affected by the presence of all the different types of distortion in power systems [A96]. This distortion may result from power electronics and other non-linear loads [H1,9,14,16, A94,131,133] or from some random events such as lightning, accidents to power lines, load regulation, etc. [H1]. Random line disturbances are the most difficult to combat and can never be eliminated completely. This requires enough redundancy in the power supply to provide uninterruptable power to sensitive loads.

The major problem with random distortion is its effect on crucial systems within today's complex technologies. Examples are memory-loss in computers and control disruptions in massive chemical and other processes, which places a high price-tag on a distortion free and uninterruptable power supply [A97]. This price is, in the majority of the cases, paid directly or indirectly by the power utility, which in turn has a negative effect on the price of energy reflected onto the energy consumer.

The method to limit distortion, which can be characterized as the result of power electronic systems under steady state conditions, is complex, but at least the solutions remain within the realm of technical feasibility and can largely be implemented. The method of analysis should, however, be sound and the measurement techniques accurate [H1, A132]. On the other hand, distortion which results from random changing loads and power electronics under dynamic loading conditions is, with the existing techniques, impossible to analyse and in most cases impossible to compensate for with presently correction systems. One of the purposes of

this study is to investigate the possibility of determining and compensating for this kind of distortion with new methods.

With corrective action taken on the part of the utilities, a differential price structure for different degrees of non-linearity in consumer loads, different short circuit capacities and different degrees of uninterruptability of power, seems to be one of the possible solutions to some of the problems associated with distortion generation, penetration and distribution in power systems. This emphasizes the urgency of accurate measurement and analysis of distortion within these contaminated power systems [A24,45,47,60,61,87,91,132,135,137,138,143]. The measurement and penetration model for the analysis of distortion is, from a utility point of view, the major problem area [H1, A4,138]. With effective measurement and analysis techniques the sources of the distortion can be identified and appropriate action can be taken.

Standards governing the limits of distortion injection into utility lines, have to be revised with different, but equally restrictive implications to the utilities, electrical systems and individual consumers. A higher penalty will have to be paid by consumers that inject harmonics into power systems, with a resultant higher responsibility on the side of the utilities to measure and identify these distortion quantities accurately. European nations have adopted a common set of standards, which set limits for each form of distortion and for each individual harmonic of the fundamental frequency [H1,10]. This resulted in less problems arising, with higher cost implications for power control equipment manufacturers and individual consumers, and higher responsibilities on the side of the power utilities.

Thus the major problem which power utilities have to face is to measure and control power system distortion accurately, in concurrence with recommended standards, without a major burden being placed on the price of electric energy.

1.3 CONSTRAINTS PLACED ON ENERGY CONSUMERS

From the viewpoint of the energy consumer, the effect of distortion on other equipment and the cost of distortion compensation, is of major concern. The distortion a specific consumer has to put up with, originates from distortion generating equipment used either by the specific individual consumer or by other consumers. In the latter case the distortion penetrates to the individual consumer via the common power supply he shares with the other consumers. The control and limitation of distortion generated by other consumers, will always be the responsibility of the utility, while distortion generated by the consumer will of course be the responsibility of the individual consumer. The cost of distortion compensation, so that the standards can be met, is affecting the general profitability of the consumer and is therefore of primary importance.

In the last 20 years, the practice has been to apply electronic power control equipment with minimum thought to the power system, feeding the existing plants. These systems have been designed haphazardly in these plants which, in some cases where the total distorted load is small compared to the total load, do not result in much of a problem. With the increased use of these systems to a point where the non-linear load accounts for more than about 20% of the total load [H21, A131-133], distortion causes problems and losses to such a degree that power electronic converters have been abandoned altogether, which resulted in the installation of early rotating machinery based power control systems, with in some cases an inferior performance [A131-133].

With careful planning, solutions to these problems can be found without massive capital investments in the first place. With some thought given to the choice of power electronic systems, control strategy of these non-linear loads, decentralized compensation of distortion and distortion monitoring, a minimum of extra capital investment is necessary.

In badly designed power plants, disastrous effects associated with distortion can result. In these cases a detailed analysis as

well as the installation of different power filter systems may be costly, but will normally be very necessary for the acceptable performance of these plants [A97,131,143].

Individual consumers have to make choices which concern the matter of centralized or decentralized distortion compensation in their plants. By centralized compensation is meant the technique to compensate the total distortion, generated within the plant, by means of centralized capacitor filter banks, harmonic power filters, thyristor controlled reactive sources or other compensation techniques. Decentralized compensation, on the other hand, implies the compensation at the point where the distortion is generated within the plant. This method has some distinct advantages over the method of centralized distortion compensation, with some associated disadvantages.

When the distortion is compensated directly at the point of generation, there are no secondary effects on other equipment coupled to the same power feeder. Normally the decentralized method is also used where the short circuit capacity of the power supply is small, with associated higher resonance frequencies and therefore less disastrous resonance problems at lower frequency harmonics. Another advantage is that the compensation systems are only operative when the power control equipment is in use. Some disadvantages are that the total cost of distortion compensation is high compared to the case of centralized distortion compensation, because the generated distortion can be compensated naturally by overrated step-down power transformers and other electrical equipment which act as natural sinks for some forms of distortion. It is also a known fact that distortion is smaller the further on-line from the point of generation it is measured [H1,14].

The co-operation between the power utilities and individual consumers should be sound, based on the collaboration between the different parties to minimize the effects of distortion penetration to such an extent where a totally polluted network, affecting all other consumers and utility equipment, is avoided.

1.4 CONSTRAINTS PLACED ON POWER CONTROL DEVICES AND SYSTEMS

During recent years much attention has been given to the design of power control systems with minimum distortion generation in mind [A7,8,38,58,105,112,118,120,149,150]. Research has also been strongly boosted by higher standards, which have been forced onto power control equipment manufacturers. With a few novel exceptions [A33,46,105], the course follow has been to use higher switching frequencies and/or modifications to pulse width modulation (PWM) control strategies in power electronic systems. This places a high burden on the cost and practical implementation of these systems because the power electronic switching frequency is directly related to the price of the system and inversely related to the power rating of the system.

Another possibility is to design novel systems which use basic power converter configurations known to generate distortion but which are cheaper in high-power applications, together with low-power systems and/or passive power components to eliminate the distortion which is generated by the total power control system. This concept has the advantage that only passive components or, in some cases, low-power compensation systems with high dynamic response, utilizing high-frequency switching power devices, may be necessary to compensate high-power control systems. This is one of the reasons why dynamic power filters have to be controlled in conjunction with other low-frequency or passive compensation systems. These combined compensation systems will in general reduce the overall size of sophisticated high-frequency compensation systems [A50].

In the lower power range (<10 kVA) the state of the art in power control systems, is to design systems to operate in the 10-100 kHz and up to as high as 1-10 MHz switching frequency range, in resonant topologies [A8,142]. This has the advantage of minimum power system distortion at a moderate cost. With high-power systems (>100 kVA), limitations in the technology and high cost require that these systems are primarily in the low-frequency switching range (<1 kHz), with the associated distortion generation problems.

A proposal to compensate high-power systems with the combination of low-power, high-frequency distortion compensation apparatus and more conventional compensation equipment, is also within the scope of this work. This is the result of the proposed fictitious power control philosophy (chapter 5).

Power control devices and systems will in general have to be designed with minimisation of distortion generation in mind. The major changes will take place in the general control strategy of these systems. The application of expert systems and high-speed signal processing will have to be included in most of the designs to optimize the distortion generation and cost restraints placed on these systems.

1.5 CLASSICAL PHASOR DEFINITION OF ELECTRIC POWER

The definition of electric power using phasors is well known, but is not relevant when the waveforms of voltage and current are non-sinusoidal. In the majority of power systems the waveforms of current and sometimes voltage are under dynamic loading conditions in fact aperiodic, which disqualifies this definition altogether. This definition of electric power is normally described in literature as the fundamental definition of electric power, it is nevertheless shown here.

The complex form of electric power, generally used in power system theory, is derived from the phasor representation of voltage and current. The voltage and current phasors are shown underneath.

$$\mathbf{U} = U.e^{j\alpha}$$
$$\mathbf{I} = I.e^{j\beta} \quad \text{and} \quad \mathbf{I}^* = I.e^{-j\beta} \tag{1.1}$$

Complex power **S**, is calculated from the product between the two quantities **U** and $\mathbf{I}^*$ and divided into the two orthogonal components active power P, and reactive power Q.

$$\mathbf{S} = \mathbf{U}.\mathbf{I}^* = U.I\, e^{j\theta}, \qquad \text{with } \theta = \alpha - \beta$$
$$= U.I \cos\theta + jU.I \sin\theta$$
$$= P + jQ \tag{1.2}$$

with $\mathbf{I}^*$ the complex conjugate of the current phasor **I** and **U** the voltage phasor, shown in eq.(1.1).

Apparent power S is obtained from the modulus of the complex power **S**, and is a measure of the loading of the power network. Apparent power is directly calculated from the effective values of voltage and current [A12].

$$S = U.I \tag{1.3}$$

with U and I the rms values of the voltage and current respectively.

Active power P, is a measure of the average rate of energy transfer from source to load, over the fundamental period T. Reactive power Q is a measure of the oscillating energy flow from source to load, without any net energy transfer. Reactive power originates from reactive load elements, while active power is characterized by the resistive load elements [A12].

The power factor Γ in a power network is defined in terms of the effective utilization of the power network.

$$\Gamma = P/S = \cos\theta \tag{1.4}$$

This definition of power is only capable of describing energy transfer from a sinusoidal supply to a linear load. Non-sinusoidal power supplies and non-linear loads cannot be described with this definition. Phasor theory was originally introduced to describe sinusoidal power supplies and linear loads in a time invariant manner. It was shown to be a good mathematical tool, capable of mathematical manipulations of sinusoidal voltage and current waveforms and adequate to describe power flow under these limitations. The theory of phasors is, however, used in general terms even for non-linear loads and non-sinusoidal voltage power supplies, which is non-valid. The same problems

with the time-invariant vector theory have been experienced in the generalized electric machine and dynamic thermodynamic theories [H5,12]. In these areas the generalized time-variant tensor theory is adopted. It is proposed that the same path is chosen for the mathematical, time-variant representation of voltage and current waveforms under non-sinusoidal conditions.

1.6 DEFINITION OF POWER WITH PERIODIC WAVEFORMS

With increased distortion in power systems, especially the increased use of non-linear loads, the fundamental phasor definition of electric power was upgraded, with the introduction of harmonic phasors by Budeanu in 1927 [A13,14]. This definition is based on Fourier's analysis of periodic voltage and current waveforms, in the frequency domain and was extended to unsymmetrical multiphase circuits by Quade in 1937 [A115,116].

In contrast to the definition of Budeanu, the time domain representation of electric power was defined by Fryze in 1932 [A69]. This definition was developed around the equivalent conductance G which was derived for the given network directly in the time domain. Despite difficulties with the design of accurate practical measurement techniques for the Budeanu concept in the early days, the Budeanu concept of distortion was accepted by most engineers when designing distortion compensation systems [H16, A20-23,128,131-133]. The reason for preferring the frequency domain approach to the time domain approach, was normally associated with the interpretation problems experienced with the time domain approach by these engineers. In later years the time domain approach was developed further, mainly by Depenbrock [A31-35, D1]. These two schools of thought regarding the definition of electric power under non-sinusoidal conditions, are normally referred to as the frequency domain and time domain approaches respectively. Both these definitions, as formulated originally, are limited to periodic waveforms of current and voltage.

1.6.1 Definition of Power in the Frequency Domain

The frequency domain approach in defining power in non-sinusoidal power systems, is characteristic of the work by Budeanu [A13,14], Rissik [H16, A117], Quade [A115,116], Erlicki and Emanuel [A42-47,57], Shepherd and Zakikhani [A122,123], Sharon [A121], Fischer [A65-67] and others. These above-mentioned formulations of the definition of reactive power are, however, not always consistent [A27].

Originally Budeanu defined power under non-sinusoidal conditions in terms of the harmonic analysis of the current and voltage waveforms [A13,14]. Periodic voltage and current waveforms can be described in terms of their harmonics, shown in eq.(1.5) and (1.6) respectively. These equations are generally true for periodic waveforms, but in special cases, with sinusoidal or DC voltages and/or currents, either one or both of them will simplify to a single term. In the formulation which follows eq. (1.5) and (1.6) are used in the form shown to make the approach as general as possible.

$$u(t) = U_0 + \sqrt{2} \sum_{n \in m} U_n \cos (n w_1 t + \alpha_n) \qquad (1.5)$$

$$i(t) = I_0 + \sqrt{2} \sum_{k \in l} I_k \cos (k w_1 t + \beta_k) \qquad (1.6)$$

where m and l denote the set of voltage and current harmonics respectively.

Under non-linear load conditions it is impossible to describe power by only two orthogonal components. Budeanu introduced a third component, called distortion power D_B, so that electric power consists of three mutually orthogonal components P, Q_B and D_B. These components are defined in eq.(1.7) - (1.10) [H10,16,21, A13,14].

$$S = \left[\sum_{n \in m} U_n^2 \cdot \sum_{k \in l} I_k^2 \right]^{1/2} \qquad (1.7)$$

$$P = U_0 . I_0 + \sum_{j \in (m \neq l)} U_j . I_j \cos (\alpha_j - \beta_j) \qquad (1.8)$$

$$Q_B = U_0 . I_0 + \sum_{j \in (m \neq l)} U_j . I_j \sin (\alpha_j - \beta_j) \qquad (1.9)$$

$$D_B^2 = S^2 - P^2 - Q_B^2$$

$$D_B = \left[\sum_{n \neq k \in (m,l)} [U_n^2 I_k^2 + U_k^2 I_n^2 - 2 U_n U_k I_n I_k \cos (\theta_n - \theta_k)] \right]^{1/2}$$

$$\text{where} \qquad \theta_i = \alpha_i - \beta_i \qquad (1.10)$$

Note that the frequency transforms of the voltage and current signals must be obtained before the power components can be calculated. Apparent power S is defined in terms of the harmonic components of the current and voltage waveforms. Furthermore the interpretation of reactive power Q_B and distortion power D_B is not associated with the physical load in the network [A25,27,48], but calculated from the inner products of voltage and current harmonic components. For the calculation of reactive power Q_B the inner products of current and voltage harmonics having the same frequencies are summed (eq. (1.9)). Distortion power D_B is calculated from the summation of the inner products of voltage and current harmonics having different frequencies (eq. (1.10)).

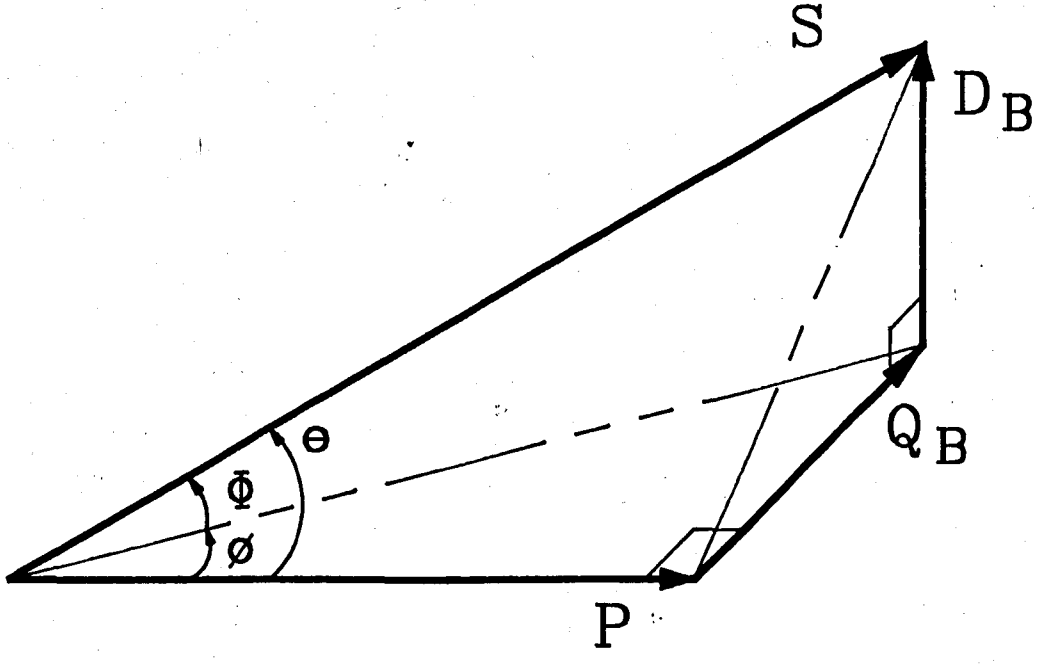

Fig. 1.1: The Relationship between the Different Power Components from the Budeanu Concept

The power components are also represented schematically in fig. 1.1 which shows the relationship between them.

The effective utilization of the power network is expressed by three utilization factors, viz. total power factor Γ, distortion factor Γ_d and displacement factor Γ_r [H16].

$$\Gamma = P/S = \cos\Theta \equiv \text{Total Power Factor}$$

$$\Gamma_r = \frac{P}{\sqrt{[P^2 + Q_B^2]}} = \cos\phi \equiv \text{Displacement Factor}$$

$$\Gamma_d = \frac{\sqrt{[P^2 + Q_B^2]}}{S} = \cos\Phi \equiv \text{Distortion Factor} \quad (1.11)$$

The disadvantages of the frequency domain approach include the fact that it cannot be used for aperiodic currents and/or voltages, because periodicity is a prerequisite for obtaining the frequency transforms. When it is used for aperiodic or unsymmetrical waveforms, inaccurate results are obtained [A25-27,48,60,109]. Even for periodic waveforms, when the measurement interval is not multiples of the period, erroneous results are obtained. Furthermore the Budeanu reactive and distortion powers are not related to the power phenomena in the network, because physical interpretation is not attained with the frequency transform [A27]. These limitations catalyzed a search for improvement [A42-44,57,64-68,115-117], but some form of periodicity was assumed throughout. Therefore these definitions do not support the design of distortion compensation systems in general [A27,48,50,109].

In the light of the above-mentioned discussion, the author abandons the harmonic analysis of voltage and/or current waveforms in the generalized definition of electric power. Power should be defined directly in the time domain and then extended to the frequency domain if the current and voltage waveforms are periodic. The use of the frequency domain should be restricted to analysis of periodic signals, e.g. in the analysis of the effects of distortion on electrical

equipment with a periodic supply and under stationary loading conditions.

1.6.2 Definition of Power in the Time Domain

In 1932 the idea of reactive power measurements in the time domain was first introduced by Fryze and in 1980 it was recommended by the International Electrotechnical Commission [A69, H10]. In the time domain definition of power, which is still formulated for periodic functions only, active power is related to the conductance G of the load. Fictitious power, which is the vector difference between apparent and active power, is physically related to the load in the form of that portion of the load which is not associated with net energy transfer. The fictitious power is not subdivided into other orthogonal components, which implies expensive distortion compensation systems, because high dynamic response power filters should be used to compensate the total fictitious power. If the fictitious power is subdivided in components with high and low dynamic characteristics, more cost effective compensation systems can be implemented [A1,50].

Apart from Fryze's work [A69], the time domain approach in defining power in non-sinusoidal power systems, is also characteristic of the work by Oberdorfer [A110], Depenbrock [A31-35, D1], Kusters and Moore [A93], Filipski [A60,61], Czarnecki [A20-27], Page [A113], Nowomiejski [A108,109], Gretsch [A77], again Fischer [A64] and others. In all these contributions the basis of the definitions is the division of current into two or more orthogonal components. Nowomiejski [A109] and Gretsch [A77] did some work on using correlation techniques to measure power in the time domain, while Nowomiejski [A109], Filipski [A61], Czarnecki [A23,24] and Fischer [A64] used the Hilbert transform to define reactive power.

The development of the time domain approach was, however, hindered to a great extend by the shortfall of accurate

measurement systems utilizing it [A31-35, D1,8]. The problem is that fictitious power is not directly measurable with standard measurement techniques; sophisticated signal processing techniques are necessary to split load current into the different orthogonal components from which the fictitious power can then be obtained [A34,60-63,77,93, D1-6,8,9].

1.6.2.1 Analysis of the Fryze definition.

In the time domain representation of the Fryze definition, the active current $i_a(t)$ has the same waveform as the voltage u(t) and its amplitude is governed by the equivalent conductance G of the network. The instantaneous value of the fictitious current $i_f(t)$ is the instantaneous difference between the network load current i and the active current $i_a(t)$.

$$i_a(t) = G.u(t)$$

$$\text{with } \overline{i_a.i_f} = 0 \quad \text{and} \quad i = i_a + i_f \tag{1.12}$$

Using these orthogonal current components, the power components of Fryze are obtained. Two orthogonal components of power, active and fictitious power, were defined and is shown in eq. (1.13) [A69].

$$\begin{aligned} S &= I.U \\ P &= I_a.U \\ F &= I_f.U \\ S^2 &= P^2 + F^2 \\ G &= P/U^2 \end{aligned} \tag{1.13}$$

The fictitious power F is a measure of the portion of the apparent power that is not associated with net energy transfer to a load. Some authors [A29,35,61,64, 76,89,93,109] subdivided the fictitious power F into several other components, but normally these components do not represent the energy phenomena associated with the network, or are unsuitable for use in the control of fictitious power compensators.

1.6.2.2 Analysis of the Depenbrock definition.

Depenbrock [D1], was mainly responsible for the rediscovery of the time domain definition, after it had been disregarded to some extent during the time span between 1932 and 1960. The Depenbrock approach [A35] is based on a division of the load and source into different orthogonal components. The source is divided into a fundamental frequency component u_g and a harmonic component u_h. Together they form the periodic component u_T. The rest of the source is characterized by the modulation portion u_m. An expanded version of the fundamental division of Fryze [A69] is applied to the load. The division of Depenbrock is shown schematically by an equivalent circuit diagram in fig. 1.2 [A35].

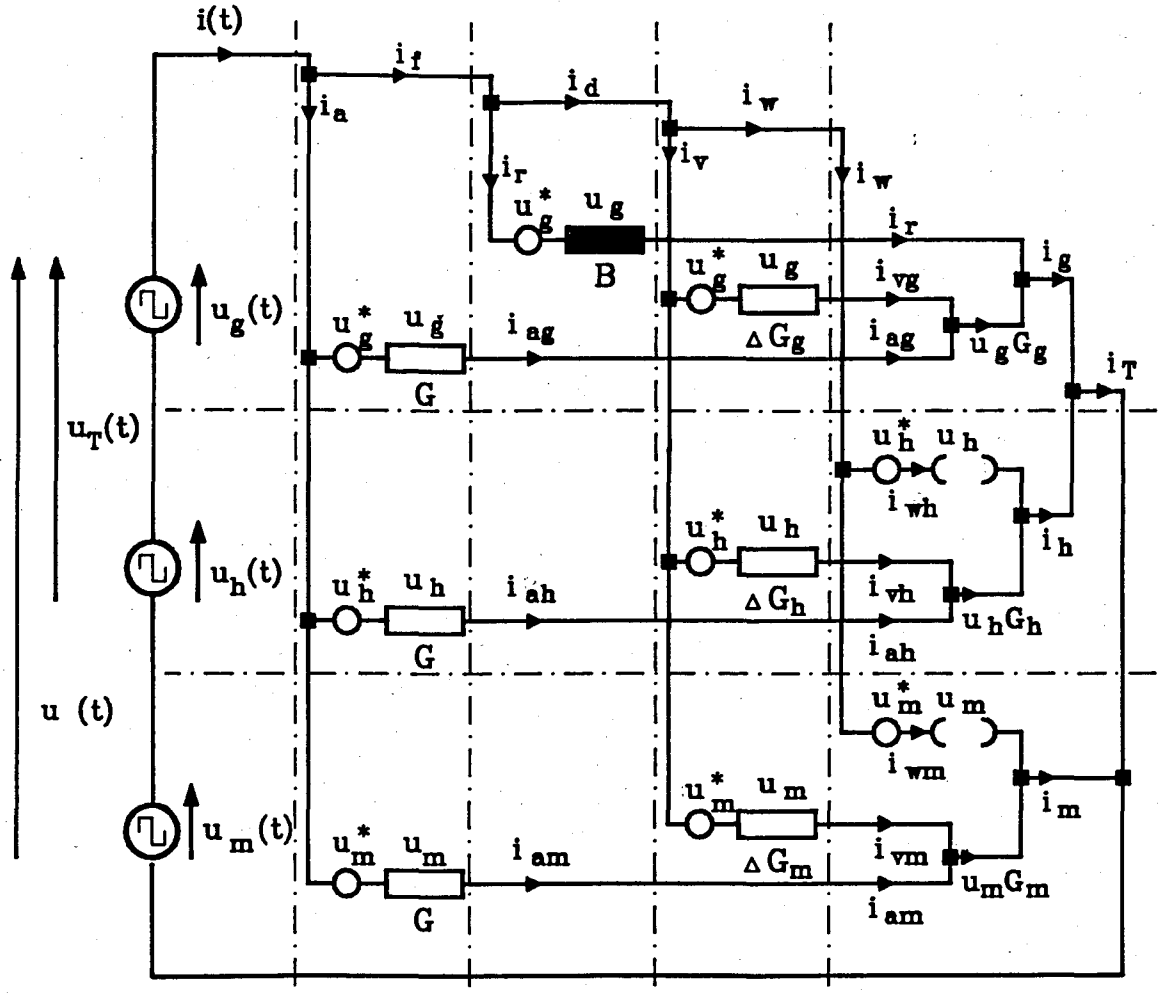

Fig. 1.2: Equivalent Circuit for Depenbrock's Definition of Power Components [A35].

The load current i(t) is divided into active current i_a and fictitious current i_f which is subdivided into displacement current i_r and distortion current i_d. The distortion current is again subdivided into conversion current i_v, resulting from the source subdivision, and rest current i_w [D1, A35,119]. The voltages shown as conjugates, for example u_g^* shown in fig. 1.2, is equivalent to $u_h + u_m$ with a negative sign. This means that only the appropriate voltage is responsible for each respective current.

In the Depenbrock approach, reactive power is defined in terms of the fundamental periodic components of current and voltage. This implies that reactive power is represented by one collective term and no harmonic reactive power is defined [A35].
This definition has some disadvantages when applied to the control of fictitious power compensation systems, because a fundamental period is assumed for the calculation of the different power components. The orthogonal power components, especially the modulation term, are difficult to measure and calculate and need highly specialized and sophisticated measurement equipment. This problem seems to be aggravated under conditions of varying frequencies, such as PWM controlled power control systems [A119, D8,11].

1.6.2.3 Analysis of the Oberdorfer definition.
Oberdorfer described non-sinusoidal periodic waveforms in terms of harmonic phasors in three phase power systems in the frequency domain [A110]. He also addressed the problem of non-sinusoidal waveforms in terms of a different time domain approach. He defined components of power directly from the instantaneous power waveforms. The basis of his time domain work is shown in the following equations [A110]:

$$P = \frac{1}{T}\int_0^T u.i \; dt \quad \equiv \text{Active power} \tag{1.14}$$

$$S_0 = \frac{1}{T}\int_0^T |u.i| \; dt \quad \equiv \text{Throughput power} \tag{1.15}$$

$$R_0 = \frac{1}{2T}\int_0^T (|u.i| - u.i) \; dt \quad \equiv \text{Return power} \tag{1.16}$$

These power components are defined in terms of the energy which is transmitted through the power network. The throughput power S_0, is defined in terms of the energy which is oscillating between load and source, while the return power is characterizing the power which is reversible (reactive power). This definition has a sound energy background. There are, however, some problems associated with the interpretation of these power components, as pointed out by Depenbrock in the form of a discussion [A110]. This definition is not waveform dependent, but, in its original form, only applicable to periodical waveforms. Furthermore the definition is not related to the power phenomena of the load, only the instantaneous power signal is concerned. Furthermore this approach does not try to divide load current into different components, which makes it unsuitable for the control of distortion compensation systems.

1.6.2.4 Analysis of the Nowomiejski definition.

Nowomiejski proposed a new generalized theory of electric power based on correlation techniques and a Hilbert transform [A109]. With this time domain definition, it is possible to define power in a time window without taking the signal period into consideration. This has many advantages for a generalized time domain definition of power (chap.3), although different values will be obtained for the power components if the measuring window is changed continuously.

The work of Nowomiejski is characterized by the use of correlation techniques [H15] to define active power. Apparent power is defined as the product of the effective values of current and voltage, which are defined over the same time window with the autocorrelation of the current and the voltage respectively [A109]. The Hilbert transform, which represents a $\pi/2$ rotation in all the frequency components [H15], is used to define reactive power. The fundamental equations of Nowomiejski are shown below [A109].

$$U = \sqrt{[R_{uu}(0)]}$$

with R_{uu} ≡ Voltage autocorrelation.

$$I = \sqrt{[R_{ii}(0)]}$$

with R_{ii} ≡ Current autocorrelation.

$$S = U.I$$

$$P = \lim_{T\to\infty} \frac{1}{2T} \int_{-T}^{+T} u(t).i(t)\, dt \qquad (1.17)$$

$$P = R_{ui}(0)$$

with R_{ui} the u(t)-i(t) cross-correlation.

$$Q_N = \lim_{T\to\infty} \frac{1}{2T} \int_{-T}^{+T} i(t).H(u(t))\, dt \qquad (1.18)$$

$$H(u(t)) = \frac{1}{\pi} \int_{-\infty}^{+\infty} \frac{i(\tau).d\tau}{\tau - t} \qquad (1.19)$$

H(u(t)) is the Hilbert transform of u(t).

$$D_N = \left[\lim_{T\to\infty} \frac{1}{4T^2} \int_{-T}^{+T}\int_{-T}^{+T} \tfrac{1}{2}|u(t).i(\tau)-u(\tau).i(t)|^2 dt d\tau \right]^{1/2} \qquad (1.20)$$

$$\Gamma = \frac{P}{\sqrt{[P^2 + D^2]}} \qquad (1.21)$$

The effective values of voltage and current, U and I, are computed from the autocorrelated voltage and current signals respectively. Apparent power S is calculated from the product of the effective values of voltage and current. Active power P is defined from the cross-correlation of voltage and current and is the amount of apparent power delivering energy over the correlation window [A108,109].

Reactive power Q_N, is defined in terms of the Hilbert transform of the voltage. Interpretation of the Hilbert transform and the physical realization of this transform is a major concern to the author. A Hilbert transform H(u) is in general non-causal for non-linear functions [H15], which implies that it is impossible to realize this transform for all signals without a prior knowledge of the waveform to be transformed. Furthermore the Hilbert transform is an indirect frequency domain transform, because the $\pi/2$ rotation is defined in the frequency domain (Appendix A4). This places a major limitation on the use of this definition for not only aperiodic signals of current and voltage, but also for non-sinusoidal voltage waveforms in the time domain (chapter 3,4) [A23,61,77,104]. The reactive power of Nowomiejski is, however, described in terms of the total frequency bandwidth of current and not only associated with the fundamental as proposed by Depenbrock.

The distortion power D_N is defined in terms of the other three components. The physical interpretation of distortion power D_N is not clear from the paper by Nowomiejski. Some other authors viz. Filipski [A61], Fischer [64] and Czarnecki [A23-26] used adaptive versions of this approach to develop time domain measurement systems and analyse power networks with non-sinusoidal voltages (chapter 4).

The problems associated with this definition are the realization and interpretation of the Hilbert transform (which is part of the generalized definition), the physical interpretation of the power components, the measurement of these components and the fact that the definition is not related to the power phenomena of the load or even the energy attributes of the network. This definition can in fact be seen as a time domain representation of the Budeanu frequency domain definition, with no explicit physical relation to the load parameters [A27].

1.7 DEFINITION OF POWER ASSOCIATED WITH APERIODIC WAVEFORMS

In the case of an aperiodic instantaneous power waveform, average power is in general defined over an infinite time span [H15] (chap. 3.2). The definition of power in aperiodic waveforms is, however, limited to the information transfer theory, where only active power can transfer useful information [H17]. The power cross-spectrum theory [H15, 17] is used in these applications. In power systems the waveforms of currents and voltages are also, in general, continuous but aperiodic as stochastical load changes are peculiar to all power systems. In the definition of electric power under these aperiodic conditions, several problems arise. They are primarily associated with determining the appropriate measurement time window and the classification of the aperiodic waveforms (chap. 3.2).

Aperiodic instantaneous power waveforms p(t), can be divided into three groups [H15]. Only two are relevant to this study. The one delivers a finite amount of energy and therefore the average power, when taken over an infinite time span, is zero. In practical terms, a single pulse of power in a relative long time span, for example a full-cycle thyristor controlled temperature controller under certain operating conditions, can be regarded as belonging to this group. The other delivers an infinite amount of energy, resulting from a continuous stochastical waveform of in-

stantaneous power. In practical terms this is the type which is normally associated with power systems, as for example an arc-furnace cycle. The third is irrelevant as it is associated with infinite average power, which is only of mathematical interest. Of the finite average power category, power associated with periodic waveforms is a special case. The classification of energy transfer can be summarized as follows: If the energy delivered to the load is associated with a continuous waveform of instantaneous power, a finite amount of average power is transferred. On the other hand, if energy is transferred to a load by means of a relatively short power pulse, it is a zero average power case (chap. 3.2).

1.7.1 Definition of Power in the Frequency Domain

A sufficient condition for the existence of the Fourier transform of a signal, is that the signal must have finite energy [H15]. In practice, however, a modification of the normal Fourier transform is necessary, because power systems normally have continuous instantaneous power waveforms and are therefore normally infinite energy systems. This modification is done by means of the so-called periodic Fourier transform with the limit theory [H15]. A frequency domain analysis of a continuous, but aperiodic, instantaneous power waveform, is therefore fundamentally impossible [H15].

Some authors try to circumvent this limitation by defining the so-called modulated or running harmonics. This is, however, mathematically incorrect and should be abandoned altogether. Probabilistic modeling of harmonics in power systems can, however, give good results when the effects of distortion on electrical equipment must be calculated and when used in the design of power factor compensation equipment [A6,47]. It is nevertheless still fundamentally impossible to analyse power systems with a continuous, aperiodic instantaneous power waveform in the frequency domain.

1.7.2 Definition of Power in the Time Domain

In principle the time domain can be used to define electric power over any chosen time window dT, without reference to a fundamental period of either voltage or current. The general time-domain definition of power is therefore independent of any period, but, for comparison purposes, fundamental periods should be used as natural time windows, if they do exist.

All the definitions described in the previous section on periodic time domain definitions, can be adapted to a greater or lesser extent for the definition of power, in the time domain, when the instantaneous power waveform is aperiodic. The division of electric power into active and fictitious power poses no fundamental problems in the majority of the time domain definitions. It is, however, the subdivision of the fictitious power into other components, which results in a lot of complications, because there is no accurate proven method to do this subdivision.

1.7.3 Power Cross-Spectral Density

The power cross-spectral density definition of power is normally found in all information theory textbooks [H15,17]. Only active power, i.e. power dissipated in a resistance, is however defined in this way. The other components of power used in power systems, viz. loading or apparent power, fictitious power, reactive power and distortion power, are of no concern in information science. The other limitation of this approach is that the finite energy criteria [H15] applicable to information systems, can only be used for power systems with discontinuous instantaneous power waveforms.

For the sake of completeness, eq. (1.22) shows the definition of active power from the power cross-spectral density, S_{ui}.

$$P = \frac{1}{T} \int_{-\infty}^{+\infty} S_{ui}(f).df \tag{1.22}$$

$$S_{ui}(f) = \lim_{T->\infty} \frac{1}{2T} \left[\; |F_u(f)|.|F_i(f)| \; \right] \tag{1.23}$$

with F_u and F_i the fourier transforms of the voltage and current signals respectively:

$$F_u(f) = \int_{-\infty}^{+\infty} u(t).e^{-j2\pi ft} \, dt \tag{1.24}$$

$$F_i(f) = \int_{-\infty}^{+\infty} i(t).e^{-j2\pi ft} \, dt \tag{1.25}$$

An interesting property of the cross-spectral density is the fact that it can be obtained from the Fourier transform of the cross-correlation of voltage and current (Appendix A4):

$$S_{ui}(f) = \int_{-\infty}^{+\infty} R_{ui}(\tau).e^{-j2\pi f\tau} \, d\tau \tag{1.26}$$

1.8 CRITICAL DISCUSSION OF THE EXISTING DEFINITIONS

In all the above mentioned definitions of power it is clear that active and apparent power are covered adequately under all the above-mentioned power definitions. In the time domain and the frequency domain definitions, active power is a measure of the average rate of net energy transfer from source to load, taken over a chosen time window. Apparent power describes the loading of the network over the same time window and this is universally defined as the product of the effective values of current and voltage.

Nearly all the definitions give different interpretations for the components of fictitious power. Some definitions give reactive power in terms of all the current and voltage harmonics and others only in terms of the fundamentals. Furthermore all the basic definitions make provision for three or more power components, eq. active, reactive and distortion power, but the difference between reactive and distortion power is not always clear. Different results are obtained when the voltage is non-sinusoidal.

It seems appropriate to define only two orthogonal components of loading power, viz. active power and fictitious power. Active power is a measure of the rate of net energy transfer from source to load and fictitious power does not result in net energy transfer. If, for some reason, it is important to have more than one power component, apart from active power, a further subdivision of fictitious power should be made. A good example for the subdivision of the fictitious power into other components is in the compensation of fictitious power in contaminated power systems. If it is possible to compensate the fictitious power by means of different techniques, which are characterized in terms of the dynamic response of the compensation systems, fictitious power with low dynamic characteristics can be compensated by means of distortion compensation systems with low dynamic characteristics, and normally of lower cost. Then only the residual amount of fictitious power, associated with high dynamic characteristics, should be compensated with costly high dynamic responsive power filters.

In the author's opinion only real-time occurring voltage and current signals should be input data for a power measurement system and no definition of power should be explicitly dependent on the analysis of current and voltage signal harmonics. Harmonic analysis can, however, be adopted for the characterization of the effects of distortion on electrical equipment and used to some extent in the design of power compensation filters. The generalized definition of power should however be in terms of the real occurring waveshapes of voltage and current.

1.9 AN OVERVIEW OF THE REST OF THIS STUDY

This thesis is divided into several chapters which focus on different aspects of the definition, analysis, signal processing, generation, penetration, effects, measurement and compensation of distortion in power systems. Each aspect of distortion is overviewed with some references to literature. New contributions are made in several aspects of this broad field of distortion in power systems. The emphasis is, however, placed on the effective definition, analysis, measurement and compensation of fictitious power under dynamic power system operation.

Experimental results high-lighting the different aspects are found throughout this thesis, with special attention given to the measurement of distortion in various power electronic systems. The philosophy of fictitious power compensation is shown experimentally in a separate chapter. It is evident that better and faster processing of voltage and current signals can make a great impact on power system distortion analysis, measurement and compensation. Throughout this study the problem of a distorted supply has nevertheless been found to have such far-reaching consequences, that a lot still needs to be done on this subject.

CHAPTER 2

CLASSIFICATION, SOURCES, PENETRATION AND EFFECTS OF DISTORTION IN ELECTRIC POWER SYSTEMS

2.1 INTRODUCTION

Non-linear electrical loads, normally the consequence of power control equipment, are known to be the major sources of power network distortion. Because these loads are generally highly efficient, both their numbers and capacities increased enormously during the last number of years and will follow this trend for the time to come. The technique of phase angle control by means of supply commutated thyristor converters, is by far the most extensively used technique to control vast amounts of power in electric power systems. These power converters do inject characteristic harmonic distortion into the power network under steady state conditions and uncharacteristic distortion under dynamic operating conditions. This forms the biggest single source of distortion in power systems. Other non-linear loads which may be singled out as major distortion generating power equipment, are arc-furnaces, arc-welders, fluorescent lighting and to a lesser extent magnetic saturation in power transformers and space harmonics caused by slot distribution in direct on-line AC machines. In this chapter these sources of distortion are synoptically reviewed to distinguish between the different types of distortion in power systems.

In the majority of cases, the effects of distortion on a power network include higher operating costs both of the power network itself and of the equipment subjected to this distortion [A97]. With better and more sophisticated designs of power control equipment, the problems associated with a distorted supply are becoming more important, because manufacturers are laying down stricter specifications for the power supply to their equipment.

The effects of distortion on electric power systems high-lighted in this chapter, can be summarized as follows [H1,8,16, A19,70, 77,82,97,98,111,128,130-133,145,148]:

a) parallel and series resonance in power systems, with associated detrimental effects on other power equipment,
b) the increase of losses in power generation, transmission and utilization,
c) excessive loading of power networks without an associated increase in the transfer of usable electric energy, or other forms of energy, from source to load.
d) early aging of power equipment or shortening of their useful operating life and
e) system maloperation caused by electromagnetic interference.

Finally the penetration of distortion into a power system is important because of the interaction between power equipment coupled to a common power supply [H1,A138].

This chapter starts with a classification of the distortion types and sources in power systems. A synoptic overview of some of the more important effects and financial constraints, distortion places on the power system, is then shown after a model for the penetration of distortion into power systems is described.

2.2 CLASSIFICATION OF DISTORTION IN POWER SYSTEMS

As described in chapter 1, distortion is seen collectively as that which causes the loading of a network to be higher than the net required rate of energy transfer from the power source to the load. This includes the extra losses in the load which result from the distortion present in the power network. A classification of distortion based on the final electric load coupled to the power network, is given underneath.

2.2.1 Distortion Caused by a Time Shift between Current and Voltage Waveforms.

This type of distortion implies a power factor lower than unity and is normally caused by reactive elements in the power network. Examples are inductances, capacitances and direct on-line AC-machines operating from a power supply with a sinusoidal voltage waveform. Under steady state conditions the extra loading of the power system, due to this type of distortion, can safely be compensated for by means of the conjugate reactive element. Under quasi dynamic conditions (when the load current does not change drastically from one fundamental period to the other) Thyristor Controlled Reactive sources (TCR's), with associated harmonic power filters, should be incorporated for compensation [H14].

2.2.2 Distortion Caused by the Correlating Harmonics of Voltage and Current Waveforms.

The distortion present, under steady state conditions, when the waveforms of voltage and current are periodic, but non-sinusoidal, normally causes extra energy losses in electric loads requiring primarily a sinusoidal voltage supply. This type of distortion also causes reactive power associated with the correlated harmonics of the voltage and current. Distortion of this nature places a higher loading on the power network, increases energy losses in equipment and shorten the equipment's useful operating life cycle. Compensation of this type of distortion can successfully be obtained with the effective use of harmonic power filter networks [H14].

2.2.3 Distortion Caused by Modulation in the Correlated Voltage and Current Waveforms.

This type of distortion is normally found in systems with a weak power supply where the current is modulated by means of power control equipment or by the presence of stochastically changing loads, for example arc-furnaces or electric machine

drives under dynamic operating conditions. The weak supply implies that the voltage is modulated together with the current. This distortion can result in reactive power associated with a time shift between the modulated voltage and current waveforms and in active power losses due to the modulation. Compensation of this type of distortion is difficult to achieve, because of the large amount of power which is modulated, the stochastical changes and low frequency of the modulation. At present large Thyristor Controlled Reactive Sources (TCR's), with reactive power ratings of between 10 and 100 MVA, are being used in large power systems [H14, A9,17]. However, with state of the art designs incorporating adaptive controllers, the dynamic control of these systems poses a major problem [A28,83,99].

2.2.4 Distortion Caused by the Uncorrelation between Voltage and Current Waveforms.

It is a known fact that waveforms of voltage and current which are not correlated, for example two sinusoids of different frequencies, result in a loading of the power network without transferring net energy. In general when the correlation between a voltage signal and a current signal decreases, the net amount of energy they transfer also decreases even though the loading of the power network may remain constant. A decrease in energy transfer without a corresponding decrease in the loading of the network, implies an increase in distortion. A typical example of a circuit in which this type of distortion occurs is the simple series connection of diode and a resistance coupled to a power supply outputting a sinusoidal voltage (Appendix A3). This very common form of distortion, found in almost all power control systems, is present under steady state operation and under dynamic operation of the electric load. Under steady state conditions, compensation can be achieved with tuned harmonic filters. Under dynamic loading conditions, a dynamic power filter with a high dynamic system response should be used for compensation [A1-3,16,50-56,81,84,86,101,139, 141].

2.2.5 Distortion Associated with Multiphase Systems.

Distortion occurs in a multiphase power system when the network is loaded unsymmetrically. This means that distortion occurs when the loads in the different phases are not equal to each other, even though they may all be linear resistances. The unsymmetrical load results in unbalanced currents and unsymmetrical load voltages, which place a higher loading on the power system. From the very nature of this kind of distortion, it is clear that it is peculiar to multiphase systems and can never be found in single-phase systems. The opposite can however also be true: a form of distortion which can be present in single-phase systems, viz. that associated with the triplen zero sequence harmonics, is eliminated in a balanced three-phase system [H1,9,14, A32, 35,40,111,127].

2.3 POWER ELECTRONIC CONTROL SYSTEMS AS A SOURCE OF DISTORTION

Controlling the shape of the line current, for the purpose of controlling the load power in an electric power system, is commonly known as phase angle control, because it is tantamount to controlling the angle between the current fundamental and the sinusoidal voltage. The systems employed for phase angle control is a more common cause of distortion than other electronic power control systems [H1,9,13, A131-133]; fundamental time-shifted distortion, correlated and uncorrelated harmonics as well as the modulated distortion may result from these systems. Furthermore, when the supply is weak, the voltage is also non-sinusoidal and thus the distortion is injected back into the power system.

Unlike phase control systems, pulse width modulated (PWM) line-side power electronic systems do not present distortion problems at fundamental voltage frequencies, because the modulation is normally sinusoidal. However, problems arise at higher frequencies and, as these systems do not in general possess waveforms with halfwave symmetry, even harmonics are generated. Furthermore these systems have complicated circuit and control

topologies, which have a negative effect on their cost and power ratings. PWM converters can also contribute to a lot of high-frequency associated distortion problems, for example electromagnetic interference in sensitive systems.

Applications of the above-mentioned converters include the following [A142]: in-cycle temperature controllers and light dimmers [H1,9,13], resonant induction heaters [H9,13], renewable energy conversion [A140], traction drives [H9, A7,106,142], industrial machine drives [H9,13, A36,75,111,130], battery chargers [A8,112], High Voltage Direct Current (HVDC) converters [A74], Thyristor Controlled Reactive sources (TCR's) [H14, A80,92,124] and power supplies for residential appliances, like television receivers [H1, A71].

In the case of these power control systems the analysis, measurement and compensation of distortion under steady state conditions seem to be difficult, but technically feasible. Under dynamic operating conditions on the other hand, the characterization, analysis, measurement and compensation of distortion are in general undefined and are seldomly referred to by authors.

Different topologies of power electronic converters may be used to obtain different power conversion results. Figure 2.1 shows several fundamentally different structures [A142]. Each topology is shown symbolically as a p-pulse converter using bi-directional on-off switching [A142]. The control strategy of these different converter topologies is the major reason for distortion generation. All these converters can be controlled by means of natural source or load commutation, PWM controlled external commutation, or even naturally resonant switching devices if reactive elements are included inside the topologies [H9, A142].

2.3.1 Analysis Under Steady State Operating Conditions

Steady state conditions exist when the time taken for changes in the load to take place is at least an order of magnitude longer than the fundamental period of the power supply voltage as defined in the time domain. Under these

conditions no load changes are anticipated during a distortion analysis interval and very small changes are anticipated from one analysis interval to the next. Typical examples are a power control system controlling temperature in a confined space and a power control system controlling an electric machine drive at constant speed and torque.

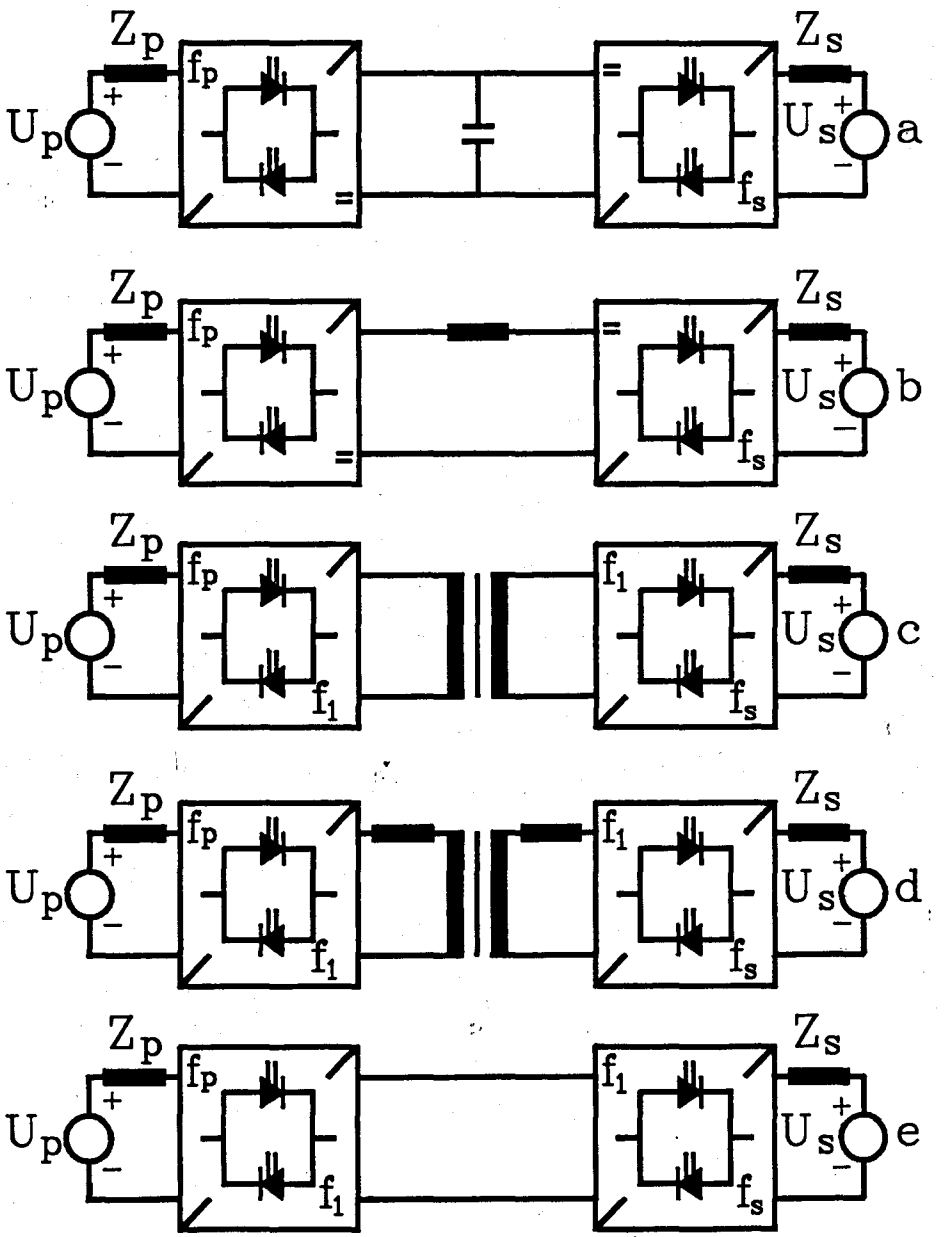

a. Direct voltage link converter
b. Direct current link converter
c. Alternating voltage link converter
d. Alternating current link converter
e. Directly linked composite converter

Fig. 2.1: Structure of Different Converter Topologies [A142]

For this type of converter the frequency domain and time domain representations give accurate results under steady loading conditions. The frequency domain can also give a good approximation of the types of distortion possibly present and is normally used in the analysis of distortion generated by these converters.

Through Fourier analysis the periodic distortion currents are described by the sums of sine waves of different frequencies [H15]. Equation (2.1) may be used to calculate the non-zero harmonic currents which are normally found with most phase controlled AC-DC converters [H1,9,13,14,16,21, A128,130-133]. This type of converter is the most used building block in the majority of power electronic systems [A142].

$$h = kp \pm 1$$
$$I_h = I_1/h \qquad (2.1)$$

where h ≡ harmonic order
k ≡ any integer 1,2,3,...
p ≡ the topology pulse number
I_h ≡ magnitude of h-th current harmonic
I_1 ≡ magnitude of current fundamental

This theoretical equation implies that for a typical six-pulse converter operating under steady conditions, the 5,7,11,13.. current harmonics exist with magnitudes of 20%, 14%, 9% .. of the magnitude of the current fundamental respectively [H1,9, A130-133].

These theoretical calculated quantities are affected by several factors, for example the thyristor overlap angle μ, unsymmetrical phase voltages and supply transformer windings, the dc-link reactances, supply transformer reactances, discontinuous current flow and fully-controlled or half-controlled topologies [H1, A128]. Figure 2.2 shows a schematic representation of a generalized phase controlled converter topology and the associated phase current [H1]. The width of the theoretical block line current through each

converter valve is inversely proportional to the pulse number p. In systems incorporating symmetrical converters the even harmonics cancel and therefore only odd harmonics are present. This result is typical for three phase converter systems and is reflected in eq. (2.1). Furthermore the triplen harmonics are also absent in symmetrical three phase systems [H1,14], because of zero sequence cancellation and thus only positive and negative sequence harmonics exist. This aspect is also reflected by eq. (2.1).

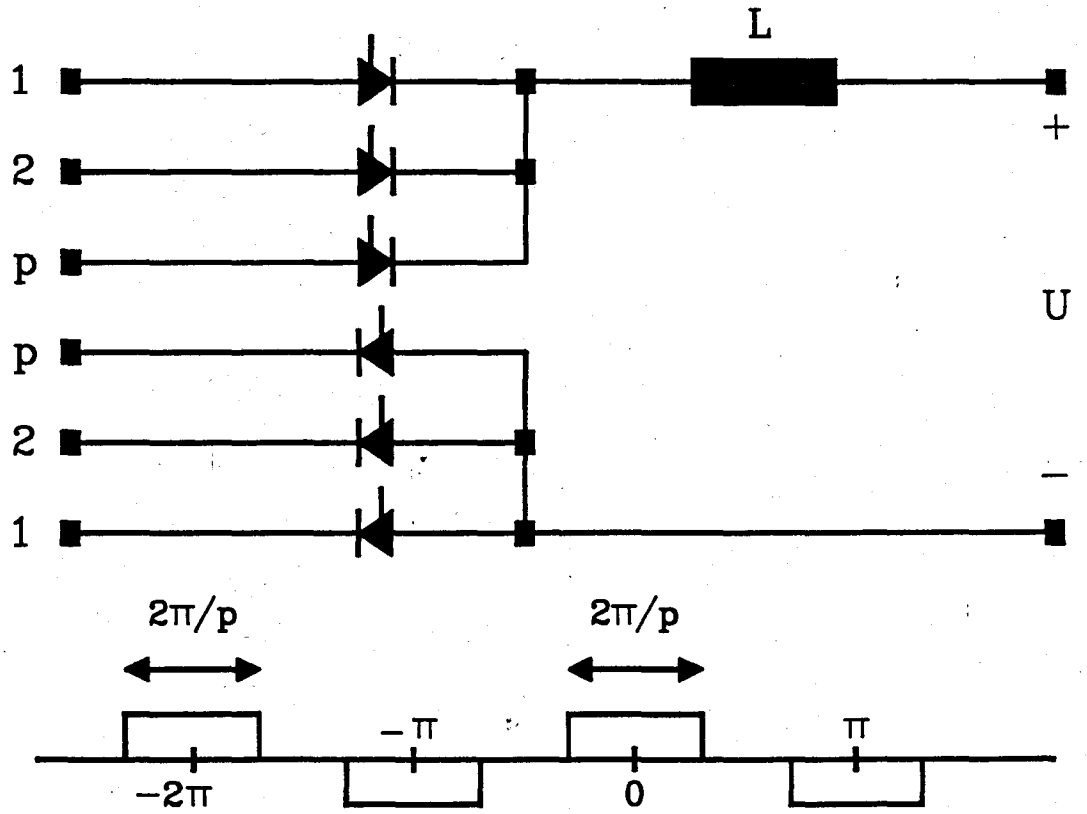

Fig. 2.2: Generalized p-Pulse Converter and Associated Block Current

The load-side harmonics in current-fed converter systems are affected by the pulse number and the load reactance [H1]. For a typical 6-pulse converter topology, the load ripple has a frequency of six times the fundamental frequency, thus the 6,12,18.. current and voltage harmonics exist. At higher power applications it is, for the reasons stated above, com-

mon practice to incorporate 12 and 24 pulse converter systems, which are normally realized by means of star-delta and zigzag transformer winding configurations.

When utilizing pulse width modulation (PWM) techniques in power converters with externally commutated power devices, the first significant harmonic occurs at the modulating frequency. In high power control systems this frequency can be as low as 200 Hz - 1 kHz which implies that the first harmonic present, is the 4th - 20th with eq. (2.1) governing its magnitude. Because the PWM waves does not have halfwave symmetry, even harmonics do exist. A vast number of authors are optimizing the PWM switching pattern and modulating frequency to minimize the distortion injected back into the power system [H1, A11,38,58,111,150].

2.3.2. Analysis under Dynamic Operating Conditions

Uncharacteristic distortion arises when a power converter is operated under dynamic conditions. Take as an example a traction drive where the traction effect can be acceleration, coasting or regenerative braking. In the majority of cases the changes are stochastical, thus making it impossible to analyse the distortion with the present characterizing approach. Some authors [A47] have done research work on stochastical harmonics, as a means of analysing these static power converters under dynamic operating conditions. This approach is based on the frequency domain, with the associated problems described in chapter 1.

From the author's point of view the frequency domain approach can only be used in the analysis of distortion under steady state or nearly steady state operating conditions of these power electronic converters. The actual waveforms in the time domain should be used in the analysis of distortion under dynamic operating conditions [A48,50,51, D3]. The proposed time domain approach for the analysis of power electronic converters under dynamic operating conditions is derived in chapter 3.

2.4 DISTORTION CAUSED BY ARC-FURNACE INSTALLATIONS

The combination of arc ignition delays and non-linear arc admittance [A94], introduces fundamental frequency harmonics. On the other hand random changes in the arc-length produce lower order distortion of the modulation type [A77]. These stochastical variances are typical in the 0,1 - 30 Hz frequency range [H1, A77,98]. Arc-furnaces can be either AC or DC based; in the latter case a cascaded power electronic converter, with associated distortion, is implemented. An arc-furnace load is known as one of the most problematic loads which can be coupled to an electric supply [H1, A77]. It is normally coupled to its own power supply and sometimes even to its own power generating plant and distribution networks. Arc-furnaces range in size from small units of a few tons with a associated power capacity of 2-3 MVA, up to 400 ton units rated at 100 MVA [A94].

Schematic diagrams of AC-based and DC-based arc-furnaces are shown in fig. 2.3(a) and 2.3(b) respectively. It has been found that DC-based furnaces are less problematic because of the current source realized by means of the link inductance [A77]. The arc current is less capable of fluctuating and only characteristic distortion, resulting from the cascaded rectifier system, is present. These DC-based systems are normally of smaller power rating than the AC system.

An arc-furnace normally has a reasonably fixed furnace cycle which can be seen as the signature of the specific furnace [A77]. The first phase, where scrap metal melting occurs, is normally the worst phase where the arc-length changes considerably and where maximum energy is required. In the second phase where the oxidation or overheating of the molten metal is performed and the third phase associated with the refining of the molten metal, only small fluctuations in the distortion generation are noticeable. Distortion associated with arc-furnaces can normally be characterized by means of probabilistic modeling, which analyses the statistical properties of this distortion [A47].

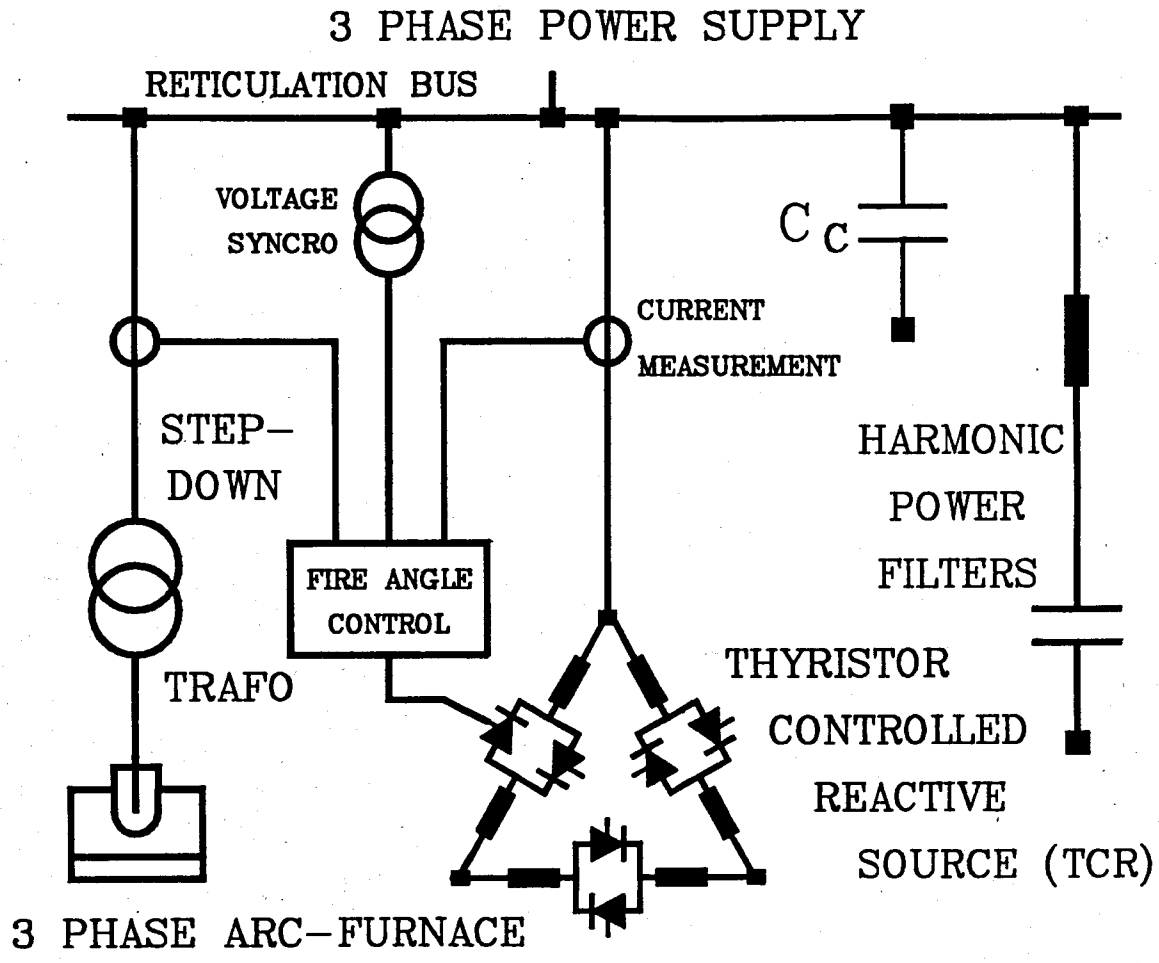

Fig. 2.3(a): Schematic Line Diagram of AC-based Arc-furnace.

Arc-furnaces have detrimental effects on the power supplies to which they are coupled. Serious light flickering occurs in the vicinity of arc-furnace installations and other electrical equipment is also adversely affected [A82].

Compensation of distortion generated by arc-furnaces is accomplished by the effective combination of harmonic power filters and in most of the cases a TCR of the same power rating as the arc-furnace [H1, A77,82,94]. The effective use of a TCR may also contribute to elimination of the flicker caused by these installations [A77,82,94].

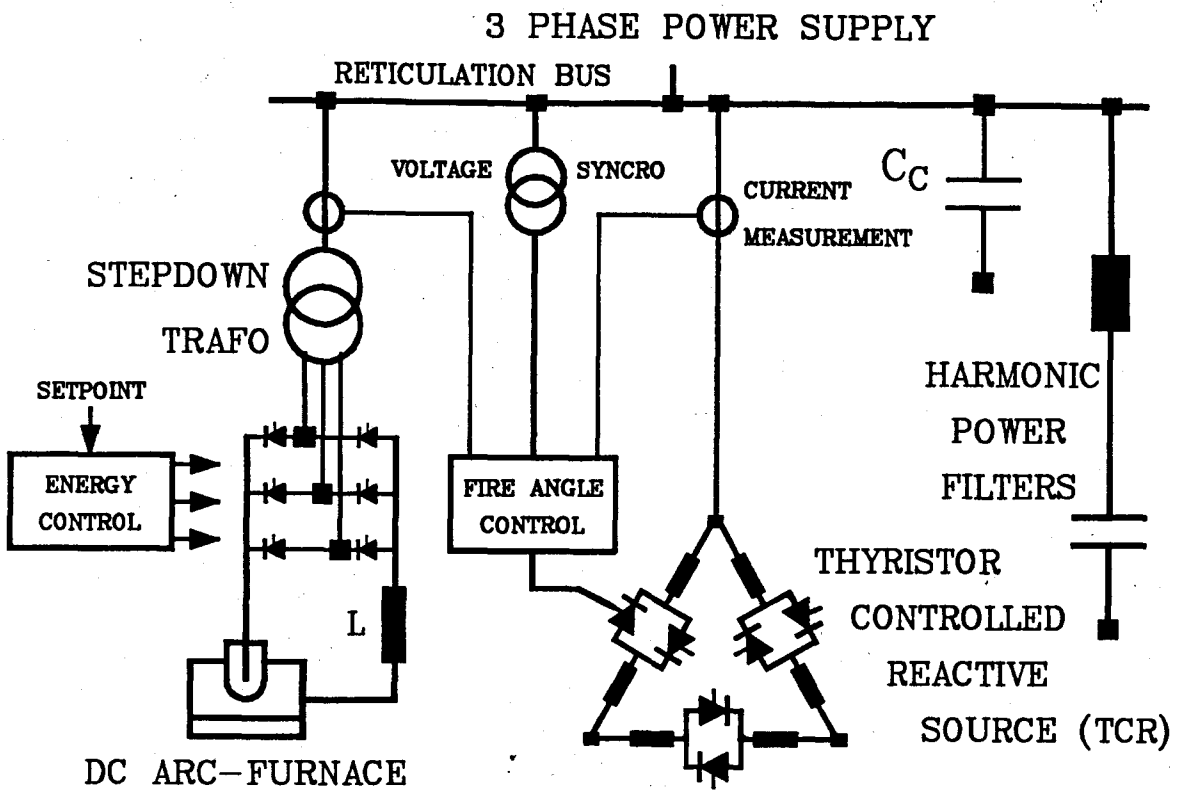

Fig. 2.3(b): Schematic Line Diagram of DC-based Arc-furnace.

2.5 SECONDARY NON-LINEAR LOADS AS SOURCES OF DISTORTION

There are a number of devices and systems which generate distortion to a lesser extend than the power electronic converters mentioned earlier and arc-furnace loads. Prior to the development of power electronic converters, distortion was primarily associated with the design and operation of electric machines and transformers. These were the major distortion generating equipment, the distortion being caused by them including the non-sinusoidal voltages generated by early electric power generators and the non-sinusoidal magnetizing and inrush current of power transformers [H1, A19].

2.5.1 Distortion Caused by Magnetic Power Equipment

Distortion from magnetic power equipment is normally associated with AC-machines and power transformers.

2.5.1.1 Distortion resulting from power transformers.

The power transformer voltage at no-load is practically balanced by the back EMF, because the effect of winding resistance and leakage reactance is negligible at low currents, thus form Faraday's law:

$$u_p = N \frac{d\phi}{dt} = \sqrt{2}.U \sin wt \qquad (2.2)$$

The flux is shown in eq. (2.3):

$$\phi = \int \frac{e.dt}{N} = \frac{\sqrt{2}U}{N.w} \cos wt = \Phi_m \cos wt \qquad (2.3)$$

This implies that the flux has a sinusoidal waveform. The magnetizing current I_m is, however, not purely sinusoidal, because the relation between flux and magnetizing current is non-linear. This stems from the facts that the magnetization curve is non-linear and that hysteresis occurs. A big third current harmonic results from this magnetizing characteristic [H1, A39]. The magnetizing current is distorted even further when an unbalanced load is connected to the transformer secondary [H1, A39,40].

Distortion also results from the economic design of power transformers, where the core material is normally utilized well, thus running the transformer into quasi saturation [H1, A39]. However, with a small increase in the supply voltage, major saturation will occur, which will increase the third harmonic current component drastically. When turning a power transformer on, the non-zero residual flux present in the core prior to turn-on can, in the worst case, result in a peak flux density of up to three times the normal peak flux density, with associated third harmonic and DC components.

Other distortion which results from power transformers, is associated with the ferro-resonance between a power system capacitance and the equivalent magnetizing reactance of the power transformer [A104]. This distortion is, however, very seldomly measured and can generally be ignored.

2.5.1.2 Distortion resulting from rotating machines

In practical machine design the machine windings are distributed along the surface with k slots per pole per phase and the MMF's of the k coils are spacially displaced from each other. For a p-phase machine the number of slots per pole is kp and the electrical angle between slots is given in eq. (2.4).

$$\alpha = \pi/(kp) \tag{2.4}$$

It can be derived from basic principles that in the case of a typical three-phase electric machine, the triplen harmonics (3,9,15) are absent. Only positive and negative sequence harmonics (5,7,11,13...) occur because of the finite number of slots per phase, as shown in eq. (2.5) [H1].

$$h = 2\,kp \pm 1 \tag{2.5}$$

where p ≡ number of phases;
k ≡ number of machine slots per pole per phase.

This distortion can also be present in a synchronous generator, so that a non-sinusoidal voltage is delivered to the power supply. In asynchronous machines a rotor slip s is present, which can result in speed dependent harmonics injected into the power supply [H1]. These types of distortion are, however, very small compared to that from other sources like static power converters and arc-furnaces.

2.5.2 Fluorescent Lighting as Source of Distortion

Distortion associated with fluorescent lightning is commonly found in office buildings. In a typical power plant fluorescent lighting comprises only a small fraction of the total non-linear load. In office buildings, however, this is no longer true. In big city office buildings, fluorescent lighting loads can be as large as 80% of the total load [A73]. In these cases serious distortion results from this highly non-linear load which can have a major effect on the other equipment, for example computers and telecommunication apparatus, in the same environment and coupled on the same power feeder.

Fluorescent tube lighting gives rise to odd-ordered current harmonics the third being the most dominant. As lighting installations often involve long distances with very little load diversity, resonance at the third harmonic is possible [A73]. For these installations it is recommended to avoid resonance by implementing centralized compensating capacitor banks adjacent to distribution boards [H1, A73].

This conclude the synoptical overview of the different sources of distortion in power systems. Other sources have a very small occurrence rate or are uncontrollable, for example lightning, and for these reasons fall outside the scope of this study. All of the above-mentioned sources contribute to the types of distortion described in section 2.2.

2.6 MODEL OF DISTORTION PENETRATION IN POWER SYSTEMS

The penetration of distortion in power system has been studied by a number of authors [H1, A4,138]. The principle of these studies is an intuitive appreciation of the relationships between the fundamental power flow and the power flow at distortion, especially at harmonic frequencies. The power flow under conditions of modulation and in cases where the supply voltage is non-sinusoidal is however not addressed. The principle of the power flow studies is shown in fig. 2.4.

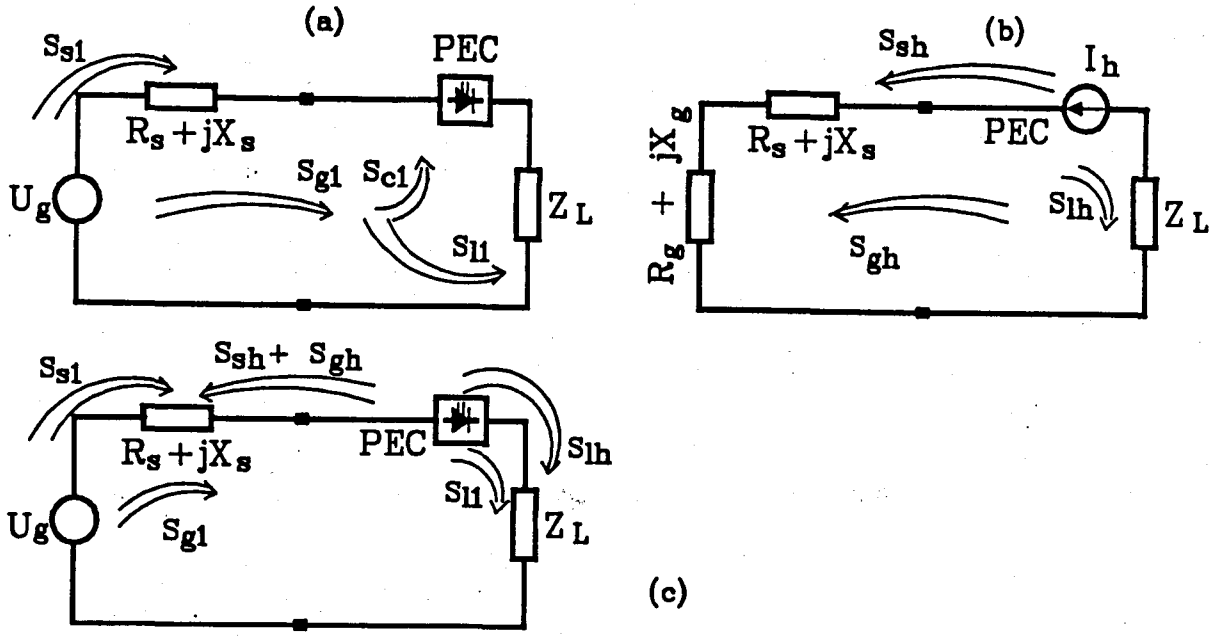

Fig. 2.4: Harmonic Power Flow with Non-linear Loads [A138].

Fig. 2.4(a) shows the fundamental power flow from source to the circuit element, while fig. 2.4(b) describes the harmonic power flow. Some of the power which flows from the source, is converted into harmonic power and flows to the load and back into the source. In this case the distortion generating equipment, which is the source of the distortion, is shown as an equivalent harmonic current source. This current is delivered to the load and to the source. Figure. 2.4(c) shows the net result of the two cases.

This approach describes the non-linear portion of the load as an active current source at the harmonic frequencies. The transfer of source power to harmonic power is not described fully by Tschappu [A138] and is from the authors point of view not justified. This approach will be amended by the equivalent network theory described in chapter 3, where the power network is divided into equivalent passive components, describing the different forms of the distortion found in a typical power network. This theory also describes how distortion penetrates back into the power system only by means of the associated non-sinusoidal voltage (chapter 3).

2.7 RESONANCES IN POWER NETWORKS

When analysing the effects of distortion in power systems there are so many factors to be considered that it will be a detailed study of its own. Some effects of distortion are, however, very important and stand out as primary problem areas; they are described here. One of the serious effects is the principle of resonance of the equivalent network reactances at harmonic frequencies [H1, A38]. Resonances in power networks can be divided into the following:-

(a) Parallel resonance of user capacitance and the supply reactance, resulting from distortion generated internally i.e. within the consumer system.
(b) Series resonance of the consumer capacitance and the supply reactance, resulting from externally generated distortion.
(c) Interactive parallel resonance between different power factor capacitor filters and harmonic power filters in the user power network.
(d) Interactive parallel resonances between different energy users on a common power supply.

These different types of resonance are described by the schematic circuit diagram shown in fig. 2.5. Any linear network can be given an equivalent Thevenin circuit as shown in fig. 2.5(a). This equivalent circuit is coupled to a non-linear load, for example a power electronic converter PEC and other linear load elements C_L, R_L and L_L shown in fig. 2.5(b). This is a typical load in power control systems. As shown in fig. 2.5(c) this circuit can form a parallel resonance circuit with R_T, X_T and C_L, at one of the harmonic frequencies generated by the non-linear load PEC. If, on the other hand, the distortion is generated externally, series resonance may result, as shown in fig. 2.5(d), while parallel resonance results with internal generated distortion on the other side. Parallel resonance can be obtained at the frequency f_p, calculated by eq. (2.6). The load inductance is dominating the load at higher frequencies, which can be equivalent to a open circuit, which implies that the load capacitance C_L is predominant at harmonic frequencies.

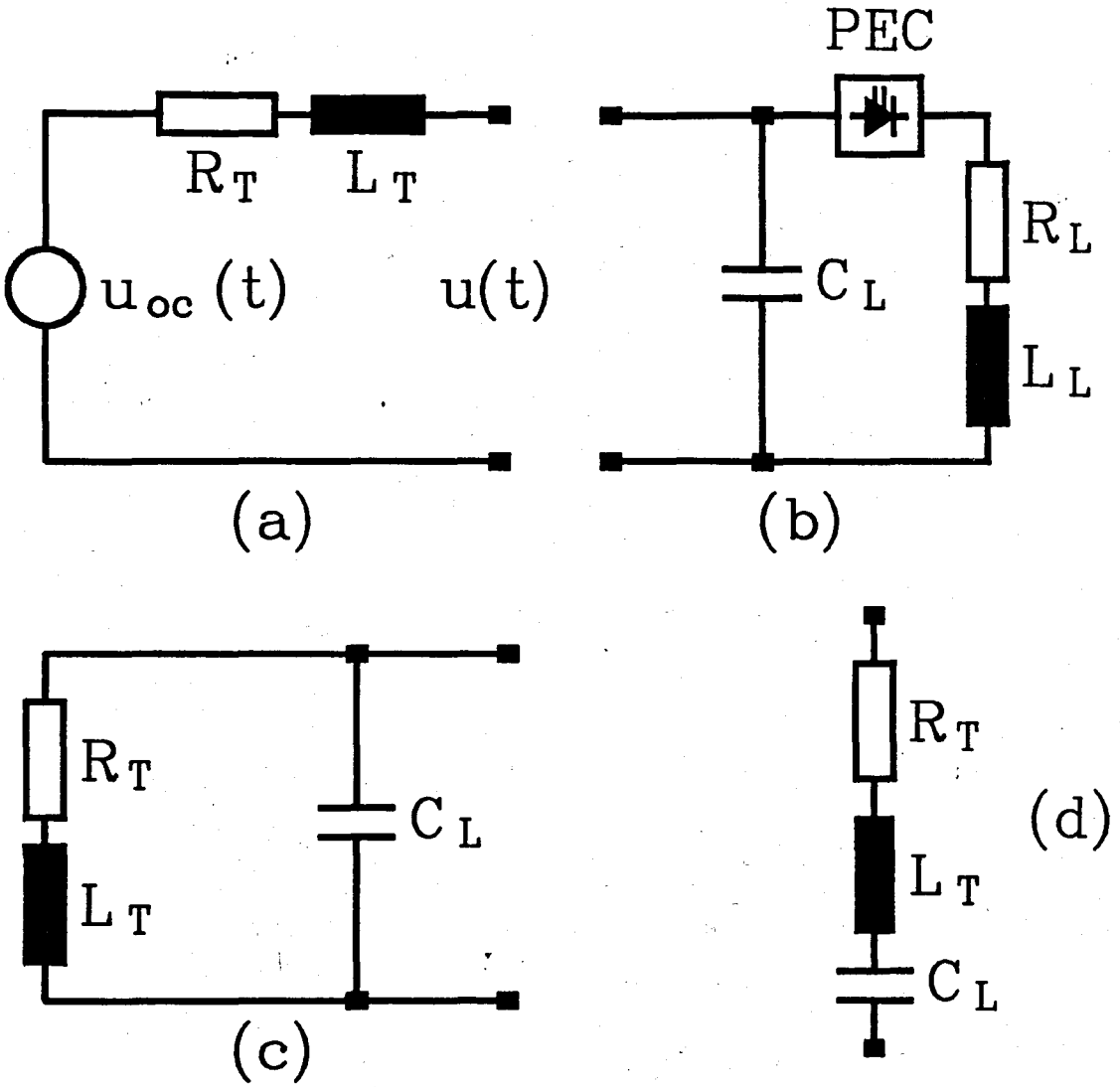

Fig. 2.5: Equivalent Thevenin Circuit with Non-linear Load

$$f_p = \frac{1}{2\pi[L_T C_L]^{1/2}} \tag{2.6}$$

or in terms of the short circuit ratings

$$f_p = f. \left[\frac{S_s}{S_c}\right]^{1/2} \tag{2.7}$$

where f ≡ fundamental power frequency [Hz]
S_s ≡ short circuit capacity [MVA]
S_c ≡ capacitor power rating at f [MVA]

If this frequency corresponds to the frequency of one of the harmonics generated by the power converter PEC, or the frequency of one of the externally generated harmonics, very high resonance voltages, damped only by the associated resistance R_T, will occur on the voltage bus. This will have detrimental effects on the power equipment connected to the feeder bus. Furthermore, this resonance can be even more severe if the power network is weak, i.e. L_T is large, which results in a low-frequency resonance. Resonances have been considered in relation to capacitors and in particular, power factor correction, harmonic power filter capacitors and TCR's [A146]. Resonances may lead to component failure and may interfere with power line signal (ripple control) for purposes of load management [H1,10].

2.8 EFFECTS OF DISTORTION ON ELECTRICAL APPARATUS AND SYSTEMS

Once the sources of distortion in power systems have been defined clearly, they must be interpreted in terms of their effects on systems and electrical equipment operation. The main effects of distortion within a power system has been summarized in the introduction to this chapter.

2.8.1 Effects on Electric Power Network Components

In general distortion implies a higher loading of all the electrical components coupled to the distorted power network. This can be seen as the fundamental effect of power supply distortion. Most of the losses results from the skin-effect [H7], caused by the AC resistance of a conductor to increase linearly with the frequency.

2.8.1.1 Rotating machinery.

Rotating machines are very sensitive to distortion of the voltage waveform, because these are primarily fundamental frequency, sinusoidal voltage-fed electromechanical power converters. Temperature rises caused by an increase in power losses in the the rotor and

torque pulsations on the axle injected into the mechanical load, are of primary concern [A19].

In the stator of these machines the eddy current and hysteresis losses are highly frequency dependent. Since only natural cooling is applicable to the stator windings of a general purpose machine, this effect affects the dimensional sizing of the machine. Furthermore the higher harmonic number frequencies are induced over the air gap to the rotor, increasing the iron losses in the rotor as well.

Although the rotor rotates at or near synchronous speed it can be seen as if at standstill for the transformed harmonic frequencies. This results in heat dissipation in the rotor [A19]. This heating effect is applicable to synchronous and asynchronous machines. The rotor of a synchronous machine subjected to harmonic distortion, is actually performing like an asynchronous machine at high slips (s>1). The familiar torque-speed curve of an induction machine can therefore be used to calculate the slip losses in the rotor.

The familiar equivalent circuit of an induction machine, shown in fig. 2.6, can be redrawn for each harmonic frequency. Positive sequence harmonic currents in the stator of an AC machine produce motoring action (i.e. positive harmonic slips s_n). The negative sequence current harmonics also produce motoring torques but in the negative direction [H1].

Because the slip is almost unity for the harmonic frequencies, the per unit values of the torques produced, by harmonic currents are very small. The Total Harmonic Distortion (THD) associated with the voltage waveform is also small (typical less than 20%), so that the torque-speed curve is flattened at the respective harmonic frequencies. Furthermore the positive and negative sequence harmonic torques tend to cancel each

other in most cases. The effects of harmonics upon the mean torque may therefore be neglected in most cases. Although harmonics have little effect upon the mean torque, they can produce significant torque pulsations, which usually have detrimental effects on the mechanical load. In most practical cases the increase in mean torque due to harmonics is insignificant compared to the possible problems associated with torque pulsations injected into sensitive loads.

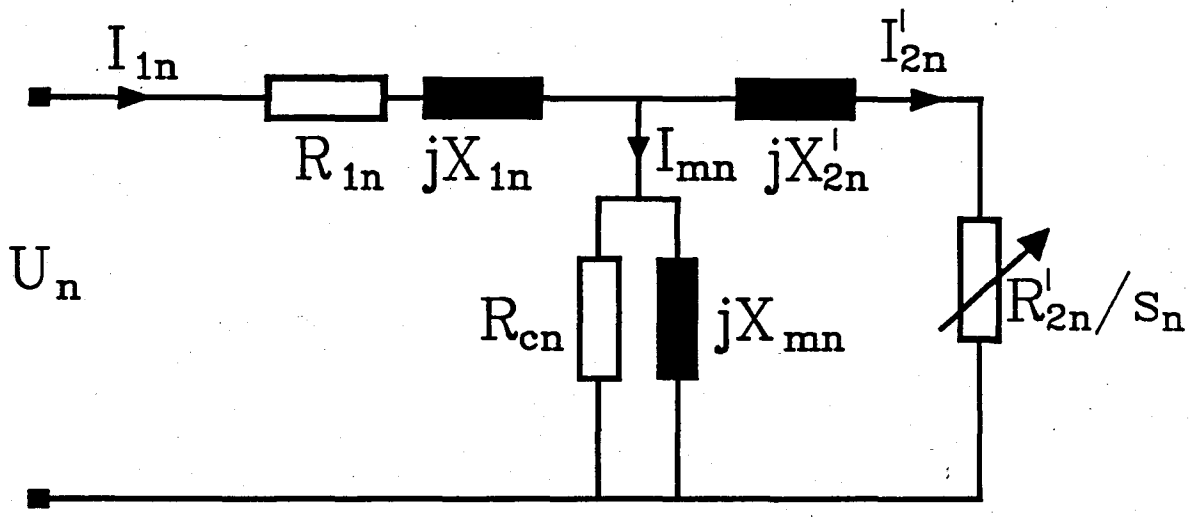

Fig. 2.6: Equivalent Induction Machine Circuit Diagram at Harmonic Frequencies

2.8.1.2 Power transformers.

The effects distorted voltages have on transformers can be summarized as increases in the hysteresis and eddy current losses and higher stresses placed on the insulation, because high voltage spikes associated with distortion can damage the insulation. Furthermore, the current harmonics present in transformers coupled in cascade with power electronic converters increase the copper losses. An important effect of distortion on power transformers, is the circulation of triplen zero sequence currents in the delta windings of the transformer. This can cause the rated currents to be exceeded and contribute to overheating and associated

breakdown. Three phase transformers supplying asymmetrical loads are also more prone to saturation of their magnetic circuit [A39,40].

2.8.1.3 Power capacitors.

Capacitors are seriously affected by voltage distortion, especially when parallel or series resonance occurs. Furthermore the loss factor, tan δ increases with frequency and therefore all harmonics cause extra power losses in the capacitor which result in overheating and and associated shorter life expectancy. This situation is worsened, because capacitors have low impedances to harmonic currents. Therefore they normally sink all the harmonic currents in the network over long transmission or reticulation power lines.

Other effects of distortion on the power plant include additional transmission losses caused by the increased effective values of the current waveforms, and the associated higher loading of the transmission system without an increase in net energy transfer.

2.8.2 Effects of Distortion on Measurement, Control, Signal Processing and Telecommunication Systems.

The effects of distortion on measurement, control, signal processing and telecommunication systems are difficult to analyse and even more difficult to compensate for. Distortion can, however, result in system maloperation and associated high costs. These systems usually have high input impedances, which make them more susceptive to the injection of higher frequency harmonics [A5,70].

2.8.2.1 Remote power control systems.

Power supply authorities normally use ripple control circuits to control street lighting circuits and to do load regulation (such as switching off domestic hot water heaters) during the peak hours of the day. Furthermore, power system protection switchgear is nor-

mally controlled by means of ripple control circuits. As a result of distortion interference, some practical difficulties have been experienced with such ripple control equipment [H1, A5,71]. Some newly developed ripple control systems employ digital filtering techniques, so that these problems are less pronounced.

2.8.2.2 Control of power electronic converters.
Power electronic converters are normally controlled in synchronism with the fundamental power supply frequency. In cases where distortion is of such a magnitude that synchronization circuits are affected, serious converter maloperation can result and in some cases even the destruction of converter equipment.

2.8.2.3 Telecommunication and control equipment
In the case of telecommunication and control equipment, higher order harmonic distortion gives rise to electromagnetic interference. Affected systems include television receivers [A71], computers in a control environment and all the other types of telecommunication apparatus. A simple equivalent circuit diagram that can be used to describe the interference in these systems, is shown in fig. 2.7.

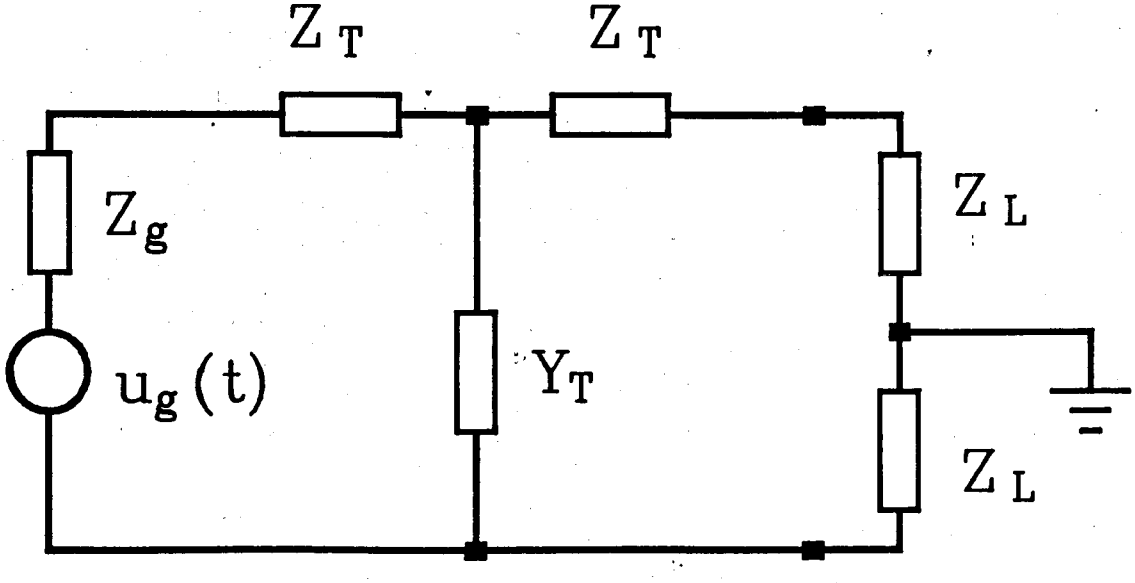

Fig. 2.7: Equivalent Circuit for Communication Systems

The ways in which high-frequency distortion will influences this circuit, depend on the following factors:

(a) Magnitude of generated high-frequency distortion.

(b) Coupling of interfering currents and voltages into the communication system, which in turn depends on the transmission impedance Z_T or the transmission admittance Y_T.

(c) Susceptibility of the communication system to higher order distortion, which in turn depends on the source impedance Z_g and the input impedance Z_L respectively.

The digital and optical technologies employed in telecommunication systems have become so immune to distortion lately, that distortion related problems can be eliminated in these applications. In the majority of control systems there are, however, analogue interfaces and analogue signal processors, which are very susceptive to distortion. Therefore distortion is still a major problem in big control systems installed in the vicinity of distortion generating equipment.

2.8.2.4 Power measurement equipment

Ferraris induction watthour meters [A5,71] and general purpose wattmeters [A62,63] are influenced by a non-sinusoidal voltage. An induction watthour meter is an electromagnetic meter which produces positive and negative torques when measuring energy on a distorted supply [A5,71]. When measuring the energy consumed by a resistive load in the presence of voltage distortion, the watthour meter reading is always too high [A5,63,71]. On the other hand, the reading may sometimes be too low when the load is non-linear and reactive [A63]. In general, however, it appears that a consumer responsible for the generation of network distortion is automatically penalized, because his apparent electricity consumption is higher than his actual electricity consumption. Wattmeters, especially time-division active power meters, are being used to measure

power, even for non-sinusoidal voltage and current waveforms. These meters do not have a high bandwidth, which results in an inaccuracy proportional to the square of the frequency [A62]. Electrodynamical meters, which are used for wattmeters and high quality voltmeters and ampere meters, are calibrated on pure sinusoidal alternating currents and subsequently give errors when used in distorted power supplies.

2.9 FINANCIAL IMPLICATIONS OF DISTORTION IN POWER SYSTEMS

The effects of distortion on some electrical equipment has been described in the previous section. The cost of distortion in power systems is difficult to calculate, because distortion adversely affects the life expectancy of electrical equipment. Furthermore the effects of resonance on the power supply are responsible for a lot of power equipment failures, and the higher loading of power supplies increase the capital cost of a power system.

Costs and containment of distortion in electric power systems are often emphasized but are seldom quantified because of the difficulty to evaluate the cost aspects in an inter linked power system [A97]. Cost can be calculated in the following categories:

(a) reduced power apparatus efficiencies;
(b) increased capital investments for fictitious power;
(c) reduced power control performance;
(d) increased maintenance costs;
(e) degrading of apparatus life expectancies;
(f) higher energy bills.

In many cases the above-mentioned distortion related cost aspects can be eliminated by a level headed approach towards distortion in power systems. Resonance effects can be eliminated, time-shifted distortion, the biggest single contributor to the total distortion, can be compensated for by means of passive reactive elements. Designs of distortion generating equipment can be im-

proved, and consumers can be more distortion conscious when purchasing power control equipment.

2.10 SUMMARY

This chapter addressed most of the distortion related problems, beginning with a classification of distortion found in electric power systems and a categorization of different known sources of distortion. The generation of stochastically changing distortion seems to be a major problem because of the lack of techniques to analyse, characterize and compensate for this type of distortion. All the other forms of distortion do not seem to be too much of a problem; standard procedures and compensation methods can be used to solve the problems related to these forms of distortion. It is however believed that the stochastically changing distortion can be analysed by means of time domain analysis techniques and compensated for by means of a power filter with a high dynamic system response.

It is clear that there is not one single magic solution to the problems associated with distortion in power systems. It should, however, be pointed out that the combination of several philosophies can give adequate results in designing systems where distortion can be tolerated and reducing distortion to such an extent, that power generation, distribution and utilization can be cost effective.

CHAPTER 3

PROPOSED GENERALIZED DEFINITION OF POWER IN ELECTRIC POWER SYSTEMS

3.1 INTRODUCTION

To be able to characterize electric power and compensate for the unwanted components of electric power under non-sinusoidal and in general aperiodic waveforms of voltage and current, it is important to have a generalized definition of electric power which is independent of the periodicity and the waveshape of the voltage and the current. Power measurements in systems with sinusoidal, periodic or constant voltages and/or currents, are then special cases of the more generalized definition of electric power.

The standard definitions of power are inadequate for the design of distortion compensation systems having to cope with aperiodic voltages and currents (chapter 1,2). These definitions are furthermore not sufficiently load-related, which gives rise to problems with the physical interpretation of the analysis of distortion in electric power systems.

A new, load-related, generalized, time domain definition of power, capable of describing all the components of electric power is proposed in this chapter. This definition gives converging results even if the waveforms of voltage and current are aperiodic, because it is only defined over a predetermined time interval. Power is defined in terms of specific equivalent network quantities or parameters and each network parameter is associated with an unique power component. This definition possesses attributes which relate to the power phenomena of the circuit; moreover, the use of this definition provides information for the design of fictitious power compensation systems.

Coupled with this power definition, a new equivalent network parameter, the disceptance K measured in Siemens, is defined. Like the susceptance B and the conductance G, the disceptance K is a component of the total admittance Y of the load. The disceptance K contains information about the uncorrelated properties of the power system and is used to characterize the non-linear portion of the load connected to the power network. In general the disceptance describes the uncorrelation between the current and voltage waveforms.

The proposed time domain definition of electric power divides the loading power S into two orthogonal components, viz. active power P and fictitious power F. This corresponds to the Fryze definition [A69]. In analysing, characterizing and controlling fictitious power, the subdivision of fictitious power into the orthogonal components reactive power Q and deactive power D, so that P, Q and D are mutually orthogonal, is advantageous and is therefore proposed in the compensation of fictitious power in chapter 5. The power components P, Q and D are associated with the equivalent network parameters, G, B and K respectively and are calculated by means of time domain correlation techniques. This subdivision of fictitious power into other power components pertains to the way in which they are generated, which emphasizes the division characteristics.

Using a digital correlation algorithm (chapter 4), simulations have been done on a personal computer to evaluate this definition for several waveforms of voltage and current. Results obtained from these simulations are shown towards the end of this chapter. The voltage and current waveforms chosen for the simulation can be found in the majority of the contaminated electric power systems and can also be analysed with other known power definitions to evaluate the accuracy of the proposed definition. The purpose of these simulations is to obtain the accuracy under static conditions with periodic waveforms. If the definition seems to be accurate under these above-mentioned conditions, it can be generalized further.

3.2 ENERGY TRANSFER IN ELECTRIC POWER SYSTEMS

Resulting from the principle of conservation of energy, any increase in the energy of a volume v must be produced by a net inflow of energy and likewise a decrease in energy must be equal to the net outflow of energy. This flow of energy takes place when electric energy is transferred from a source to a load. Power in a power system is associated with the rate of this energy flow. The original work of Poynting [A114] describes the transfer of energy through a volume v with surface area s by means of the well-known Poynting vector, defined as the cross-product between the electric field vector **E** and the magnetic field vector **H**. The Poynting vector is equivalent to the power density in the volume v enclosed by the surface s [H7,11].

$$\oint_s (\mathbf{E} \times \mathbf{H}) \cdot d\mathbf{s} = \oint_s \mathbf{P} \cdot d\mathbf{s} \qquad (3.1)$$

where **P** is the instantaneous Poynting vector.

$$\Rightarrow \mathbf{P} = \mathbf{E} \times \mathbf{H} \qquad [W.m^{-2}] \qquad (3.2)$$

$$p(t) = \oint_s \mathbf{P} \cdot d\mathbf{s} \qquad [W] \qquad (3.3)$$

where p(t) is the instantaneous power.

This instantaneous Poynting vector is normally extended to the time-average Poynting vector P_{av}, by expressing the electric and magnetic fields, varying sinusoidally with time, in phasor form [H7,11]. This extension is, however, not valid in systems where the fields are non-sinusoidal and another way to calculate average power should be used. The instantaneous Poynting vector is, however, a function of the geometrical shape of the volume v in which it is calculated, and is therefore a function of the specific circuit under consideration. The currents and voltages can, however, be measured in any circuit, without reference to the respective fields in the circuit. From these measurements the instantaneous power p(t) can be calculated as shown in eq. (3.4):

$$p(t) = u(t).i(t) \quad [VA] \tag{3.4}$$

Average active power is defined over the time span between $t = -\infty$ and $t = +\infty$, as shown in (3.5) [H15], and is associated with the rate of net transfer of energy from the source to the load. This average active power is the only component of power which can be calculated from the instantaneous power, because no other power component can be related to net energy transfer.

$$P = \lim_{T \to \infty} \frac{1}{2T} \int_{-T}^{+T} p(t).dt \quad [W] \tag{3.5}$$

This expression where active power is averaged over a time interval tending to infinity is not useful for practical power measurements in a power system; a measurement interval of the order of the dynamic system response should be chosen. To be able to obtain an effective measurement interval under dynamic conditions, the instantaneous power should be categorized as described in paragraph 1.7.

This categorization can be described as follows: If the energy delivered to the load is associated with a continuous instantaneous power waveform p(t), it is an example of the finite average power case. Note that power associated with periodical waveforms is a special case of finite average power. On the other hand, if energy is transferred to a load by means of a relatively short power pulse, a discontinuous power waveform p(t) results. This is an example of zero average power and thus the finite energy case.

This classification of the dynamic behavior of the instantaneous power can be helpful when determining the appropriate measurement interval dT. When choosing the measurement interval dT, the time constant of the dynamic system response of the power network under consideration should be kept in mind. In general the measurement interval should also be changed to correspond to the changes in the dynamic system response. In finite energy systems the

measurement interval should be very long compared to the power pulse duration, but in infinite energy systems a much shorter measurement interval dT is appropriate. It should be noted that the average power components are not defined over an infinite time interval, resulting in the fact that the different power components are dependable on the measurement time interval over which they are defined. This implies that the power components are only averages over the specific time interval, in general dT.

3.3 DEFINITION OF LOADING POWER QUANTITIES

The electric power in any electric network has a generation function and a loading function, one of these being the voltage and the other the current. In this analysis it will be assumed that the voltage is the generating function and the current the loading function. Note however that whether the source voltage is the generating function and the load current drawn from the power supply the loading function, or the current is the generating function and the voltage the loading function, the loading function is still dependent on the load.

The power components defined underneath, are formulated in terms of the energy transfer in the power network which implies that the power components are formulated in terms of average values. Instantaneous currents are however also derived from these average power values which should be interpreted as the representation of the power flow in the network. These currents can also be used in the compensation of fictitious power and can only be derived after the measurement interval has elapsed and the average power components derived. The instantaneous currents should not be seen as the definition of the power components. In some cases it is even possible to derive other waveshapes of instantaneous currents to describe the power flow for the same average power components, which implies that there may be a large number of representations which can be the result from the same average power components.

Loading power S is no more than a new name for what has been known as the apparent power in a power network. This new name is however proposed firstly to minimize the possibility of confusing it with fictitious power and secondly it is a more accurate term, S being a measure of the network loading. S is still defined as the product of the effective values of voltage and current over a measurement interval dT, as shown in eq. (3.6). This implies that loading power is a constant average value over the measurement interval dT.

$$S = U.I \quad [VA] \quad |_{dT} \tag{3.6}$$

For the calculation of loading power in the case of periodic generating and loading functions, the effective values of voltage and current are normally calculated from eq. (3.7).

$$u(t+T) = u(t); \quad i(t+T) = i(t)$$

$$U^2 = \frac{1}{T}\int_0^T u^2(t).dt \quad [V^2]; \quad I^2 = \frac{1}{T}\int_0^T i^2(t).dt \quad [A^2] \tag{3.7}$$

where T is the period of the functions.

The calculation of loading power in power systems with aperiodic voltage and current waveforms disqualifies eq. (3.7) altogether.

3.3.1 Definition of Loading Power in the case of Aperiodic Voltage and Current Waveforms

The effective values of aperiodic voltages and currents over a time interval dT, can be obtained from a time domain autocorrelation [H15] (Appendix A4). The square of the effective value of a periodic voltage, calculated over the fundamental period T of the waveform, is shown in eq. (3.7), while the autocorrelation of a voltage signal over an arbitrarily chosen time interval dT, is shown in eq. (3.8). If the autocorrelation shift variable τ is equated to zero and dT is equal to T, eqs. (3.7) and (3.8) are identical (appendix A4). The same result can be obtained for currents.

$$R_{uu}(\tau) = \frac{1}{dT}\int_{t-dT}^{t} u(t).u(t-\tau).dt \quad [V^2] \qquad (3.8)$$

This implies that using a time domain autocorrelation, the effective values of any periodic or aperiodic waveform can be calculated over any time window dT, as shown in eq. (3.9). To compare the results for typical periodic waveforms it is a requirement to use the same measurement interval, thus dT = n.T.

$$\begin{aligned} U &= [R_{uu}(0)]^{1/2} \quad [V]; \\ I &= [R_{ii}(0)]^{1/2} \quad [A] \end{aligned} \Big|_{dT} \qquad (3.9)$$

Using eq. (3.9), the average loading power specific to a particular time interval dT is given as:

$$S = U.I = [(R_{uu}(0)).(R_{ui}(0))]^{1/2} \quad [VA] \Big|_{dT} \qquad (3.10)$$

3.3.2 Equivalent Admittance in Power Networks

The loading power S is a measure of the loading of the power network. This loading is associated with the loading of the generating function, in this case the source voltage, by the loading function, in this case the load current. This load current results from an equivalent instantaneous load admittance y(t). The average value of the load admittance Y, is related to the loading power formulated over the time interval dT, as formulated in (3.11). The instantaneous values are shown schematically in fig. 3.1.

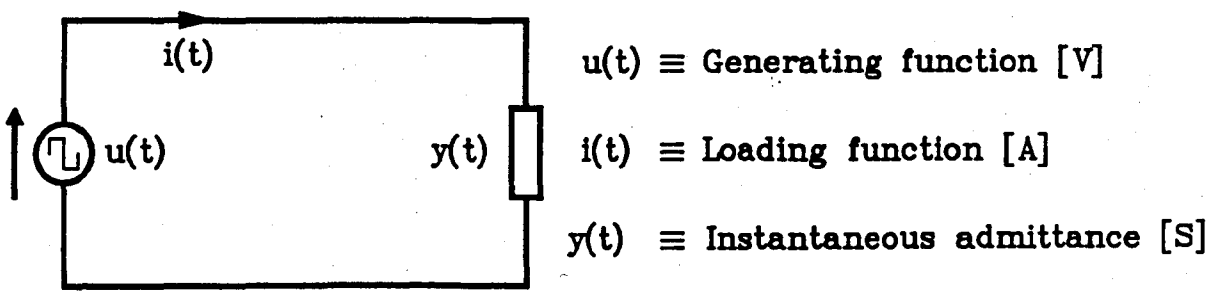

Fig. 3.1: Schematic Representation of Network Loading

$$I = Y.U \quad [A]; \qquad S = U.I = U^2.Y \quad [VA] \quad |_{dT} \tag{3.11}$$

3.4 DEFINITION OF ACTIVE POWER QUANTITIES

Average **active power** P is defined over the time span between $t = -\infty$ and $t = +\infty$, as shown in eq. (3.5). As this cannot be used in practical power measurement techniques, the formulation as shown in eq. (3.12), was adopted for periodic voltages and currents. In this case P is defined over one fundamental period T.

$$P = \frac{1}{T} \int_0^T u(t).i(t).dt \quad [W] \tag{3.12}$$

3.4.1 Definition of Active Power in the case of Aperiodic Voltage and Current Waveforms

It should be pointed out that active power is a measure of the average rate at which net energy is transferred from a source to a load and must therefore be defined over a time interval dT for the definition to be physically interpretable. The active power over a time interval dT, can be calculated from the result of a cross-correlation between the voltage and the current at zero time shift. The active power, delivered by periodic voltage and current waveforms, over the fundamental period T, is calculated from eq. (3.12), while the cross-correlation between voltage and current over an arbitrarily chosen time interval dT, is shown in eq. (3.13). If the cross-correlation shift variable τ is equated to zero and dT is equal to T, eqs. (3.12) and (3.13) are identical (Appendix A4).

$$R_{ui}(\tau) = \frac{1}{dT} \int_{t-dT}^{t} u(t).i(t-\tau).dt \quad [VA] \tag{3.13}$$

This implies that using a time domain cross-correlation, the average active power can be calculated for any waveform over any time window dT, as shown in eq. (3.14). Active power is

then associated with the average rate at which net energy is transferred from a source to a load over the measurement interval dT. The active power is thus the average rate of net energy transfer from source to load over the interval dT.

$$P = R_{ui}(0) \quad [W] \quad |_{dT} \tag{3.14}$$

3.4.2 Equivalent Conductance in Power Networks

The physical interpretation of active power P implies that the load should consist of an equivalent conductance G. The conductance G is a linear equivalent network parameter measured in Siemens S and as shown in eq. (3.15), it is formulated over the measurement interval dT in terms of the active power P and the effective voltage U. The instantaneous value and the average value of the conductance over the time interval dT is equivalent.

$$G = P/U^2 \quad [S] \quad |_{dT} \tag{3.15}$$

3.4.3 Definition of Active Current

The effective value of the **active current** I_a is defined in terms of the transfer of the active power P from the source to the equivalent conductance G. The instantaneous representation of the active current i_a, has the same waveform as the voltage and its amplitude depends on the equivalent conductance G; therefore it is defined generally as shown in eq. (3.16) and represented schematically as shown in fig. 3.2.

$$i_a(t) = G.u(t) = g(t).u(t) \quad [A] \tag{3.16}$$

The effective value of the active current is also formulated over the measurement interval dT, as shown in (3.17).

$$I_a = G.U \quad [A] \quad |_{dT} \tag{3.17}$$

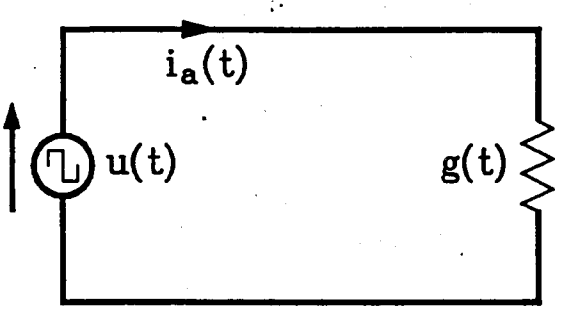

u(t) ≡ Source voltage [A]

$i_a(t)$ ≡ Active current [A]

g(t) ≡ Equivalent conductance [S]

Fig. 3.2: Representation of Active Power Quantities

3.5 DEFINITION OF FICTITIOUS POWER QUANTITIES

When analysing power components, orthogonality between the different power components is normally assumed by the majority of the authors [A1,12-14,20-27,31-35,60-61,69,93,109,110,113,115-116,131-122,127]. In this study all the components are also defined orthogonal. **Fictitious power** F is a measure of the inability of the load to absorb energy delivered by the source. Fictitious power is therefore a result of the non-conductance portion of the load and can be distributed through the network by means of the generating function. It is clear from the classical definition of reactive power for sinusoidal waveforms that fictitious power includes reactive power, but with non-sinusoidal and aperiodic waveforms, fictitious power includes all components of power which cause the loading power to be higher than the active power.

Applying the principle of orthogonality [H15,24], **fictitious power** F is defined as the vector difference between loading and active power which is an average value over the interval dT, as shown in eq. (3.18).

$$F = \sqrt{[S^2 - P^2]} \quad [VA] \quad |_{dT} \tag{3.18}$$

The effective value of the **fictitious current** I_f transports the fictitious power F to the load. The instantaneous representation can be shown as the result of the difference between load current i(t) and active current $i_a(t)$, as shown in eq. (3.19).

$$i_f(t) = i(t) - i_a(t) \qquad [A] \tag{3.19}$$

The effective value of the fictitious current over the measurement interval dT is calculated from eq. (3.20).

$$I_f = \sqrt{[I^2 - I_a^2]} \quad [A] \quad |_{dT} \tag{3.20}$$

For the analysis, characterization, compensation and control of fictitious power, it is advantageous to subdivide fictitious power F into two orthogonal components **reactive power** Q and **deactive power** D. This subdivision is based on the fact that these two components are generated differently and is realized in terms of the cross-correlation between the voltage and current signals (Appendix A4).

3.6 DIVISION OF FICTITIOUS POWER INTO REACTIVE POWER (Q)

The proposed reactive power differs from previously defined time domain reactive power quantities [A25,61,65,109], in the sense that it is defined as a component of fictitious power; moreover, it is defined as that component of fictitious power that correlates between the generating and loading functions. The proposed **reactive power** Q is defined in terms of the correlated time shift between the generating and loading functions and is calculated from the time shift in the cross-correlation function, $R_{ui}(\tau)$. Reactive power thus results from the time shift between the generating and loading functions. This correlated fictitious power can be associated with the oscillating energy flow between the source and an equivalent load susceptance B. This susceptance is defined in terms of the reactive power and the effective voltage. Reactive power is thus modeled in terms of an equivalent susceptance which can absorb energy and transport it back to the source over a measurement interval dT.

3.6.1 Calculation of Reactive Power from the Cross-correlation

Within the time interval dT, the maximum value of the cross-correlation between voltage and current $\hat{R}_{ui}(\tau)$, occurs at the point of maximum similarity between the voltage and current waveforms. This point on the cross-correlation function is equivalent to all the power which is the result of the correlation between the loading and the generating functions. This principle can be used to derive the value of the extra loading power required for a time shift between voltage and current, if one takes into account that the value of the cross-correlation between voltage and current at $\tau = 0$, $R_{ui}(0)$ represents the active power (eq. (3.14)). Equation (3.21) shows how the reactive power Q, associated with the time shift between the correlated voltage and current waveforms, can be derived from these quantities.

$$Q = [\hat{R}^2_{ui}(\tau) - R^2_{ui}(0)]^{1/2} \quad [VA] \quad |_{dT} \tag{3.21}$$

This equation is of paramount importance in the subdivision of fictitious power into reactive and deactive power. The peak value of the cross-correlation over the interval dT, shows the point where there is maximum correlation between the loading and generating functions. Power which results from the correlation between the loading and generating function is characterized as the active and reactive power components. Thus by eliminating the active power from the correlated power, only reactive power results. Deactive power, described in the next paragraph, is not the result of correlation in the loading and generating functions and is not part of this correlated power.

3.6.2 Equivalent Network Susceptance Associated with Reactive Power

Reactive power Q is associated with an equivalent load susceptance B. Reactive power, a measure of the correlated time

shift between the voltage and the current, can also be described as a measure of the oscillating power flow between the source and this equivalent load susceptance B. The susceptance, measured in Siemens S, is formulated in terms of the reactive power Q and the effective voltage U, as shown in eq. (3.22). The average susceptance has a constant value over the measurement interval dT.

$$B = Q/U^2 \quad [S] \quad |_{dT} \tag{3.22}$$

3.6.3 Definition of Reactive Current

Reactive current I_r, is formulated as the current which is responsible for the flow of reactive power. The formulation of the instantaneous signal of the reactive current requires an orthogonal time shift over the total measurement bandwidth. From an analysis of the cross-correlation between the generating and loading functions, it is clear that in general, some portion of the loading function does not correlate with the generating function. Furthermore the generating and loading functions may correlate even if the loading function has no active portion. Using these facts and the principle that the power components are mutually orthogonal, the fictitious current can be divided into a reactive and deactive current. The waveform of the reactive current is derived from the waveforms of the other current components. Equation (3.23) shows that the the deactive and the active current, or the instantaneous susceptance must be known before the reactive current can be derived. This is no problem as the active current has already been derived and the current, representing the uncorrelation between the loading and generating functions, will be derived in the following paragraph.

$$i_r(t) = b(t).u(t) \quad = i(t) - i_a(t) - i_d(t) \tag{3.23}$$

The effective value of the reactive current over the time interval dT is calculated from eq. (3.24), using the average susceptance and the effective voltage.

$$I_r = B.U \qquad [A] \quad |_{dT} \tag{3.24}$$

In cases where the generating function is periodic, reactive power can be subdivided even further into fundamental reactive power and residual reactive power. This secondary subdivision has the distinct advantage that fundamental reactive power can be compensated for by means of passive inductive or capacitive components, while tuned harmonic filters or dynamic power filters should be used for the compensation of residual reactive power (chapter 5). It should be pointed out that these components are still the result of the time shifted correlation between the generating and loading functions and that the subdivision of reactive power into fundamental and residual components can only be obtained if the generating and the loading functions have periodic waveforms.

3.6.4 Fundamental Reactive Power (Q_f)

Reactive power in the fundamental components of voltage and current is calculated by using the Fourier series, as shown in eq. (3.25).

$$Q_f = U_1.I_1 \sin \phi_1 \qquad [VA] \quad |_T \tag{3.25}$$

where U_1 and I_1 are the effective values of the voltage and current fundamentals and ϕ_1 is the phase angle between them. This component can also be called inductive or capacitive reactive power, depending on the means of passive compensation [A93].

3.6.5 Residual Reactive Power (Q_r)

After fundamental reactive power has been eliminated, the correlated fictitious, or reactive power, still present in

the harmonics and modulation of the voltage and current waveforms, can collectively be called residual reactive power. The residual reactive power, sustaining orthogonality is formulated in eq. (3.26).

$$Q_r = \sqrt{[Q^2 - Q_f^2]} \quad [VA] \quad |_T \tag{3.26}$$

The above-mentioned secondary subdivision is only applicable to periodic voltage and current waveforms and is indeterminable when the voltage and/or current are aperiodic.

3.7 SUBDIVISION OF FICTITIOUS POWER INTO DEACTIVE POWER (D)

The second component of fictitious power, viz. **deactive power** D, is associated with the non-similarity or uncorrelation between the generating and loading functions and is also described as uncorrelated fictitious power. Deactive power is a result of the non-linear portion of the load and uncorrelated properties of the power network, which is characterized and analysed in terms of the newly defined equivalent network parameter, the disceptance K. Deactive power can be calculated from the orthogonality between the different components of power. The newly defined network parameter; disceptance K describes the uncorrelation between the generating and loading functions.

3.7.1 Calculation of Deactive Power from the Other Power Components

By making use of the assumed principle of orthogonality, the deactive power, for the measurement time span dT, can be calculated as shown in eq. (3.27). The deactive power cannot be derived directly from the cross-correlation function, because it does not result from the correlation between loading and generating functions. Deactive power is however increasing the value of the loading power S, thus (3.27).

$$D = \sqrt{[S^2 - P^2 - Q^2]}; \quad |_{dT} \tag{3.27}$$

3.7.2 Equivalent Network Disceptance Associated with the Deactive Power.

The equivalent disceptance K describes the uncorrelation between generating and loading functions and is formulated in terms of the deactive power D and the effective voltage U, as shown in eq. (3.28). The average disceptance is measured in Siemens S and is constant over the measurement interval dT which implies that is a function of dT.

$$K = D/U^2 \quad [S] \quad |_{dT} \tag{3.28}$$

3.7.3 Definition of Deactive Current

Deactive current I_d is defined in terms of the transfer of the deactive power D from the source to the equivalent disceptance K. The instantaneous representation can be derived directly from the cross-correlation between the generating and loading functions. As described in paragraph 3.6.3 deactive current is that component of the load current which does not correlate with the voltage. As shown in eq. (3.29), the instantaneous deactive current is derived from the difference between the total load current i(t) and that part of it that correlates with the voltage, which is in its turn calculated from the conductance G, susceptance B and a time-shifted version of the voltage.

$$i_d(t) = k(t).u(t) \quad = i(t) - \sqrt{[G^2 + B^2]}.u(t-\hat{\tau}) \tag{3.29}$$

where $u(t-\hat{\tau})$ is the voltage delayed by $\hat{\tau}$ units of time.

The time delay $\hat{\tau}$ is no more than that value of the correlation shift variable τ for which the cross-correlation between the voltage and current reaches its maximum value $\hat{R}_{ui}(\tau)$ and can therefore be obtained directly from the cross-correlation function $R_{ui}(\tau)$. The maximum value of the cross-correlation function is the point where the correla-

tion between the loading and generating functions are the highest, thus including all the power associated with the correlation between the generating and loading functions, reactive and active power.

The effective value of the deactive current over the time interval dT is shown in eq. (3.30).

$$I_d = K.U; \qquad I_d = \sqrt{[I^2 - G^2.U^2 - B^2.U^2]}$$

$$I_d = \sqrt{[I^2 - I_a^2 - I_r^2]} \quad [A] \quad |_{dT} \tag{3.30}$$

For a schematic representation of the different current components the average network parameters and effective values of the current components or the instantaneous values of both currents and parameters can be shown. In the representation of fig. 3.3, the instantaneous values are shown which implies that the susceptance and disceptance are also shown as instantaneous values. The fictitious current i_f is subdivided into reactive current i_r and deactive current i_d, which flow through the equivalent instantaneous susceptance b(t) and disceptance k(t) respectively.

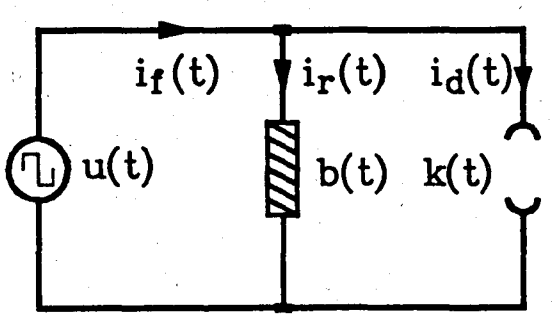

$u(t) \equiv$ Source voltage [V]
$i_f(t) \equiv$ Fictitious current [A]
$i_r(t) \equiv$ Reactive current [A]
$i_d(t) \equiv$ Deactive current [A]
$b(t) \equiv$ Equivalent susceptance [S]
$k(t) \equiv$ Equivalent disceptance [S]

Fig. 3.3: Representation of the Subdivision of Fictitious Current with Associated Equivalent Network Parameters

This generalized definition of electric power has been formulated in terms of the cross-correlation between the voltage and current waveforms. The equivalent load parameters have been defined from the different components of power and the effective voltage,

while the different current components have been obtained from these equivalent load parameters, the instantaneous voltage and the voltage-current cross-correlation. It should however be pointed out that the instantaneous values of the different orthogonal current components can be obtained only after the measurement interval has elapsed, the cross- and autocorrelations (power components) have been determined and the equivalent network parameters have been calculated.

In applications where real-time power measurements and fictitious power compensation are of the utmost importance, adaptive signal processing techniques [H6,23] should be employed to derive the instantaneous values or waveforms of the different orthogonal current components (chapter 5). The above-mentioned fundamental limitation of power calculation only after the measurement interval has elapsed, arises from the fact that the definition of power is based on averages, this being the only way to calculate load-related power components.

3.8 ANALYSIS OF DISTORTION USING EQUIVALENT NETWORK PARAMETERS

As explained in the previous paragraph each component of electric power is associated with a distinct equivalent network parameter. The mutual relationships between the equivalent parameters are represented in fig. 3.4. Instantaneous values are shown in fig. 3.4, but it should be noted that the power components are computed from averaging techniques.

It has also been explained earlier that the generating function is assumed to be the voltage u(t) and the loading function the current i(t). It is clear that all the average load parameters, viz. the conductance G, susceptance B and disceptance K, are passive components. This implies that the penetration model of Tschappu [A138] is no longer necessary for the analysis of distortion in power systems; the equivalent network parameters G,B and K characterize the network distortion unambiguously. The penetration of distortion in a power system is a result of the generating function u(t) and the equivalent load parameters only.

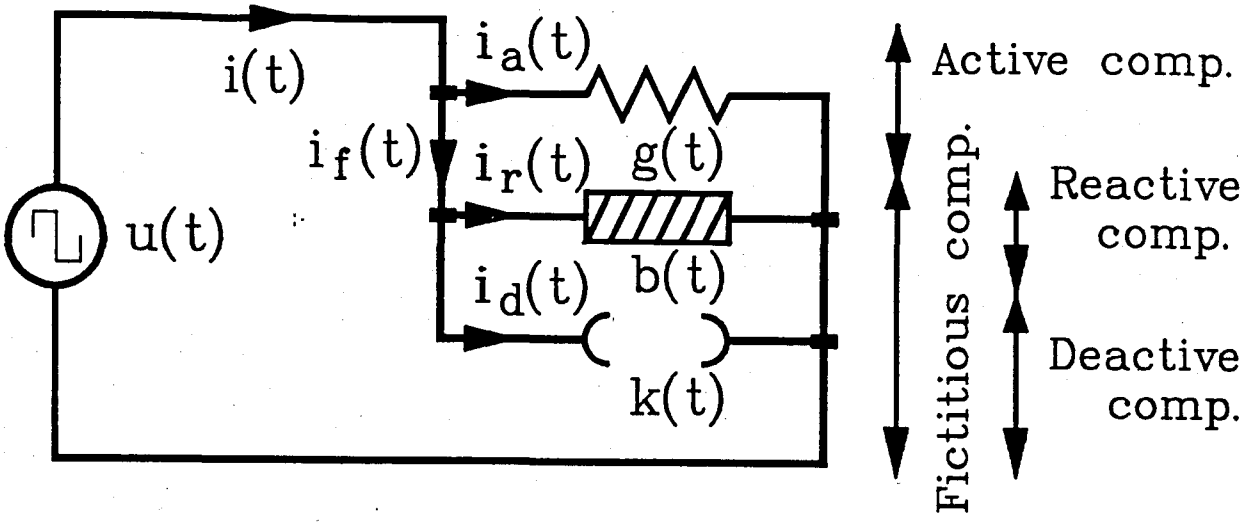

$$I = Y.U \qquad i_a(t) = G.u(t) \qquad I_a = G.U$$

$$i_d(t) = i(t) - \sqrt{G^2+B^2}.u(t-\hat{\tau}) \qquad I_r = B.U$$

$$i_r(t) = i(t) - i_a(t) - i_d(t) \qquad I_d = K.U$$

Fig. 3.4: Schematic Diagram of Equivalent Network Parameters

The equivalent internal admittance of the power network results in distortion of the generating function in the presence of a non-linear loading function. In this way distortion is distributed to other consumers and systems on the common power feeder bus. The equivalent network parameters also describe the weakening of the distortion as you get further and further away from the point where it is generated.

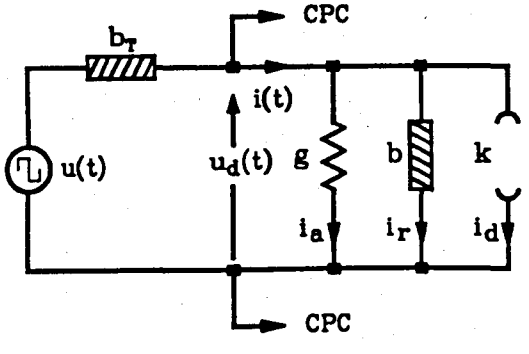

CPC	≡	Common Point of Coupling
u(t)	≡	Source voltage [V]
$u_d(t)$	≡	Distorted voltage at CPC [V]
i(t)	≡	Loading function [A]
$i_a(t)$	≡	Active current [A]
$i_r(t)$	≡	Reactive current [A]
$i_d(t)$	≡	Deactive current [A]
b_T	≡	Network susceptance [S]
g, b, k	≡	Equivalent load parameters [S]

Fig. 3.5: Penetration of Distortion by Means of the Generating Function

Figure 3.5 shows the equivalent schematic diagram of a power system in which the supply has an equivalent instantaneous supply susceptance b_T. The non-linear loading function i(t) and equivalent supply susceptance b_T are responsible for a distorted generating function $u_d(t)$ by means of which the distortion penetrates to all the other consumers on the Common Point of Coupling CPC. The analysis and characterization of distortion in power systems are claimed to be more effective with the use of the equivalent network parameters shown in fig. 3.4.

3.9 ORTHOGONALITY OF GENERALIZED POWER QUANTITIES

The components active power, reactive power and deactive power are defined to be mutually orthogonal. In appendix A1 an orthogonal representation of the power components is derived and analyzed mathematically. A summary of the different orthogonal power components is shown underneath. All the derived components are derived by means correlation averaging techniques. The instantaneous values are shown for the purpose of physical interpretation.

$$U = \sqrt{[R_{uu}(0)]} \quad [V]; \quad I = \sqrt{[R_{ii}(0)]} \quad [A] \quad |_{dT} \tag{3.31}$$

$$S = U.I = U^2.Y \quad [VA] \quad |_{dT} \tag{3.32}$$

$$P = R_{ui}(0) = U.I_a = U^2.G \quad [W] \quad |_{dT} \tag{3.33}$$

$$F = \sqrt{[S^2 - P^2]} = U.I_f = U^2.\sqrt{[Y^2 - G^2]} \quad [VA] \quad |_{dT} \tag{3.34}$$

$$Q = \sqrt{[\hat{R}_{ui}^2(\tau) - R_{ui}^2(0)]} = U.I_r = U^2.B \quad [VA] \quad |_{dT} \tag{3.35}$$

$$D = \sqrt{[S^2 - P^2 - Q^2]} = U.I_d = U^2.K \quad [VA] \quad |_{dT} \tag{3.36}$$

$$S^2 = P^2 + F^2 = P^2 + Q^2 + D^2$$

$$U^2.I^2 = U^2.I_a^2 + U^2.I_f^2 = U^2.I_a^2 + U^2.I_r^2 + U^2.I_d^2 \tag{3.37}$$

$$\overline{i_a.i_f} = 0; \quad \overline{i_a.i_r} = 0; \quad \overline{i_a.i_d} = 0; \quad \overline{i_r.i_d} = 0 \tag{3.38}$$

$$Y^2 = G^2 + B^2 + K^2 \tag{3.39}$$

$$i(t) = i_a(t) + i_f(t) = i_a(t) + i_r(t) + i_d(t)$$

$$i(t) = g(t).u(t) + b(t).u(t) + k(t).u(t) \tag{3.40}$$

In fig. 3.6 these power components are represented schematically in a three dimensional real-imaginary function space with unit

vectors **k** and **j**. The imaginary components of the function space are represented by the two unit vectors **k** and **j** and describe the two fictitious power components reactive and deactive power respectively, while the real part is representing active power. This representation is analyzed in Appendix A1 further by means of quaternions.

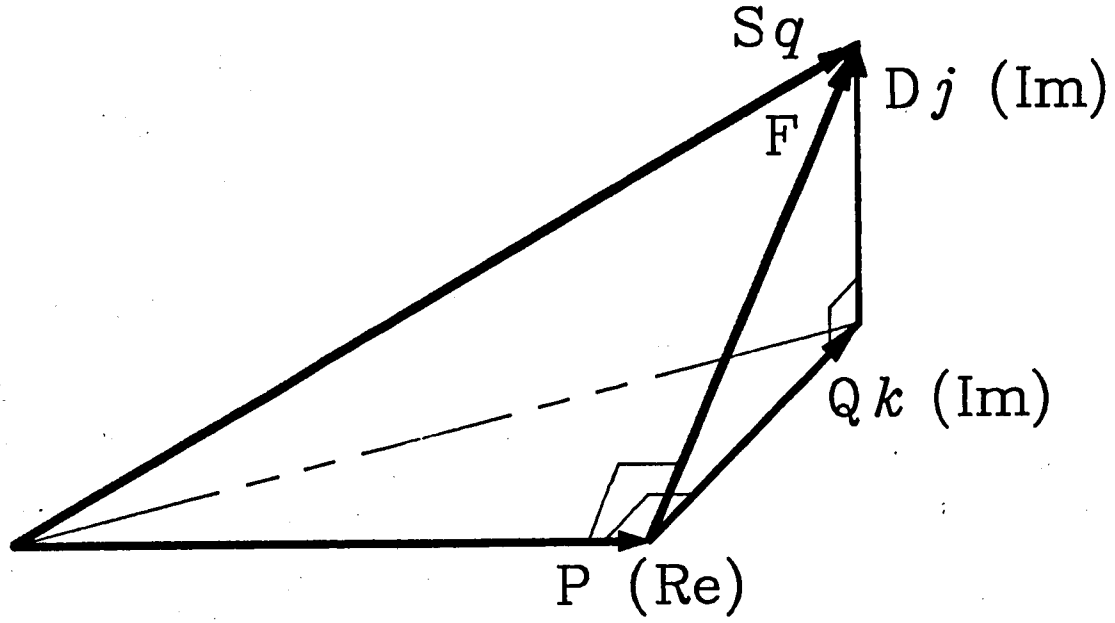

Fig. 3.6: Schematic Representation of Orthogonal Power Components

3.10 DEFINITION OF POWER UTILIZATION FACTORS

For the characterization of electric power and to be able to compensate for the unwanted power components in a power network, it is important to have a measure of the utilization of the power network. The utilization is defined in terms of the three factors shown below:

$$\Gamma = P/S \equiv \text{Power Factor}$$
$$\Gamma_r = Q/S \equiv \text{Displacement Factor}$$
$$\Gamma_d = D/S \equiv \text{Uncorrelation Factor}$$
$$\Gamma^2 + \Gamma_r^2 + \Gamma_d^2 = 1 \qquad (3.41)$$

The power factor is a measure of the utilization of the network measured in terms of energy transfer from the power source to the

load. On the other hand the displacement factor is a measure of the energy storing or time shifting capabilities of the power network, while the uncorrelation factor describes the utilization of the network by non-linear or uncorrelated loads. An uncorrelated load implies that a loading function arises which does not correlate with the generating function. These utilization factors have the same characteristics as the respective equivalent network parameters.

3.11 FREQUENCY DOMAIN ANALYSIS USING THE PROPOSED DEFINITION

Distortion analysis in the frequency domain has distinct advantages when the generating and the loading functions are periodic. A 50 Hz power supply network is a typical example of a network where the generating function can be assumed periodic and in the most of the cases also sinusoidal. These systems normally include electrical apparatus operating from sinusoidal voltage generating functions, for example electric rotating machines and power transformers. In the analysis of the distortion having temperature effects on these and other apparatus and causing harmonic power losses, frequency domain analysis techniques can be used successfully. This analysis can be performed using the known techniques of voltage and current harmonic analysis, normally used in these situations (chapter 1, 2). A different approach, which is based on the proposed cross-correlation power definition, is proposed to extend the present analysis techniques into the frequency domain.

Using the properties of the cross-spectral density, described in chapter 1 and in appendix A4, the proposed generalized time-domain cross-correlation definition of power, can be used to represent spectral power components. By performing the magnitude and phase frequency transform on the cross-correlation function R_{ui}, the two correlated power components, active power and reactive power, can be decomposed into their harmonic components. However, because deactive power is uncorrelated, it cannot be decomposed into different harmonic components. The power cross-spectral density function is shown in eq. (3.42):

$$S_{ui}(f) = \int_{-\infty}^{+\infty} R_{ui}(\tau).e^{-j2\pi f\tau}.d\tau \qquad (3.42)$$

The correlated power k-th harmonic component can be derived from the power cross-spectral density as shown in eq. (3.43) and (3.44). The k-th active power harmonic component is expressed as P_k and the k-th reactive power harmonic component as Q_k.

$$P_k = |S_{ui}(k)| \cos \phi_k \qquad (3.43)$$

$$Q_k = |S_{ui}(k)| \sin \phi_k \qquad (3.44)$$

where $|S_{ui}(k)|$ is the magnitude of the k-th power cross-spectral density and ϕ_k the phase of the k-th power cross-spectral density.

It should, however, be emphasized that the frequency transform has its limitations, as described in chapter 1, and no generalized definition of electric power can be dependent on the harmonics of the voltage, the current and their cross-correlation. The above approach is only applicable to the analysis of distortion in power networks with periodic generating and loading functions and is an extension of the time domain analysis techniques.

3.12 COMPUTER SIMULATIONS OF TYPICAL VOLTAGE AND CURRENT WAVEFORMS

Using a digital signal processing algorithm, the proposed power definition has been evaluated by means of typical power waveform simulations done on a personal computer. The algorithm is based on digital correlation and calculates the power components and quantities from the equations shown in the previous paragraphs. The digital auto- and cross-correlations are shown in eqs. (3.45) - (3.47).

$$R_{ui}[j] = \frac{1}{N} \sum_{k=0}^{N-1} U[k].I[k-j] \qquad j = -N+1...N-1 \qquad (3.45)$$

$$R_{uu}[j] = \frac{1}{N} \sum_{k=0}^{N-1} U[k].U[k-j] \qquad j = -N+1...N-1 \qquad (3.46)$$

$$R_{ii}[j] = \frac{1}{N} \sum_{k=0}^{N-1} I[k].I[k-j] \qquad j = -N+1...N-1 \qquad (3.47)$$

where N is the number of samples, R_{ui} the voltage-current cross-correlation, R_{uu} the voltage autocorrelation and R_{ii} the current autocorrelation.

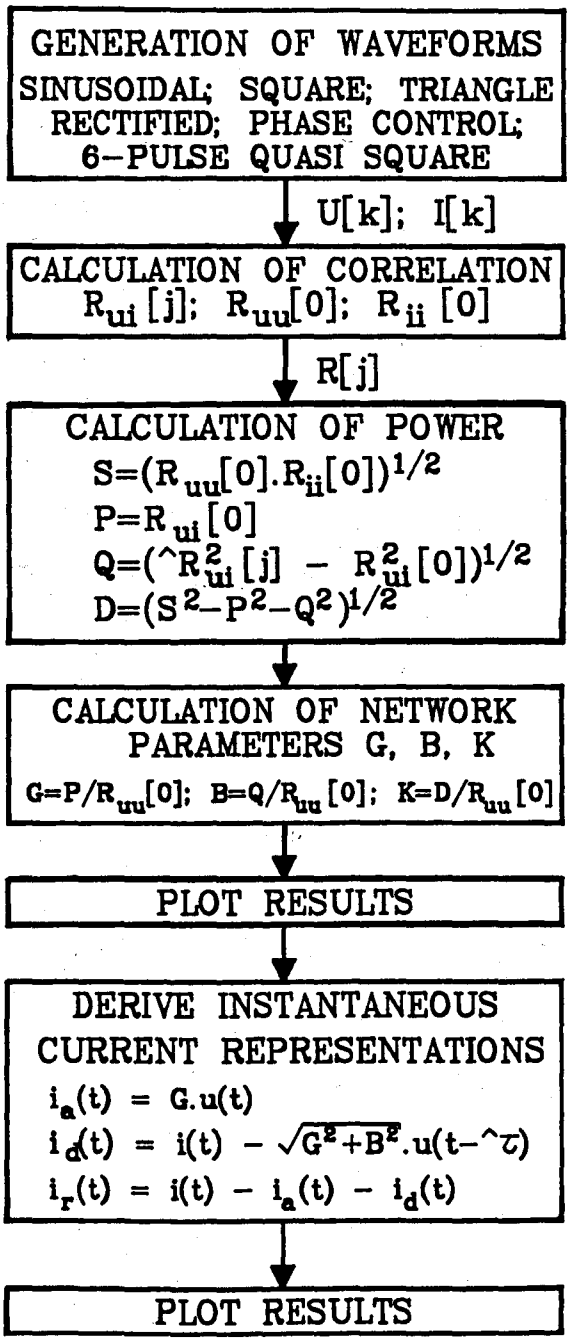

Fig. 3.7: Software Algorithm for Power Waveform Simulations

The software algorithm is shown in fig. 3.7 and the Pascal coded program in appendix B1. The first part of the algorithm generates different voltage and current waveforms, while the second part calculates all the different power components from the correlation between these voltage and current waveforms. After the calculation of the power components and network parameters, the results are plotted.

The plotted results include the following: Voltage and current waveforms in separate windows, the waveform of the cross-correlation function R_{ui} in another window and the power components and quantities in yet another window. The waveforms of the different current components are shown in a different figure and are determined as described previously. For comparison purposes, certain voltage and current waveforms are also analysed with the generalized time domain definition proposed by Nowomiejski [A109] and realized by Filipski [A61].

Throughout these analysis the amplitude of the voltage is chosen as 100 V, the current amplitude 10 A, the frequency 1 Hz and the measurement interval 3 fundamental periods. This implies that the measurement interval is chosen to be a multiple of the fundamental frequency period T. The main reason for this choice is to have comparable measurement time intervals so that the results can be analyzed with other known definitions as well.

The representation of instantaneous currents are based on eq. (3.23) and (3.29). There may however be other methods to represent the different instantaneous currents resulting from the same values of the average power components. These representations give acceptable results for the majority of the waveshapes under consideration.

3.12.1 Analysis of Simulated Sinusoidal Waveforms

Power in sinusoidal waveforms of current and voltage is analysed in fig. 3.8. The calculated power components are shown in fig. 3.8(a), while the waveforms of the current components are shown in fig. 3.8(b). The cross-correlation shows that the time shift $\hat{\tau}$, used to determine the waveform of the deactive current, is the result of the 45° phase shift between the voltage and current waveforms.

Loading power calculated from the autocorrelation of voltage and current (eq. (3.32)) agrees with the product of effective values of voltage and current (500 VA). The calculated values of active and reactive power correspond with those obtained from the fundamental phasor definition. Deactive power is zero, because the voltage and current waveforms correlate. The equivalent network parameters are calculated from the different power components.

In fig. 3.9 a sinusoidal voltage is correlated with a sinusoidal current with a DC-offset of 10A. Except for the DC-offset, everything, including the 45° phase shift, is the same as the previous example resulting in the active and the reactive power also being the same as the previous example. The loading power is however much higher because of the DC-offset in the current which does not correlate with the voltage waveform and thereby give rise to deactive power. The equivalent conductance and susceptance are the same as in the previous simulation, but the disceptance now has a non-zero value. The current has a deactive component which represents the DC-offset as shown in fig. 3.9(b).

The next simulation, shown in fig. 3.10, is done for a sinusoidal voltage and a sinusoidal current having different frequencies. The two waveforms are not correlated, which implies that all the loading power is deactive power and reactive and active power are zero. Figure 3.10(b) shows that the current has no active or reactive component and that the load current is also the deactive current.

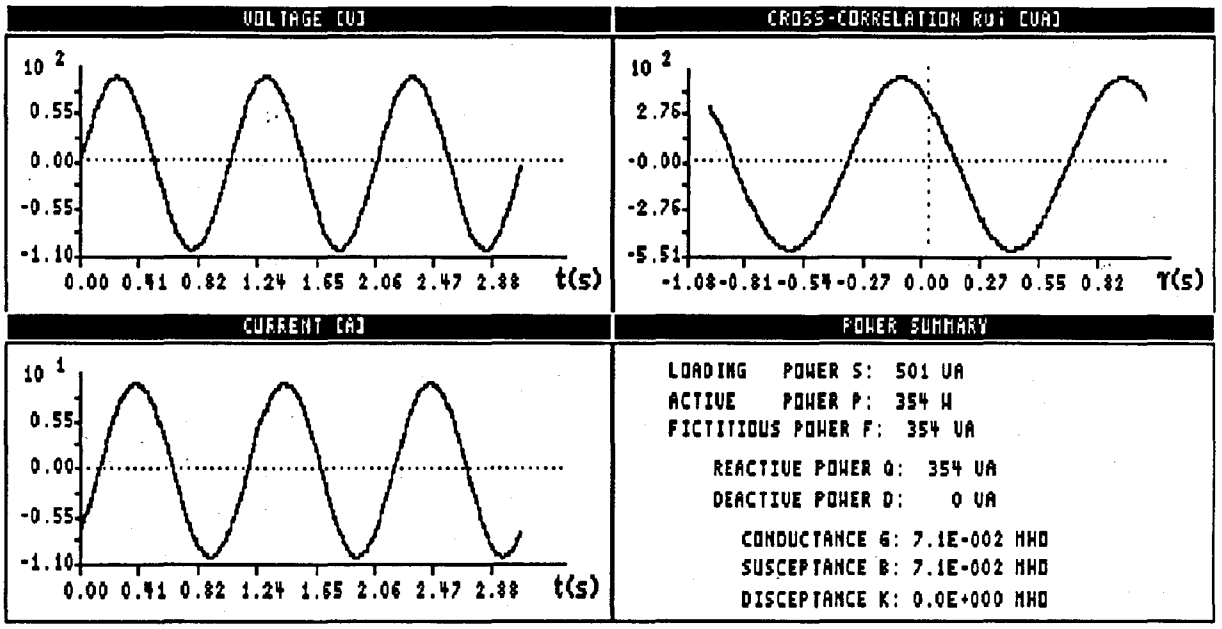

(a) Calculated Power Components

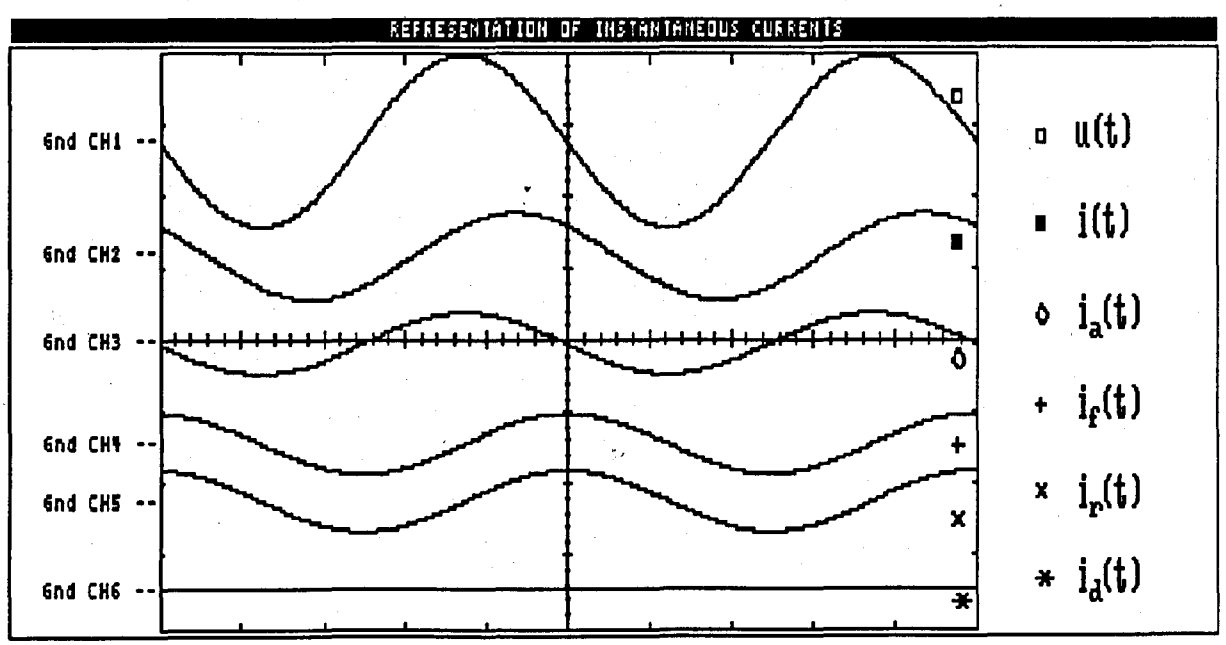

(b) Waveforms of Current Components

Fig. 3.8: Simulation of Sinusoidal Voltage and Current Waveforms

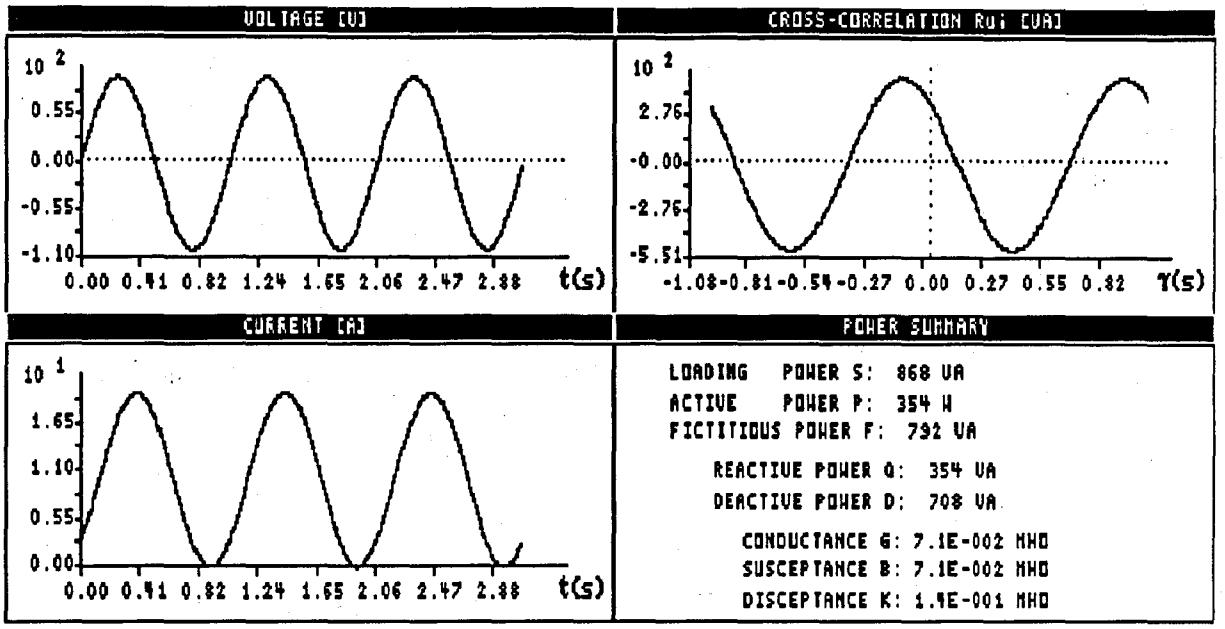

(a) Calculated Power Components

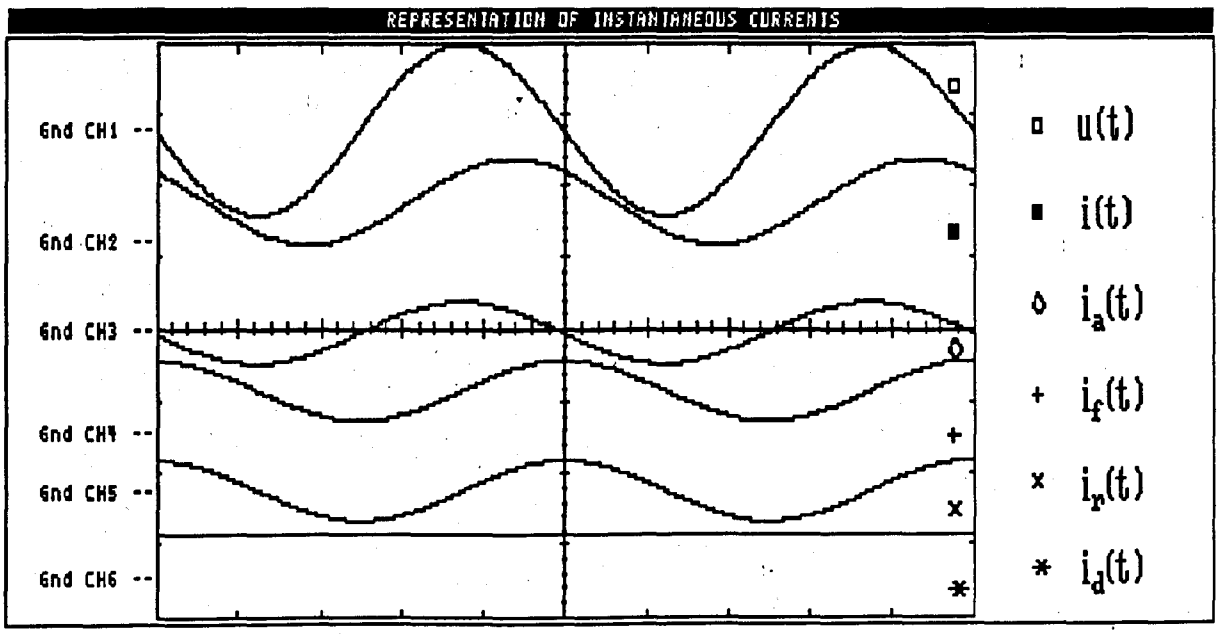

(b) Waveforms of Current Components

Fig. 3.9: Simulation of a Sinusoidal Voltage and a Sinusoidal Current with a DC-offset

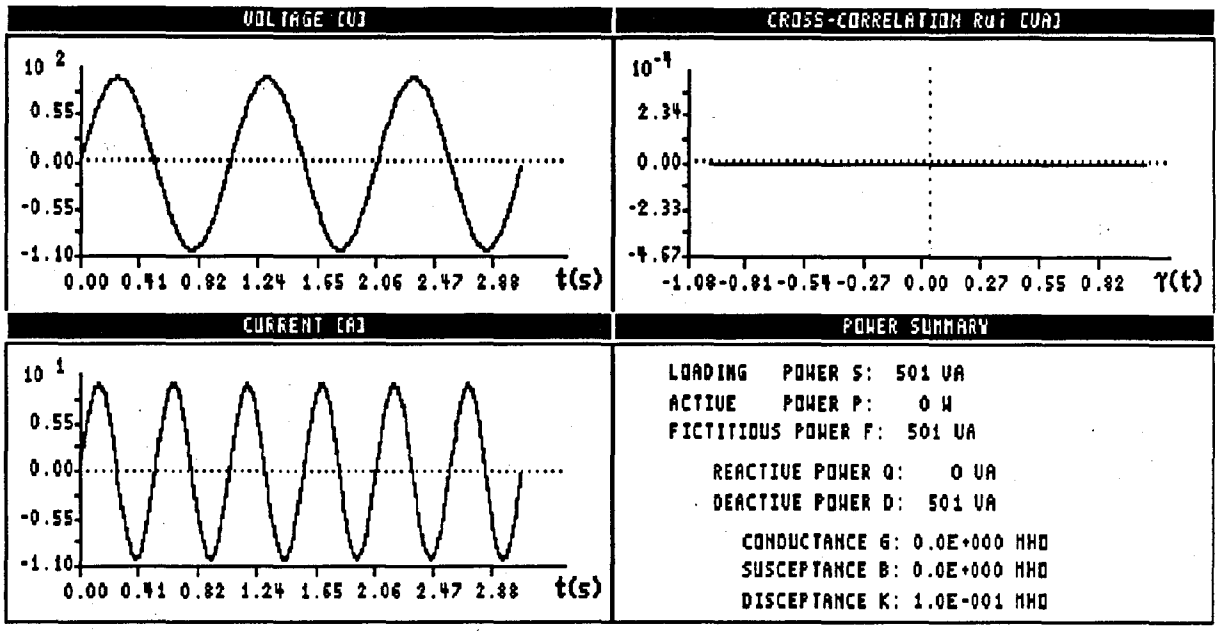

(a) Calculated Power Components

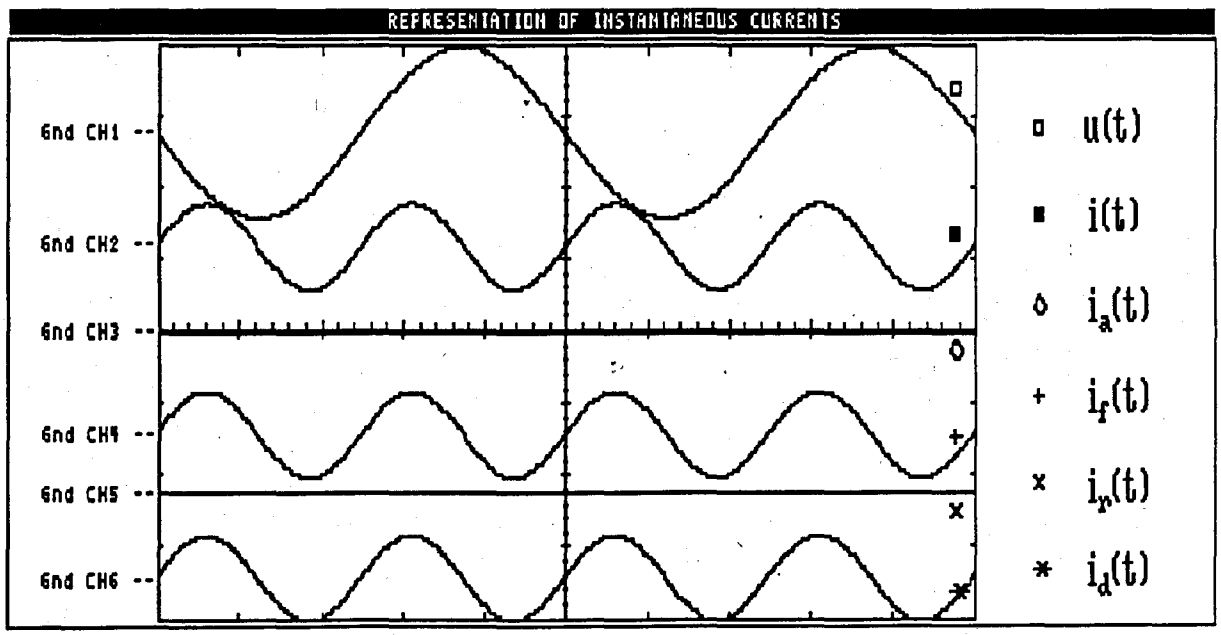

(b) Waveforms of Current Components

Fig. 3.10: Simulation of Uncorrelated Voltage and Current Waveforms.

3.12.2 Analysis of Simulated Non-sinusoidal Voltage and Current Waveforms

Voltage and current waveforms that are different or not correlated result in uncorrelated fictitious power, or deactive power.

Figure 3.11 shows the results for a sinusoidal voltage and square wave current with no fundamental time shift, while fig. 3.12 shows the result for the same waveforms, but with a fundamental time shift giving rise to reactive power. There is clearly no reactive current present in fig 3.11(b). If these waveforms are analysed with the other time domain definitions the same result is obtained because the voltage is sinusoidal.

As shown in fig. 3.11 and fig. 3.12, the deactive power and current are independent of the time shift. This is because reactive and deactive power are generated differently.

Figure 3.13 shows the case where the current and voltage are both square waves, their fundamentals being phase-shifted by 45°. According to the proposed correlation based power definition, deactive power should be zero, because the voltage and current waveforms correlate exactly. Figure 3.13(a) shows that deactive power is in fact zero, resulting from this exact correlation. When deriving the instantaneous signals for the different current components, shown in fig. 3.13(b), the deactive current is found to be zero and the reactive current, which is in this case of zero deactive current, identical to the fictitious current, is a quasi square wave. The current components shown in fig. 3.13(b) are clearly mutually orthogonal.

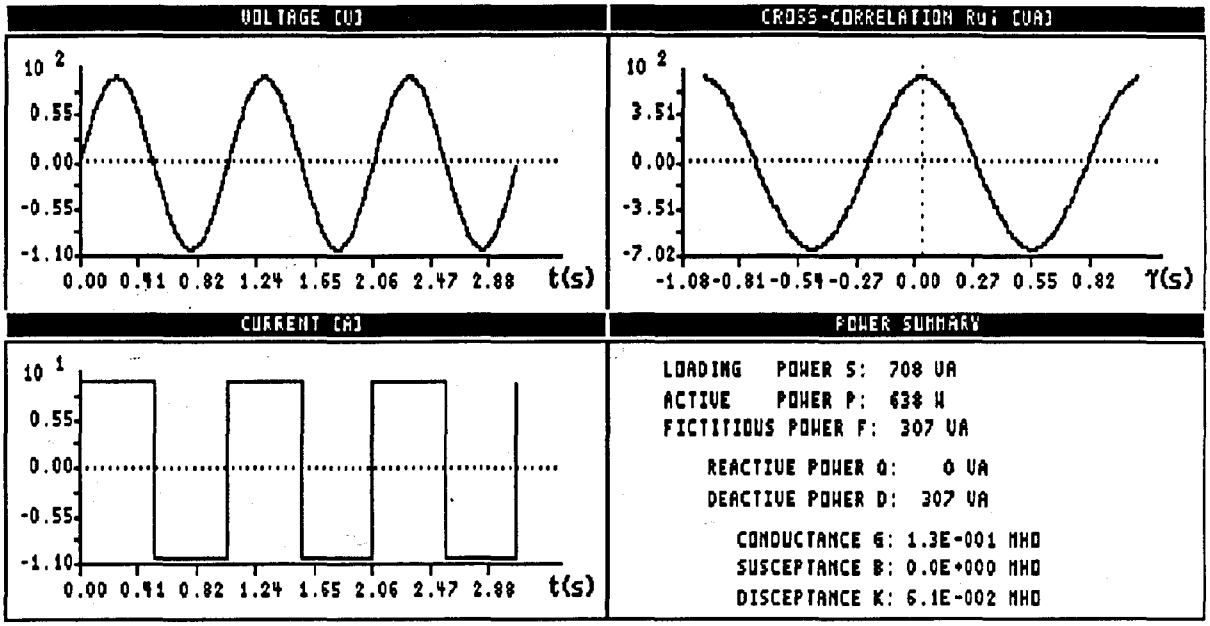

(a) Calculated Power Components

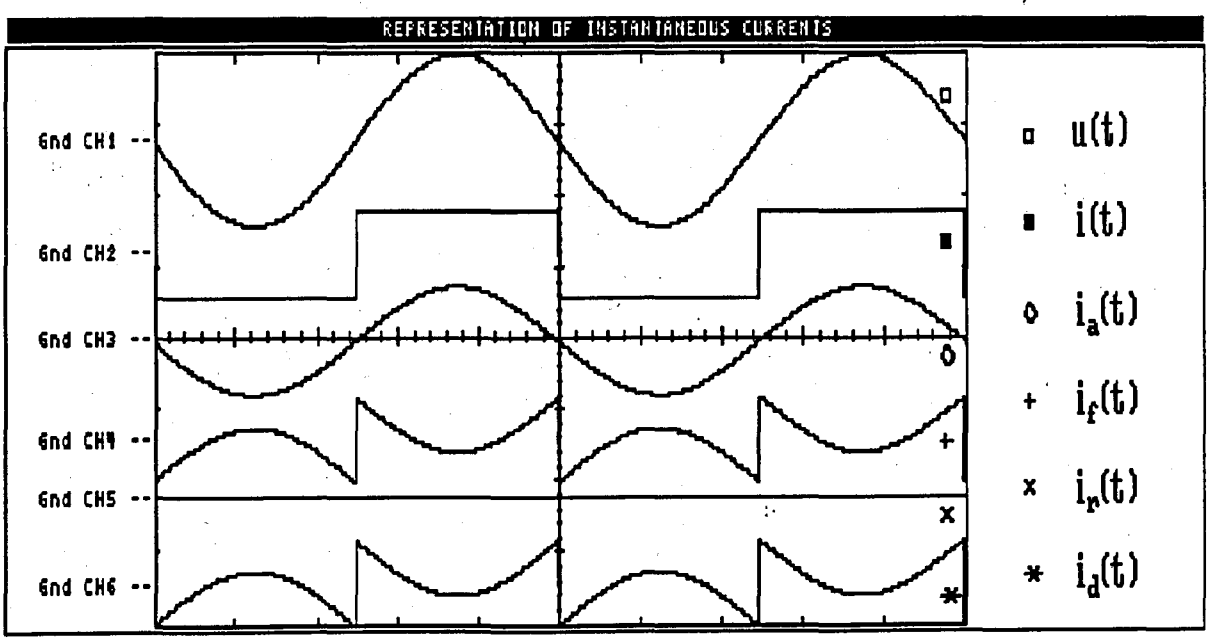

(b) Waveforms of Current Components

Fig. 3.11: Analysis of Simulated Sinusoidal Voltage and Square Wave Current

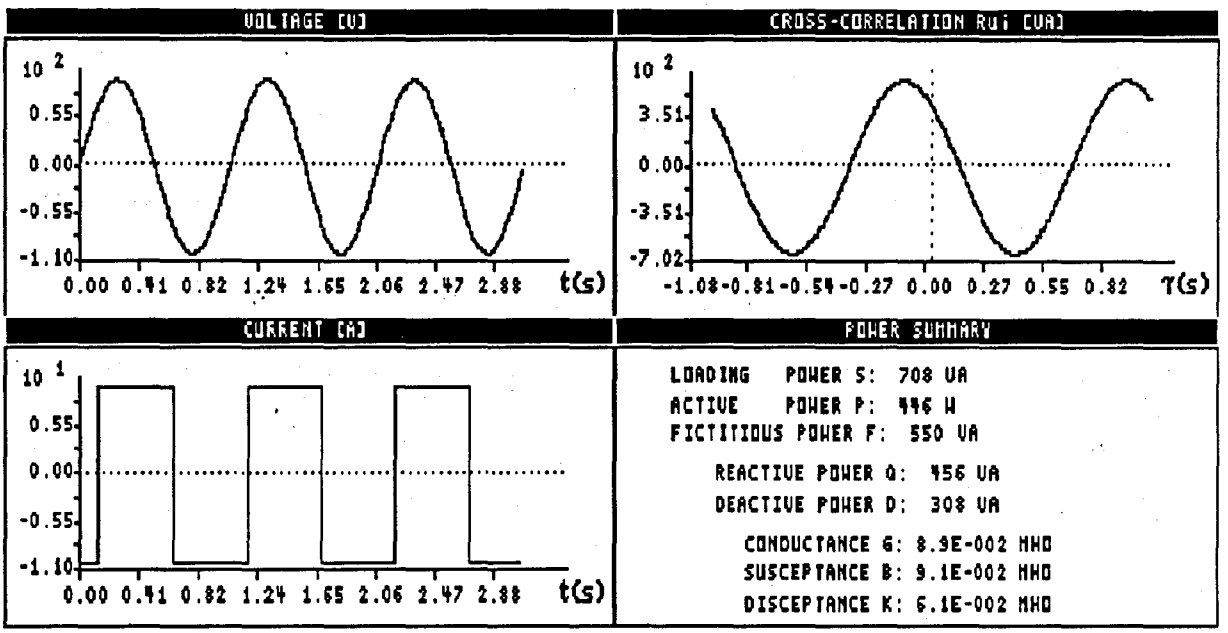

(a) Calculated Power Components

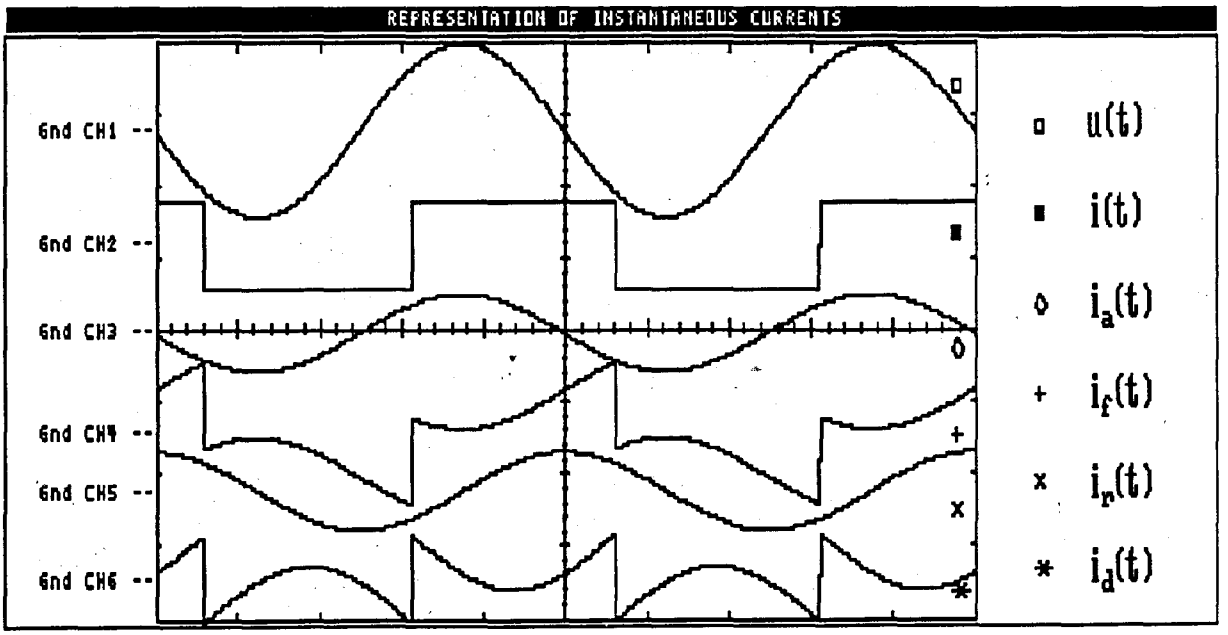

(b) Waveforms of Current Components

Fig. 3.12: Analysis of Sinusoidal Voltage and Time Shifted Square Wave Current

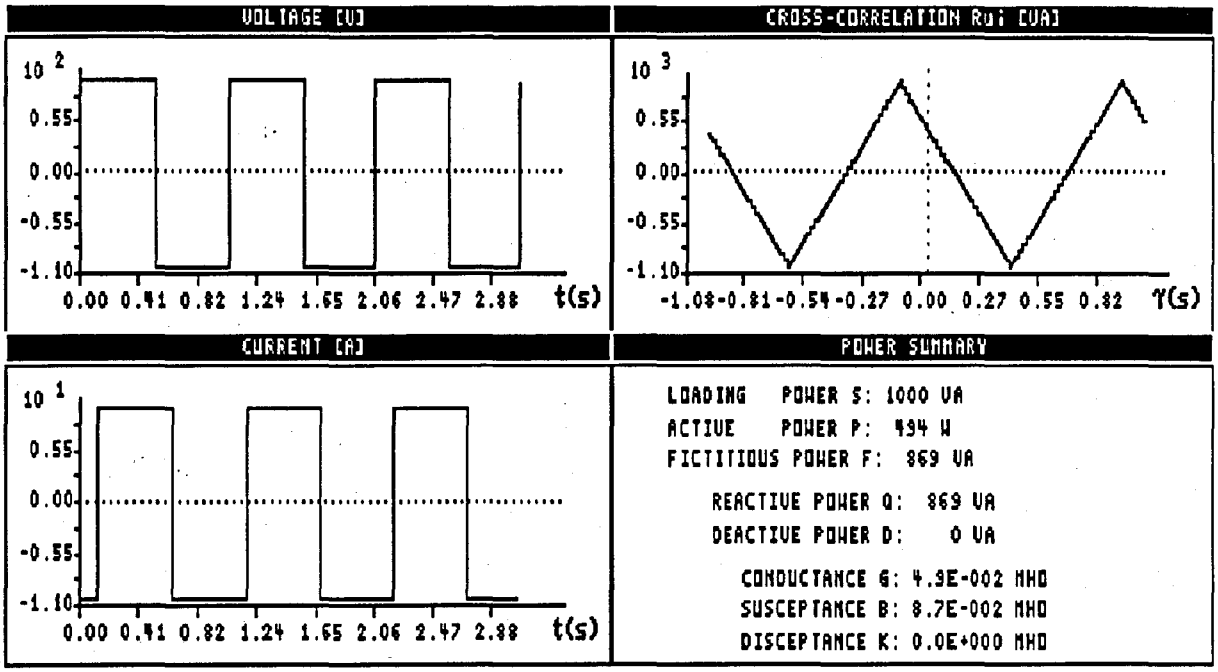

(a) Calculated Power Components

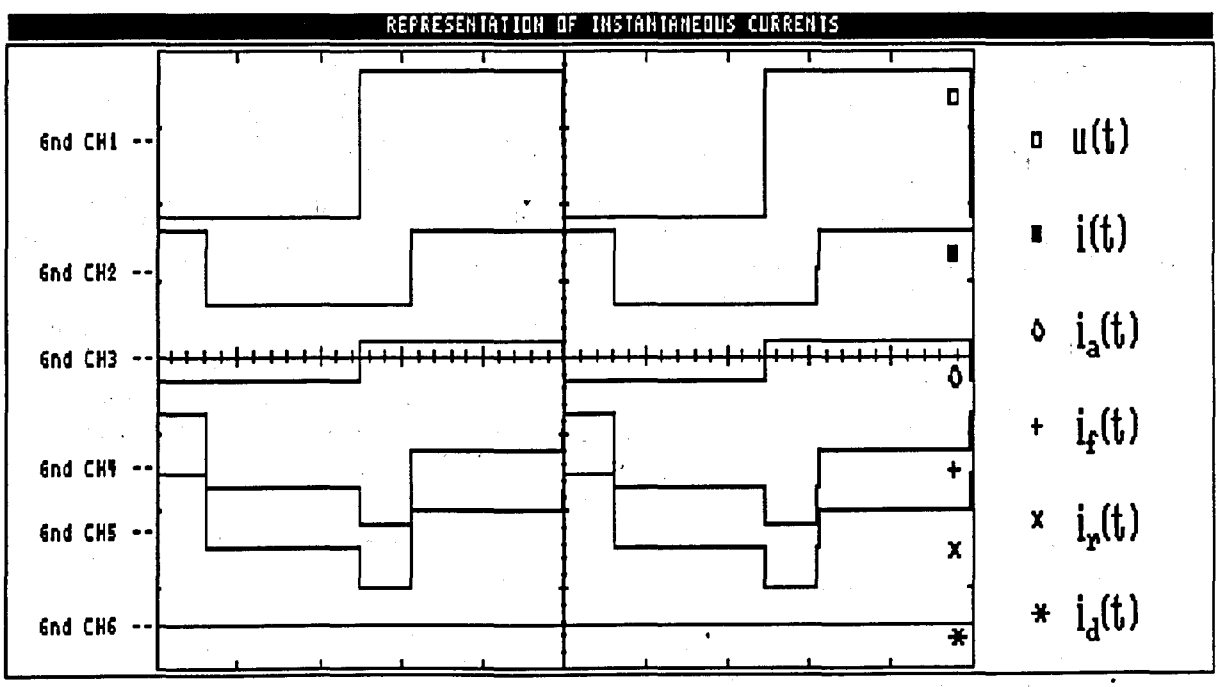

(b) Waveforms of Current Components

Fig. 3.13: Analysis of Shifted Square Waves for Voltage and Current

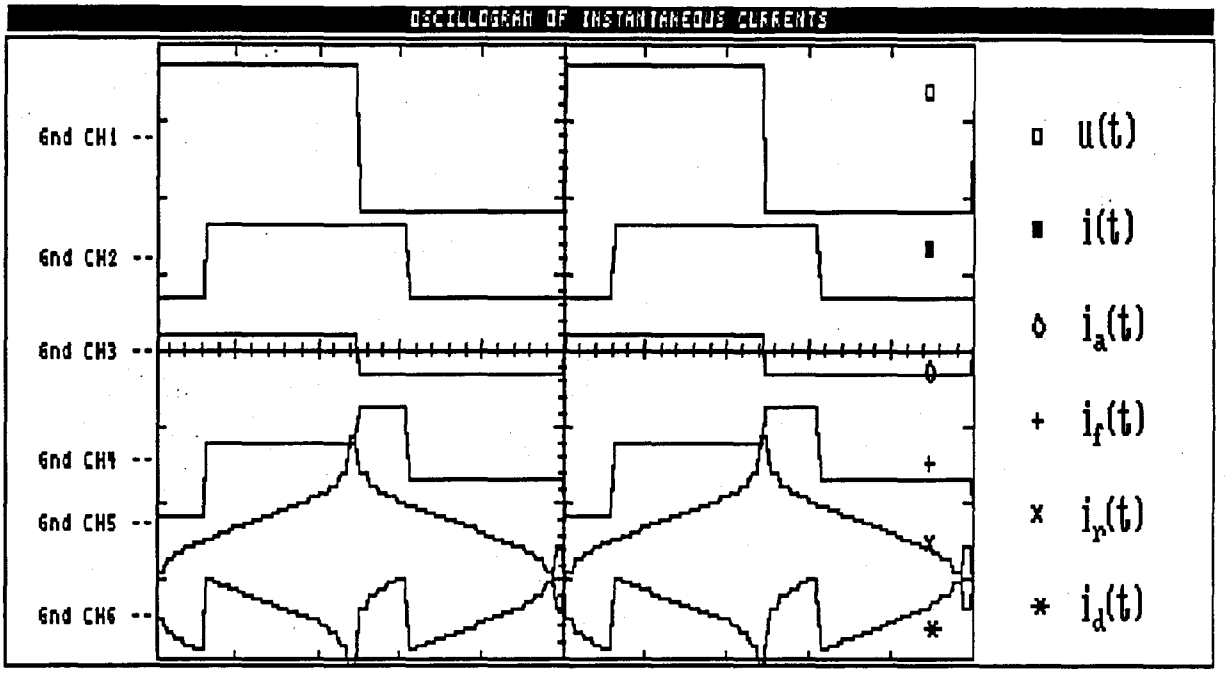

(c) Waveforms of Nowomiejski's Current Components [A109]

Fig. 3.13: Analysis of Shifted Square Waves for Voltage and Current

The same waveforms are used to derive the instantaneous current components according to Nowomiejski [A109]. Characteristic of this approach is the fact that a Hilbert transform is used to define reactive power and to decompose the current into its orthogonal components as described in chapter 1, paragraph 1.6.2.4 and in Appendix A4. The Hilbert transform based definition is, however, not related to the power phenomena in the network and for this reason inconsistent results are obtained when the voltage signal is non-sinusoidal. In systems where the generating functions are sinusoidal, as in the examples in the previous paragraph, all the power definitions give equivalent results. This is not the case when the generating function is non-sinusoidal as shown in fig. 3.13(c). The reactive current in fig. 3.13(c) shows the characteristic Hilbert transform of a square wave, in this case the square wave voltage (appendix A4). Resulting from the reactive current waveform, the Nowomiejski distortion current is non-zero, which implies

that the Nowomiejski distortion power D_N also has a non-zero value. These results are inconsistent with the proposed definition based on correlation. The Depenbrock approach will give a non-zero value for the distortion (deactive) current, because the reactive current will be sinusoidal [A35]

Figure 3.14 shows the analysis of a square wave voltage and a triangular wave current. Their commutation points coincide, which implies that the reactive power calculated from the correlation based power definition will be zero. This is confirmed by fig. 3.14(b), which shows that the current has no reactive component. Figure 3.15 shows the same waveforms, but without the coinciding commutation points. Figure 3.15(b) shows a non-zero reactive current corresponding to the non-zero reactive power. The active current in fig. 3.15(b) is zero, corresponding to the fact that the active power is zero, as shown in fig. 3.15(a). Again the Depenbrock and Nowomiejski approaches each result in different reactive and distortion (deactive) currents, which are the result of the non-sinusoidal voltage [A35,109].

3.12.3 Simulation of Power Electronic Converter Waveforms

Figure 3.15 shows the case where the commutation points of the triangular current is 90° later than those of a square wave voltage. This case is obtained when a purely inductive load is subjected to a square wave voltage. As expected there is no active power (inductive load) and the deactive power and the loading power are the same as in fig. 3.14. The reactive power is the result of the inductive load, but is however smaller than the loading power. Firstly this phenomena seems odd because the load is a simple inductance. This network, when characterized in terms of the loading and generating function, is however uncorrelated. The inductive load results only in a correlated loading function if the generating function is sinusoidal, therefore this network is uncorrelated and deactive power results.

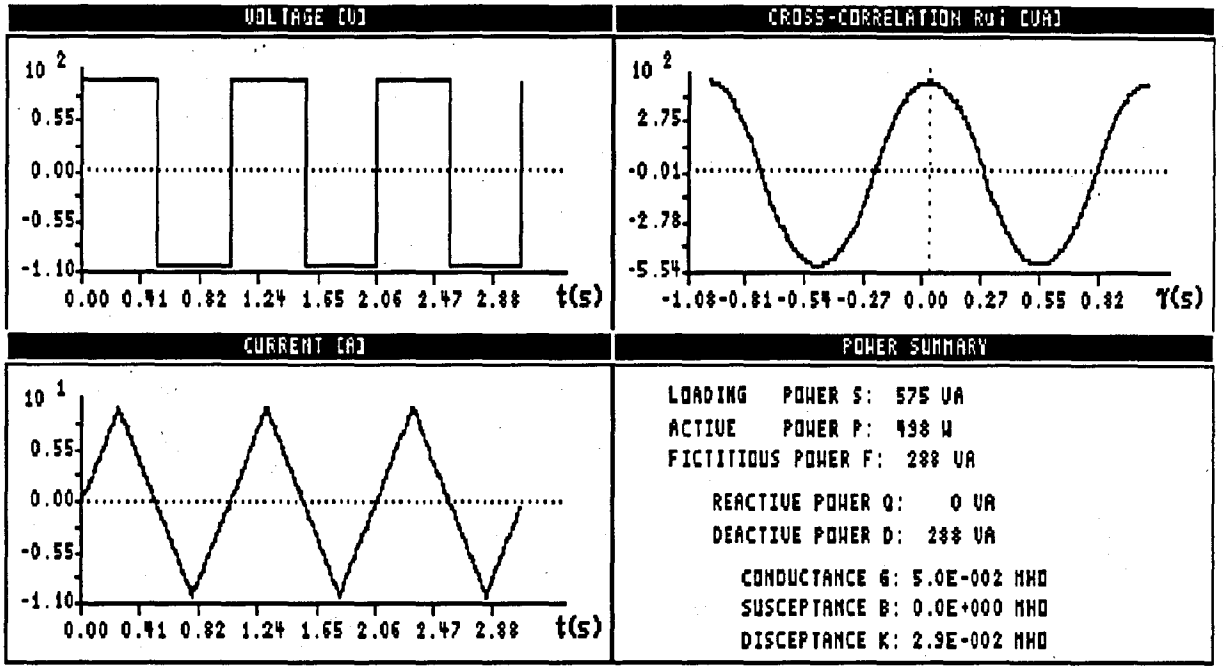

(a) Calculated Power Components

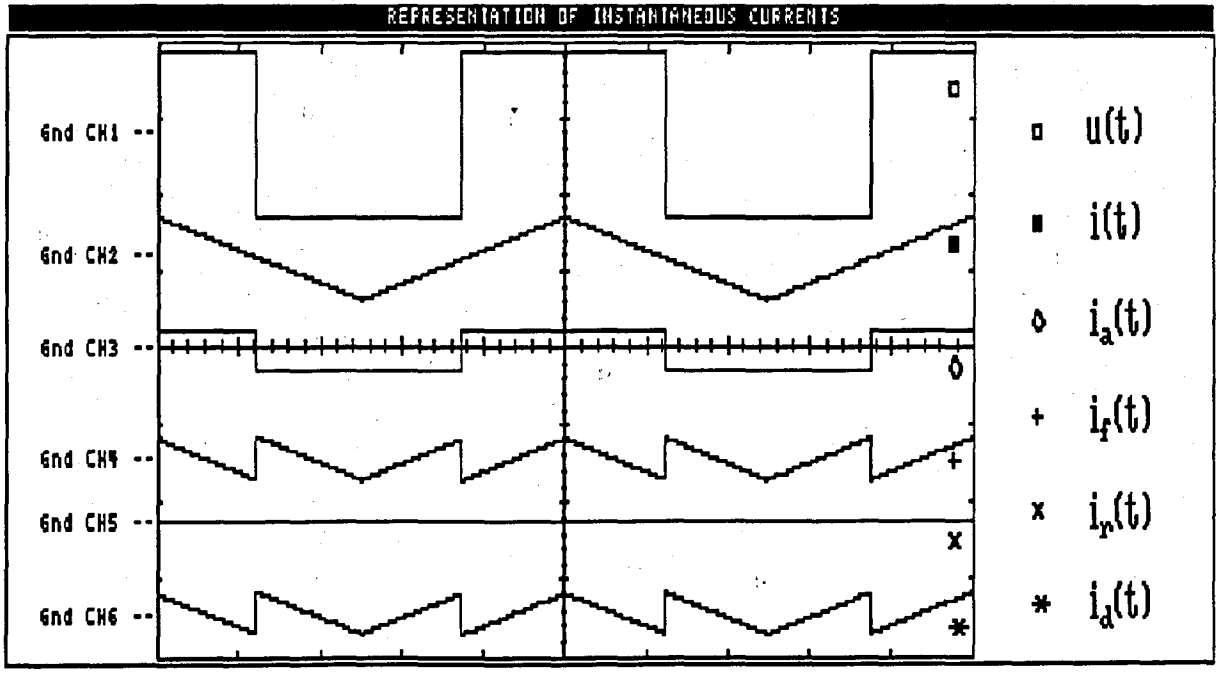

(b) Waveforms of Current Components

Fig. 3.14: Simulation of Square Wave Voltage and Triangular Current

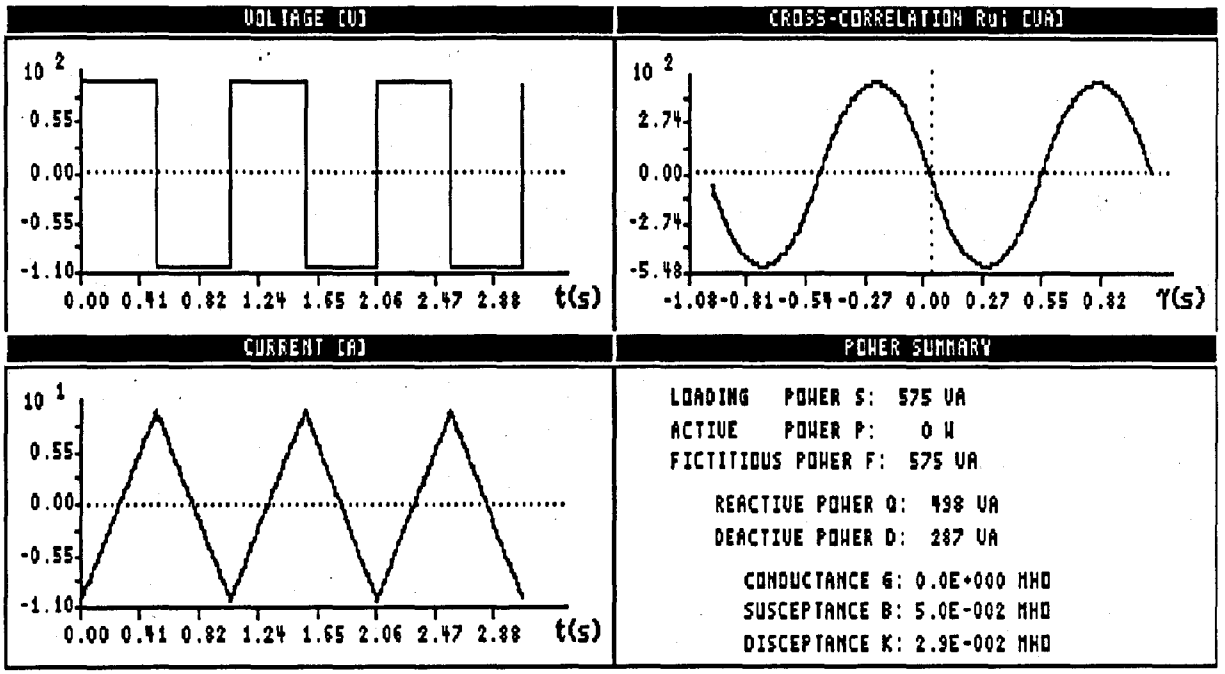

(a) Calculated Power Component

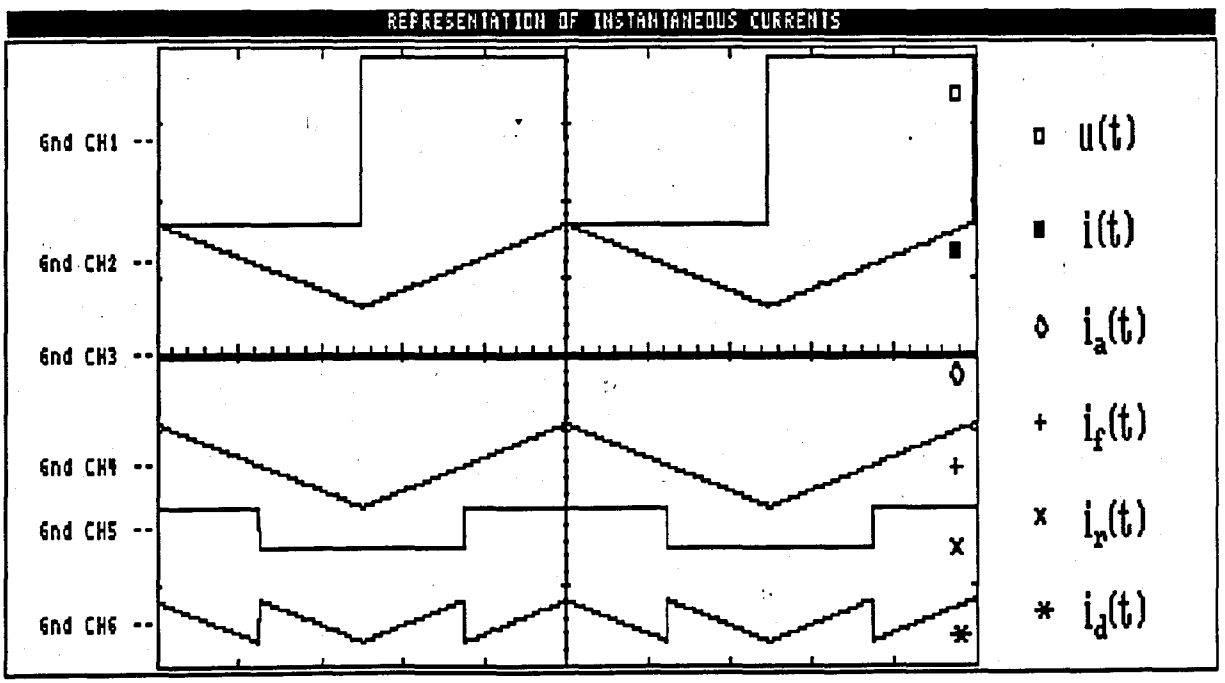

(b) Waveforms of Current Components

Fig.3.15: Simulation of Square wave Voltage and Triangular Current, Resulting from an Inductive Load

Figure 3.16 shows the analysis of the case where the generating function is a sinusoidal voltage and the load consists of a simple diode in series with a pure resistance. In Appendix A3 this case is analysed mathematically with all the major power definitions. The diode in the network is responsible for deactive power. In this case reactive power is however zero, because there is no time shift present in the two waveforms. The fictitious power is only the result of the non-similarity between the generating and loading functions.

Figure 3.17 shows the analysis of a sinusoidal voltage as generating function and a six-pulse current as loading function with the control angle α set to zero, while fig. 3.18 shows the analysis when the control angle α is set to 45°. As expected, the loading power is constant in both cases and active and reactive power are proportional to cos α and sin α respectively. The deactive power stays the same, because the correlation between voltage and current does not change with the control angle α. These simulation shows typical voltage and current waveforms for the majority of phase angle controlled power converters where a DC link is employed.

In fig. 3.19 a six-pulse voltage-fed converter with an inductive load, typically found in three phase variable speed voltage-fed induction machine drives, is analysed. The phase voltage is a quasi square wave while the line current is sinusoidal because of the magnetizing and leakage inductance. Power electronic converters generating the above mentioned waveforms, are analysed experimentally in chapter 4.

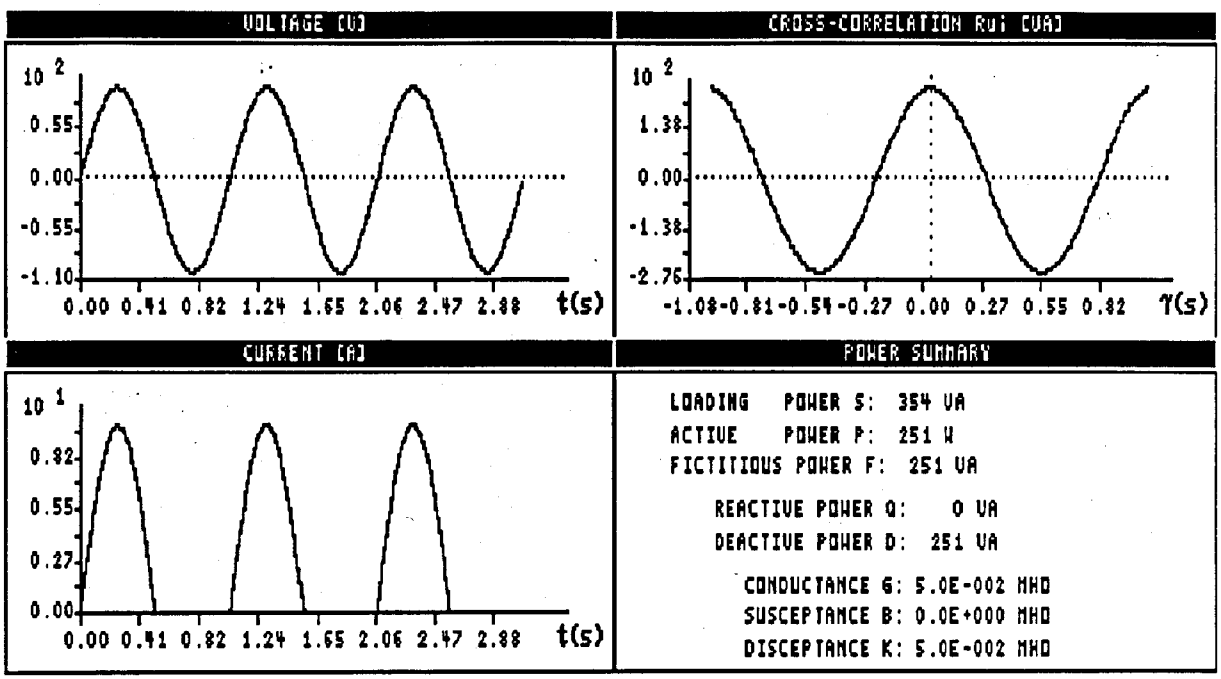

(a) Calculated Power Components

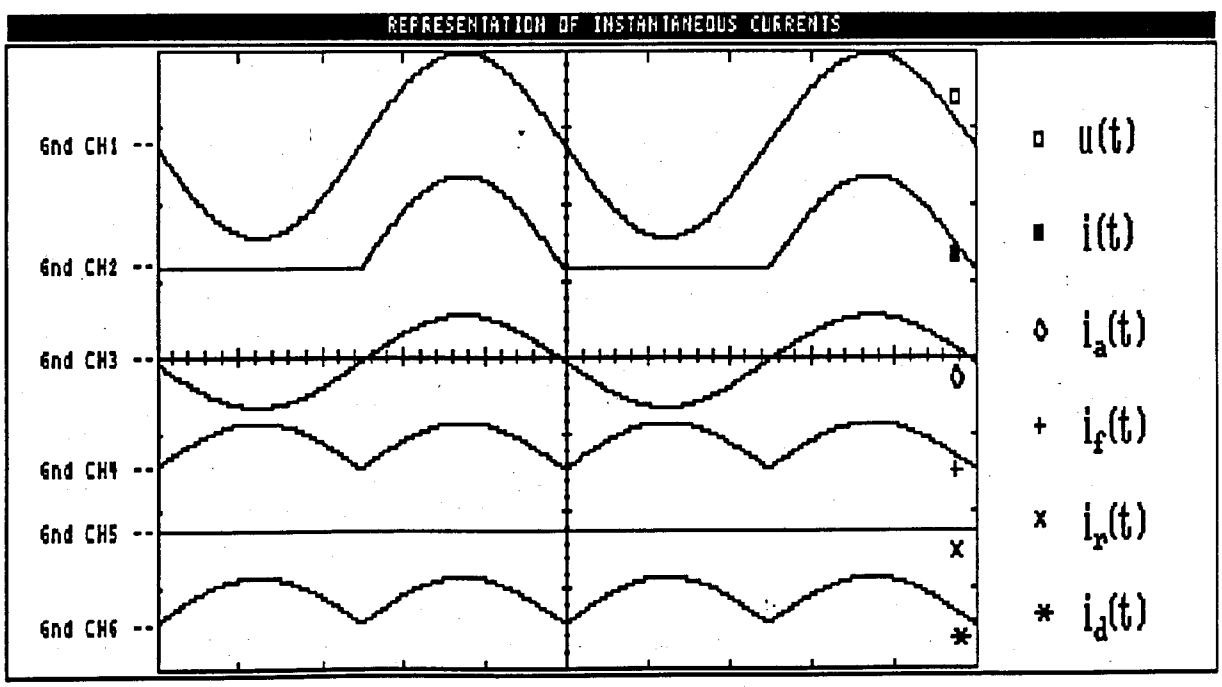

(b) Waveforms of Current Components

Fig. 3.16: Simulation of the Diode-Resistance Network

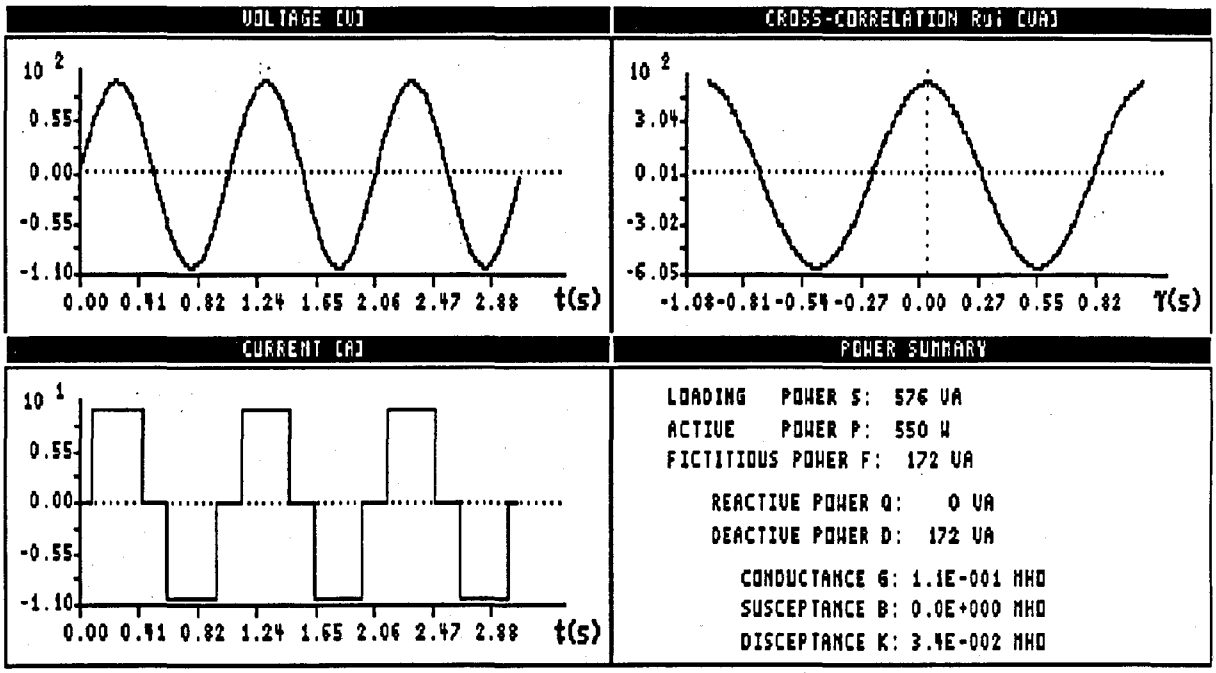

(a) Calculated Power Components

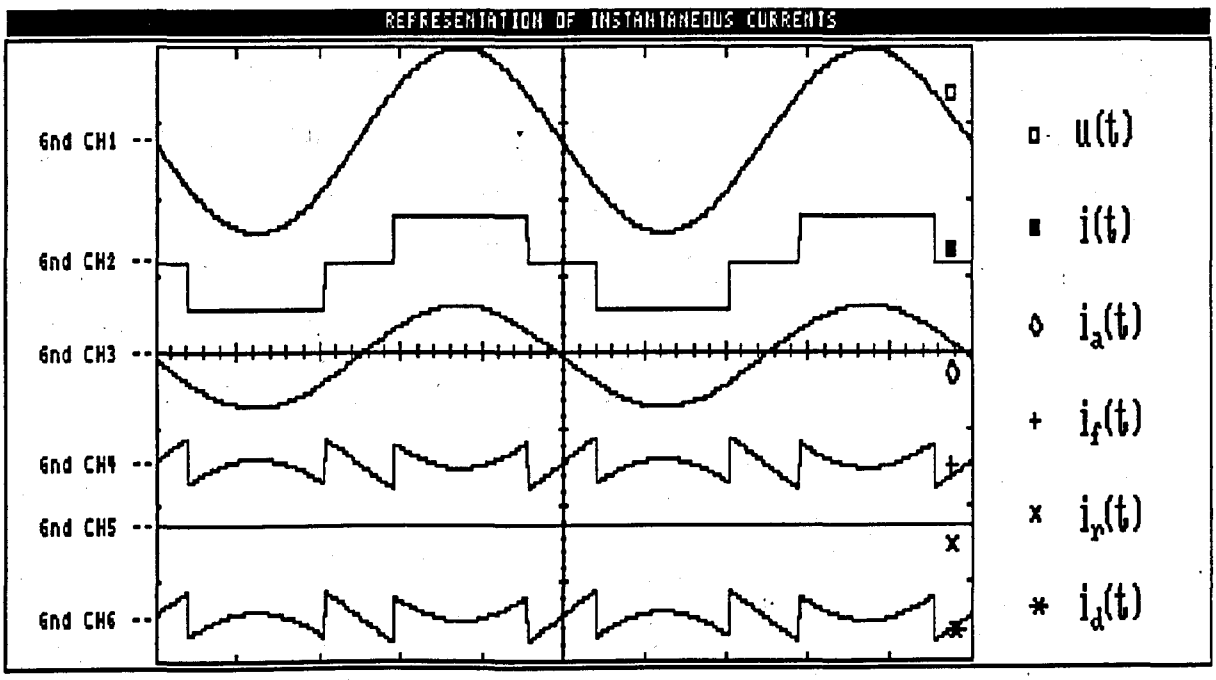

(b) Waveforms of Current Components

Fig. 3.17: Simulation of Six-pulse Converter with $\alpha = 0°$

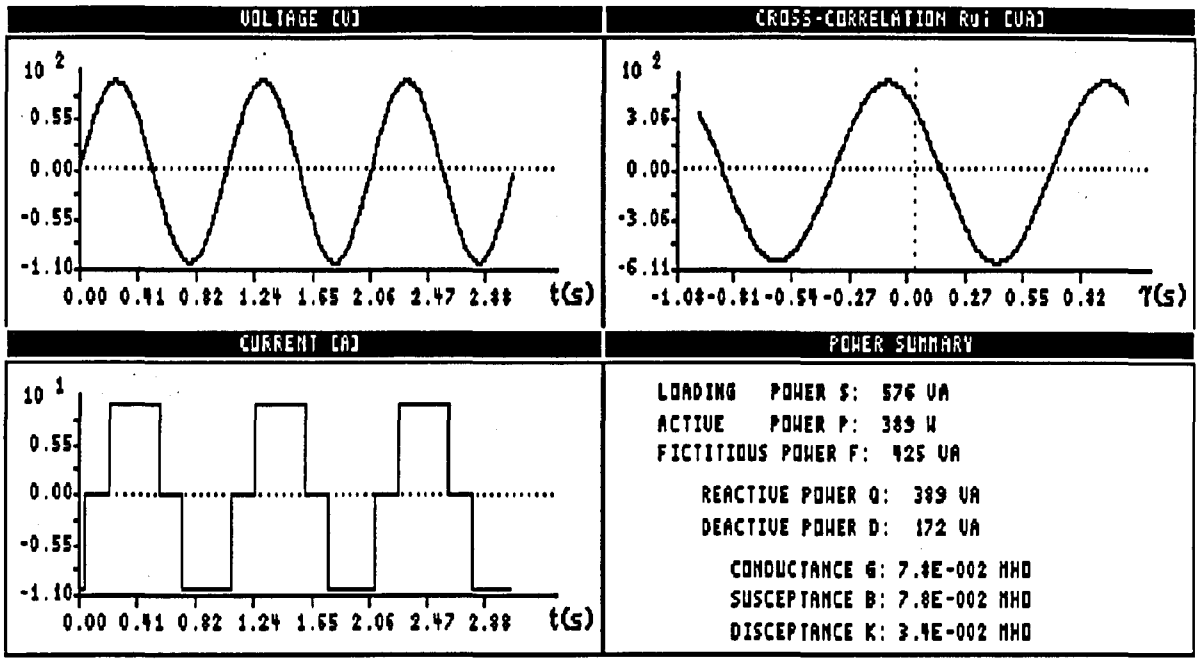

(a) Calculated Power Components

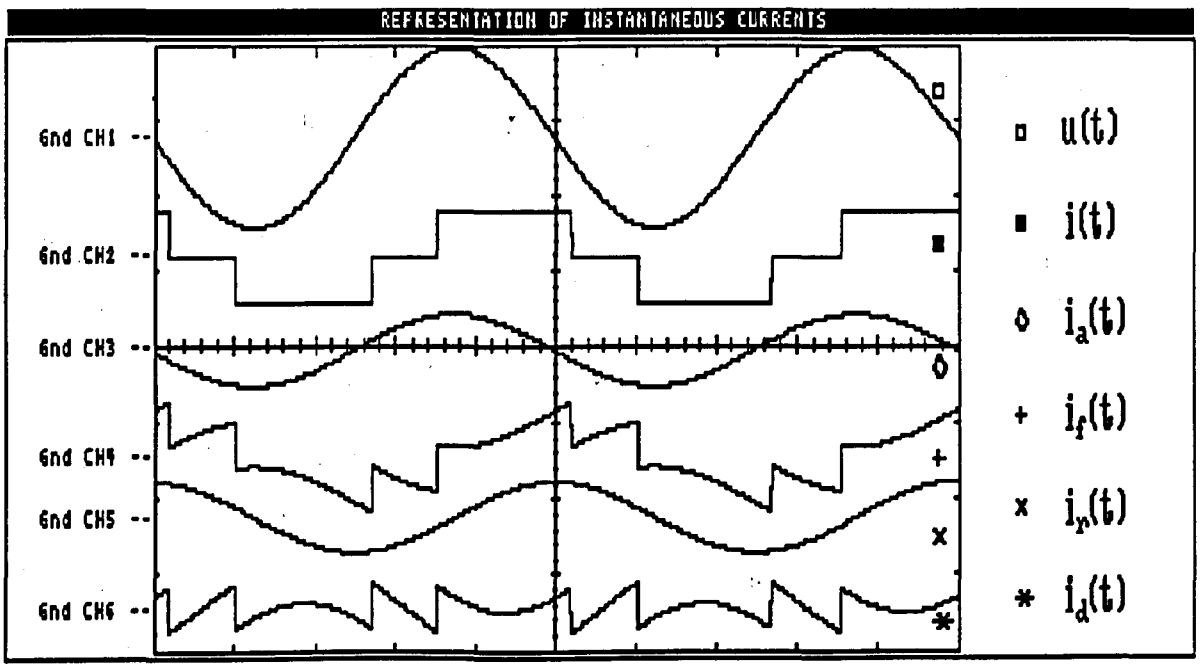

(b) Waveforms of Current Components

Fig. 3.18: Simulation of Six-pulse Converter with $\alpha = 45°$

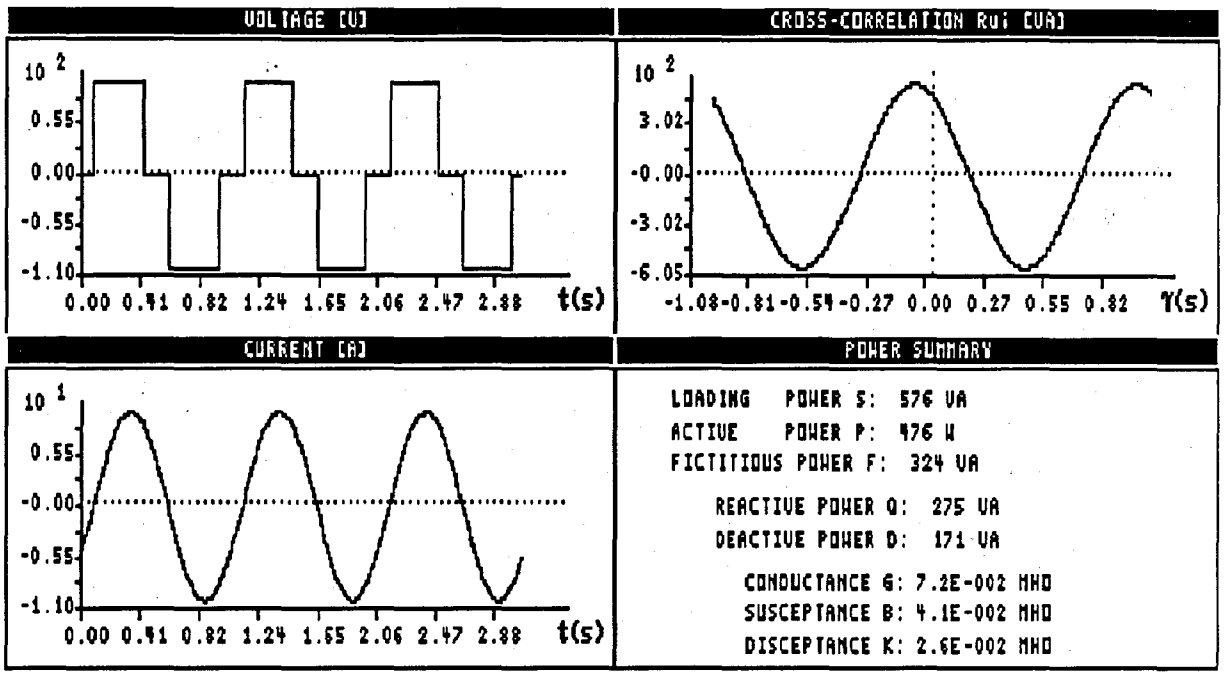

(a) Calculated Power Components

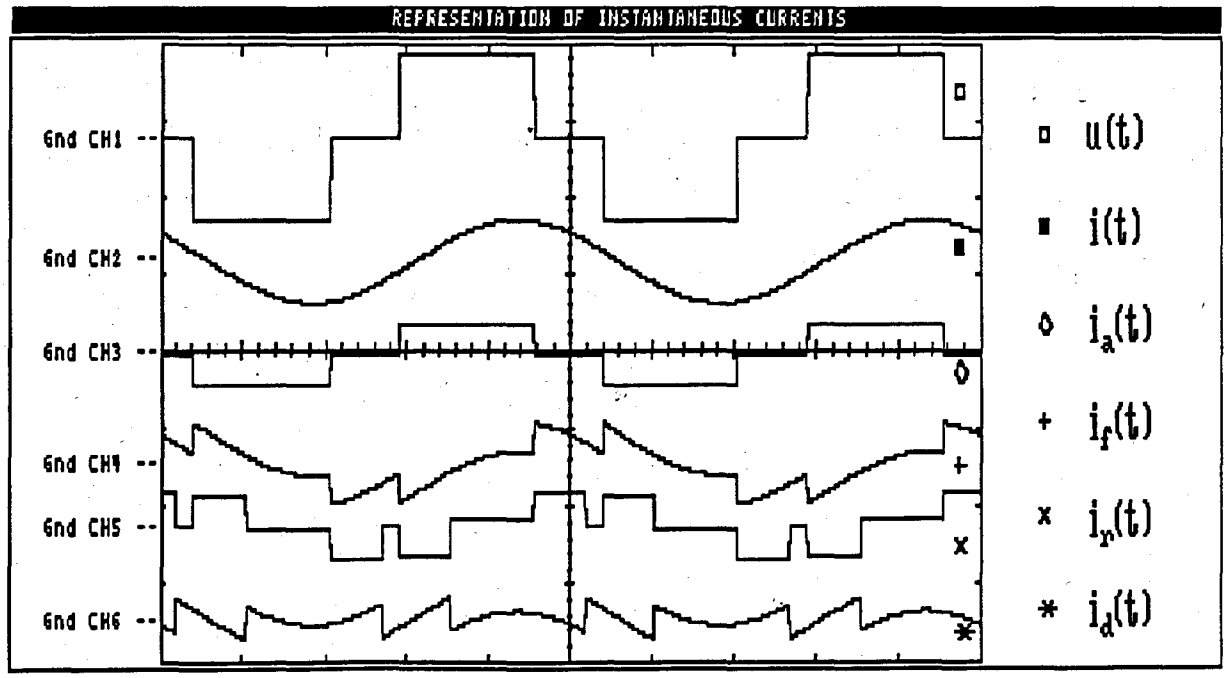

(b) Waveforms of Current Components

Fig. 3.19: Simulation of a Six-pulse Voltage-fed Converter with an Inductive Load

Controlling the firing angle α of a phase controlled power electronic converter is tantamount to controlling the equivalent conductance and susceptance in the power network. Figure 3.20 shows the case where the diode-resistance network analysed in fig. 3.16, is replaced by a thyristor-resistance network with the fire angle α set to 60°. Although there is no inductance in the load, the equivalent susceptance has a non-zero value due to the control of the fire angle α. This implies that the schematic circuit diagram does not describe the power phenomena in the network, but only the circuit elements. The proposed equivalent parameter diagram, fig. 3.4, does, however, describe the power quantities and should be used when characterizing networks as analysed in fig. 3.20. Fire angle control implies that a reactive current, describing the reactive power flow, arises without any physical inductance in the network. This result corresponds with the result from the Depenbrock [A35] and Nowomiejski [A109] approaches.

When the thyristor in the previous simulation is replaced by an anti-parallel thyristor pair, the results shown in fig. 3.21 are obtained. In this case the fire angle α is also set to 60°. This is a typical circuit in light dimmers and other phase controlled circuits. Again the reactive power is proportional to sin α and the active power to cos α.

In fig. 3.22 the power components for the anti-parallel thyristor-resistance network analysed in fig. 3.21, is plotted as a function of the fire angle α. It can be seen that the fictitious, reactive and deactive power follow the same trend, proportional to sin α, while the loading and active power follow a cos α proportionality. At an angle of $\alpha = 90°$ the fictitious power exceeds the active power.

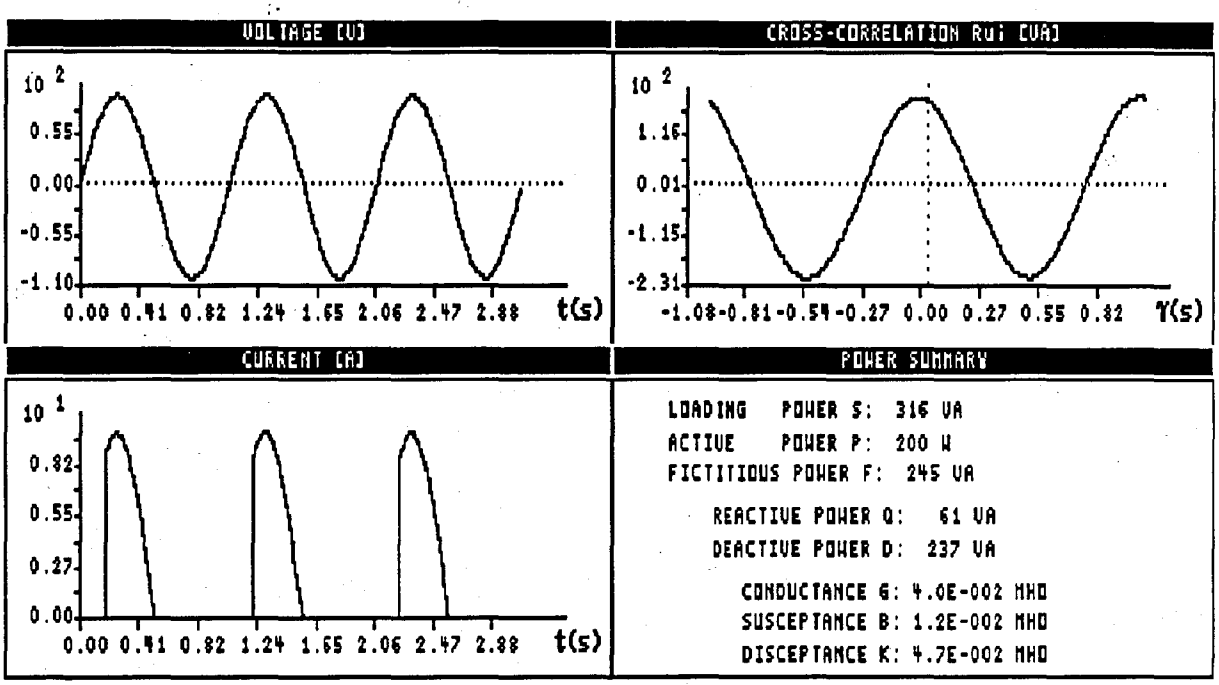

(a) Calculated Power Components

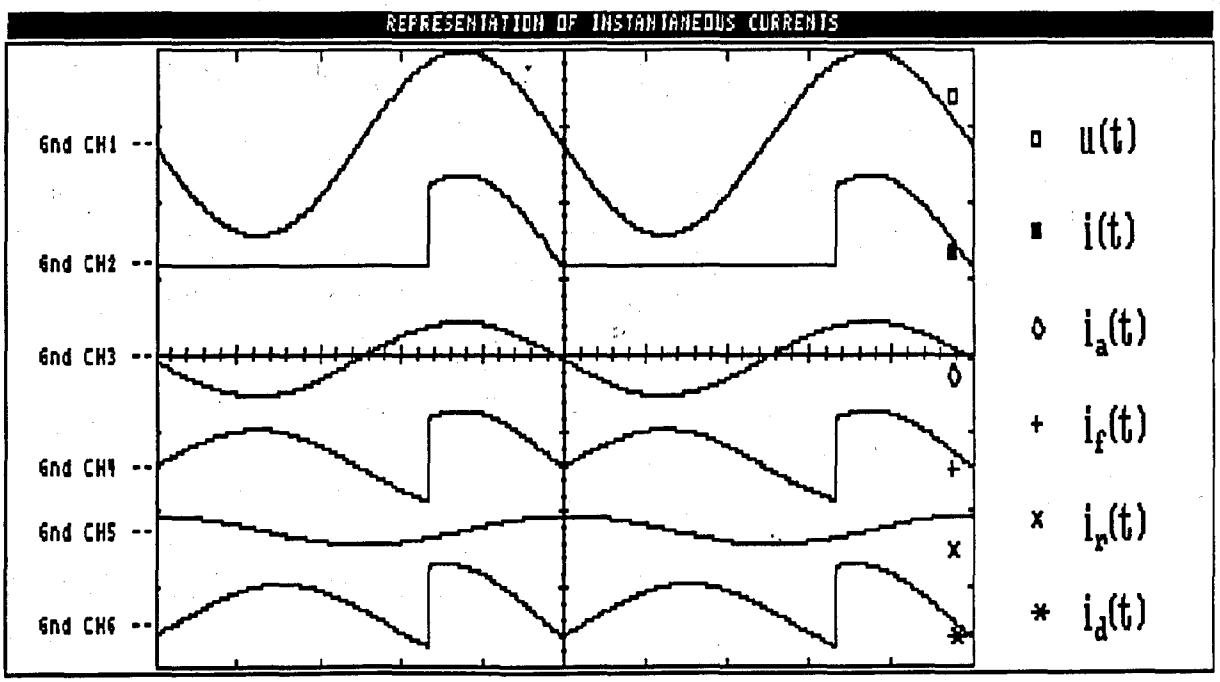

(b) Waveforms of Current Components

Fig. 3.20: Simulation of Thyristor-resistance Network with the Firing Angle α set to 60°

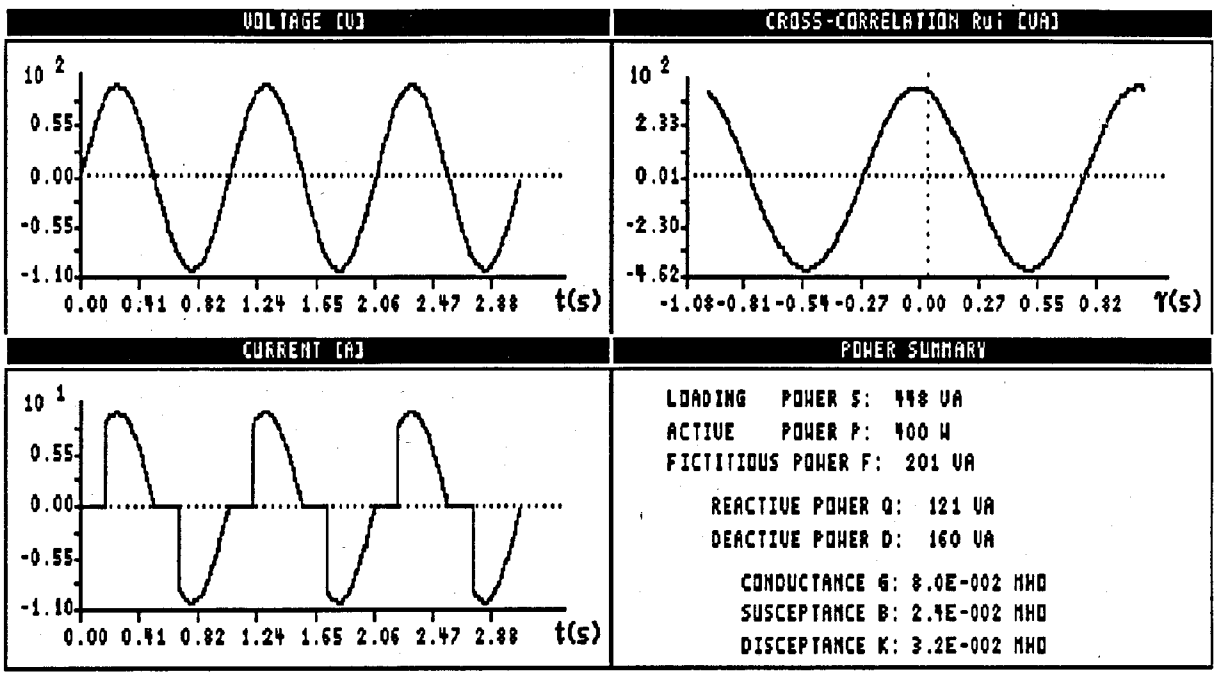

(a) Calculated Power Components

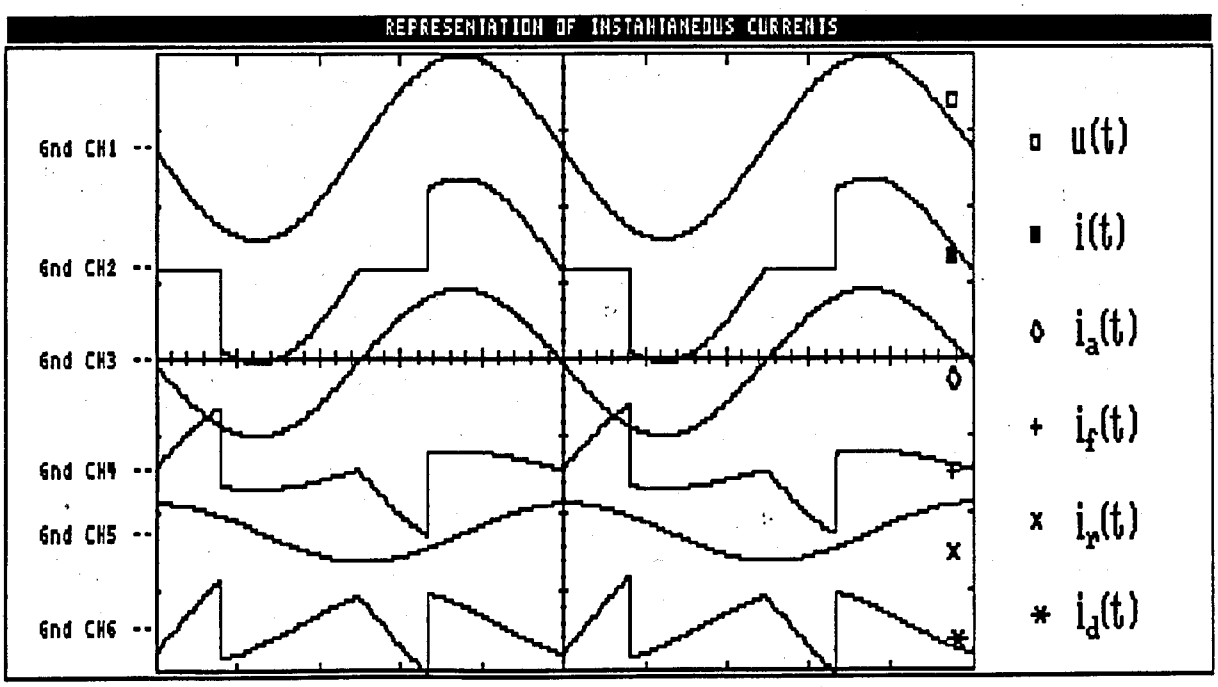

(b) Instantaneous Current Representations

Fig. 3.21: Simulation of Anti-parallel Thyristor-resistance Network with $\alpha = 60°$

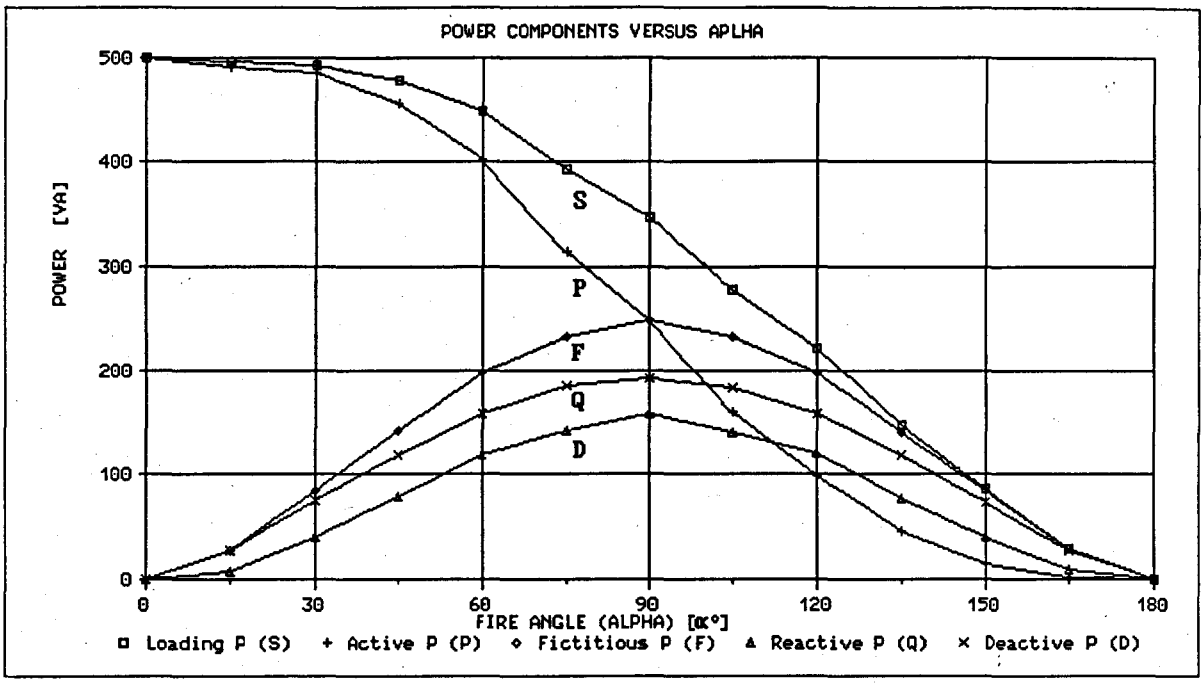

Fig. 3.22: Power Components in an Anti-parallel Thyristor-resistance Network versus Firing Angle α

3.13 EXTENSION OF THE POWER DEFINITION TO MULTIPHASE SYSTEMS

The principle of conservation of energy establishes that the total active power in a multiphase system must be equal to the algebraic sum of the active powers in the individual phases. Furthermore the active power dissipated in the equivalent conductance must be equal to the active power supplied. The total active power in a multiphase system can therefore be calculated either by the summing of the active powers in the individual phases algebraically or by measuring the power transfer along the power lines [A127]. If the total fictitious power in a multiphase system, and therefore also the total reactive and deactive power, is however calculated by summing the fictitious, or reactive or deactive powers in the individual phases algebraically, anomalities arise under conditions of unbalanced and unsymmetrical waveforms [A32,35,40,115,127]. Furthermore there are different methods for the calculation of loading power in m-phase systems [A127]:

(a) Vector total = $\sqrt{(\Sigma P_n)^2 + (\Sigma F_n)^2}$, where P_n is the active power in phase n and F_n is the fictitious power in phase n.

(b) Arithmetic total = $\Sigma U_n I_n$, where U_n and I_n are the effective values of the n-0 phase voltage and associated line current respectively.

(c) Equivalent copper-loss total = $U.\sqrt{[\Sigma I_n^2 + I_0^2]}$ where U is the effective value of the line voltage (assumed symmetrical) and I_n is the effective value of the current in line n and I_0 is the effective value of the neutral current.

These three methods yield identical results under balanced conditions, but increasing values in the order (a), (b), (c) in the presence of an unbalance. In the presence of unsymmetrical voltages, the results are even more adversely affected.

For this study the total active, fictitious, reactive, deactive and loading power are calculated as shown beneath:

$$S = \sum_{n=1}^{m} S_n \text{; where } S_n \text{ is the loading power in phase n} \quad (3.48)$$

$$P = \sum_{n=1}^{m} P_n \text{; where } P_n \text{ is the active power in phase n} \quad (3.49)$$

$$F = \sum_{n=1}^{m} F_n \text{; where } F_n \text{ is the fictitious power in phase n} \quad (3.50)$$

$$Q = \sum_{n=1}^{m} Q_n \text{; where } Q_n \text{ is the reactive power in phase n} \quad (3.51)$$

$$D = \sum_{n=1}^{m} D_n \text{; where } D_n \text{ is the deactive power in phase n} \quad (3.52)$$

The equivalent parameter circuit described in paragraph 3.8 can be adapted to multiphase systems. It should, however, be pointed out that the equivalent parameters may have values different to those in the separate phases when the power supply is unsymmetrical. Depenbrock [A35, D1] subdivided the equivalent network into a symmetrical and unsymmetrical portion. This is however not sustained here for reasons of complexity.

Each phase has a separate combination of equivalent network parameters with the values determined in the same way as

described in the previous paragraphs; the parameters are again calculated from the measured effective values of voltage and current and calculated power components.

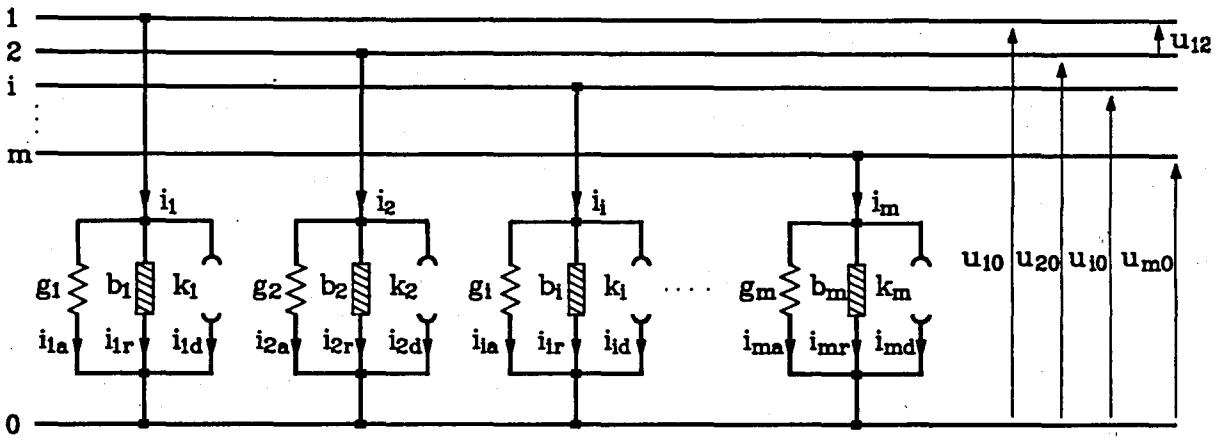

Fig. 3.23: Equivalent Network Parameters in Multiphase Power Systems

3.14 **SUMMARY**

This chapter is devoted to the proposed definition of electric power under generalized conditions of voltage and current. This definition is formulated over a measurement interval dT and has meaning only over this measured time interval dT. The length of this time interval is chosen with the dynamic response of the power network being analysed, in mind and should be adapted to the dynamic system response. To have comparable results in periodic voltage and current systems, multiples of fundamental periods have to be analyzed or real-time processors, calculating continuous cross-correlations, should be implemented.

The generalized definition is described in terms of equivalent network parameters, which describes the power phenomena of the circuit unambiguously. The network is described by means of a generating function and a loading function, the loading function being dependent on the load characteristics, analysed in terms of the equivalent conductance, susceptance and disceptance. The conductance describes the phenomenon of the transfer of a net amount

of energy from source to load, the susceptance the equivalent of oscillation of energy between source and load and the disceptance the uncorrelation phenomena of the network, normally characterized in terms of a non-linear load.

Instantaneous current waveforms are derived for the representation of the power flow through the network and the control of fictitious power. The instantaneous currents and equivalent network parameters are derived from the average power components and average equivalent network parameters after the measurement interval has elapsed. The way in which distortion penetrates a power network is described in terms of an equivalent network admittance resulting in the distortion of the generating function shared by multiple users. The generalized definition is shown to be accurate in the analysis of characteristic voltage and current waveforms and is superior in power systems with non-sinusoidal and in general aperiodic waveforms of voltage and/or current. Figure 3.24 shows a schematic representation of the division of loading power into the different power components.

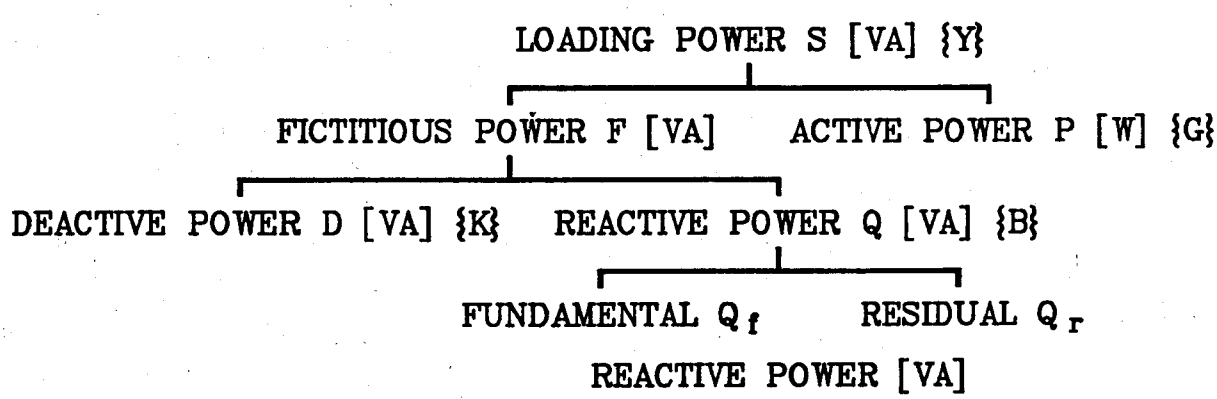

Fig. 3.24: Schematic Representation of Loading Power Division

This definition will be used in the measurement system described in chapter 4. Furthermore the possibility of effective fictitious power compensation, by using this approach, will be pointed out in chapter 5. The derivation of the instantaneous currents is still problematic because the definition is based on average values and therefore there are multiple possible instantaneous current representations.

CHAPTER 4

MEASUREMENT OF ELECTRIC POWER USING THE PROPOSED DEFINITION

4.1 INTRODUCTION

Several possibilities have arisen in the effort to measure voltage and current signals, calculate the different power components and the equivalent load parameters of the power network and divide the power into its orthogonal load related components. The fundamental requirement is to calculate the different power quantities directly in the time domain, from the measured voltage and current signals and to do it in the shortest possible time. In dynamic power filtering, chapter 6, the prerequisite for real-time measurement and signal processing calls for a rather sophisticated measurement and signal processing system.

Real-time measurement of average power is, however, contradicting in principle, because average power can only be measured after some time has elapsed, and any real-time calculation of power components is therefore at least one time window old. In systems where it is considered to use dynamic power filters for dynamic power compensation, real-time power measurement is a fundamental prerequisite. In chapter 5 adaptive signal processing is proposed and evaluated for the measurement and control of these systems. For the purpose of power definition evaluation and general power measurements, on-line, but not necessarily real-time, measurements are required. In this chapter, different on-line measurement and computation systems are described and evaluated, with special reference to digital signal processing (DSP) techniques. The experimental measurement system, used in this study, is based on a time domain digital signal processing technique. Attention is also paid to frequency domain techniques, in order to be able

to compare the different power definitions and analyse the effects of distortion on power apparatus.

To evaluate the proposed definition of electric power in power conditioning systems, a personal computer based measurement system has been developed. This basic measurement system consists of a combination of analogue and digital signal processing circuits, also used as a control system for the dynamic power filter, discussed in chapter 6. This system is used to evaluate the power definition's usefulness for fictitious power compensation, but is not proposed in the final control system, because the system is not capable of real-time power component calculation.

In dynamic power filter applications where real-time measurement and calculation of power components and parameters are fundamental prerequisites, dedicated digital signal processing systems are necessary. Some basic characteristics of a Texas Instruments TMS 320 based digital signal processing system are also discussed in this chapter [H2,20,22, A96].

4.2 POWER MEASUREMENT WITH ANALOGUE SIGNAL PROCESSING TECHNIQUES

The analogue effective value meters and analogue electro dynamic wattmeters, used for power measurement in systems with sinusoidal voltage and current waveforms, are examples of early analogue measurement systems and give very accurate results under these conditions. With distorted waveforms, these measurement systems are inadequate and systems using a combination of analogue and digital electronic circuits were investigated [A59,63,87,135, 137]. The majority of these systems uses the instantaneous values of voltage and current to calculate the effective and average values with dedicated analogue integrated circuits. These systems have response times of between 100 ms and 3 s.

A different approach for the calculation of power components with analogue electronic circuits, was adopted by Harashima [A81], Filipski [A60] and Page [A113] and a more complex approach by Schwan [A119,D8]. Both of these approaches make use of the prin-

ciple of orthogonal current division to measure the different power components, with associated response times between 40 ms and 2 s.

4.2.1 Conventional Measurement Systems

Since the end of the previous century, power has been measured with an electro dynamic instrument, the well known wattmeter. This instrument consists of one or two fixed coils and one moving coil. The output torque is proportional to the average value of the product of current in the moving coil, current in the fixed coil and the phase angle between the two currents. The current in the one coil is calibrated for voltage, while the other is proportional to the network current. The meter is therefore calibrated to read active power (W).

This instrument is normally calibrated for frequencies between 40 Hz and 60 Hz. Inaccurate results are obtained when current and voltage signals are non-sinusoidal. The loading power is calculated from the product of the effective values of current and voltage, measured accurately with electro dynamic instruments.

There are a lot of problems associated with this type of instrumentation, especially in energy and power metering in power networks [A71]. Inaccurate results have been obtained by Electricity Supply Utilities under conditions of non-sinusoidal current and voltage waveforms [A91].

Some later electronic instruments take the time product of instantaneous current and voltage and have an averaging output, which gives better results for non-sinusoidal current and voltage waveforms. With this approach only active and loading power can be measured [H21, A59].

4.2.2 Orthogonal Current Division

Another measurement approach with analogue techniques, or in some cases a combination of analogue and digital techniques, is the application of the original time domain definition of power according to Fryze, where the current waveform is divided into the orthogonal components i_a and i_f as shown in eq. (4.1) [A60,61,69,81,119].

This measurement system was developed by Harashima [A81], Page [A113] and Filipski [A60]. Schwan [A119,D8] used the division of Depenbrock [A35] as basis for the development of an orthogonal current divider calculating all the Depenbrock current components, as described in reference A34 and paragraph 1.6.2.2. The Schwan system is very complex, being based on microprocessor controlled digital electronics, to reduce the calculation time. The Harashima system, described in paragraph 6.4, is used in dynamic power filter control. These approaches are in principle equivalent and involve orthogonal current division.

The Filipski and Page device, which is a simpler configuration, consists of only two multipliers, a summation circuit, a high gain amplifier with gain K and a low-pass filter with a long filter constant τ [A60,113]. Orthogonality is obtained with the low-pass filter which limits the dynamic response of this measurement system. Figure 4.1 shows a functional block diagram of the orthogonal current divider developed by Filipski and Page. The voltage u(t) is fed to the multipliers A_1 and A_2. After the active current $i_a(t)$ has been calculated from the equivalent conductance G, the load current i(t) is diferentially summed with the calculated active current $i_a(t)$, to form the fictitious current $i_f(t)$. The gain K has to be very high for satisfactory operation. Mathematically the divider is evaluated as follows:

$$\begin{aligned} i_a(t) &= G.u(t) \\ i_f(t) &= i(t) - i_a(t) \\ \overline{i_a.i_f} &= 0 \qquad \text{with conductance } G = K.\epsilon \end{aligned} \tag{4.1}$$

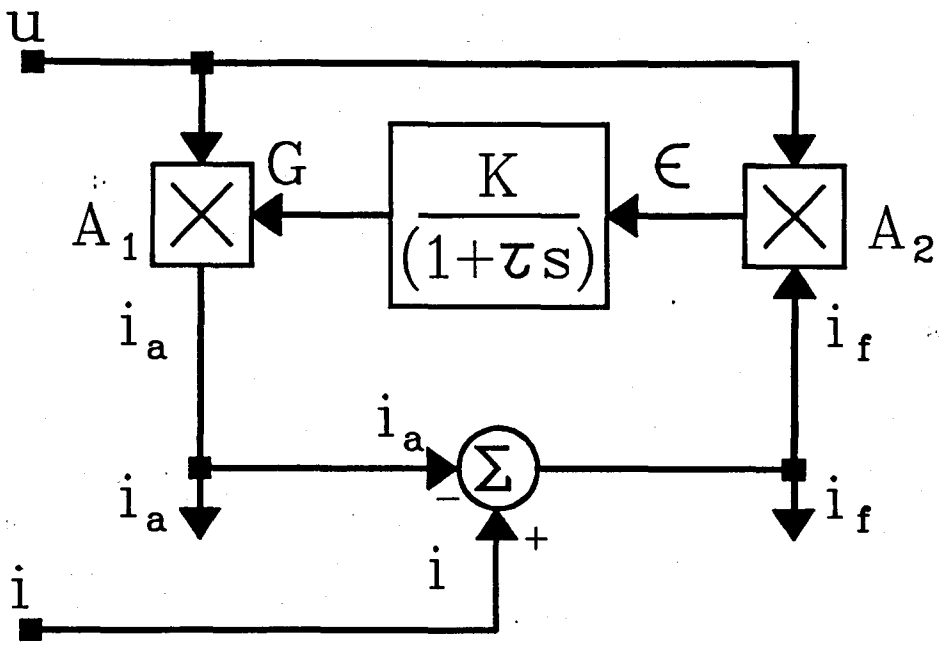

Fig. 4.1: Current Divider According to Filipski and Page

If the gain K is assumed to be very high, the error signal ϵ approaches zero. The error is derived from the following expression:

$$\epsilon = \overline{u.(i - G.u)} \approx 0 \qquad (4.2)$$

$$\Rightarrow \quad G.U^2 = \overline{u.i} \equiv P$$

$$G = P/U^2 \qquad (4.3)$$

Equation (4.3) is equivalent to the conductance G in any network. The average value of the product of conductance G and instantaneous voltage u(t) therefore gives the instantaneous active current $i_a(t)$, which corresponds with the Fryze definition [A69]. The products of the effective values of the current components and the voltage result in the different power components as shown in eq. (4.4).

For the subdivision of fictitious current $i_f(t)$ into other orthogonal components, Filipski proposed a Hilbert transform [A61], after the generalized definition of Nowomiejski [A108,9] (Paragraph 1.6). The Hilbert transform, shown in eq. (4.5), results in a function orthogonal to the argument throughout the full frequency spectrum of the signal and the

same effective value as the argument (Appendix A4). The subdivision of fictitious current into reactive and deactive current by means of the Hilbert transform and two orthogonal current dividers, equivalent to one shown in fig. 4.1, is shown in fig. 4.2 in block diagram form. This system incorporates two orthogonal dividers O_1 and O_2 and a Hilbert transform of the voltage H{u}. The Hilbert transform was realized by Filipski with the aid of phase shift circuits, tuned to specific harmonics [A61]. Equation (4.4) shows how the power components are calculated from the effective values of all above-mentioned currents and the network voltage.

$$S = I.U; \quad P = I_a.U; \quad F = I_f.U; \quad Q = I_r.U; \quad D = I_d.U \qquad (4.4)$$

$$H\{u\} = \frac{1}{\pi} \int_{-\infty}^{+\infty} \frac{u(\tau).d\tau}{\tau - t} \qquad (4.5)$$

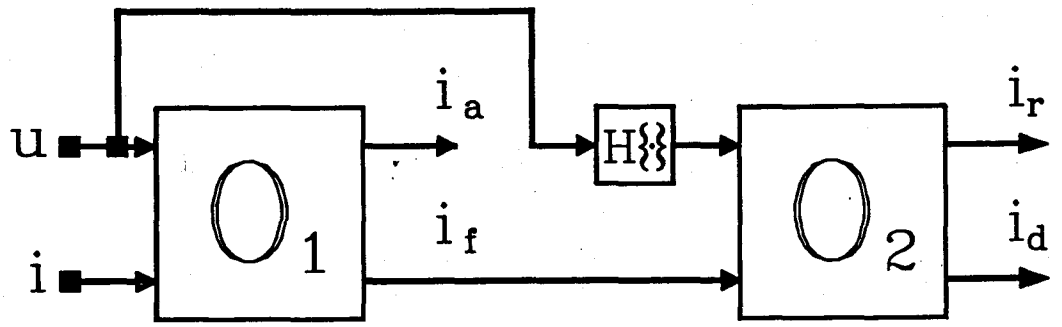

Fig. 4.2: Full Orthogonal Current Divider

The current $i_f(t)$ is the fictitious current, $i_r(t)$ the reactive current and $i_d(t)$ the Nowomiejski distortion current. The results obtained with the PC-based measurement system, employing the proposed definition, agree with the Filipski results for characteristic waveforms under steady state conditions and where the voltage (generating function) is a sinusoidal waveform [A61,D4].

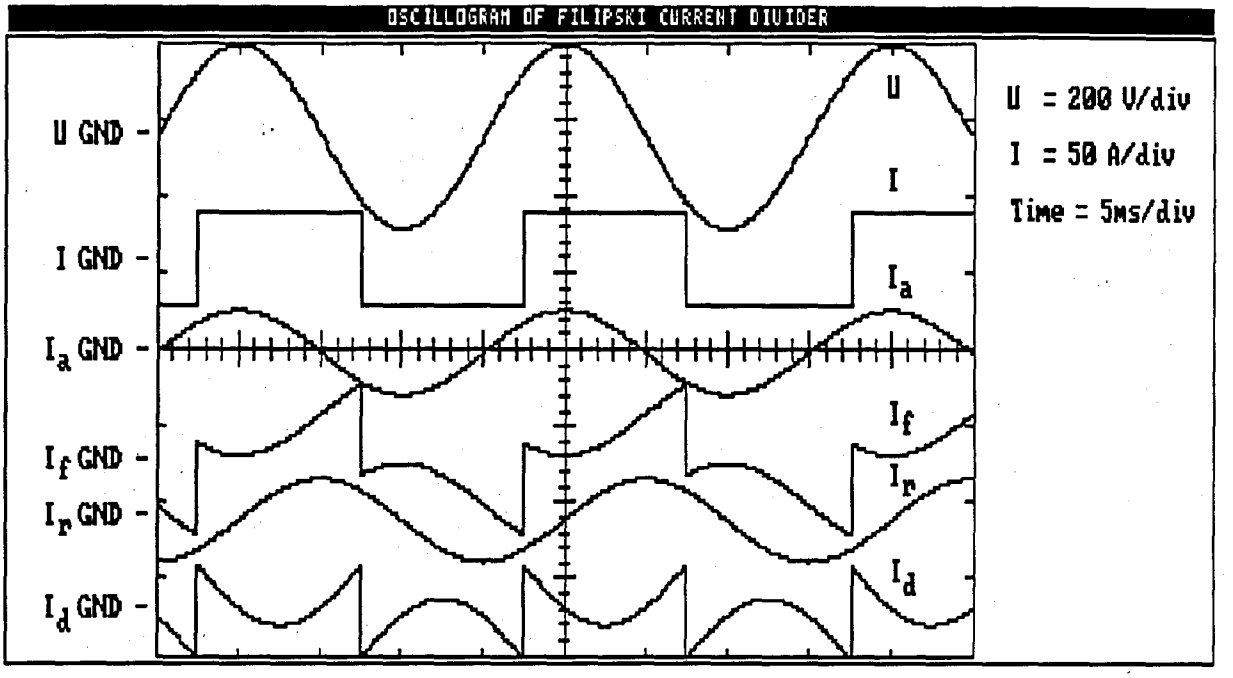

(a) Oscillogram of Filipski Decomposed Current Components

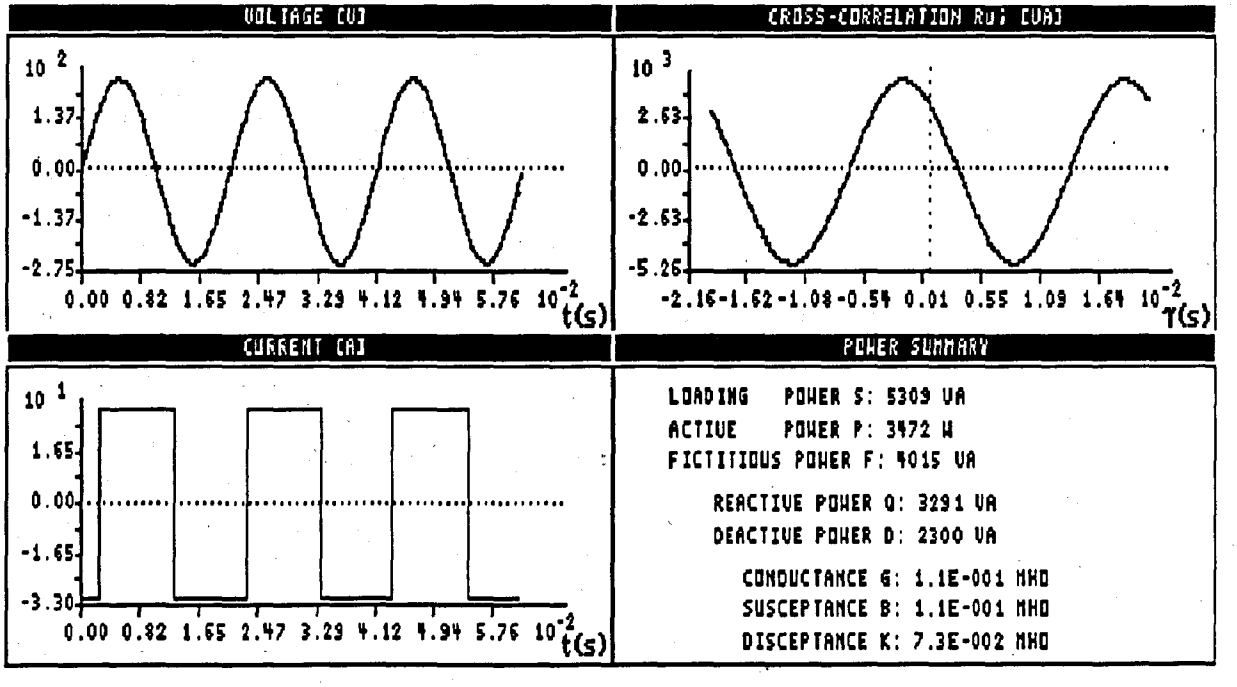

(b) Power Components Analysed with Proposed Approach

Fig. 4.3: Experimental Results from the Filipski Division

This system has been evaluated experimentally with a result shown in fig. 4.3(a) [D3]. The Hilbert transform is responsible for the orthogonal division of i_f into i_r and i_d. Figure 4.3(a) shows a sinusoidal voltage and a square wave current with the fundamentals of voltage and current phase shifted by 45°. Using the first orthogonal current divider O_1 from fig. 4.2, i_a and i_f are derived, as shown in fig. 4.3(a). The second current divider O_2 and the Hilbert transform H{u} are used to derive i_r and i_d. Comparing this result with fig. 3.12(b) shows that the same results are obtained from the Filipski divider and the proposed time domain approach, if the voltage is a sinusoid. The Hilbert transform is responsible for the fact that inconsistent results are obtained when the voltage is non-sinusoidal, see fig. 3.13(c). The same waveforms, as in fig. 4.3(a), are analysed with the proposed time domain approach from chapter 3. The analysed result is shown in fig. 4.3(b). This result corresponds with the Nowomiejski calculations from eq. (4.4). In practical terms, it is difficult to keep the Hilbert transform well tuned, furthermore the bandwidth is limited to the tuned harmonics [A61].

Because of its simple design and low component count this Filipski orthogonal current division system, without the Hilbert transform, is also incorporated in a control system for dynamic power filters, where it is used together with a digital signal processing system (chapter 6). Under steady state conditions, accurate results are obtained [D5].

4.3 POWER MEASUREMENT WITH DIGITAL SIGNAL PROCESSING TECHNIQUES

Digital sampling wattmeters, which make use of fast A/D converters and high performance low cost microprocessors, can be used for relatively accurate power measurements in power systems with non-sinusoidal periodic voltage and current waveforms. These instruments use equally spaced samples of current and voltage and either a Fast Fourier Transform (FFT) in the frequency domain or time averaging techniques directly in the time domain; there are

two schools of thought. In existing systems [A59], the minimum measurement time needed for reliable results is typically between 2 and 100 fundamental voltage periods, with a calculation time of several seconds.

Some other systems use dedicated instruments, for example spectrum analysers and control computers, to measure the frequency spectra of the voltage and current signals and calculate the power components from these frequency spectra, directly in the frequency domain [A135,137,143]. Algorithm times of between 2 and 3 s have been achieved [A143], while an average algorithm time is between 0,1 and 2 minutes [A135,137].

The proposed time domain definition, chapter 3, is illustrated by means of a personal computer based measurement system. This system uses a time domain digital signal processing correlation algorithm, unlike the normal frequency domain FFT algorithm. The present PC-based system has a total algorithm time of 5 s and no hardware signal processing circuitry is employed. It uses a time window of 3 fundamental periods and has a resolution of 200 samples per fundamental period. This setup can be varied, but if accuracy is improved calculation time will be impaired and vice versa. The basic system uses a 150 MHz digital storage oscilloscope as digitizer at 8-bit resolution, which implies that the measurement system can be used to analyse high frequency power electronic converters as well as typical 50 Hz power systems [A48,50,51,53,54, D3,4].

4.3.1. Power Measurements in the Frequency Domain

In the frequency domain approach, sophisticated instrumentation is needed for accurate measurements of the power components. These systems normally use the Budeanu concept of electric power under non-sinusoidal conditions, with the associated limitations (paragraph 1.6) [H16, A13,14,87,135, 137,143]. One of the more serious limitations is the fact that the fundamental period of the waveforms must be known before a frequency domain approach can be adopted. Because

this approach needs sophisticated instrumentation capable of very fast FFT algorithms, it was 50 years after Budeanu had defined the power components, before on-line measurement equipment, using dedicated spectrum analysers, were developed [A135,137,143].

Typical instrumentation consist of a hardware spectrum analyser and a control computer. The spectrum analyser must have two channels capable of amplitude and phase spectrum analysis. The computer is normally used to control the equipment and to compute the power components in the different harmonics of the current and voltage signals. High bandwidth current and voltage probes are essential to measure the high frequency components. The current probe normally uses the Hall-effect to measure all components from dc to 5 MHz. Figure 4.4 shows a block diagram representation of a typical instrumentation system for the measurement of power in a non-sinusoidal load with the frequency domain approach [A143].

In aperiodic signals, it is however impossible to find a fundamental frequency and therefore this technique is inadequate for accurate power measurements under dynamic conditions, or where aperiodic currents or voltages are observed. Furthermore the fundamental frequency drift within any power system causes these techniques to give inaccurate results. Even a small mismatch on the measurement window can give catastrophic results. Windowing of data does make the results more acceptable [H1], but these systems can be used properly only under steady state conditions. Furthermore, the calculated values of the power components can be incorrect, even under steady state conditions [A20-27].

A single FFT takes a long time in terms of real-time compensation techniques (typically longer than 20 ms with dedicated spectrum analysis techniques) and no results can anyway be obtained before at least one period of a 50 or 60 Hz signal has elapsed. The measurement window should also be exactly synchronized with the fundamental period, otherwise

the results will be inaccurate. Because of the finite computation time and the mathematical interpretation of the FFT approach, real-time compensation techniques can not be controlled explicitly by measurements obtained in the frequency domain [A143].

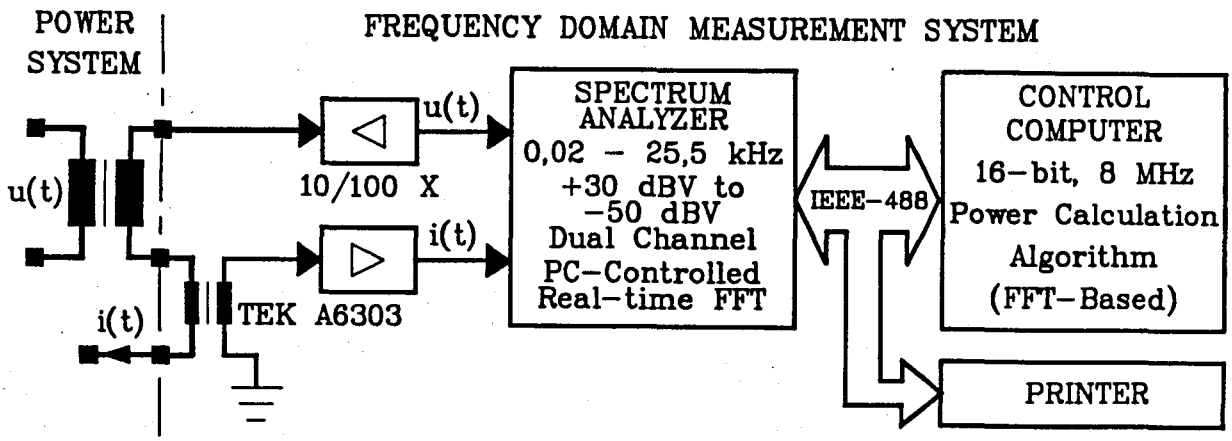

Fig. 4.4: Typical Instrumentation in the Frequency Domain Approach [A143].

For the reasons stated above, the frequency domain approach is not completely acceptable for the majority of power measurements. However, frequency domain analysis techniques can provide a lot of insight into power factor compensation and filter design and also information regarding distortion analysis [H1, A104,123,130-135,137,143,147]. Therefore it is from the author's point of view necessary to define power in both the time domain and the frequency domain. In cases where both approaches are defined, for example in systems with steady state periodic waveforms of voltage and current, they should then give consistent results.

4.3.2 Personal Computer Based Measurement System

The developed time domain measurement system consists of a current and a voltage probe, a digitizer and an AT-compatible personal computer with a digital time domain signal processing algorithm. Signals of voltage and current are measured and digitized and these sampled waveforms are

transported via an IEEE-488 interface bus to the personal computer. The different power components and parameters are then calculated by means of this digital signal processing algorithm. This basic measurement system is adaptable to a variety of measurement applications, because of the PC-based control and the high-level language based software algorithm.

4.3.2.1 Schematic diagram of the measurement system.

Figure 4.5 shows a schematic diagram of the current and voltage probes, the digitizer and the personal computer with the digital signal processing algorithm. The current probe is an active Tektronix A6303 Hall element based transducer and matching amplifier with a bandwidth of 5 MHz. Currents of up to 100 A can be measured over this bandwidth. The normal 10 or 100 times attenuated companioning Tektronix oscilloscope probe, with a nominal capacitance of 15 pF, is used as voltage probe. This probe is capable of measuring voltages of up to 2,2 kV. The 150 MHz Tektronix 2430 digital storage oscilloscope is used as digitizer. The sampling rate of this oscilloscope is a function of the timebase setting, with a record length of 1024 samples per window. The oscilloscope has 8-bit resolution with simultaneous sampling of both channels and an effective bandwidth of 40 MHz per channel.

The oscilloscope is connected to an AT-compatible personal computer via the National Instruments IEEE-488 interface bus, which is controlled from the Turbo Pascal high level computer language. This interface bus has an effective throughput rate of 1 MHz, with a real-time clock for synchronization purposes. The AT-compatible personal computer used in this analysis, is a Hewlett Packard VECTRA computer with a 80286 based microprocessor and a numerical 80287 co-processor under an adapted MS-DOS 3.1 operating system. The time domain digital signal processing algorithm has been

written in TURBO PASCAL Ver. 3, using the numerical co-processor with an adapted Turbo Graphics library for the graphics display.

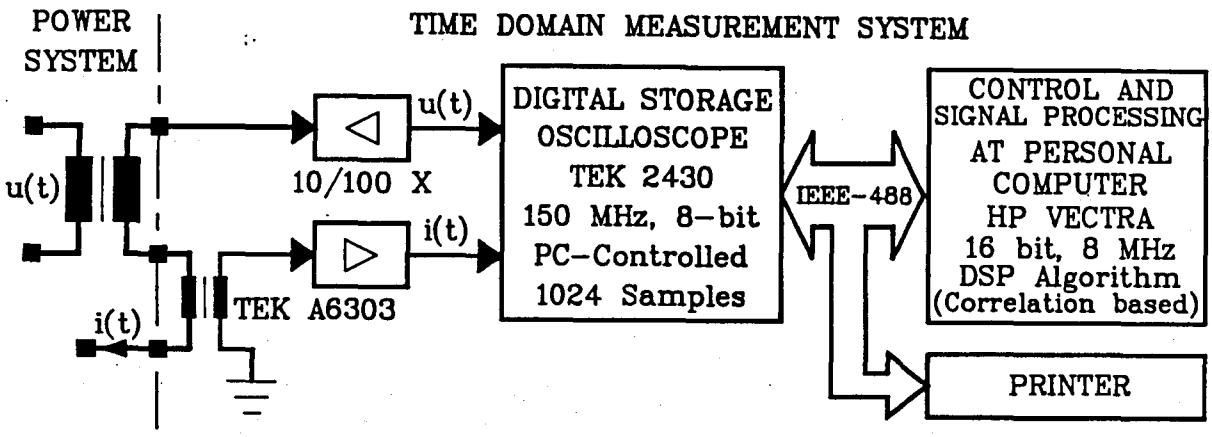

Fig. 4.5 : Schematic Representation of PC-based Measurement System

4.3.2.2 Software computer algorithm.

It has been shown in chapter 3 that power can be calculated with correlation techniques in the time domain. This PC-based measurement system uses a digital auto- and cross-correlation algorithm to calculate the different power components and parameters. The digital cross-correlation $R_{ui}[j]$ is given in eq. (4.6), while the digital autocorrelations of voltage $R_{uu}[j]$ and current $R_{ii}[j]$ are shown in eq. (4.7) and (4.8) respectively (Appendix A4).

$$R_{ui}[j] = 1/N \sum_{k=0}^{N-1} U[k].I[k-j] \qquad (4.6)$$

$$R_{uu}[j] = 1/N \sum_{k=0}^{N-1} U[k].U[k-j] \qquad (4.7)$$

$$R_{ii}[j] = 1/N \sum_{k=0}^{N-1} I[k].I[k-j] \qquad (4.8)$$

$$j = -N+1 \ldots N-1$$

where N is the number of samples

The autocorrelation is used to calculate the effective values of voltage and current and from them the loading power, while the cross-correlation is used to calculate active and reactive power. Deactive power is then calculated with the orthogonality principle from the other components. The different network parameters are then derived from the calculated power components (chapter 3). This basic algorithm is shown in block diagram form in fig. 4.6. $\hat{R}_{ui}[j]$ is the maximum value of the digital cross-correlation over the measurement window dT.

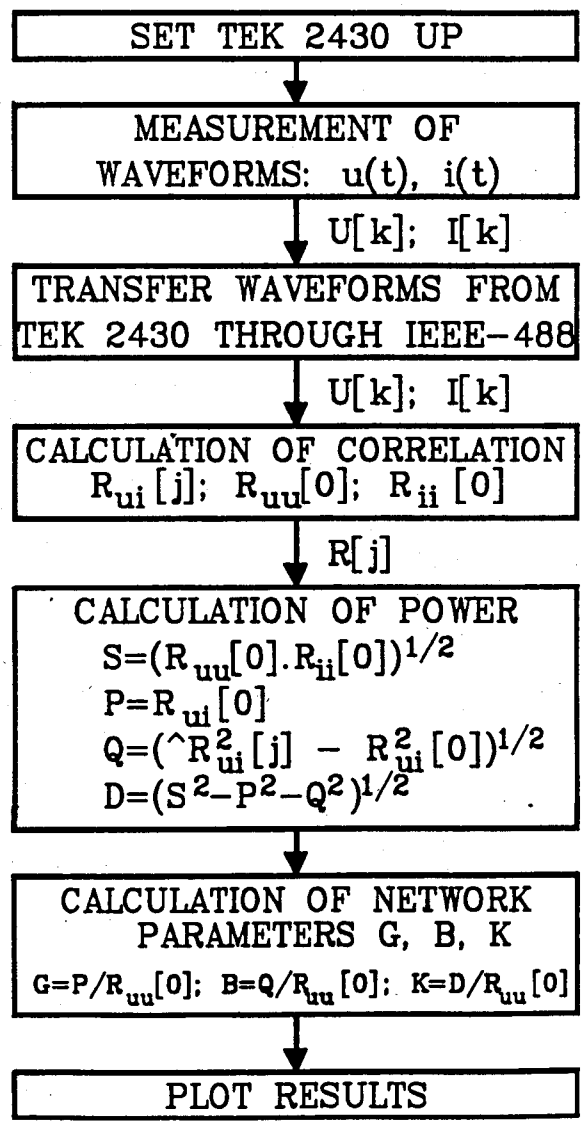

Fig. 4.6 : Time Domain DSP Algorithm implemented in the PC-Based Measurement System.

The details of the software Pascal program is shown in Appendix B1. In the analysis of the measurement algorithm calculation time, it is evident that the longest time is consumed by the digital cross-correlation algorithm (4 sec.). The shortening of this calculation time is a fundamental requirement.

4.3.3 Dedicated DSP Microprocessors

The PC-based system described in the previous paragraph has some severe limitations in applications where real-time measurements are a fundamental requirement, for example in the control system of a dynamic power filter. By "real-time measurements" is meant that the power components are calculated on-line in such a way that the total measurement, data acquisition and power components calculation time, is at least an order of magnitude smaller than the measurement time window dT. This implies that when the measurement time window is in the order of 50 - 100 ms, then the total measurement and calculation time should be smaller than 5 - 10 ms.

This calls for a rather sophisticated calculation and power measurement system, which should be capable of high speed signal processing. Of all the signal processing microprocessors available, only a few dedicated processors adapted to high speed signal processing can therefore be used to realize such a system, in applications of real-time measurements.

When the time domain algorithm discussed in the previous paragraph is analysed, it is found that the longest processing time is needed for performing the digital correlation. This correlation algorithm consists of multiplications and summations, which can very easily be implemented with digital techniques within dedicated DSP microprocessors. Some digital signal processing processors have a very fast internal analogue multiplying architecture. This makes it possible to do a correlation, with reasonable resolution,

within a few hundred microseconds. One of these families of processors is the Texas Instruments TMS 320 series which has a separate hardware implemented 16 x 16 bit parallel multiplier, capable of performing a 16 x 16 bit multiplication within one clock cycle (100 ns for the TMS 320C25) [H22, A96]. This makes it possible to do a full 64 point correlation within 400-500 microseconds [H2,20]. Again an improvement in the resolution will impair the calculation time and vice versa.

The Texas Instruments TMS 320 family of DSP microprocessors has found a vast number of applications during recent years. These applications include voice processing, telecommunication modems, control systems, instrumentation and others where high speed signal processing is a fundamental requirement [H2,20,22, A96]. Two generations of the TMS 320 series are already available and a third is in the development phase [H22, A96].

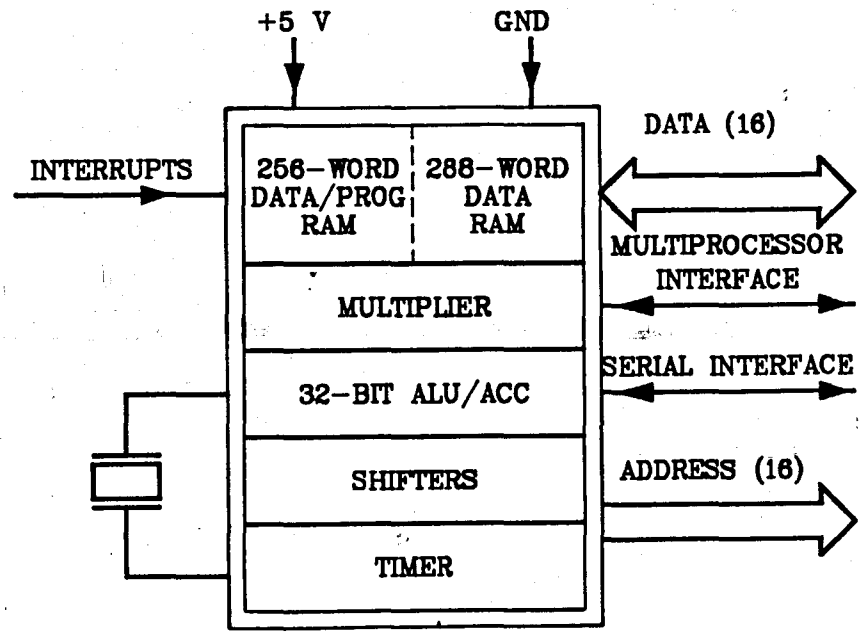

Fig. 4.7: Block Diagram Representation of the TMS 320C25 DSP-Processor Architecture

The second generation includes two products, the TMS 32020 and TMS 320C25, where the C25 has a higher clock speed (40 MHz), an instruction cycle of 100 ns and an extended in-

struction set. A block diagram representation of the TMS 320C25 processor is shown in fig. 4.7 (Courtesy of Texas Instruments) [H22, A96].

This TMS 320C25 is a 16-bit addressable, 16-bit data line processor and has a 32-bit accumulator with an integrated hardware multiplier, capable of a 16 X 16 bit multiplication in one 100 ns instruction cycle. Parallel processing is a standard feature with the multi-processor interface circuitry. The TMS 320 series is backed up by development tools and championed by third party software and hardware [H22].

The following schematic representation applies to the real-time measurement of the defined power components, which forms an integral part of the control system of a dynamic power filter.

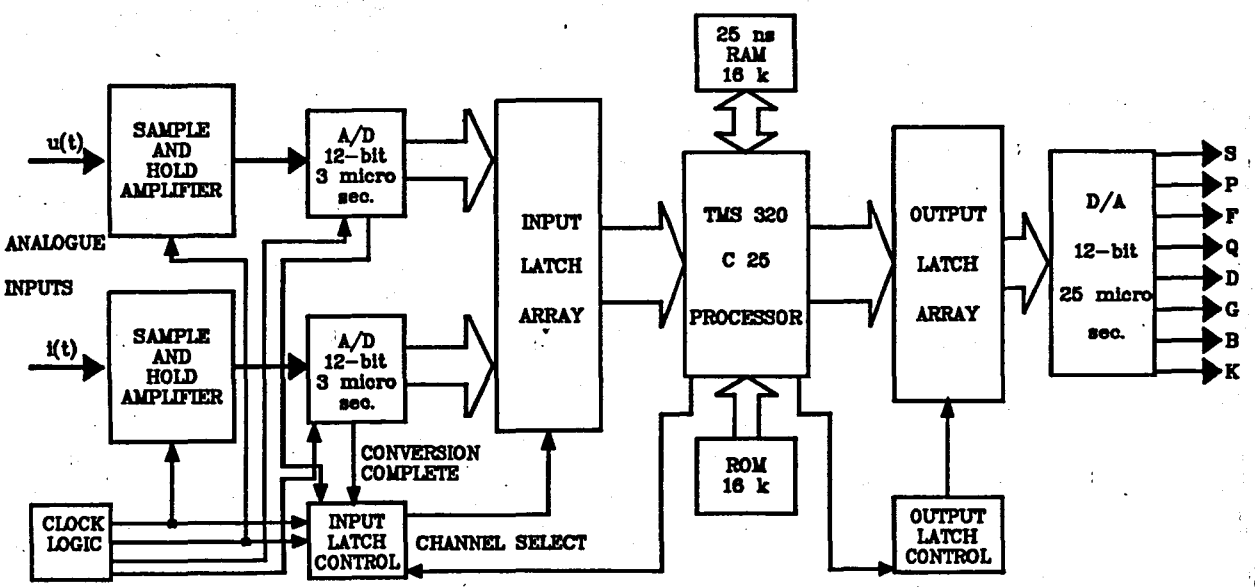

Fig. 4.8: Schematic Representation of TMS 320 Based Measurement System

The TMS 320 is responsible for the processing of the voltage u(t) and current i(t) input signals. Twin A/D devices should be incorporated for maximum conversion speed. The resolution of the converter is also of primary importance. The output of the system is sent through a 12-bit D/A converter. To obtain the final analogue outputs of the different power components and network parameters, one must employ either

several D/A converters of medium conversion speed in parallel or an output multiplexer.

4.4 POWER MEASUREMENT WITH SURFACE ACOUSTIC WAVE (SAW) DEVICES

Correlation can be very time consuming in digital signal processing algorithms, even when implemented with dedicated DSP-microprocessors. Techniques to do fast correlations without microprocessors, are therefore also investigated for real-time power measurement applications. For this reason a real-time correlator in the form of a Surface Acoustic Wave (SAW) mechanical correlator is investigated. At this stage, the solutions offered by dedicated signal processing integrated circuits and optical electronics do not seem practicable, because of high costs and high component count associated with it [H2,20, D8]. However in the future to come optical processing systems seem to be an alluring proposition.

Surface Acoustic Waves (SAW) [H19, A107] are used in high-frequency signal processing applications for example chirp FFT or pulse compression microwave filtering, FM chirp filtering, delay lines in digital filtering and high-frequency oscillators, to name only a few. The major advantages of SAW technology are the simplicity of the signal transformer design and its low cost.

A basic SAW converter consists of two mechanical resonators or interdigital transducers (IDT), which are manufactured by metallised thin film techniques, deposited onto piezoelectric substrates, to form the basic mechanical signal processor. The transition of signals through these devices is directly coupled to their physical dimensions. The mechanical wavelength of the comb resonator is given in eq. (4.9).

$$\Gamma_o = v/f_o \qquad (4.9)$$

where Γ_o is the mechanical signal wavelength [m],
v is the SAW plane velocity [m/s] and
f_o is the signal frequency [Hz]

The fundamental constraints and possible experimental realization of a SAW-based power signal correlator are described in Appendix A2. The basic structure of a SAW correlator is shown in figure 4.8. The in-line convolving plate electrode between the input and output IDT's forms the summing device, while the other two IDT's form the delay line to obtain the shift in the correlation function. Multiplication is done on the substrate between the two direct IDT's.

The output of the SAW-correlator is sent through a low pass filter (LPF) to give the cross-correlation between the voltage and current signals. To get the average power, it is necessary to average the correlation output over a longer time span. The surface acoustic wave seems to be an attractive proposition in real-time power measurement. It appears to be necessary to have some form of memory device to be able to average the device output in order to calculate the power components over a longer time span (Appendix A2).

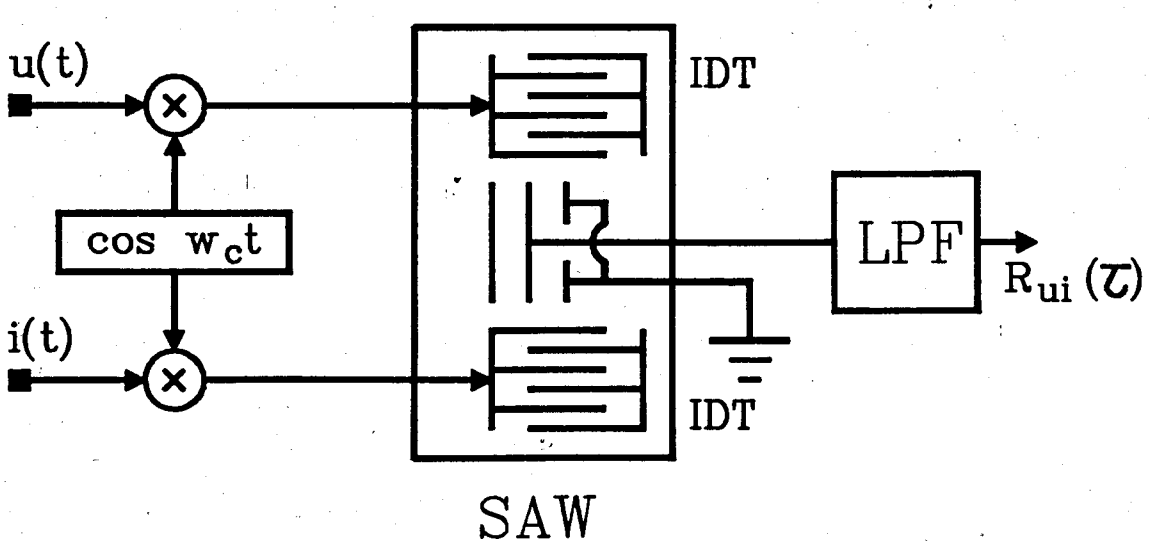

Fig. 4.9 : Block Diagram Representation of a SAW Power Convolver in a Correlation Application.

To derive the loading power S with a SAW-device, the same structure as in figure 4.9 can be used, the only difference being that an autocorrelation is performed. This means that both input signals will be voltage or both will be current. All the power components defined in chapter 3 can therefore be obtained by realiz-

ing cross- and autocorrelation with SAW-technologies. The SAW-cross- and autocorrelation devices can be coupled to a fast digital signal processing microprocessor to calculate power directly. It is even possible to model a Kalman filter as a power network parameter estimator, as described in paragraph 6.4.4.

4.5 EXPERIMENTAL TIME DOMAIN RESULTS OBTAINED FROM POWER ELECTRONIC CONVERTERS

Different power electronic circuits have been analysed with the proposed definition, using the PC-based measurement system described in the previous paragraph. The analysed systems include 50 Hz supply commutated converters as applied in light dimmers, space heater controllers and variable speed electric machine drives. Converters with forced commutated power switches and high-frequency link power stages as applied in AC-machine drives and Uninterruptable Power Supplies (UPS).

4.5.1 Phase Controlled In-cycle Power Controller

A schematic diagram of a power converter based on an in-cycle control strategy is shown in fig. 4.10.

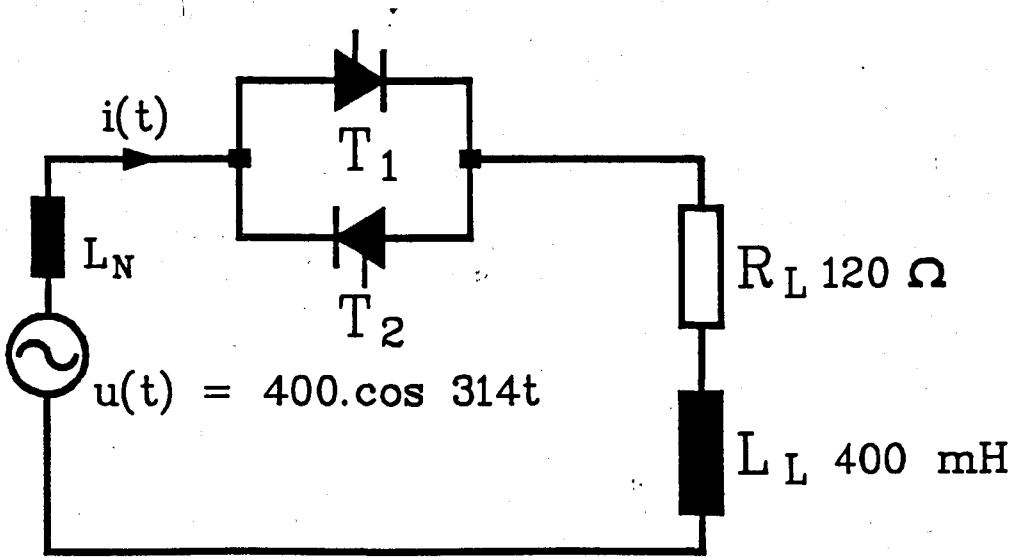

Fig. 4.10: In-cycle Supply Commutated Power Converter

The converter consists of two 800 V, 10 A thyristors, T_1 and T_2, in anti-parallel, a sinusoidal 50 Hz voltage generating function with 10 mH equivalent source impedance, resulting from the isolation transformer, and a complex R-L load. Some simulations of this circuit are included in chapter 3, fig. 3.21 and 3.22. The experimental results obtained from this system are shown in fig. 4.11 - 4.14. The experimental system is a converter rated at 250 V, 2 kVA designed for space heating. The control strategy has been designed for in-cycle as well as burst power control.

Figure 4.11 shows the results obtained when the converter is loaded with a complex R-L load and the fire angle α is set to 60°. The same setup, but without the inductive portion of the load, gives rise to the results shown in fig. 4.12.

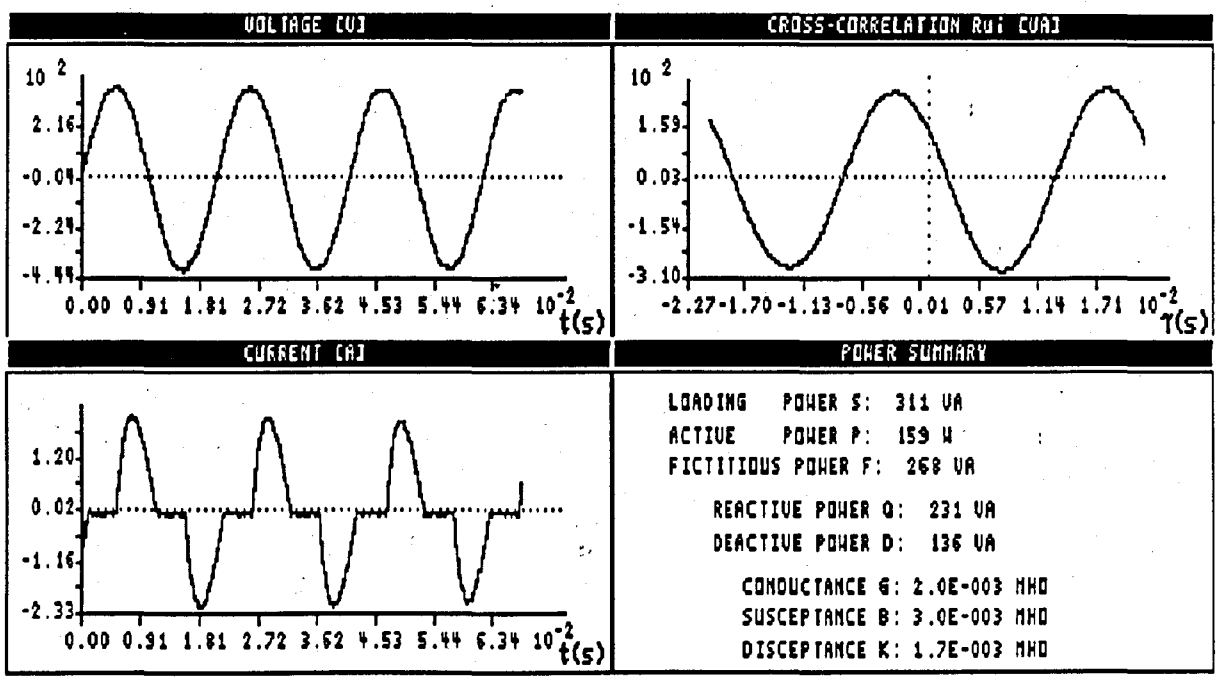

Fig. 4.11: Analysis of In-cycle Converter with Complex R-L Load under Steady State Operating Conditions

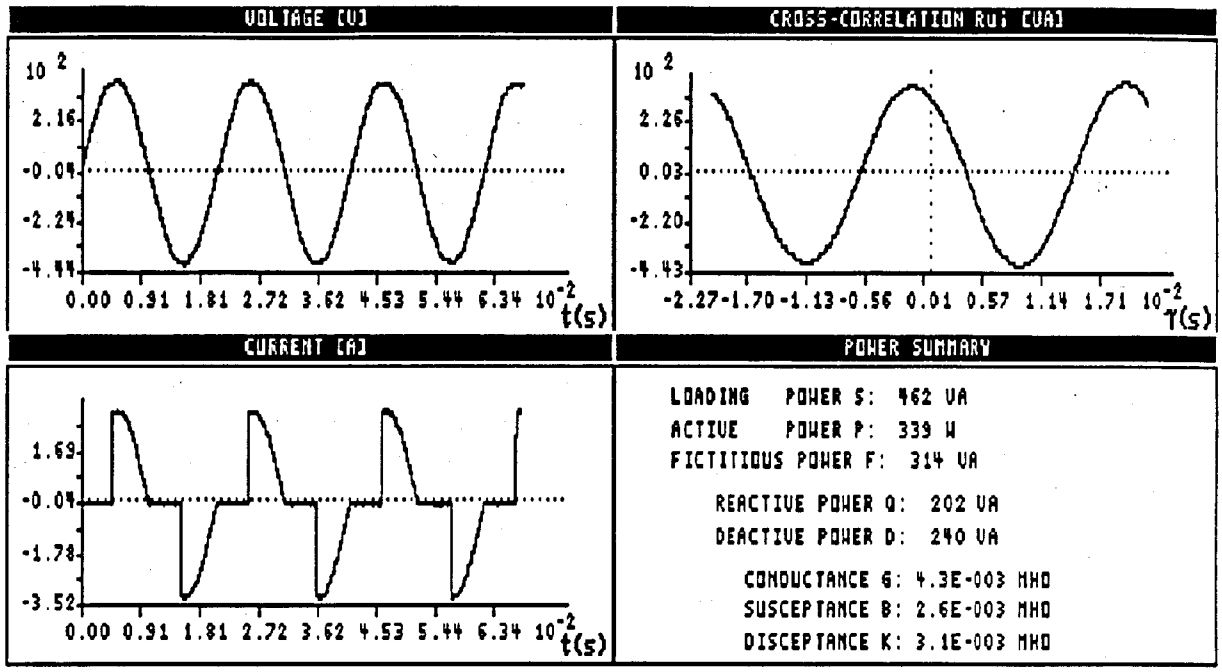

Fig. 4.12: Analysis of In-cycle Controller with Resistive Load under Steady State Operating Conditions

When fig. 4.12 and fig. 4.11 are compared, it is clear that more deactive power with more active power and loading power is analysed. Percentage wise, less deactive power is analysed in fig. 4.11, because the waveforms are more correlated in fig. 4.11 than in fig. 4.12. The fire angle α is responsible for the reactive power analysed in fig. 4.12. These phenomena correspond with the power waveform simulations performed in chapter 3. Figure 4.13 and 4.14 show the operation of the converter under dynamic operating conditions. The fire angle α is controlled dynamically to give the outputs shown in the figures below. The results are again obtained with and without the inductance L_L in the load.

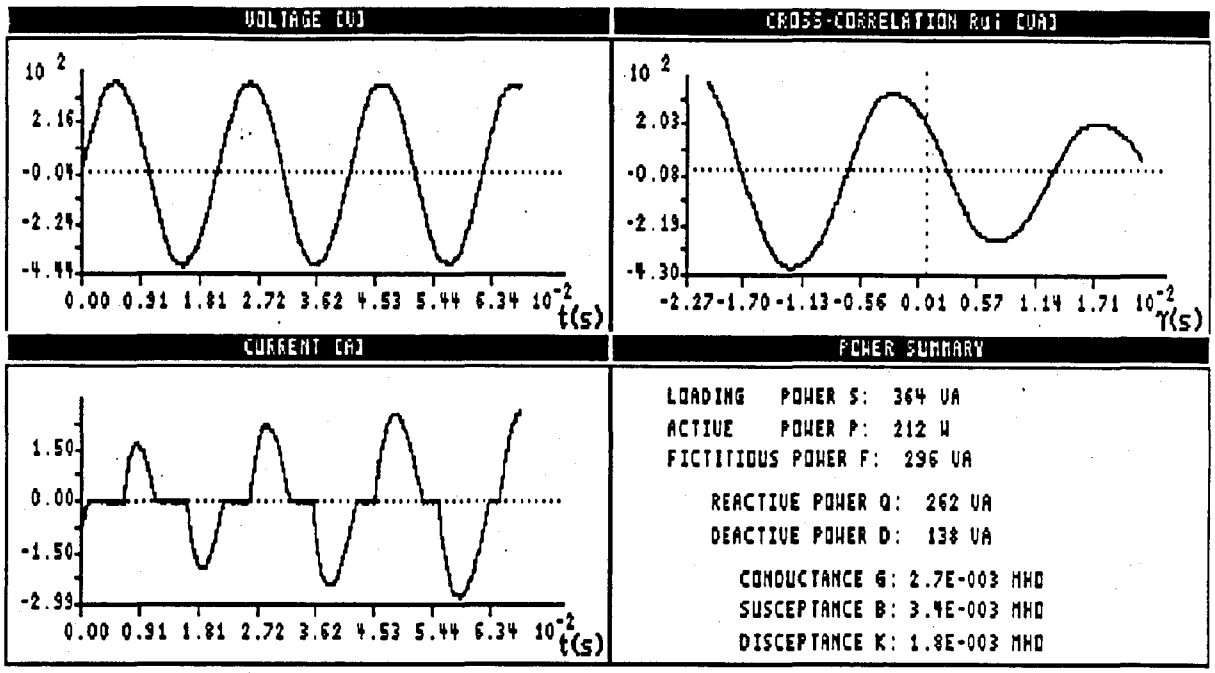

Fig. 4.13: Analysis of In-cycle Converter with Complex R-L Load under Dynamic Operating Conditions

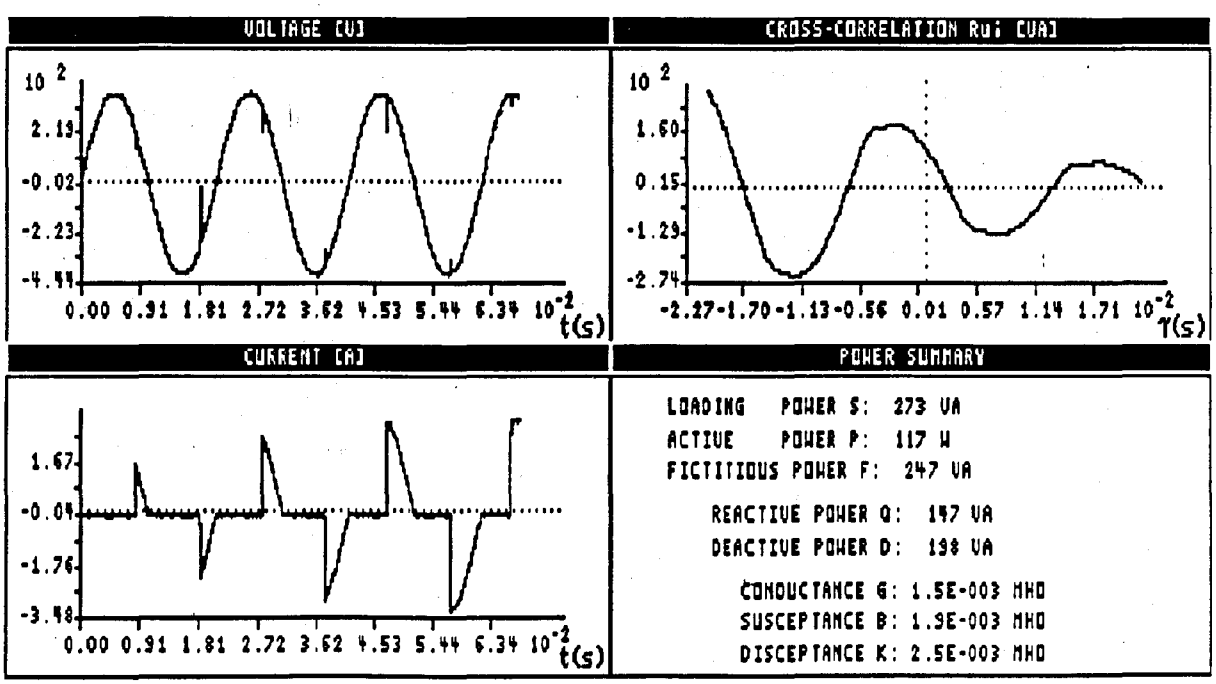

Fig. 4.14: Analysis of In-cycle Converter with Resistive Load under Dynamic Operating Conditions

Any time window can be used for the calculation of the different power components, but the best results will be obtained when the measurement interval corresponds with the time constant of the dynamic system response. In the above-mentioned case, 5-10 fundamental voltage periods seems to be an appropriate choice.

4.5.2 Phase Controlled Six-Pulse DC-Drive Converter

DC-machine drives are well-known and used extensively in high-power speed control machine drive applications. A 100 kW DC-machine with a 93 kVA brushless synchronous machine, has been used in the analysis of the distortion generated by typical six-pulse, supply commutated, phase controlled power converters.

Figure 4.15 shows the schematic diagram of the DC-machine drive. The synchronous machine SM is used as load for the DC-machine DCM, which is operated as motor in the first power quadrant. The speed of the DC-machine is controlled by a phase controlled six-pulse power converter rated at 120 kVA. The equivalent network reactance, consisting mainly of a step-down transformer leakage inductance, has been measured as 1 mH. The link inductance consists of the DCM armature inductance only and has been measured as 4 mH. The supply has a line voltage of 400 V and an equivalent reactance of 1 mH. The DCM has a constant 300 V field excitation, while the brushless SM has a 60 V controlled excitation. The SM is loaded with a 3 Ω, 3 ϕ load resistance.

The voltage and currents in this system has been simulated in chapter 3, fig. 3.17 and 3.18. In the experimental analysis, the phase voltage u_{TN} and line current i_T have been measured as shown in fig. 4.16. The familiar six-pulse current and voltage with noticeable commutation spikes have been obtained.

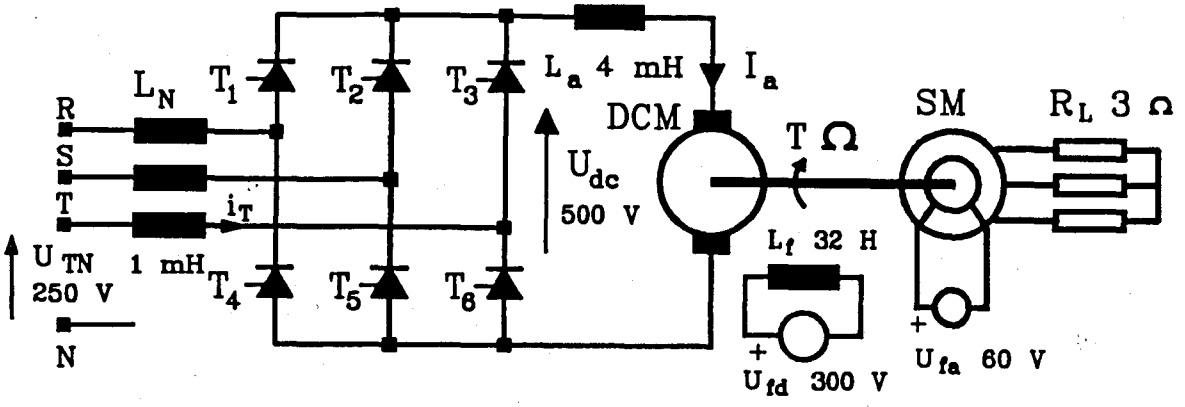

Fig. 4.15: Schematic Diagram of DC-machine Speed Drive

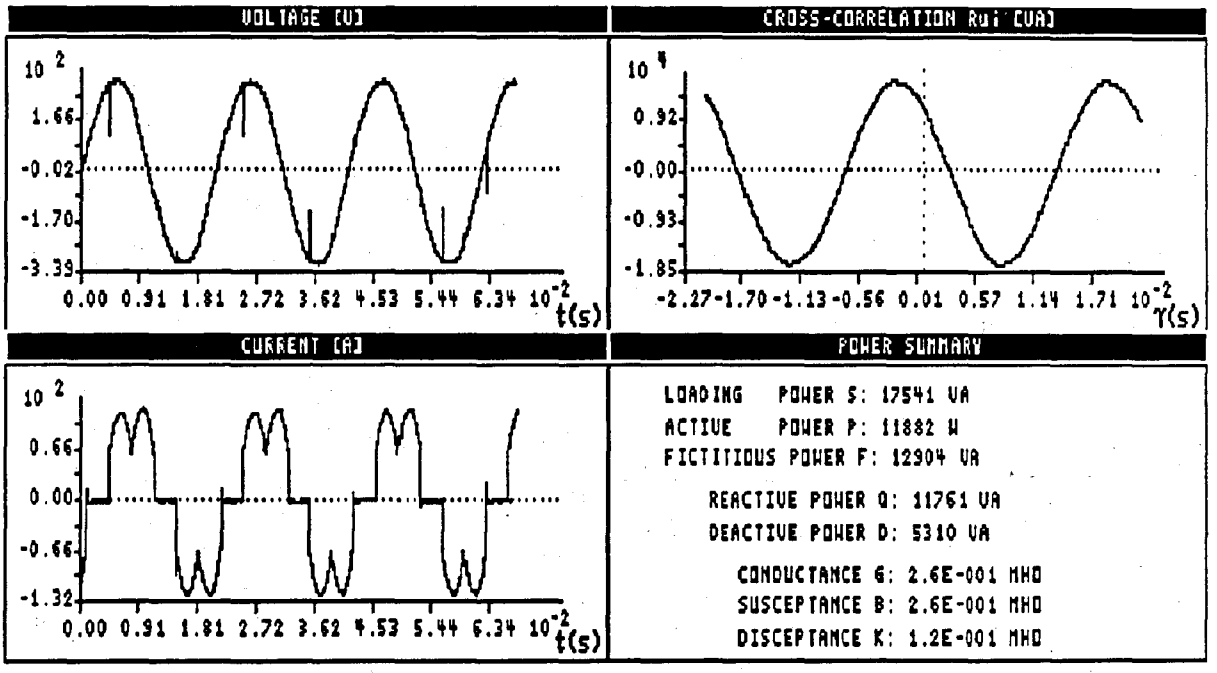

Fig. 4.16: Distortion Analysis of the Six-pulse DC-machine Drive

From fig. 4.16, it is clear that the fictitious power is higher than the active power. Reactive power forms the major portion of this fictitious power because of the 42° fire angle α, while the relatively small amount of deactive power is the result of the uncorrelated waveforms. Phase controlled circuits generally generate less deactive power than reactive power, which is distinctly advantageous for the compensation of fictitious power in these converters: the deactive power can generally be compensated for by means of

deactive power compensation systems with lower ratings than their reactive power peers (chapter 5,6).

4.5.3 Voltage-Fed Asynchronous Machine Drive

In resent years, AC-machine drives, especially induction machine speed drives, have become very popular as small to medium size industrial machine drives. The speed of squirrel cage induction machines can be controlled most effectively by controlling the stator voltage frequency proportional to the desired speed and keeping the air gap flux constant at the same time [H9,13, A142]. This implies that at speeds lower than synchronous speed, the frequency of the rotating air gap field should be reduced with an associated decrease in applied stator voltage to ensure constant flux operation. On the other hand, increased speeds are associated with higher field frequencies and higher stator voltages.

This control strategy implies that the magnitude and frequency of the stator voltage should be changed proportionally. Recent AC-drive designs incorporate current-fed inverters (CFI) with forced commutated PWM machine side converters and supply commutated or forced commutated PWM line side converters [A142]. The supply commutated line side converters give rise to the same distortion characteristics as those shown in fig. 4.15 and 4.16. Older AC-machine drives with lower power ratings normally implement voltage-fed converters with link choppers controlling the voltage links and line side uncontrolled rectifiers. Such a design is shown in fig. 4.17.

A 50 Hz power supply with a line voltage of 400 V and a equivalent network reactance of 3 mH, primarily associated with an isolation transformer, is used for the voltage-fed converter. The power converter consist of a 5 kVA induction machine coupled to a 4 kW DC-machine and fed from a 5 kVA voltage-fed power electronic converter. The voltage-fed converter consists of a three phase uncontrolled rectifier, a down-chopper and a voltage-fed inverter.

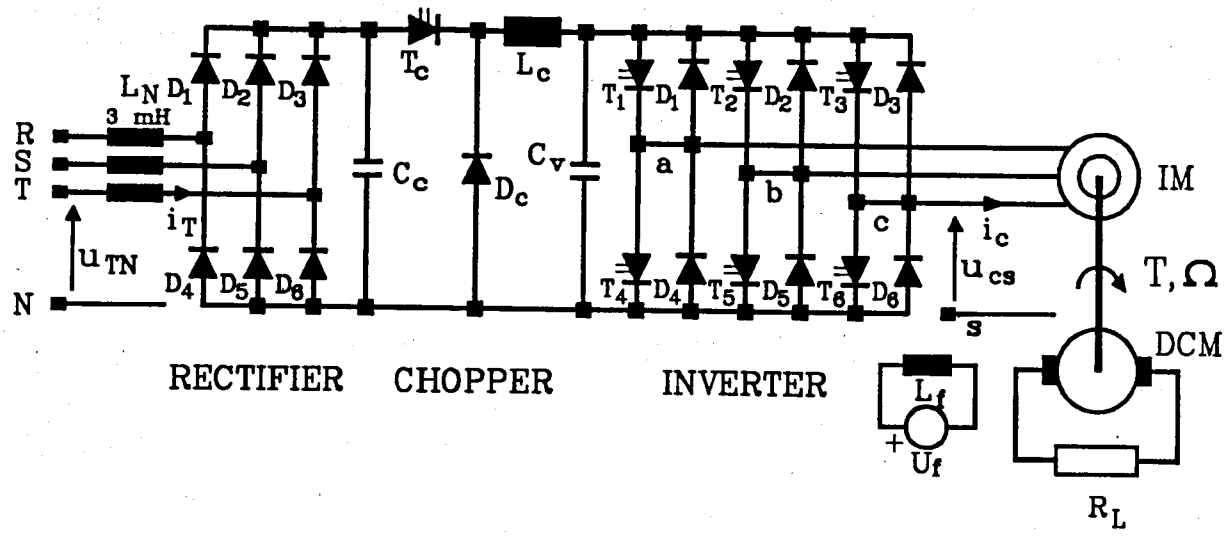

Fig. 4.17: Voltage-fed Induction Machine Drive

Distortion analysis has been performed both on the supply side and on the machine. The distortion analysis on the supply side, u_{TN} and i_T, is shown in fig. 4.18, while the distortion analysis on the machine side, u_{cs} and i_c, is shown in fig. 4.19.

A simulation of the six-pulse voltage-fed converter is shown in chapter 3. The supply voltage deviates from the fundamental sinusoidal because of the highly distorted current and high equivalent source reactance. Because of the capacitor C_c, coupled to the output of the rectifier, the current has the uncharacteristic waveshape, shown in fig. 4.18. Furthermore, the fundamental current is nearly in phase with the fundamental voltage, with only a small amount of reactive power resulting from the leading fundamental current. The fictitious power is mainly the result of uncorrelation between the voltage and current signals. This distortion is furthermore uncharacteristic due to the aperiodic current waveshape and can therefore be compensated for only by means of a dynamic power filter, chapter 6. The current waveform is aperiodic even under steady state mechanical load conditions, because of the mismatch between supply and machine frequencies.

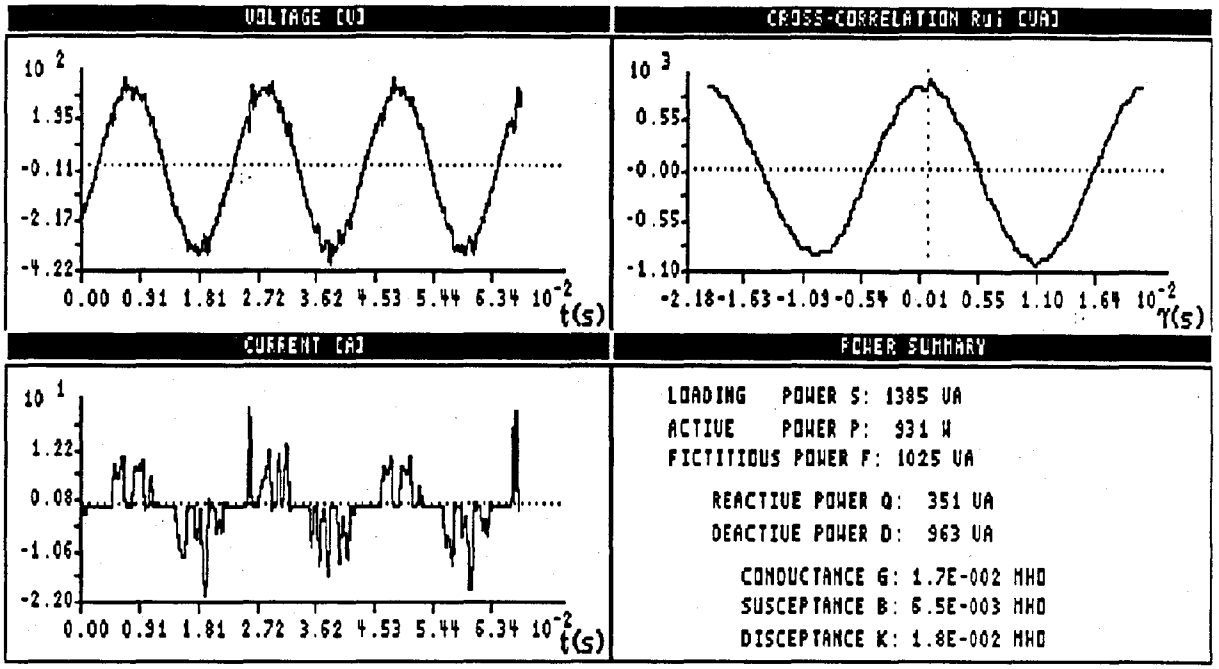

Fig. 4.18: Supply-Side Distortion with Voltage-fed Induction Machine Drive

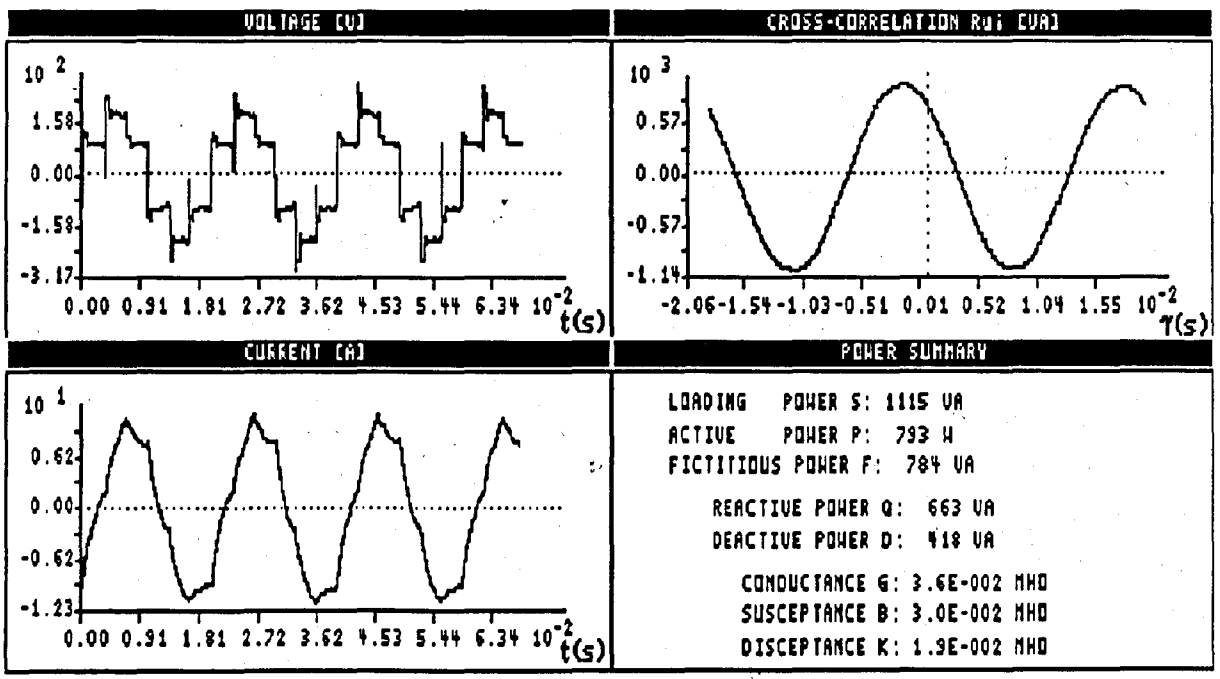

Fig. 4.19: Machine-Side Distortion with Voltage-fed Induction Machine Drive

Figure 4.19 shows the distortion analysis under the same steady state operating conditions, but on the machine side. In fig. 4.19, the current i_c and the voltage u_{cs} are correlated. In this analysis the majority of the fictitious power is the result of the magnetizing reactance of the induction machine, which is responsible for the lagging line current. The line voltage has the familiar six-pulse characteristic, with some commutation spikes clearly visible. The phase voltage and current are plotted in fig. 4.19 to calculate the phase power quantities. A comparison between fig. 4.18 and 4.19, shows that there is a decrease of 270 VA in loading power and a decrease of 140 W in active power, this is the result of losses in the converter. A comparison between the utilization factors results in the following:

		Line Side :	Machine Side
Total Power Factor :-	$\Gamma = P/S$	0,67	0,71
Displacement Factor :-	$\Gamma_r = Q/S$	0,25	0,60
Uncorrelaton Factor :-	$\Gamma_d = D/S$	0,70	0,38

From this comparison it is clear that the distortion on the line side is mainly the result of the non-linear characteristics of the current, causing uncorrelation between the voltage and current waveforms. Distortion on the machine side is the result of a reactive element, more specifically the machine's magnetizing and leakage inductance.

4.5.4 Scherbius Rotor Cascade Asynchronous Machine Drive

Cascaded wound rotor induction machines have been used in early slip recovery speed drives for induction machines. In new developments with forced commutated solid state converters, this type of drives has been discarded to some extent because of more complicated machine structures. In renewable energy converters, especially Variable Speed Constant Frequency (VSCF) converters for wind or hydro turbine alternators, this drive configuration is very interesting [A140]. One of the major advantages of this type of drive is that the configuration can, with a simple one quadrant rotor

cascade converter, operate collectively as an induction motor and an oversynchronous induction generator, which is ideal for wind and hydro turbine applications. Furthermore only half of the rated power passes through the rotor cascade power electronics during generator operation at a speed to twice synchronous speed [A140].

Such a converter, based on the well known Scherbius rotor cascade induction machine drive, is shown schematically in fig. 4.20. The 9 kVA induction machine is stator-fed from a 400 V, 50 Hz supply. The induction machine slip power is fed through a 4,5 kVA uncontrolled rectifier RB and inverted back to the 50 Hz supply by means of a supply commutated current-fed inverter IB. The rotor power is sent through a step-up transformer, which is not shown to simplify the diagram. The drive is loaded by a DC-machine with parallel field excitation.

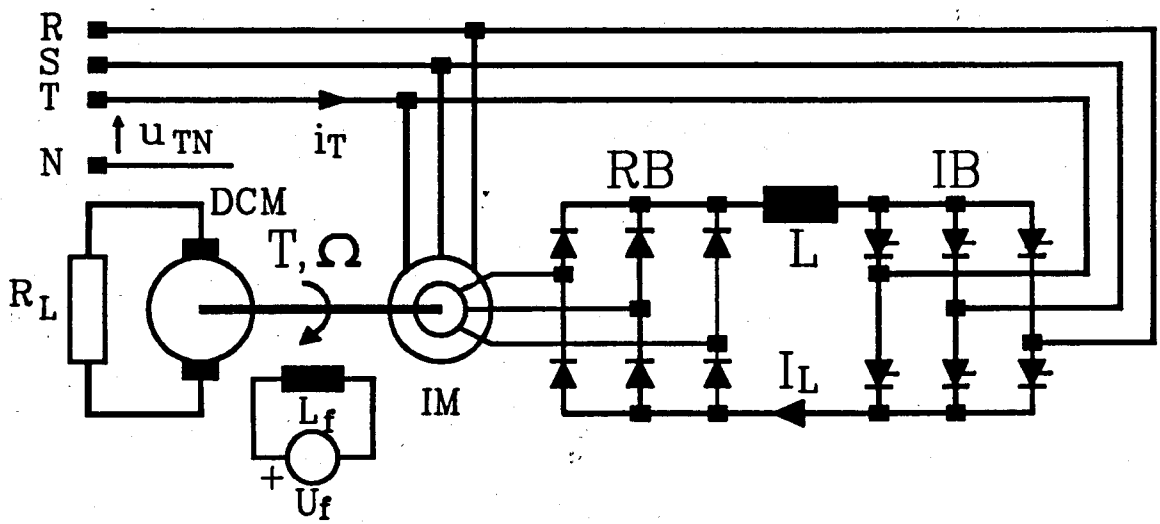

Fig. 4.20: Schematic Diagram of a Scherbius Rotor Cascade Induction Machine Drive

The analysis is shown in fig. 4.21. The current i_T and voltage u_{TN} are correlated, resulting in the characteristic per phase distortion shown in fig. 4.21. The phase controlled rotor inverter is responsible for the high value of the reactive power present in the fictitious power. The deactive power is, as is normally the case with phase controlled circuits, small in comparison with the reactive power.

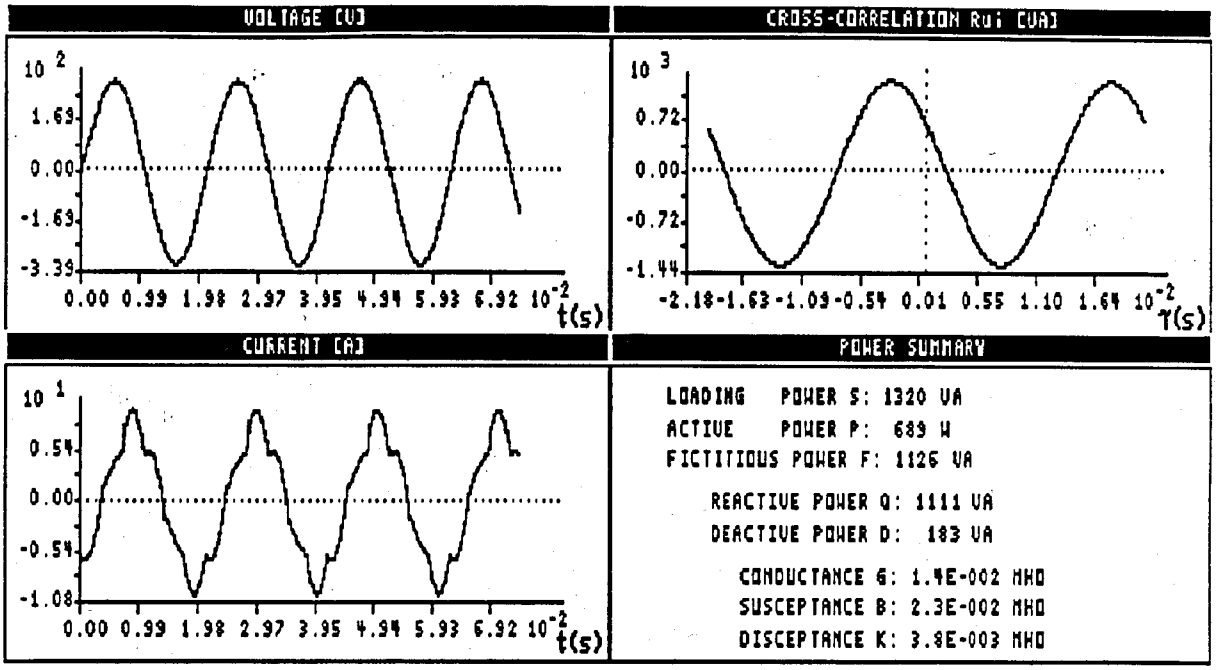

Fig. 4.21: Distortion Analysis of Scherbius Cascade Induction Machine Drive

4.5.5 High-Frequency Link Power Converter Systems

In the search for converters which generate less distortion, high-frequency link converters seem to be an alluring proposition [A49,142]. These converters normally consist of a high-frequency (1-100 kHz) link, generated by means of a forced commutated inverter from a DC-bus. This high-frequency link voltage is normally converted to a variable or fixed low-frequency voltage (0-100 Hz). The applications of these converters include variable speed AC-drives, uninterruptable power supplies and frequency changers [A49,142].

This converter type can be used in multiple configurations, shown in block diagram form in fig. 2.1, chapter 2. Figure 4.22 shows a typical primary converter, while fig. 4.24 represents the secondary converter, configured as a high-frequency cyclo-converter [A49,142]. The total block diagram of this type of converter is shown in fig. 2.1(c). Distor-

tion analysis has been done on the primary and secondary converters shown in fig. 4.22 and 4.24 respectively.

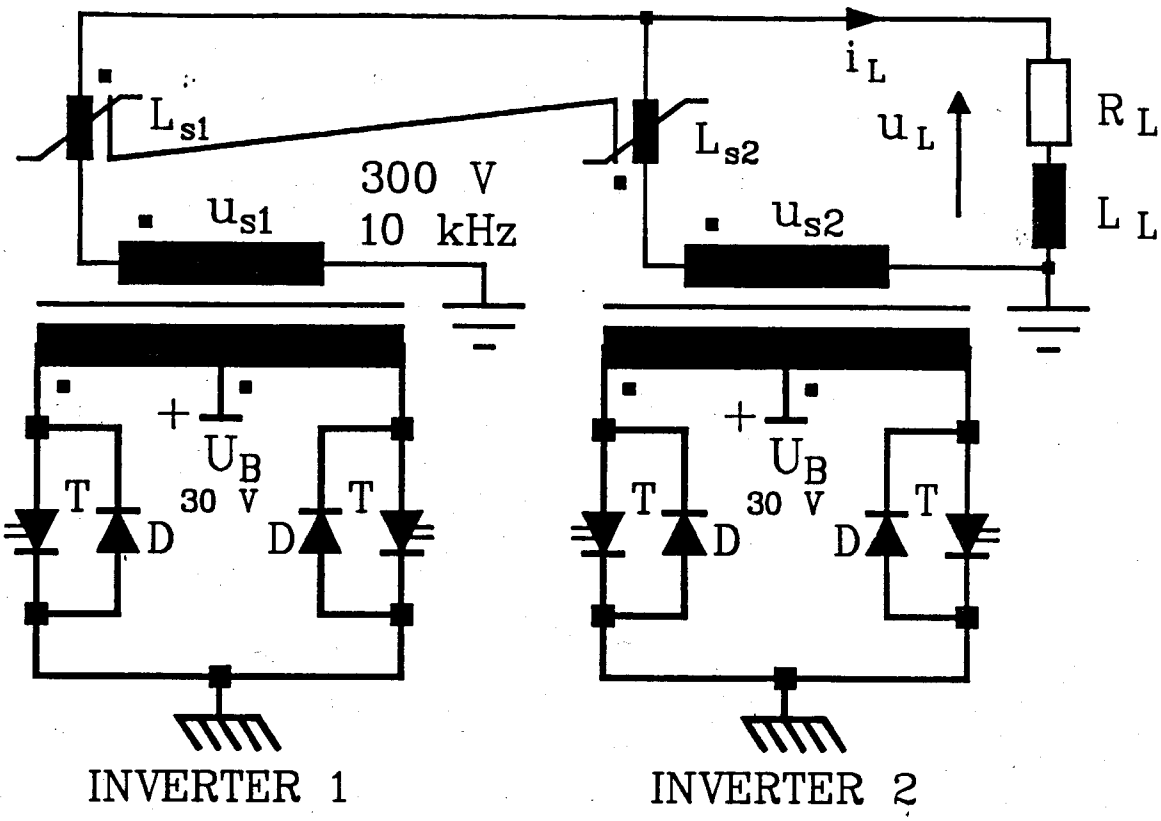

Fig. 4.22: Schematic Representation of High-frequency Inverter

Figure 4.22 shows the schematic diagram of a 10 kVA high-frequency (10 kHz) inverter [A49]. A center-tap topology is used because of its low component count, simple base drive and low input voltage U_B (30 V DC). The forced commutated power switches are realized with bipolar power transistors with collector currents of 150 A each, which emphasize the need for paralleled converters in higher power applications [A49]. Asynchronous power transistor switching in the two inverters results in unwanted circulating currents during the switching times. To limit this effect the high-voltage secondaries of the two inverters are paralleled via novel saturable inductance circuits L_{s1} and L_{s2} [A49]. The load for the converters consists of a linear resistance R_L (11 Ω) and an inductance L_L (160 μH) in series.

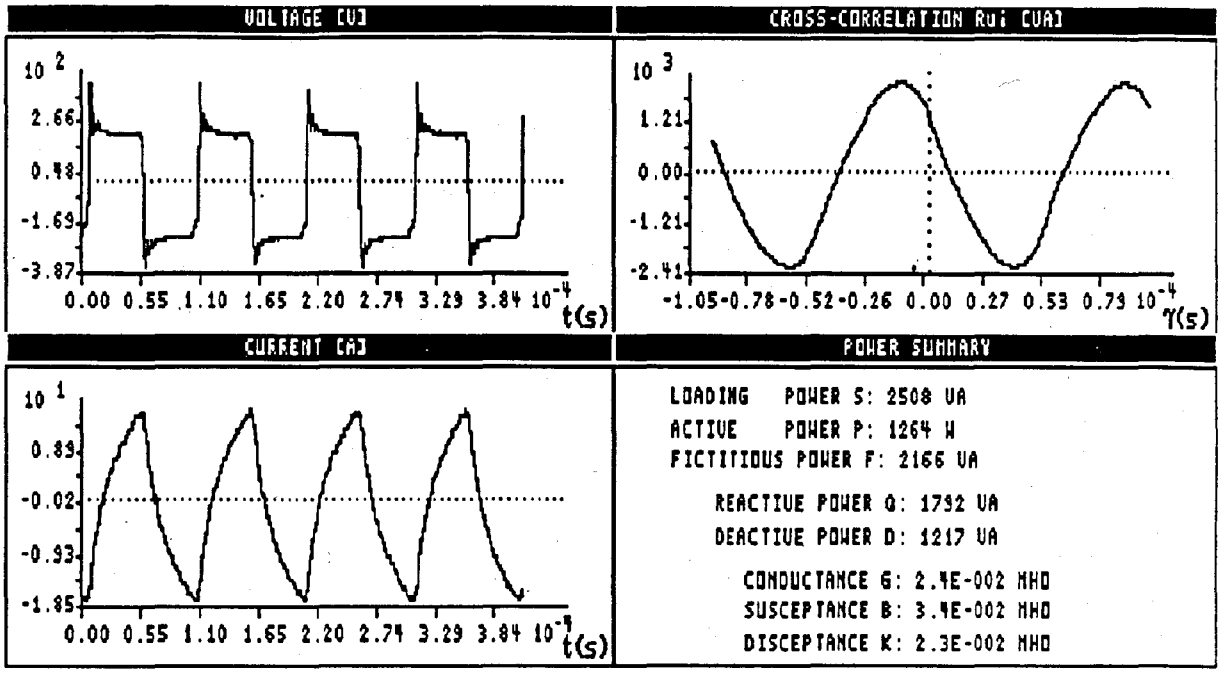

Fig. 4.23: Analysis of Distortion in High-frequency Inverter

Figure 4.23 shows the results of the distortion analysis. The load current i_L and the load voltage u_L are correlated to give the different power components. Although the load consists of only inductance and resistance, the equivalent disceptance has a non-zero value, which implies that the network is uncorrelated and therefore deactive power results. The inductive load loads the network in an uncorrelated manner, resulting from the non-sinusoidal generating function. The major portion of the fictitious power is caused by the time shifting characteristic of the reactive element L_L.

A schematic diagram of a secondary converter of the high-frequency link type is shown in fig. 4.24. The converter is fed from a high-frequency square wave voltage (300 V, 10 kHz), which can be obtained from a converter analogous to the one shown in fig. 4.22.

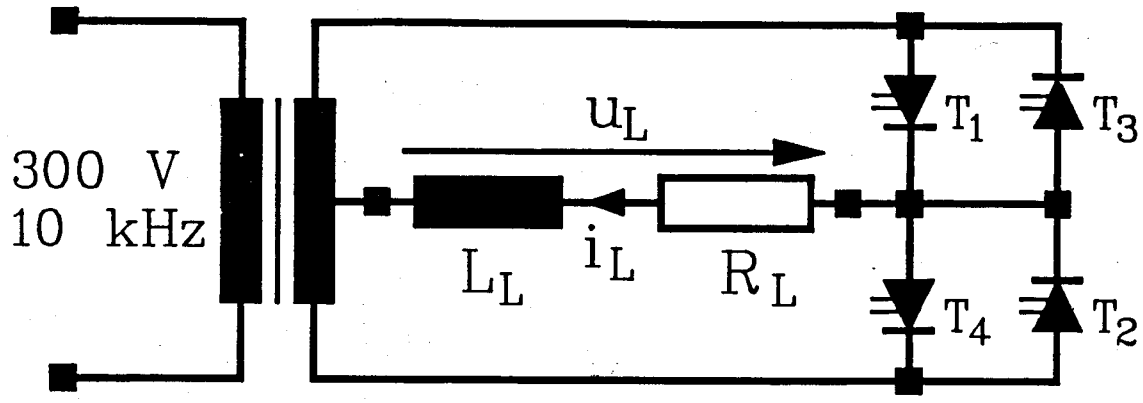

Fig. 4.24: Schematic Diagram of High-frequency Secondary Converter

The secondary of the high-frequency transformer consists of a center-tap winding with a simple cyclo-converter coupled as indicated to yield the desired load characteristics. The cyclo-converter operates with four power switches (Gate Turn-off Thyristors (GTO's) are used in this system) and is generally supply commutated. The converter operates as a full-wave rectifier when T_1 and T_2 are conducting and the inversion is obtained by a switch over to T_3 and T_4. This converter is controlled using the principle of delta modulation [A142].

The analysis of the distortion in the secondary converter is shown in fig. 4.25. This is a typical case where the generating function is the current (sinusoidally modulated). The voltage signal is sent through a small signal, digital, minimum phase shift, 3 kHz, averaging output filter (built into the digitizer), to minimize aliasing in the sampled waveform. The load consists of a single phase induction machine magnetizing inductance L_L (300 mH) and a resistance R_L (185 Ω). The output current is controlled to have a frequency of 50 Hz. Because of the high value of the inductance, which is a reactive element, the major portion of the fictitious power is reactive power. The deactive power is again caused by the uncorrelation between the generating function and the loading function.

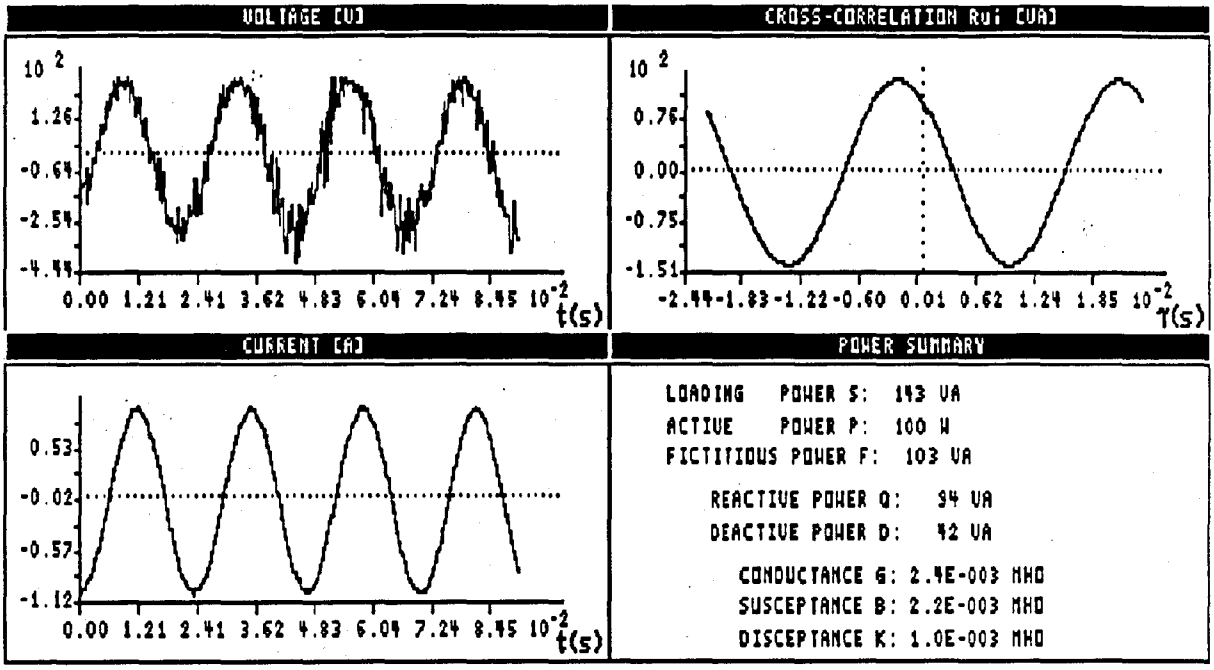

Fig. 4.25: Analysis of Distortion Present in the Secondary Converter of a High-frequency Link Converter

4.6 SUMMARY

This chapter describes the measurement of power, especially fictitious power, in different power systems. This includes an investigation into appropriate measurement techniques in the time domain and, to a lesser extent, also in the frequency domain. Some attention is focused on the development of a PC-based time domain measurement system. This system can be used to measure the different power components directly on-line in the time domain, as described in chapter 3.

A dedicated DSP microprocessor based measurement system, in which the correlations could be performed by a SAW convolver, is proposed for real-time power measurements. As described in the rest of this thesis, real-time measurements are required for fictitious power compensation.

The PC-based measurement system has been used for the measurement and analysis of the distortion generated by different power electronic converter systems. The analysed systems are systems used frequently in industrial power conditioning systems. Their power ratings range from 100 VA to 100 kVA and their operating frequencies from 50 Hz to 10 kHz.

CHAPTER 5

PHILOSOPHY FOR FICTITIOUS POWER COMPENSATION USING ADAPTIVE SIGNAL PROCESSING TECHNIQUES

5.1 INTRODUCTION

The analysis of distortion, using the proposed correlation approach to describe all the different parameters, quantities and time representations in a contaminated power system, seems advantageous to other techniques (chapter 3 and 4). Furthermore it is shown in the previous two chapters that fictitious power loads the power network without delivering net energy to the load. In power systems, with sinusoidal generating and loading functions, the term power factor correction is normally used to indicate a compensation method to limit the VA-value of the measured loading power to the W-value of the measured active power in the power system. This is normally realized with a capacitor bank or synchronous machine operating as an appropriate equivalent susceptance.

In power systems with non-sinusoidal loading and/or generating functions, distortion compensation is, however, a riddle which has given rise to extensive discussion in literature [H1, A1-3, 21-27,42-46,50,51,56,60,61,78,81-86,102,108-110,113,115-118,121-126,128,130-134,136,139,141,144,145]. One of the major causes of concern is the resonance of the compensation capacitances with the equivalent short circuit susceptance of the network, at harmonic frequencies. These resonances have detrimental effects, destroying the fictitious power correction capacitors and other equipment coupled to the power network (chapter 2). For this reason the compensation of distortion is normally limited to systems with a sinusoidal generating function.

The distortion compensation techniques can, however, be extended to power systems with non-sinusoidal generating and loading functions, when implementing appropriate analysis and compensation techniques. The previous two chapters showed a principle difference in the generation of distortion, which is either the result of the time-shifted correlation or the uncorrelation between the generating and loading functions. The time-shifted correlation is caused by the equivalent load susceptance, while the uncorrelated fictitious power is caused by the uncorrelated load characteristics, characterized as the equivalent disceptance.

The compensation of these distinct forms of distortion is addressed in this chapter, using different compensation systems collectively, with special reference to the implementation of a new fictitious power control philosophy. When distortion compensation systems are individually implemented in these contaminated supplies, a decrease in the total power factor Γ without an associated decrease in loading power can result [A25-27]. A typical example is a power factor compensation capacitor bank in a supply with a non-sinusoidal voltage as generating function. For this reason it is of the utmost importance to design the fictitious power compensation equipment accurately by introducing power filters with appropriate dynamic response, which in a well designed system, can compensate for all the components of fictitious power [A2,3,50,81,84,86,101,139,141, D5,9].

These dynamic power filters consist of forced commutated converters, with high dynamic response and a passive reactive element (chapter 6) which can be a very expensive compensation method in high-power contaminated power networks. In general, these cost constraints placed on these converters, prevent their wide-spread application in distorted power systems. These systems can, however, bring-about a peripety in fictitious power compensation, if they can be engineered as cost effective compensators using a control philosophy that utilizes their positive characteristics in an effective way. Such a control philosophy is derived in this chapter.

In general the control philosophy derived in this chapter use the diversity of all the known fictitious power compensation systems, in such a way as to utilize the advantageous aspects and eliminate the disadvantages of each system. This control philosophy is based on the generalized power definition proposed in chapter 3 and evaluated experimentally in chapter 4. In the realization of this control philosophy for real-time applications, adaptive signal processing techniques are proposed and evaluated, resulting in an adaptive control scheme for fictitious power compensation apparatus.

5.2 FICTITIOUS POWER COMPENSATION PHILOSOPHY

All the components of electric power, mentioned in chapter 3, are associated with equivalent load parameters, each having a specific loading function characteristic. In the control philosophy of fictitious power compensation apparatus, these different load parameters can be used in different control loops, to control the magnitude of each equivalent network parameter and in the process compensating the unwanted fictitious power by eliminating the unwanted equivalent network parameters. Figure 5.1 shows a block diagram of this power compensation philosophy, while fig. 5.2 shows the schematic diagram of the compensation philosophy.

The total compensation system consists of a susceptance B portion (Reactive power compensation) and a disceptance K compensation portion (Deactive power compensation), which forms a sink for the reactive and deactive currents characterized in the load, leaving the network in the ideal case with only an equivalent conductance G. The susceptance B and disceptance K, present in the non-linear load, have been cancelled by the compensation system by generating the conjugate susceptance B and disceptance K. The reactive power compensation system generates the current $-i_r(t)$, the deactive power compensation system the current $-i_d(t)$, thus compensating the reactive and deactive currents from the load and only active current $i_a(t)$ is drawn from the power supply.

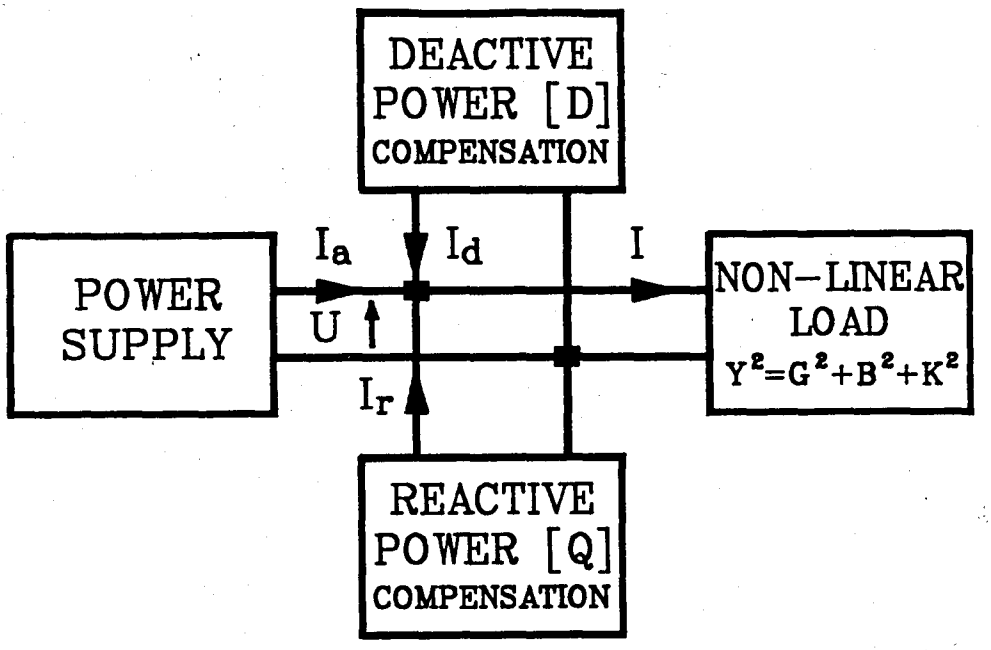

Fig. 5.1: Block Diagram Representation of the Fictitious Power Compensation Philosophy.

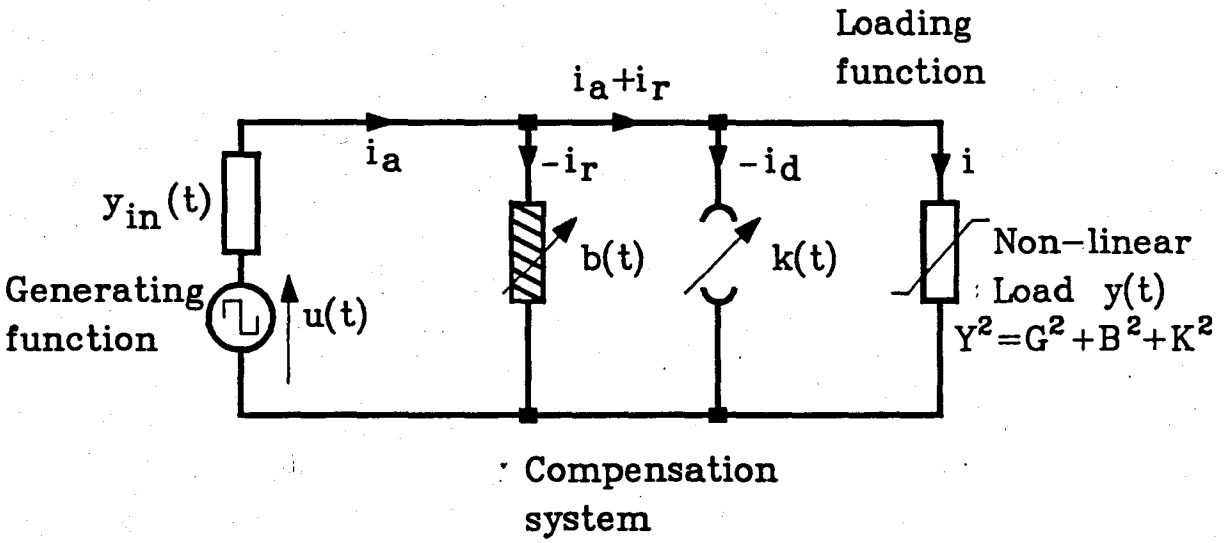

Fig. 5.2: Schematic Diagram of the Fictitious Power Compensation Philosophy.

Fictitious power compensation systems can be classified on the basis of their dynamic system response and their maximum power rating which, in practical systems, follow a reciprocal relationship. The cost of these compensation systems is proportional to their dynamic response and the maximum compensation power rating. [H14, A81,141]. Fictitious power compensation systems are classified into the following categories for the purpose of this thesis:

(a) **Fixed static power filters with a constant power rating:** power factor correction capacitors or inductors; tuned harmonic power filters (F > 10 MVA, no dynamic response);
(b) **Quasi-dynamic power filters with a variable power output:** relay controlled reactive components; tunable harmonic filters; thyristor controlled reactive sources; reactive power generating synchronous machines (100 kVA < F < 15 MVA, dynamic response 10 s > τ > 30 ms);
(c) **Dynamic power filters:** PWM controlled current or voltage-fed reactive loaded, forced commutated power converters (1 kVA < F < 100 kVA, dynamic response 20 ms > τ > 100 μs).

Each of the above types of compensation systems can fulfill an important role in the compensation of distortion in a contaminated power supply.

The properties of the load and the proposed definition of reactive power, implies correlated fictitious power which does not change within a typical measurement interval. For this reason fixed power filters under steady state conditions and quasi-dynamic filters under dynamic conditions can be used for reactive power compensation. Power filters with high dynamic response can also be incorporated but will, however, have a negative effect on the cost of reactive power compensation.

For deactive power compensation it is, however, important to compensate within a typical measurement time interval and for this reason the majority of quasi-dynamic filters do not have an adequate system response. Forced commutated Pulse Width Modulated (PWM) current- or voltage-fed reactive loaded converters have been proposed for dynamic power filters (DPF) [A1-3,16,55,56,81, 84,86,101,139,141]. Compensation of deactive power and, under dynamic load changing conditions, residual reactive power is proposed to be effective with the use of dynamic power filters. The proposed power definition makes a prominent distinction between fundamental reactive power and residual reactive power. Fundamental reactive power can safely be compensated by means of a fixed reactive component like a capacitor, while residual reactive power should in general be compensated by means of a DPF.

Under steady state conditions tuned harmonic filters may be used to compensate the residual reactive power.

The total compensation system forms an integral part of the load in the network, which means that the compensation system can individually contribute to the distortion compensation or generation in the network. Some compensation systems can compensate some of the fictitious power components, while in the process generating another. This is generally true for compensation systems like thyristor controlled reactive sources TCR's which compensate fundamental reactive power, but generate some deactive power in the process and draw some active power from the supply to compensate the losses [H14].

This unfortunate situation can in some cases, if no other type of compensation system is incorporated, increase the total loading power or give rise to dangerous parallel or series resonance. To eliminate these catastrophic conditions, the TCR should be operating in conjunction with a dynamic power filter (DPF) or, under steady state conditions, a fine-tuned harmonic power filter (HPF).

The parallel operation of different fictitious power compensation systems is not only essential in some situations, it can result in a cost effective compensation system in general. In practice it is necessary to compensate deactive power in a network with a DPF, this DPF should be rated for all the fictitious power in the network which can be very expensive. The reactive power portion of the fictitious power could, however, be compensated partially or fully by means of a cost effective low dynamic response compensation system, as for example a capacitor bank or even a TCR, leaving the DPF to compensate only the deactive power and in general a small amount of the reactive power. This will result in a much lower power rating DPF and an associated more cost effective compensation system in total.

On the other hand the compensation of one power component results in the reduction of the other because the different power components are mutual orthogonal, thus a reduction in reactive power

result in an associated decrease in the loading power which again implies a reduction in the resultant deactive power under the same operating conditions. An a-priori reduction of the reactive power will thus have a positive effect on the compensation of deactive power. This phenomena will be shown experimentally in chapter 6.

This philosophy of fictitious power compensation has many advantages in the realization of the compensation apparatus: Small dynamic power filters DPF's, economical power compensation in high-power rated networks, higher compensation system capacities and the possibility of an integral design of compensation systems within distortion generating systems, as for example high-power rated power electronic converters. Furthermore this philosophy makes provision for the compensation of non-sinusoidal supplies using a combination of passive low and high-dynamic response filter components.

The advantages described above are clear when the generating function (voltage) has a nearly sinusoidal waveform because it is easy to generate a sinusoidal reactive current by means of passive reactive components, i.e. inductors and capacitors. When the voltage is, however, non-sinusoidal and the network operates at steady state conditions, all the reactive power can also be compensated by means of passive components, i.e. inductors, capacitors and tuned harmonic power filters. With a non-sinusoidal generating function and the network operates under dynamic loading conditions, a portion of the reactive power, associated with the dynamic operating conditions, has to be compenated by means of a dynamic power filter.

5.3 REACTIVE POWER COMPENSATION SYSTEMS

Reactive power compensation is seen as the compensation of a portion of the fictitious power, which is associated with a correlated time shift between the generating and loading functions and calculated from the cross-correlation between these two functions (chapter 3) [A50,51]. Reactive power can in general be compen-

sated by means of simple reactive components, if the generating function is sinusoidal and with a combination of tuned harmonic filters if the generating function is periodic but non-sinusoidal. In systems with an aperiodic generating function, the major portion of the reactive power can be compensated with these low dynamic response power filters, while the rest should be compensated by means of high dynamic response power filters.

For reasons stated above the principle of the matter is to compensate the major portion of the fictitious power by means of passive reactive components with a low dynamic response. For this reason it is advantageous that not only reactive power and deactive power are split, but that reactive power is subdivided into fundamental and residual components, as proposed in chapter 3.

PART I:- **Fundamental Reactive Power Compensation**

The leading current to voltage characteristics of a capacitor and leading voltage to current characteristics of an inductor is in general utilized in fundamental reactive power compensation systems. Fundamental reactive power is calculated from the cross-correlation function $R_{ui}(\tau)$, by implementing a minimum phase low-pass or band-pass filter (or a Fourier transform if harmonic powers are of interest) in cascade with the cross-correlation. The fundamental reactive and active power can be obtained in this manner, as shown in eq. (5.1) (chapter 3).

$$Q_f = \hat{R}_{1ui} \sin \Phi_1 \quad \text{and} \quad P_f = \hat{R}_{1ui} \cos \Phi_1 \qquad (5.1)$$

with Q_f ≡ fundamental reactive power

P_f ≡ fundamental active power

$\hat{R}_{1ui}$ ≡ peak value of fundamental cross-correlation

Φ_1 ≡ fundamental cross-correlation phase shift

This value of the fundamental reactive power can be used to design fundamental reactive power compensation systems with low and quasi-dynamic response, viz. fixed capacitors, synchronous machines, thyristor controlled reactive sources.

The design of fixed capacitors/inductors rated for the daily average of the fundamental reactive power can be implemented as standard practice. The perturbation around the average can be compensated by means of a quasi-dynamic fundamental reactive power compensation system viz; switched reactive components; synchronous machine condensers or thyristor controlled reactive sources.

5.3.1 Fixed Static Reactive Components

Fixed static capacitor or inductor installations, depending on the leading or lagging loading characteristics, which are rated for the long time averages of the fundamental reactive power, should be implemented in any cost effective reactive power compensation system. Systems with power ratings of > 400 MVA have been installed in HVDC-converter installations [A74].

5.3.2 Rotating Synchronous Machine Compensators

The synchronous machine, which can deliver field-controllable fundamental reactive power, is the workhorse in power systems. The mechanical time constant of these systems are in the order of 1 - 5 seconds, which limits this type of compensation system to quasi-dynamical compensation applications [H14]. Typical rotating systems in HVDC-converter installations are rated for 300 MVA, which put a different perspective to power ratings of quasi-dynamic compensation systems [H14]. Figure 5.3 shows a schematic diagram of a network with a rotating synchronous machine in a role of fundamental reactive power compensation, under quasi-dynamic conditions.

Inherent advantages of rotating systems are extra reserve kinetic energy for better power system short-circuit capabilities, uninterruptable power supply (UPS) capability and an improvement of power system dynamics [H1,14].

Thyristor controlled reactive sources are based on a line commutated thyristor converter which is reactively loaded. By controlling the fire angle α, the fundamental reactive current forms a controllable reactive source.

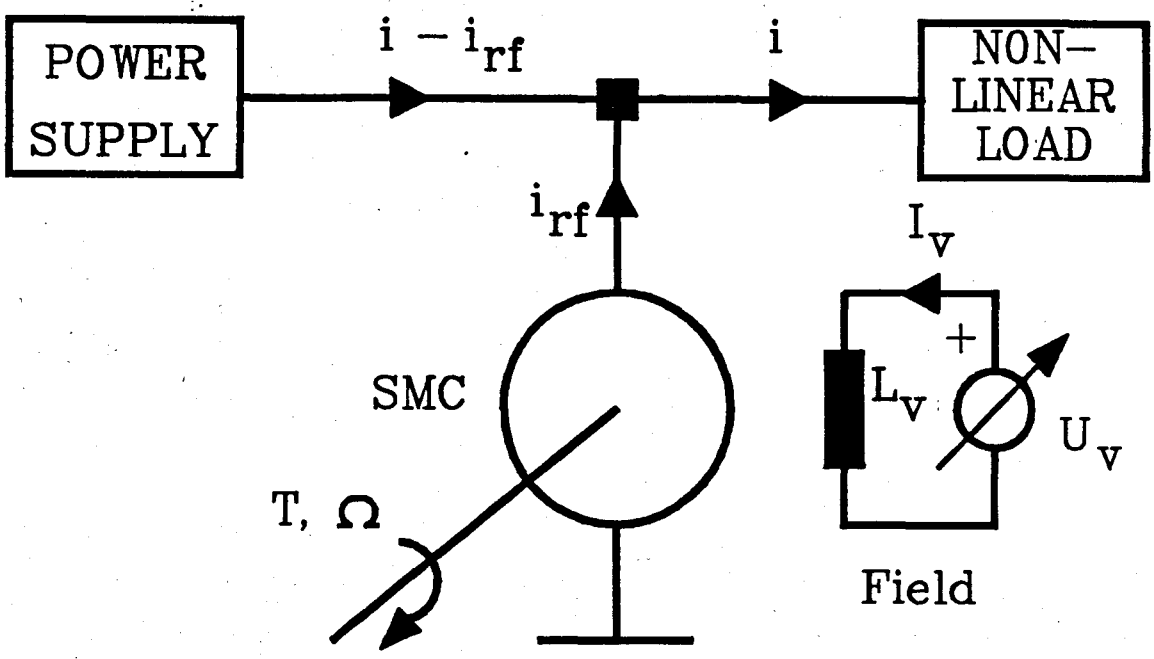

Fig. 5.3: Schematic of Synchronous Machine Fundamental Reactive Power Compensation System.

5.3.3 Thyristor Controlled Reactive Source

To compensate reactive power loads in dynamic variable environments, as for example non-linear power converter loads and arc-furnaces [H14, A18,78,82], it is necessary to change the reactance of these passive components dynamically to coincide with the change in the reactive power.

Resulting from their method of operation, these systems generate deactive power in the effort to compensate the fundamental reactive power, which imply that tuned harmonic power filters should be used collectively to compensate the generated deactive power [H14]. Normally the quality factor of the filters is designed to accommodate small shifts in the fundamental frequency and harmonics. In fig. 5.4 a thyristor controlled reactive source is shown. The system

consists of a fixed capacitor bank C and a thyristor controlled inductance. Other topologies are also used in power systems [H9,14]. Dynamic responses of between 20 and 50 ms with power ratings of between 30 and 100 MVA have been obtained [H14, A74].

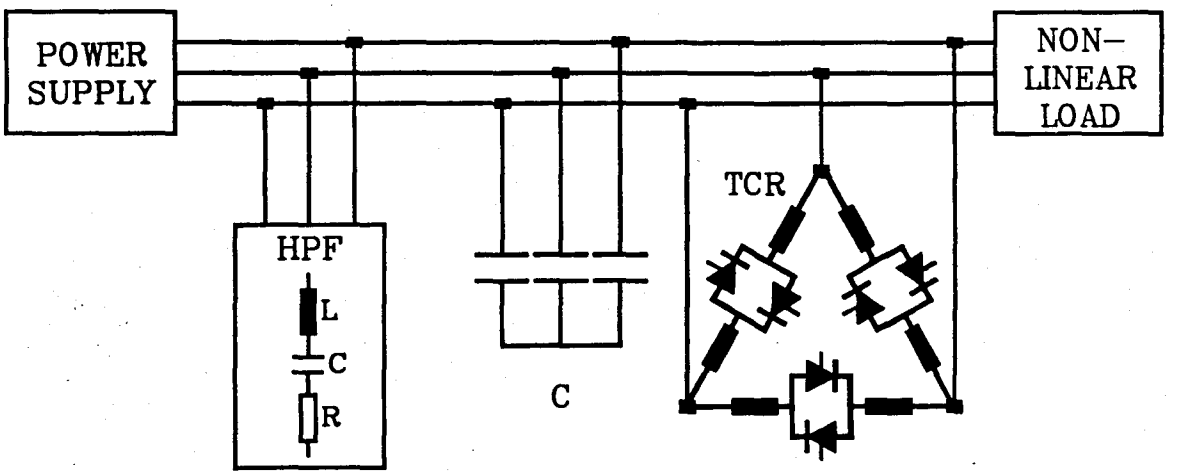

Fig. 5.4: Schematic of Thyristor Controlled Reactive Source

PART II:- **Residual Reactive Power Compensation**

Residual reactive power arises when the generating function is non-sinusoidal. This amount of reactive power cannot be compensated by means of a single capacitor or inductor, because of the frequency dependence of the susceptance of these components. This amount, which in practical systems are small compared to the fundamental reactive power, has to be compensated by means of high-dynamic response power filters, generating the negative of the residual reactive current $-i_{rr}$. An ideal fundamental frequency band-pass power filter on the loading function will also compensate this amount, but is only practical in high-frequency systems. In typical 50 or 60 Hz power systems the physical sizes of the filter components are too big.

These low-frequency power systems, which have normally relative low-distorted sinusoidal generating functions, result

in a small amount of residual reactive power. Prominent generating function harmonics, as for instance the 3rd, 5th and 7th can be cancelled from the loading function by means of tuned harmonic power filters, leaving a very small high-frequency content in the loading function, with negligible associated residual reactive power.

5.4 DEACTIVE POWER COMPENSATION SYSTEMS

For the purpose of full compensation of the fictitious power, a deactive power compensation system, compensating the uncorrelated fictitious power, should be implemented in parallel with the reactive power compensation system. This normally involves a high-frequency pulse width modulated (PWM), power electronic converter operating in a voltage- or current-fed configuration. Figure 5.5 shows the two different topologies. The principle of working can be described as a system which generates the required deactive current. The full description and classification of these systems are shown in chapter 6.

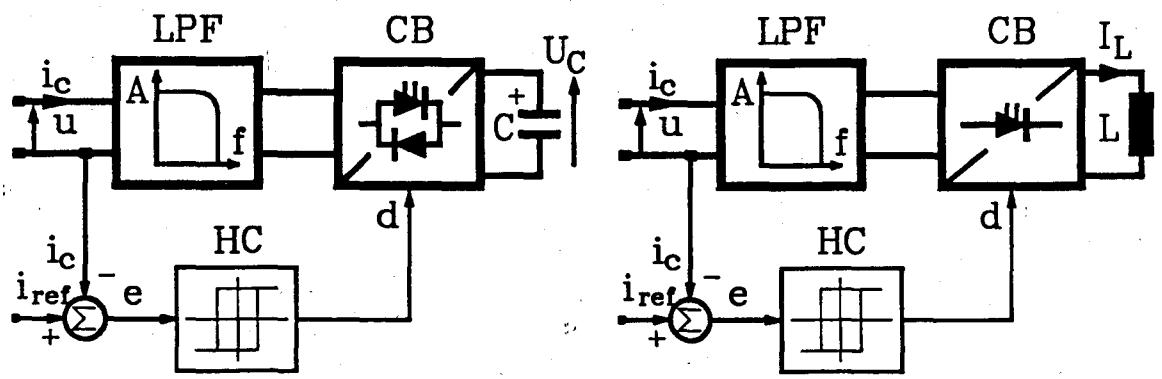

(a) Voltage-fed (b) Current-fed

Fig. 5.5: Block Diagram of Dynamic Power Filter Topologies

Both systems consist of a bridge type (single or three phase) converter (CB). They are either fed from a capacitor C to form the voltage-fed topology, with associated energy stored in the capacitor electric field, or fed from an inductor L in the current-fed topology, with associated energy stored in the inductor magnetic field. A low-pass power filter LPF is incorporated

to remove high-frequency ripple from the generated current waveform. Efficiency in the voltage-fed converter system is one of the major advantages, while more reliable control is advantageous in the current-fed converter system [A1-3,50,81,139,141, D9].

The reference current i_{ref} (in general the current to be compensated) is calculated outside the DPF. This current forms the input to the DPF, the actual compensation current i_c is measured and fed back to close the feedback loop. The error signal is sent through a hysteresis controller HC to form the duty cycle d of the bridge CB.

The major electrical difference between the thyristor controlled reactive source (TCR) (a supply commutated converter) and the dynamic power filter (DPF) (a forced commutated converter) is the compensation time constants. Fictitious power control on the TCR system occurs in steps, with an associated time lag of between 2 to 10 periods of the fundamental voltage [H14]. Conceptually the conventional TCR systems are intended to compensate only the fundamental reactive power, which does not change within a typical 50 Hz power signal. Under dynamical conditions the inherent delay of the conventional TCR system may be too long for effective compensation of rapidly varying loads, as for example in arc-furnace and power electronic converter loads [A17,18].

The dynamic power filter on the other hand has a time constant of 100 μs to 1 ms, an order of two faster than the TCR. This make the DPF ideal for compensation within one fundamental period and thus ideal for the compensation of deactive power. To compensate deactive power in any unbalanced three-phase load, a converter employing three single phase bridge converters or a converter capable of unsymmetrical compensation should be implemented [A37,139,141].

The core of the matter in dynamic power filtering, is the effective signal processing of the reference current and the control of the filter converter [A1,2,50]. This outstanding problem has

to be addressed and solved, before effective DPF systems are to be utilized in power systems. In chapter 6 the control loop of a 15 kVA three phase DPF is evaluated. It is felt that with more effective signal processing, the fundamental limitations and disadvantages of the DPF can be overcome.

Under steady state conditions prominent loading function harmonics can be compensated by means of tuned harmonic power filters, to make the residual deactive power smaller. It is, however, impossible to compensate all the deactive power by means of tuned filters.

5.5 ADAPTIVE SIGNAL PROCESSING IN APPLICATIONS OF FICTITIOUS POWER COMPENSATION

In the analysis of distortion in electric power systems it is incessantly showed that the different average power components can only be calculated after the measurement interval has elapsed. This implies that any calculation of power components or network parameters are at least one measurement interval old. In the previous paragraph it has been shown that the deactive current, representing the non-linear portion of the load, has high-frequency characteristics. For this reason the possibility of adaptive signal processing is investigated in the control of fictitious power compensation systems [A51, D7]. The proposed adaptive signal processing is based on the statistical properties found in the equivalent network parameters, as formulated in chapter 3.

These equivalent network parameters G,B,K, are describing the equivalent circuit of the power network at any given instant and are used to derive the instantaneous signals for the respective currents i_a, i_r, i_d. From the simulations, which are performed in chapter 3, it has been found that these network parameters are independent from each other, the dynamic behaviour describing the equivalent parameters are unknown, but they are in the majority of the cases statistically predictable.

5.5.1 Signal Processing on Power Waveforms

The combination of digital and analogue signal processing techniques makes it possible to optimize calculation time in adaptive parameter estimation. The short time constant of the average non-linear load, which has to be analysed and compensated, necessitates high speed signal processing, coupled with parameter estimation techniques, which can best be obtained by a combination of digital and analogue methods.

After serious considerations of the possible systems, needed to generate the reference currents in fictitious power compensators [A1,34,35,61,81,113,119,139,141], various signal processing techniques were investigated. The chosen signal processing system should be used to compute the different power components, the equivalent network parameters and the instantaneous waveforms of the respective currents in real-time. The real-time implementation is based on network parameter prediction and therefore a dedicated microprocessor based signal processing system is proposed. A Texas Instruments TMS320 series processor is proposed to realize the fictitious power control scheme (chapter 4). A software adaptive signal processing algorithm, to be used in the control system of fictitious power compensation systems (chapter 6) is derived in, reference D7 and is shown in this chapter.

5.5.2 Choice of the Adaptive Signal Processing Process

In fundamental estimation theory [H3,6,18,23] there are two distinct types of processes. The first type is the non-recursive processing and is known as classical estimation theory while the second type is concerned with recursive processing, called modern estimation theory. The Kalman filter algorithms are based on the recursive type of es-

timators, while the Wiener algorithms are based on non-recursive estimation theory [A85,129]. In estimators the input and outputs of normal digital filters are changed to form the signal y and the prediction of the signal $\hat{x}$.

5.5.2.1 Non-recursive filter as an estimator

A digital non-recursive or finite impulse response (FIR) filter implemented as an estimator is shown schematically in fig. 5.6. The estimator uses a fixed number of sampled input values and results in an output prediction $\hat{x}$.

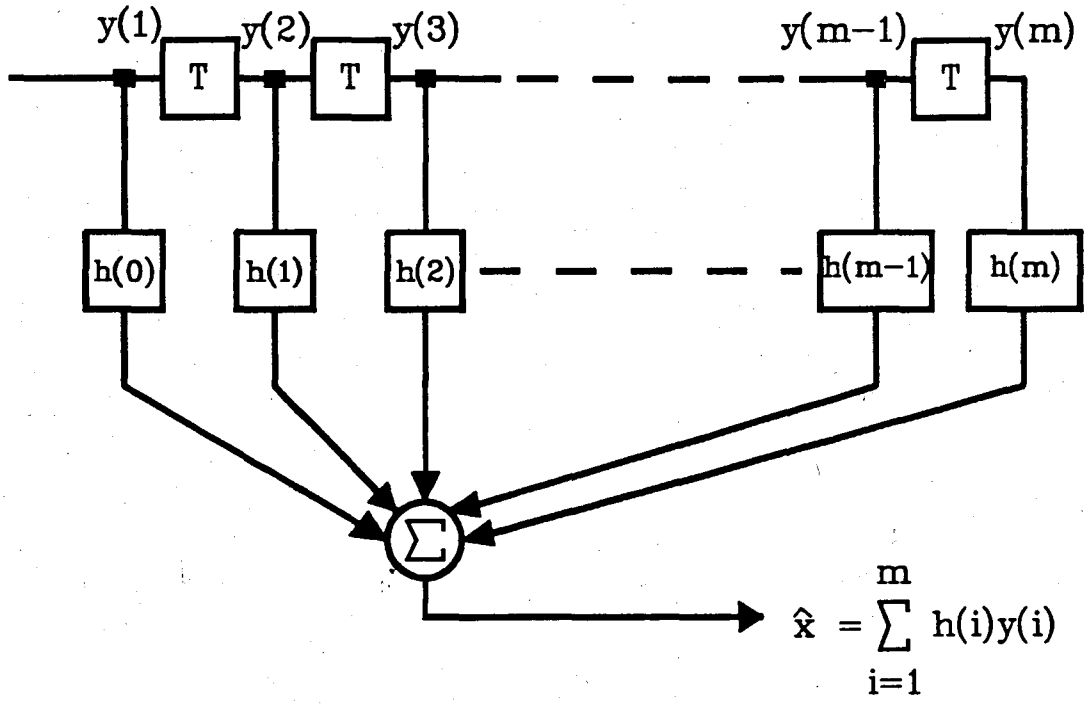

Fig. 5.6: Non-recursive Filter as an Estimator

The input data y(i), i = 1,2,3,..m, must be available as a batch. The input is stored, multiplied by weights h(i), i = 1,2,3..m, and the result is summed and produce the predicted value $\hat{x}$. Equation (5.2) shows the output of a typical non-recursive filter estimator.

$$\hat{x} = \sum_{i=1}^{m} h(i).y(i) \qquad (5.2)$$

The observation time (k) is an important parameter to be considered in the design of non-recursive filters. This time (k) must be longer than the finite filter length (m). This implies that the sampled input must be observed longer than the predicted calculation, otherwise the estimation does not have realistic meaning.

The mean-square error of an estimator is the basic measurement of the accuracy of the estimated value $\hat{x}$. The mean-square error is normally inversely proportional to m, the amount of different input samples used in the digital filter. This implies that a better estimation will result if more samples and therefore a longer observation time of the input array is used.

These types of estimator filters have certain disadvantages. Firstly a lot of memory and secondly a long observation time is needed, which implies a big and slow digital processor. For this reason modern estimators make use of recursive digital filters.

5.5.2.2 Recursive digital filter estimators

The recursive or infinite impulse response (IIR) filter is shown schematically in fig. 5.7. This filter requires a feedback loop, describing the dynamic response of the experimental system by means of the parameter a. The major difference between the two types of filters is that the output of the recursive filter consists of the present input and a weighted previous output, while the non-recursive filter uses a weighted summation of a large sum of consequent inputs.

The weight a (always less than 1) is multiplied by the previous input, delayed by T. The output-input transfer function can be written in the relationship shown in eq. (5.3).

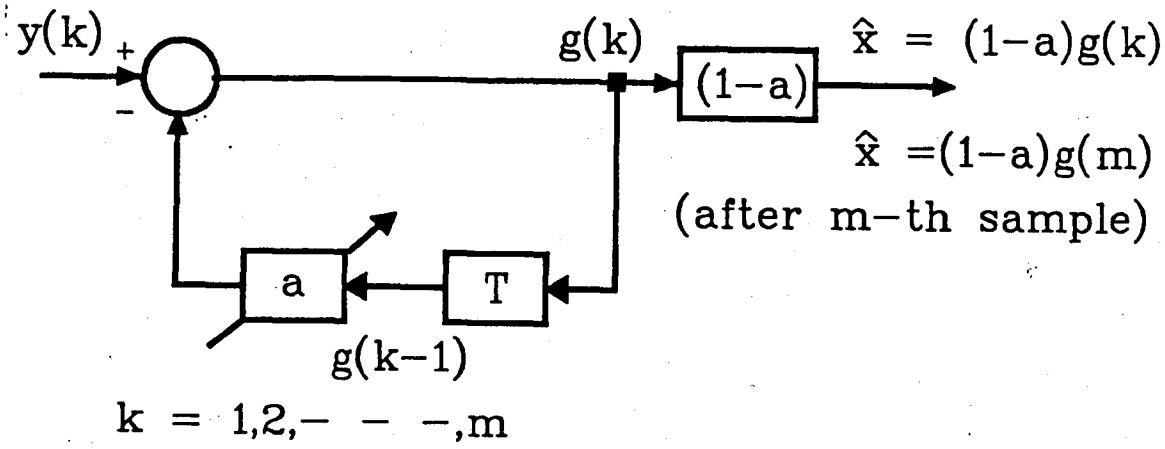

Fig. 5.7: A Schematic Representation of a First-order Recursive Estimator

$$g(k) = y(k) + a.g(k-1) \tag{5.3}$$

This filter continually updates the output, adding a new data sample y(k) to a fraction of the previous output a.g(k-1). The result of such a process can be derived from a sequential input [H2,3,18]. From these results the estimate can be derived and is shown in eq. (5.4)

$$\hat{x} = (1-a).g(m) \tag{5.4}$$

where $\hat{x}$:- estimated value
a :- weighted value ($a<1$)
$g(m)$:- output after m sequential inputs.

This means that the output (1-a).g(m) is taken as an estimate of the signal x, after the m-th input sample has been processed. To assess the accuracy of the basic recursive estimator, the mean-square error at the input and output is calculated. The mean-square error p_e at the output, after the m-th sample has been processed, is calculated as shown in eq. (5.5) [H3,18].

$$p_e = a^{2m}.\Sigma_m + \frac{\sigma_v^2.[(1-a)(1-a^{2m})]}{(1-a)} \tag{5.5}$$

with $\sigma_v^2 = E\{(\hat{x} - x)^2\}$

input mean-square error after one sample.

and $\Sigma_m = E\{x^2\}$ the mean-square signal.

This mean-square error has two distinct portions. The first can be associated to the fact that a^m is not equal to zero and the other is associated to noise, which is directly proportionally to the input mean-square error σ_v. In optimal estimators it is essential to minimize the mean-square error. This is done by changing the filter gain a to correspond to minimum mean-square error. The optimum recursive estimator consists of a measurement system which has a time-varying gain to follow a minimized mean-square error, between predicted output and real output (x and $\hat{x}$). [H3,18, A85,100].

The recursive process seems to be used in a wide variety of systems [H23]. There are some advantages which make the recursive estimator a better choice. These include shorter calculation time and good performance on systems which show a reasonable constant dynamic behaviour [H2,3,18, A85,100]. The most recent measurement has the highest effect on the prediction, which implies that the filter has a good dynamic response, but will result in stability problems in systems with fast stochastically changing system response. Furthermore the response is infinite which implies that the history of the dynamic system response will influencing the filter transfer function. For reasons of short algorithm time and high dynamic response, the recursive process is used in this analysis. The recursive process are normally implemented with a Kalman algorithm [A85,129].

5.5.3 Dynamics of the Experimental System

The experimental system consists of a typical power system analysed over a measurement interval dT. As stated in chapter 2 and 3 the choice of the measurement interval should be changed adaptively to coincide with the system response. For power systems with a voltage generating function of 50 or 60 Hz, the dynamic responses are, in the majority of cases, of the same magnitude, (10-200 ms). When a measurement interval of 20-50 ms is taken, reasonable accurate distortion characterization will result. This implies that an estimation of the network parameters should be made every 10-20 ms. Estimation of only G and B are performed because only these two parameters are needed to calculate the instantaneous current signals.

The conductance and susceptance G and B, are shown to be independent of each other with network related dynamic characteristics. The long time averages of the parameters are described by means of the determinable average loading of the power network. Their short term characteristics are unknown but can be described by means of a statistical process.

5.5.4 Kalman Prediction Algorithm to Estimate Network Parameters

The prediction of the conductance and susceptance can be obtained by means of two independent scalar Kalman predictors. An assumed model that describes the dynamic behaviour of these two parameters have been set up. Seeing that these two parameters are independent and relatively fast variable parameters, their behaviour is assumed to be described by an first order autoregressive process. Taking into account the fundamental prerequisite of real-time fictitious power compensation, two independent scalar Kalman predictors save a lot of computation time [A51, D7].

Furthermore, the parameters that describe the dynamic behaviour of the conductance and susceptance are not known, which emphasizes the need of a Kalman parameter estimator in parallel with the conductance and susceptance prediction algorithm. This implies that an estimation of the algorithm parameters are made each time a network parameter prediction is performed.

Assuming that B and G are two independent signals to be predicted simultaneously, time-varying samples of these two quantities are denoted as b(k) and g(k), with k the instantaneous time sample (k = 1,2,3,...,n). Taking the assumption that the conductance and susceptance are generated by first order autoregressive processes into account, the two processes are represented by the following equations [H3,18, A95,100,129]:

$$g(k) = a_g.g(k-1) + w_g(k-1) \tag{5.6}$$
$$b(k) = a_b.b(k-1) + w_b(k-1) \tag{5.7}$$

where the process noise, w_g and w_b are assumed to be Gaussian white noise with zero-mean and independent of all the others. In vector form:

$$\mathbf{x}(k) = \mathbf{A}.\mathbf{x}(k-1) + \mathbf{w}(k-1) \tag{5.8}$$

$$\mathbf{x}(k) = \begin{bmatrix} g(k) \\ b(k) \end{bmatrix}; \quad \mathbf{w}(k) = \begin{bmatrix} w_g(k) \\ w_b(k) \end{bmatrix}; \quad \mathbf{A} = \begin{bmatrix} a_g & 0 \\ 0 & a_b \end{bmatrix}$$

Assume further that in predicting the signal vector $\mathbf{x}(k)$, two simultaneous noisy measurements at time instant k are made. These two measured samples are labelled $y_g(k)$ and $y_b(k)$. These two measured samples are the calculated values of the equivalent conductance and susceptance of the electrical network.

$$y_g(k) = c_g.g(k) + v_g(k) \tag{5.9}$$
$$y_b(k) = c_b.b(k) + v_b(k) \tag{5.10}$$

which can be written in a vector equation:

$$\mathbf{y}(k) = \mathbf{C}.\mathbf{x}(k) + \mathbf{v}(k) \tag{5.11}$$

From the two vector eqs. (5.8) and (5.11) and minimization of the mean-square error, the vector Kalman predictor can be derived [A100]. We obtained the following set of equations [A51, D7]:

1) **Predictor equation**

$$\hat{\mathbf{x}}(k+1) = \mathbf{A}.\hat{\mathbf{x}}(k) + \mathbf{G}(k).[\mathbf{y}(k)-\mathbf{C}.\hat{\mathbf{x}}(k)] \tag{5.12}$$

2) **Kalman gain**

$$\mathbf{G}(k) = \frac{\mathbf{A}.\mathbf{P}(k).\mathbf{C}^T}{\mathbf{C}.\mathbf{P}(k).\mathbf{C}^T + \mathbf{R}(k)} \tag{5.13}$$

3) **Prediction mean-square error**

$$\mathbf{P}(k+1) = [\mathbf{A} - \mathbf{G}(k).\mathbf{C}].\mathbf{P}(k).\mathbf{A}^T + \mathbf{Q}(k) \tag{5.14}$$

with $\mathbf{R}(k) = E\{\mathbf{v}(k).\mathbf{v}^T(k)\}$ and $\mathbf{Q}(k) = E\{\mathbf{w}(k).\mathbf{w}^T(k)\}$

$\mathbf{R}(k)$ is the covariance of the measurement noise and $\mathbf{Q}(k)$ is the covariance of the process noise. The decoupled scalar Kalman predictor can be obtained from the above mentioned Kalman vector equations [D7]. The parameters a_g and a_b, that describe the dynamic behaviour of the conductance and susceptance respectively, are unknown and time-varying, mainly because the characteristics of the electrical load are non-linear. This implies that it is impossible to make an estimation of the network parameters if the dynamic behaviour of the system is unknown [H6,18]. One possible solution is to do an estimation of the dynamic behaviour of the parameters, before an actual estimation of the network parameters is performed [H18].

5.5.5 Estimation of the Dynamic Behaviour of Network Parameters

The dynamic behaviour of the power system is described by means of the algorithm parameters in the **A**-matrix, a_g and a_b. The following set of equations is used to determine these two parameters when the vector state Kalman predictor is used [A51, D7]:

1) **Parameter estimation equation:**

$$\hat{\mathbf{a}}(k+1) = \hat{\mathbf{a}}(k) + \mathbf{G}(k).[\mathbf{y}(k) - \mathbf{M}(k).\hat{\mathbf{a}}(k)] \qquad (5.15)$$

2) **Kalman gain**

$$\mathbf{G}(k) = \frac{\mathbf{P}(k).\mathbf{M}^T(k)}{\mathbf{M}(k).\mathbf{P}(k).\mathbf{M}^T(k) + \boldsymbol{\Sigma}_{vv}(k)} \qquad (5.16)$$

3) **Estimated mean-square error**

$$\mathbf{P}(k+1) = \mathbf{P}(k) - \mathbf{G}(k).\mathbf{M}(k).\mathbf{P}(k) \qquad (5.17)$$

with $$\mathbf{M}(k) = \begin{bmatrix} \hat{g}(k) & \hat{b}(k) & 0 & 0 \\ 0 & 0 & \hat{g}(k) & \hat{b}(k) \end{bmatrix}$$

and $$\mathbf{a}(k) = \begin{bmatrix} a_g(k) \\ 0 \\ 0 \\ a_b(k) \end{bmatrix}$$

with $\hat{g}(k)$ and $\hat{b}(k)$ the previous predicted value of the conductance and susceptance [D7]. $\mathbf{A}^T(k)$ and $\mathbf{x}(k)$ the input matrix of the conductance and susceptance and $\boldsymbol{\Sigma}_{vv}(k) = E\{\mathbf{v}(k).\mathbf{v}^T(j)\}$ the covariance matrix of the measurement noise.

The parameters that describe the dynamics of the conductance a_g, and the susceptance a_b, are unknown. Their average

values are the same as the parameters that describe the measurement process, c_g and c_b, thus

$$c_g = c_b = 1 \quad \text{and} \quad E\{a_g\} = E\{a_b\} = 1 \tag{5.18}$$

A dynamic penalizing function is introduced to stabilize the estimation filter after a change in the dynamic behaviour is experienced [A51, D7]. The penalizing function takes the ratio of the predicted values and multiply the Kalman gain G with these factors to stabilize the output:

$$PG(k) = \hat{g}(k)/\hat{g}(k-1); \quad PB(k) = \hat{b}(k)/\hat{b}(k-1) \tag{5.19}$$

These estimated values $\hat{a}_g(k+1)$ and $\hat{a}_b(k+1)$, are used in the state predictor to make a prediction of the conductance and susceptance at the time instant (k+1), given the data at time instant k. The predicted states $\hat{g}(k+1)$ and $\hat{b}(k+1)$ are also multiplied by the correction factors PG(k) and PB(k) respectively to form the actual predicted values (eq. 5.15). This is necessary to speed up the convergence of the predictor [D7].

5.5.6 Results of Network Parameter Estimation Algorithm

To illustrate the prediction of network parameters under dynamic conditions, two network parameters, G and B, were estimated by means of an estimation simulation algorithm, implemented on a personal computer [D7].

5.5.6.1 Computer algorithm of network parameter estimation simulation

A flow diagram of the simulation process is shown in fig. 5.8. The waveforms of voltage and current are generated, with appropriate dynamic response, to evaluate the accuracy of the predictor under dynamic conditions [D7]. After the generation of waveforms, the auto- and cross-correlations are performed on the generated data, followed by the calculation of the conductance G and

susceptance B, over the previous measurement interval dT. The calculated network parameters are used to make an estimate of the dynamic response, followed by a prediction of the network parameters over the next measurement interval dT. A full description of the simulation process is shown in reference D7.

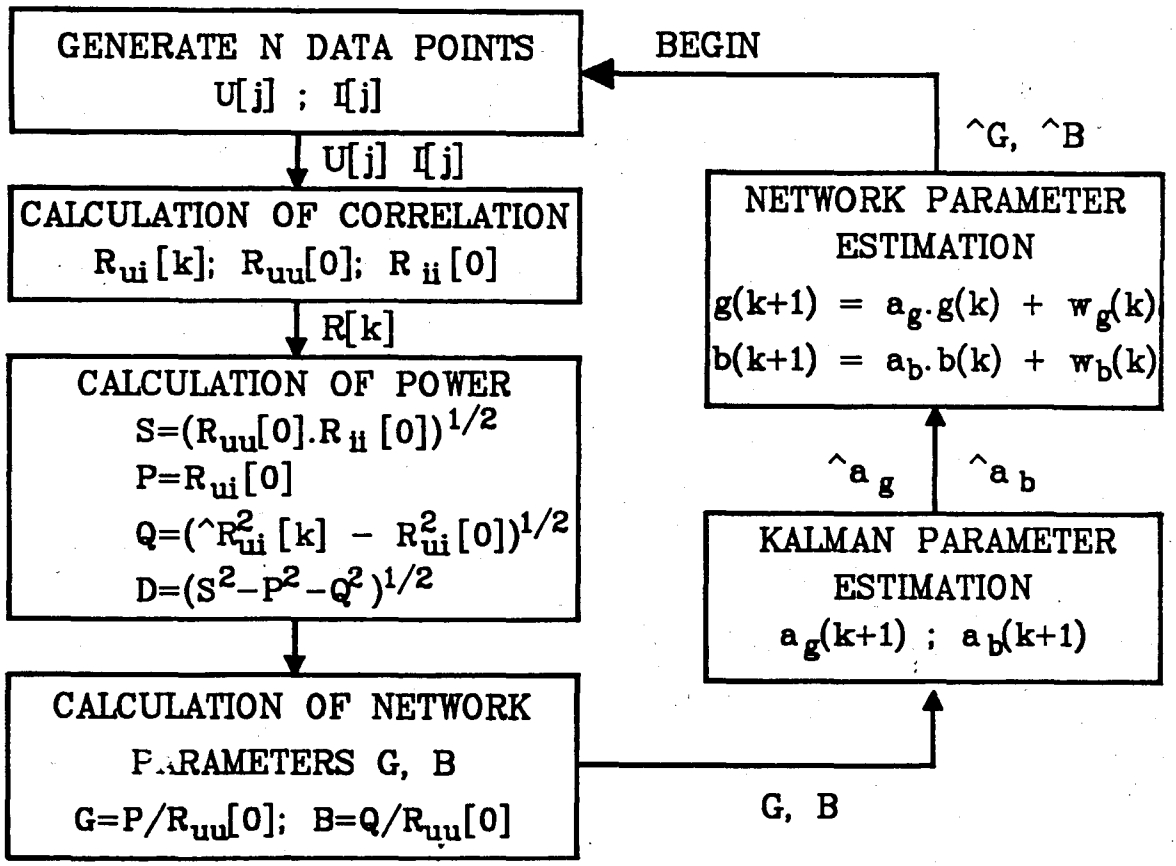

Fig. 5.8: Representation of the Simulation Process.

5.5.6.2 Results obtained from simulation algorithm

The prediction algorithm is tested under dynamic response. The first result, which shows the simulation of the Kalman prediction algorithm, is concerned with the accuracy of the predictors, demonstrating that only a few values are needed for a prediction. The second important result shows that the predictor resumes operation after one of the states had become zero. Typical results are shown in fig. 5.9 and 5.10 respectively.

The predictor gives accurate results when the dynamic response is known (in the linear portions of fig. 5.9). When the dynamic response of the system is, however, changed, the predictor makes a mistake of only one point, adapting very fast to the new dynamic response, as shown in fig. 5.9.

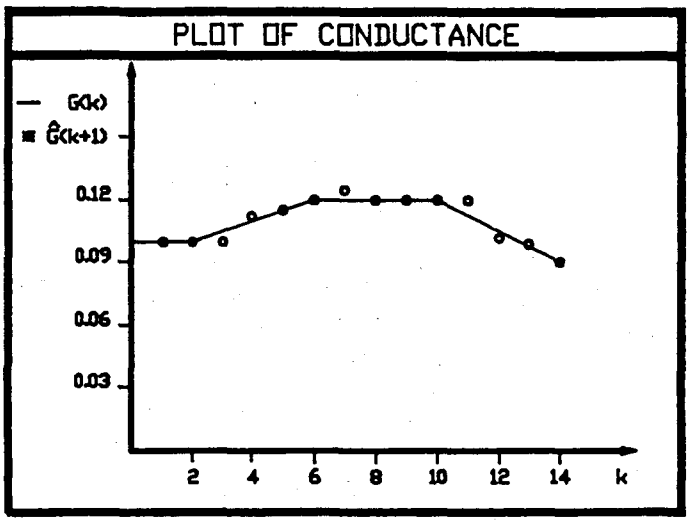

Fig. 5.9: Accuracy of Prediction Algorithm.

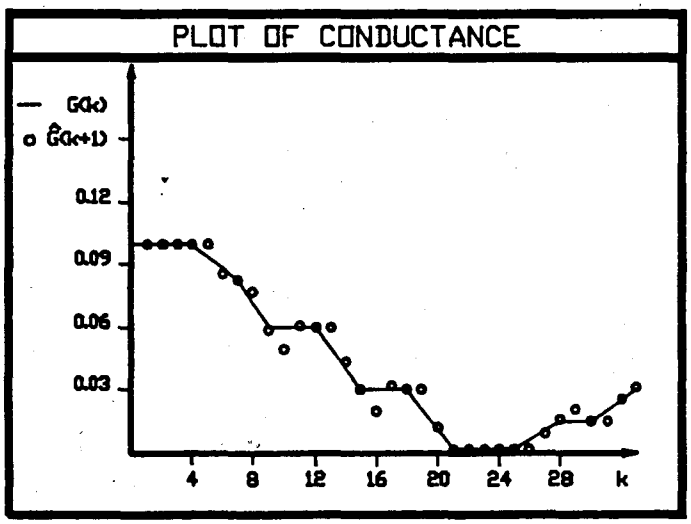

Fig. 5.10: Prediction after a Zero State.

Instability problems have been experienced when one of the network parameters, to be predicted, became zero [A51, D7]. The problem is solved by means of the penalizing function described in the previous section and analysed in reference D7. Figure 5.10 shows the

predictor when one of the parameters, in this case the conductance, has become zero. From these two results it is clear that the prediction algorithm adapted to the changes in the dynamic response of the power system quite fast. It is, however, important to note that the measurement interval should be chosen an order shorter than the average system response, otherwise the predictor is inaccurate.

5.5.6.3 Result obtained from experimental estimation of network parameters

The network parameter estimation algorithm is evaluated experimentally on a power electronic system. The system is described in chapter 4 and shown schematically in fig. 4.20. The experimental system consists of a 10 kVA Scherbius rotor cascade induction machine drive with speed control by means of the six-pulse inverter, controlled by the fire angle α. The dynamic load changes are performed by changing this fire angle α. The results of the estimator is shown in fig. 5.11. The calculated network parameters are shown on the same plot as the estimated values. Any inaccurate estimations can easily be detected.

The dynamic behaviour of the load is changed to test the robustness of the estimation under dramatic load changes. From fig. 5.11 the algorithm converges very fast to the new values within two or three calculations. Some overshoots have been experienced with the step response which is a matter for further investigation. Generally speaking, the estimation algorithm seems to be stable and well worthwhile in implementing in applications of real-time fictitious power compensation and measurement.

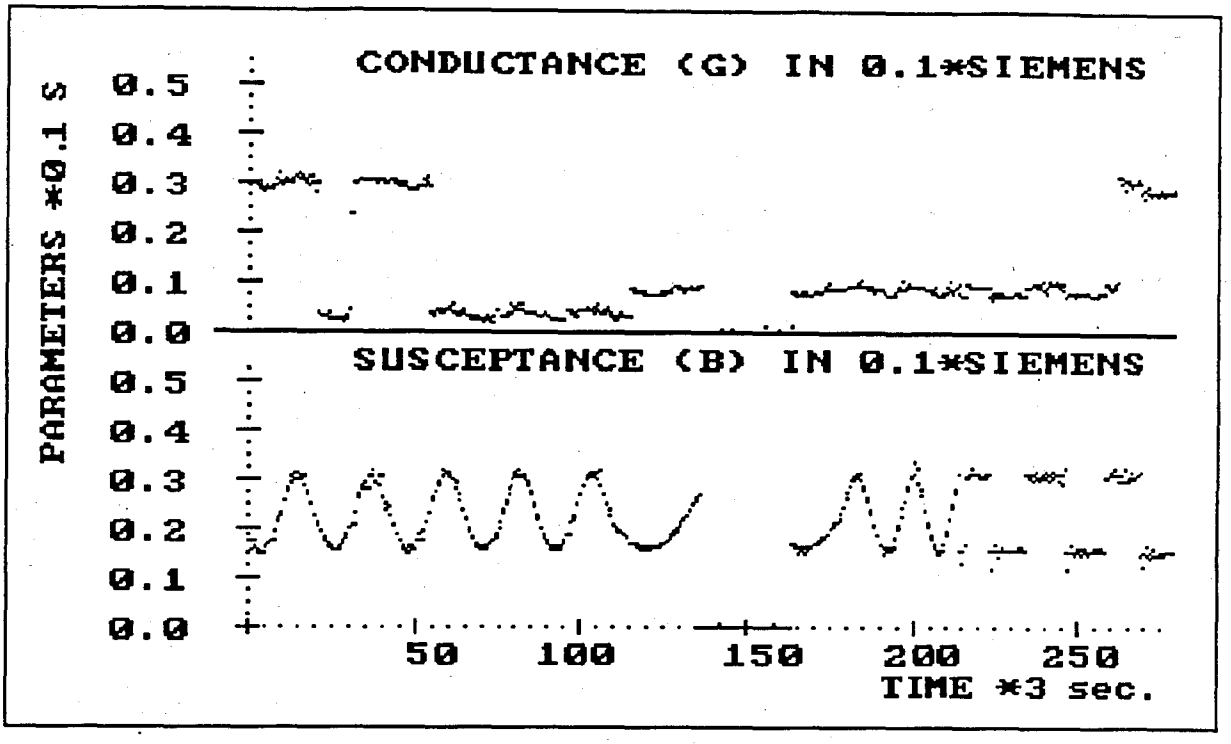

Fig. 5.11: Result of Estimation Algorithm in an Experimental Power Electronic System

5.6 SUMMARY

In this chapter the basic problems associated with the compensation of fictitious power in electric power systems are stated and a new philosophy for fictitious power compensation is derived. This philosophy is based on the definition of electric power showed and evaluated in chapter 3.

Diversity in the different fictitious power compensation systems, can advantageously be implemented in the control of fictitious power by means of a combination of these systems and is having a positive effect on the cost of fictitious power compensation in general. The principle of this philosophy is to have different systems, with different dynamic responses controlling different portions of fictitious power.

The problem of real-time control of power compensation systems is one of the major constraints placed on fictitious power compensation systems, furthermore the control philosophy of high dynamic response power filters is one of the reasons why these systems are not in commercial use in the compensation of highly contaminated power supplies. This chapter proposed adaptive signal processing techniques to calculate the instantaneous signals of the divided loading functions, active, reactive and deactive currents.

The adaptive signal processing system is based on the calculation of power components and network parameters on-line and the implementation of a first order autoregressive process of the network parameters. This process is simulated in power systems under dynamic loading conditions to evaluate the operation of the estimation process. Actual measurements are performed on typical power electronic converters.

This paper proposes a new philosophy for fictitious power control based on correlation. The possibility of measuring different power components with the aid of correlation signal processing techniques was highlighted with some actual measurements on a Scherbius rotor cascade induction machine drive. The control of dynamic power filters, a major outstanding problem, is proposed to be more effective with fast analogue and digital signal processing techniques.

A fundamental problem in power networks is, however, the variation of the parameters. Estimation was investigated for the defined conductance and susceptance of the power network, and shown to be practically feasible when using Kalman techniques under the assumptions reasonably acceptable in power networks.

CHAPTER 6

STRUCTURE, DEVELOPMENT AND CONTROL OF DYNAMIC POWER FILTERS

6.1 INTRODUCTION

Dynamic power filters were introduced in the seventies by Harashima et al [A81], influenced by increased distortion caused by power electronic converters and advantages made on forced commutated power converters with high switching frequencies. The high capital and running expenditure of these dynamic compensators, hinder their wide spread use in contaminated industrial power networks. It has been found that the cost of these dynamic power filters, at moderate power levels, is so high that the power network can rather be operated at a higher tariff, without these compensation systems. Furthermore the compensation system should, in the majority of cases, be dimensioned for the same order of magnitude as the power network, which implies that it is better to design low-distortion generating power converters in the first instance. This fundamental limitations can, however, be overcome if the dynamic power filter (DPF) is not dimensioned for all the fictitious power, but rather for a small quantity which have high dynamic characteristics. This portion of fictitious power is analysed and characterized as deactive power in this thesis (chapter 3,4).

To demonstrate the superiority of subdividing fictitious power into reactive and deactive powers, an experimental three-phase dynamic power filter (DPF) is controlled by means of the derived fictitious current and the derived deactive current. Impressive results showing the operation of the DPF with these two control inputs, are shown towards the end of this chapter. The structure and classification of dynamic power filters are also addressed for clarity reasons in this chapter.

A three-phase DPF is developed with unsymmetrical current compensation capabilities [A139, D9]. This experimental system consists of three, single phase PWM converters which are individually controlled [A139, D10]. The DPF is designed with a power rating of 5 kVA per-phase. Digital and analogue signal processing techniques are used in the calculation of the current reference signal within the control scheme of the DPF. Different methods to derive the reference current for the DPF, as proposed by other authors [A1,35,37,61,81,119], are evaluated. A control scheme comprises the defined power components and adaptive signal processing techniques, shown in chapter 3 and 4 respectively, is evaluated experimentally in this chapter.

6.2 STRUCTURE AND CLASSIFICATION OF DYNAMIC POWER FILTERS (DPF)

Fictitious power compensation systems are classified in chapter 5 on the basis of their dynamic system response. It is also shown that these compensation systems have a reciprocal relationship between dynamic system response and compensation power rating. In this paragraph the high dynamic response power filters are characterized further. Dynamic power filters are based on reactive loaded, forced commutated converters with a high switching frequency (at least one or two orders higher than the fundamental frequency of the generating function associated with the contaminated power network).

The converters can normally be characterized either by means of the voltage or current-fed topologies and by means of their unsymmetrical power compensation capabilities. Furthermore the classification can be extended to passive and active systems, the first implies that no external power supply is utilized for internal loss compensation of the DPF while the latter implies that an external power supply is used for this purpose. The passive system uses energy from the contaminated supply to compensate the losses, realized in the control strategy of the dynamic power filter.

6.2.1 Voltage and Current-fed Topologies

Figure 6.1 shows the two different systems in block diagram form. The voltage-fed system, fig. 6.1(a), is characterized by having a capacitor imposing a relative constant voltage onto the converter bridge CB, while the current-fed system has the inductor L, imposing a relative constant current onto the bridge CB.

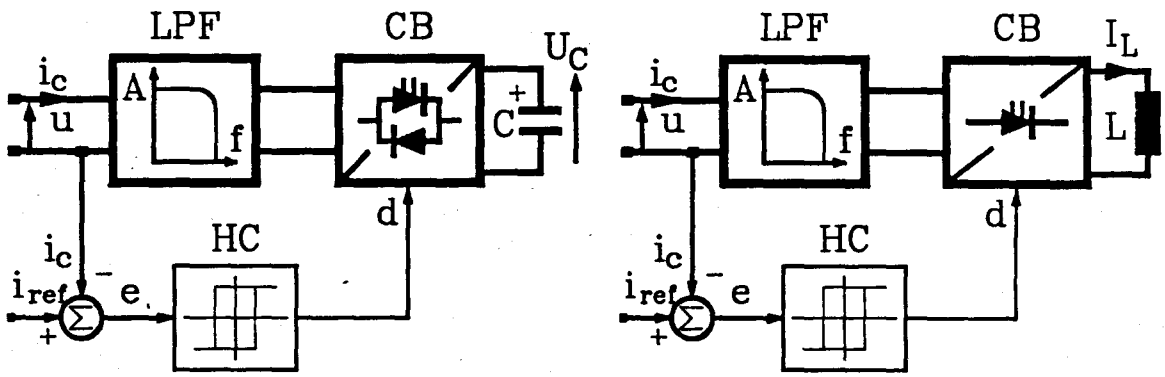

(a) Voltage-fed (b) Current-fed

Fig. 6.1: Voltage and Current-fed DPF-topologies.

The rest of each compensation system consists of the same components; a low-pass filter LPF and converter control. This diagram shows a simple hysteresis controller HC, controlling the switching of the bridge. The current-fed system has to be controlled in such a manner as to always leave a path for the source current I_L, while the voltage-fed system has a freewheeling path with a control strategy that minimized a source short circuit. The advantages and disadvantages of each system and the dimensions of the energy storage components have not been addressed successfully in literature and is a study on its own.

6.2.2 Unsymmetrical Multiphase Compensation.

To compensate fictitious power in multiphase systems, where an unbalanced loading of the different phases are predominant, the compensation system should have the capability of four wire operation in a three phase system.

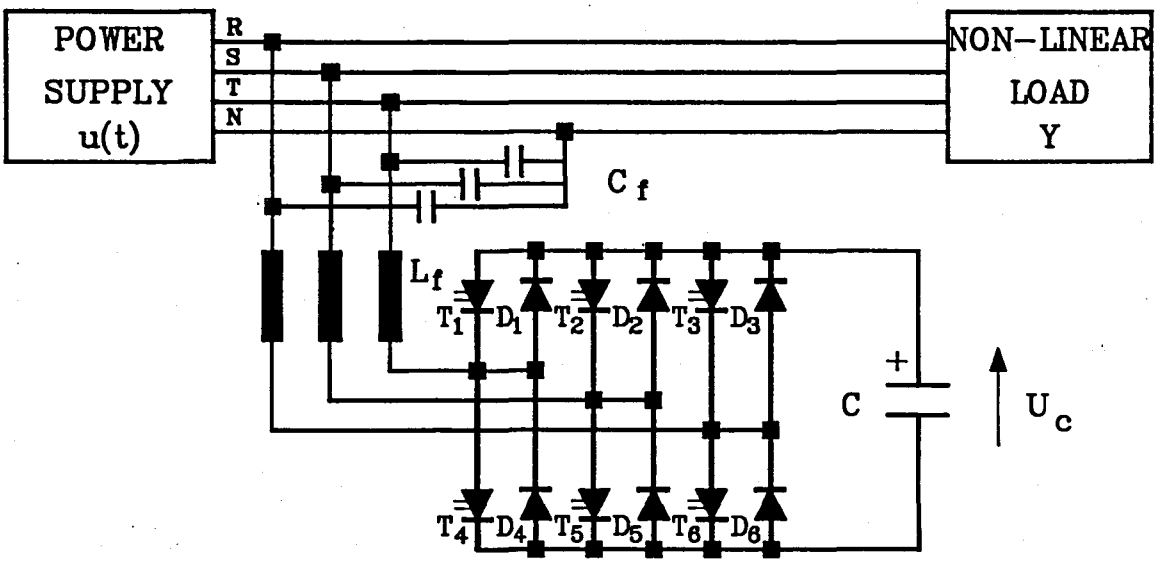

Fig. 6.2: Multiphase DPF Incapable of Unsymmetrical Compensation.

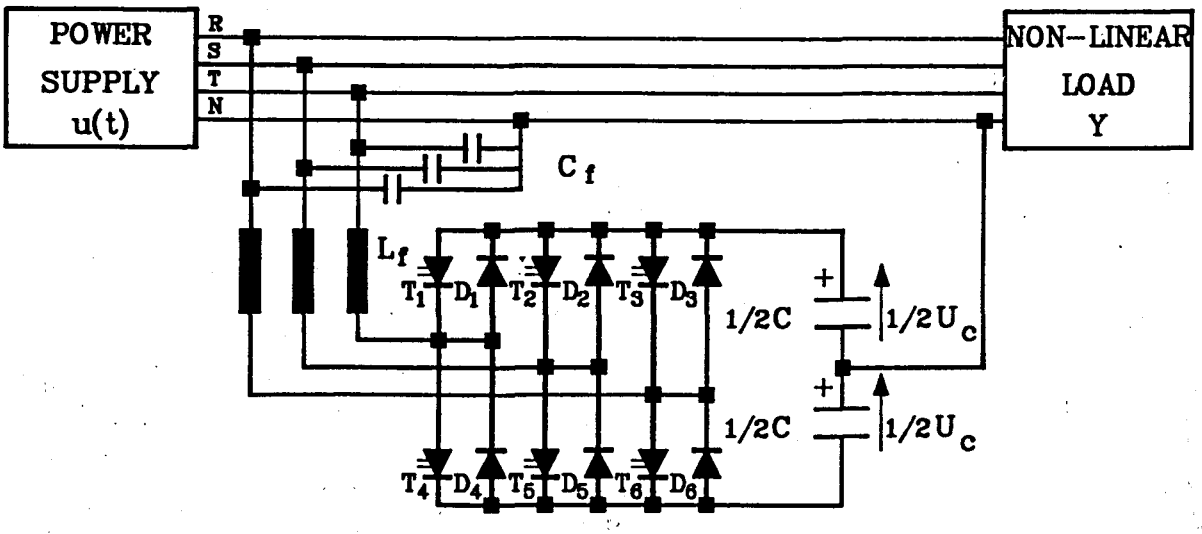

Fig. 6.3: Multiphase DPF Capable of Unsymmetrical Compensation.

This can either be performed by means of three separate single phase converters which are individually controlled [A139], or by means of a more complicated single converter with more switching elements [A37]. The latter has less switching elements than the first and a single reactive ele-

ment is collectively used by all three phases, again voltage and current-fed topologies may be used [A37].

Figure 6.2 shows the voltage-fed topology incapable of unsymmetrical compensation [A1], while fig. 6.3 shows the same topology which is capable of unsymmetrical compensation [A37]. The control scheme of these two systems are quite different [A1,37].

6.2.3 Active Versus Passive Dynamic Power Filters

Dynamic power filters are, as with all power converters, not loss-less. The losses associated with the low-pass filter LPF, the converter bridge CB and the reactive element C/L have to be compensated either by means of the power supply common to the load and the compensation system, implemented by means of the control scheme, or by means of an external power supply independently controlled. The latter implies an easier control strategy and seems to be better in power systems with a high dynamic response. The system which compensates the power losses in the DPF, can be a small converter charging a small battery or capacitor. The second converter is only rated for the losses in DPF and can easily be realized by means of high-frequency switching devices with minimum distortion generated back into the supply. Figure 6.4 shows schematic diagrams of the two systems.

The active converter type can be realized in a voltage or current-fed topology, with the voltage-fed converter easily realized with a small battery or capacitor as energy storage element. The second power bridge LCB is used to compensate the losses in the DPF, calculated as $I_{al}.U$, with I_{al} the effective value of active current drawn from the power supply. The control of this system can easily be realized under dynamic loading conditions of the DPF because the two converter systems are controlled separately. The same separate control strategy can be utilized in a passive DPF, if the reactive element is exchanged for a battery or other energy storage element.

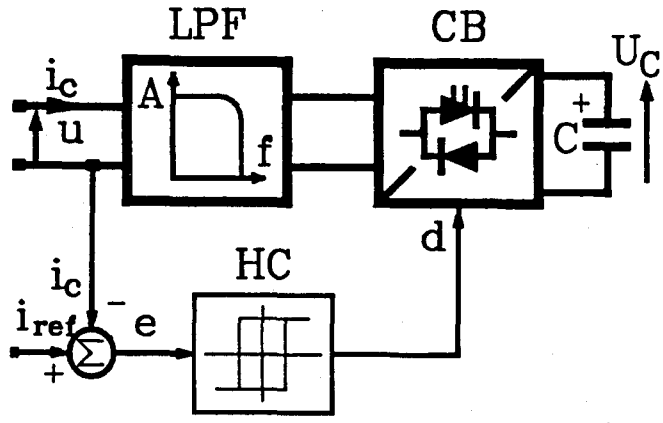

(a) Passive DPF

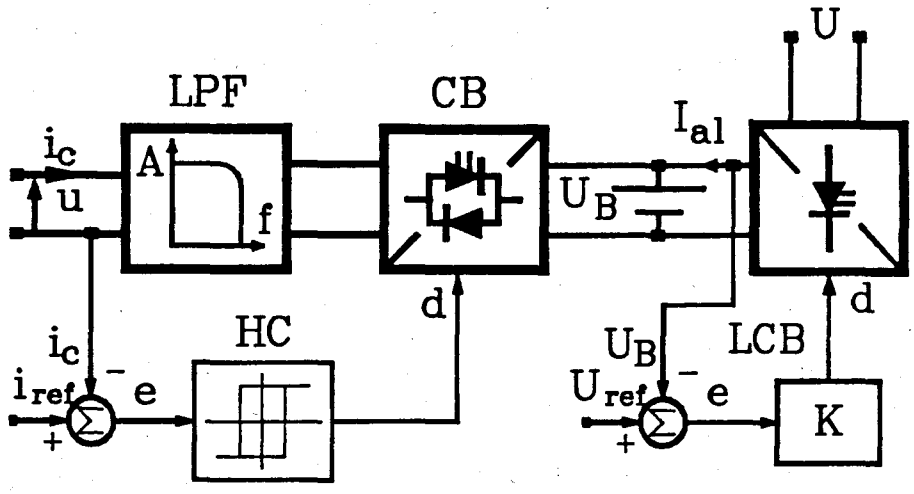

(b) Active DPF

Fig. 6.4: Passive and Active DPF Topologies.

In the passive DPF the losses are compensated for by means of an external derived current i_{al}, which is an active current component summed together with the reference current i_{ref}. The derivation of this current component under dynamic loading conditions is a troublesome task [A1,50,101, D5,10]. The classification of dynamic power filters, as shown above, is used in the analysis of these compensation systems in the rest of this chapter. The experimental system, used for the evaluation of the fictitious power control philosophy, is a passive 15 kVA three-phase DPF, based on three individual single phase converters operating separately in each phase. The loss compensation of the experimental DPF is performed

within the control scheme of the converter, with energy drawn from the contaminated power supply.

6.3 BLOCK DIAGRAM REPRESENTATION OF A 15 kVA PASSIVE DPF

The schematic circuit diagram of the experimental passive dynamic power filter is shown in fig. 6.5. The system is based on a full-controlled bridge in a current-fed topology [A139, D10].

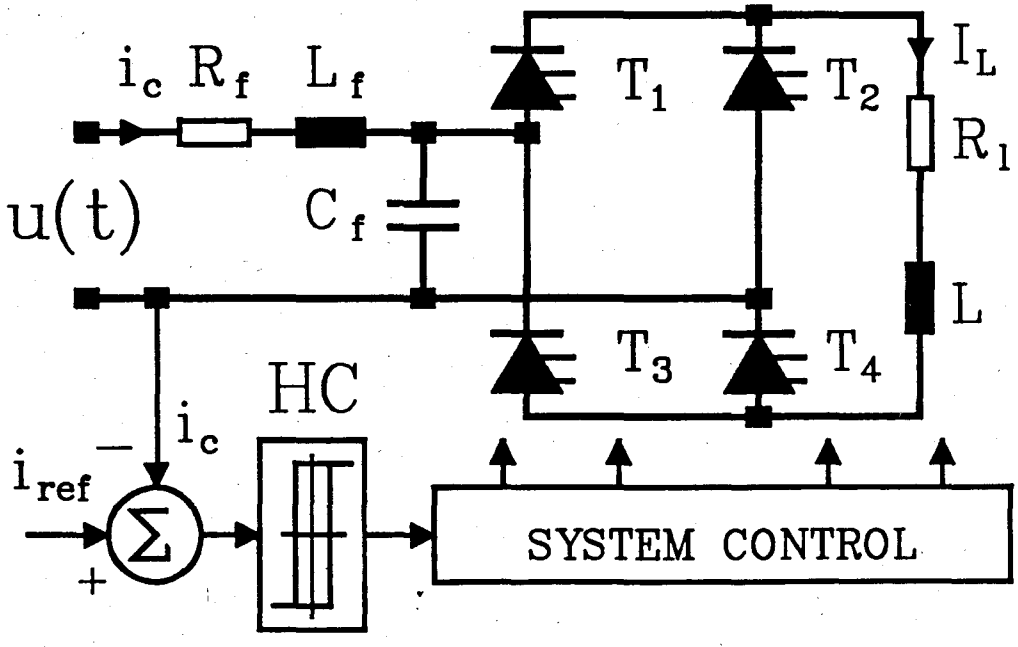

Fig. 6.5: Schematic Circuit Representation of Experimental Dynamic Power Filter DPF [A139]

The single phase system consists of a bridge power electronic converter with bipolar transistor switches and associated snubbing, control circuitry, inductive energy storage element L and low-pass filter LPF. The low-pass filter is incorporated within the isolation transformer leakage inductance L_f and filter capacitor C_f. This puts a fundamental limitation on the bandwidth of the DPF, but is necessary for high-frequency filtering. Copper resistances in the inductor L and isolation transformer IT are shown as R_l and R_f respectively.

The block diagram representation of the DPF is shown in fig. 6.6. The basic control of the bridge is achieved by means of a hys-

teresis controller HC. Limit-cycle problems, associated with the hysteresis controller, were experienced within the compensation control loop and for this reason an active compensation filter is included in the feedback loop [A139, D10]. The active filter is designed for optimal pole placing, which consist of two poles and two zeros in the s-plane, this pole placing is a function of the system and should be changed if other components are used [A139, D10].

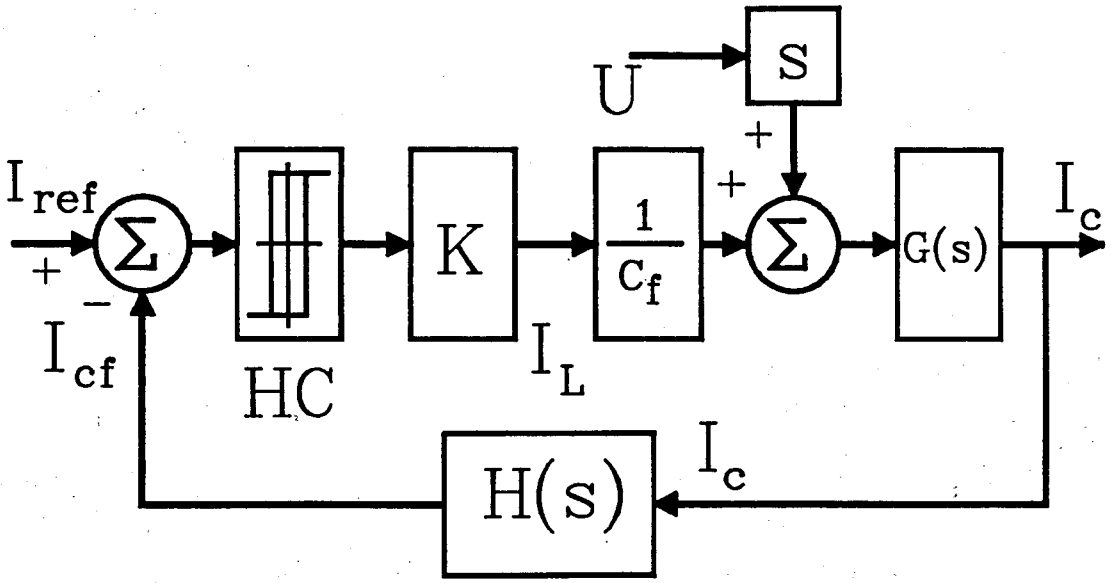

Fig. 6.6: Block Diagram Representation of DPF with Active Filter Compensation.

The transfer function G(s) of the DPF power circuit is expressed as follows:

$$G(s) = \frac{1}{L_f.s^2 + R_f.s + 1/C_f} \qquad (6.1)$$

The active filter compensation circuit (AFC) has a transfer function H(s) with two poles and two zeros, as shown in eq. (6.2) [A139, D10]:

$$H(s) = \frac{K_1(as^2 + bs + c)}{as^2 + ds + 1} \qquad (6.2)$$

with K_1 the filter gain and a, b, c and d filter constants describing the poles and zeros of the filter. The limit-cycle is found to have a frequency of 1 kHz in this experimental DPF. The active filter compensation was designed with complex poles and real zeros to compensate for the limit-cycle [D10].

6.4 INTERNAL LOSS COMPENSATION OF THE DPF

A problem with passive DPF systems, is the compensation of the losses by means of the control strategy. This problem is addressed and solved under steady state and quasi dynamic operating conditions [D5].

6.4.1 Characteristics of Converter Losses

Losses associated with the passive DPF power circuit have to be compensated for by means of active power drawn from the power network. In characterizing the losses associated with the compensation system, it has been found that there are fundamentally three types of losses [D5,10]:

(a). Losses in the power semiconductors, which include on-losses and switching losses. Both are a function of compensation current because the switching frequency is also changed by means of the hysteresis controller, proportional to the compensation current.
(b). Copper losses associated with the current-fed inductor L. This power loss is a function of the inductor current I_L, which is not directly a function of the compensation current.
(c). Copper losses associated with the isolation transformer. These losses are directly proportional to the compensation current.

From the above mentioned losses it is clear that the losses in the total DPF are not directly proportional to the loading and can vary with component manufacture, temperature, time and loading. For these reasons it is necessary to have

a current feedback loop, stabilizing the inductor current I_L. Through careful analysis of the system losses, it is found that 52% of total losses in the converter is associated with the semiconductor power bridge circuit, 35% with the inductor and 13% with the isolation transformer. The values are related to a full load of 5 kVA per phase and an overall efficiency of 92% [D10].

6.4.2 Current Feedback Loop for Inductor Current

The energy stored in the inductance should be kept at a constant value if only deactive power compensation is of interest. The energy E_L stored in the inductor L, at any given time, is described by eq. (6.3)

$$E_L = \tfrac{1}{2} L . I_L^2 \qquad (6.3)$$

The total power losses in the compensation system can be compensated by means of an active current component, which is drawn from the power network. The value of the product of this active current component and supply voltage is equivalent to the total power losses in the DPF. The active current component is added to the reference of the required compensation current i_c. This will increase the active power drawn from the network.

$$i_{ref} = i_c + i_{al} \qquad (6.4)$$

The active current i_{al}, necessary for power loss-compensation, is derived from the equivalent loss-conductance G_l and the network voltage signal u(t) [D5].

$$i_{al} = G_l . u \qquad (6.5)$$

The equivalent conductance associated with the losses in the converter G_l, is derived directly from the inductor current I_L. This loss-compensation which is implemented in the control strategy, is realized by means of a secondary control loop, controlling the inductor current I_L by means of an in-

ductor current reference value I_{Lm} [D5]. The error between the reference value I_{Lm} and the actual inductor current I_L, is proportionally controlled with a relative high gain and associated low-pass filter with a long time constant τ_L. The block diagram of the transfer function between I_L and G_l is shown in fig. 6.7.

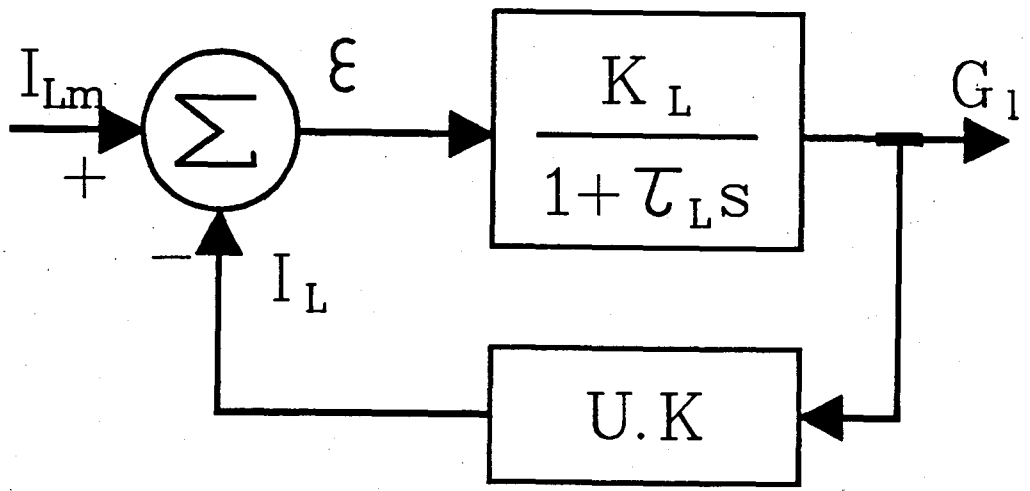

Fig 6.7: Block Diagram Representation of Loss-compensation Controller

The power converter of the DPF and the steady state supply voltage is shown in the feedback loop with gain K and voltage U respectively. The close loop transfer function for the controller is shown in eq. (6.6) [D5]:

$$\frac{G_l}{I_{Lm}} = \frac{K_L.(1 + \tau_L.s)^{-1}}{1 + U.K.K_L.(1 + \tau_L.s)^{-1}} \qquad (6.6)$$

This loss compensation system, incorporated in the total control strategy, is shown in the block diagram representation of fig. 6.8 [D5]. From eq. (6.6) (derived in reference D5) the gain has to be much higher than one for ϵ to result in a small value. Under steady state conditions, the total transfer function in eq. (6.4) simplifies to 1/(K.U) [D5].

This implies that high gain in the feedback loop K (DPF converter gain) results in smaller equivalent loss conductance G_l. In the practical system the gain K_L is increased

together with an increase in the low-pass filter time constant τ_L until satisfactory results are obtained. The time constant τ_L is set at 8 seconds and the gain K_L to 12. If the time constant τ_L is decreased, the converter acts as an aperiodic current generator, rather than a power filter. This emphasizes the fundamental problems associated with loss-compensation control [A50, D5].

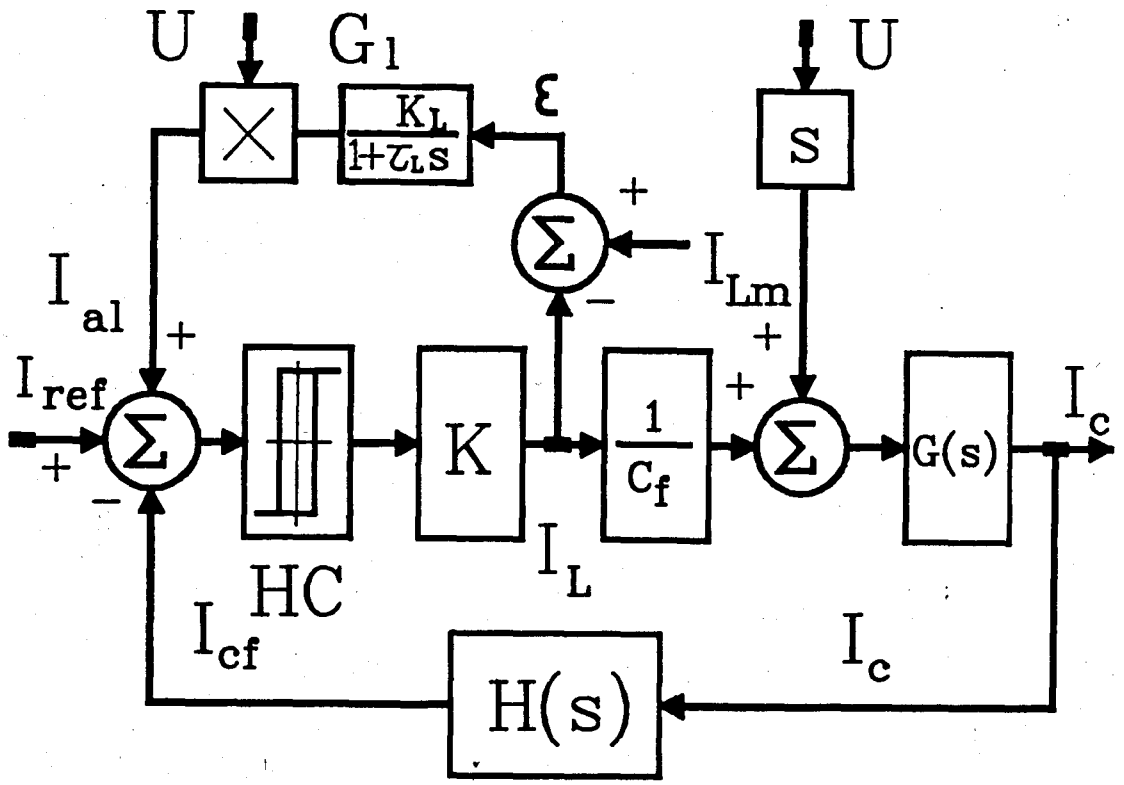

Fig. 6.8: Total Block Diagram Representation of Converter with Loss-compensation Control

This time constant τ_L of the loss-compensation loop places a fundamental limitation on the response of the energy stored control of the reactive element, which again has a negative effect on the dynamic response of the total dynamic power filter. If a passive DPF is to be used in power systems with the effective values of the compensation current having a high dynamic response, the loss-compensation control scheme, as described above, has to be adapted or an active DPF with a secondary loss-compensation converter or control strategy should be implemented.

6.5 ORTHOGONAL SUBDIVISION OF NON-LINEAR LOAD CURRENT

In the previous paragraph the losses of the converter are compensated with an extra current component i_{al} summed together with the reference of the compensation current i_c. Deriving the reference value i_{ref}, is the major interest of this chapter. The division of active current i_a and fictitious current i_f, (chapter 3) forms the fundamental principle of generating the reference value i_{ref} for the purpose of controlling the DPF.

The division of load current is done on the fundamental principle of orthogonality between i_a, i_f, i_r and i_d (chapter 3).

$$\overline{i_a . i_f} = 0 \quad \text{and} \quad \overline{i_r . i_d} = 0 \tag{6.7}$$

This is the fundamental limitation and implies that averages have to be taken for the calculation of the orthogonal components. The time interval dT over which the averages of the different current waveforms is calculated has to be a function of the generating and loading functions. In quarterwave symmetrical waveforms for generating and loading functions, the time interval has to be at least a quarter of the fundamental period. In aperiodic waveform conditions the time interval should be longer than the dynamic response of the system. Many authors have proposed methods to decompose the different orthogonal current components, in a power system with a voltage generating function, in the shortest possible time [A1,35,37,61,81,119]. These approaches are critically evaluated below. An adaptive signal processing approach, utilizing the proposed definition (chapter 3) is used in the control of the DPF.

6.5.1 Current Subdivision According to Harashima

Harashima et al introduced one of the first experimental dynamic power filters in 1975/1976 [A81]. They used the fundamental definition of Fryze [A69] to divide the load current into active and fictitious currents. The equivalent conductance G, associated with the power network, is calcu-

lated through the functional block diagram shown in fig. 6.9. The conductance G can be expressed as follows:

$$G = U^2/P \tag{6.8}$$

Where U is the effective value of the network voltage u(t) and P is the average active power over the time interval dT.

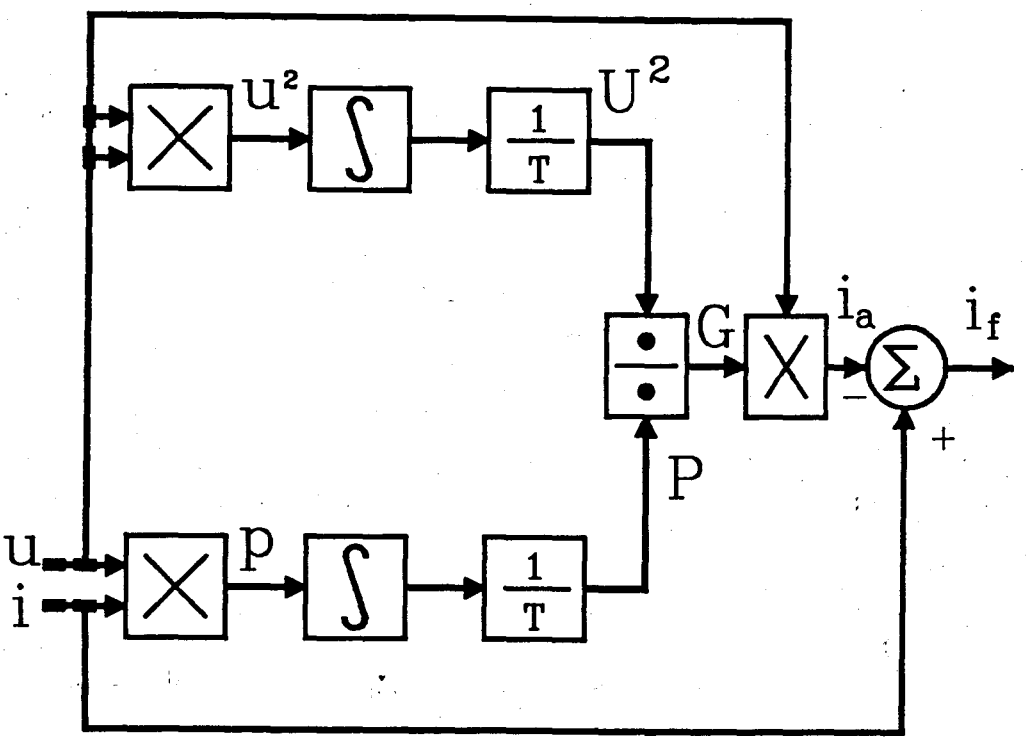

Fig. 6.9: Functional Block Diagram of Harashima Current Divider in the Time Domain.

The block diagram of the reference current generation circuit, as shown in fig. 6.9, can be realized by means of simple analogue electronic devices. This system can only calculate conductance G for periodical waveforms, because the time interval is proportional to the fundamental period T of the voltage signal. The fastest calculation can be performed when both current and voltage have quarterwave symmetry.

This limitation places a limitation on the calculation of conductance G under aperiodic waveforms for current and/or voltage. Furthermore this division can only be used to com-

pensate the total fictitious power, no provision is made to subdivide the fictitious power into other components, as proposed in chapter 5.

6.5.2 Generalized Theory of Instantaneous Power

This generalized theory of instantaneous reactive power, was developed by three researchers Akagi, Kanazawa and Nabae [A1,2]. This theory is developed to control DPF's in three-phase applications and can not be used in its basic form for unsymmetrical and single phase systems. This division of load current is based on an orthogonal mathematical transform of the load current, but does not represent fictitious power, because it is not derived from average power values.

The instantaneous imaginary power q and the instantaneous real power p in a three-phase circuit, excluding zero-sequence components, are defined by the authors in reference A1. This division is based on an orthogonal mathematical transformation of the instantaneous three-phase voltages u_r, u_s and u_t into two orthogonal co-ordinates α and β. The same principle is adopted for the three-phase currents i_r, i_s and i_t. Equations (6.9) and (6.10) show the relationships.

$$\begin{bmatrix} u_\alpha \\ u_\beta \end{bmatrix} = \sqrt{(2/3)} \begin{bmatrix} 1 & -1/2 & -1/2 \\ 0 & \sqrt{3}/2 & -\sqrt{3}/2 \end{bmatrix} \cdot \begin{bmatrix} u_r \\ u_s \\ u_t \end{bmatrix} \qquad (6.9)$$

$$\begin{bmatrix} i_\alpha \\ i_\beta \end{bmatrix} = \sqrt{(2/3)} \begin{bmatrix} 1 & -1/2 & -1/2 \\ 0 & \sqrt{3}/2 & -\sqrt{3}/2 \end{bmatrix} \cdot \begin{bmatrix} i_r \\ i_s \\ i_t \end{bmatrix} \qquad (6.10)$$

The instantaneous power is again a transformation of the orthogonal co-ordinates of voltage and current. Figure 6.10 shows the instantaneous space vectors u_α, u_β, i_α and i_β.

The transformation of the instantaneous power into two orthogonal components is performed in eq. (6.11) and (6.12).

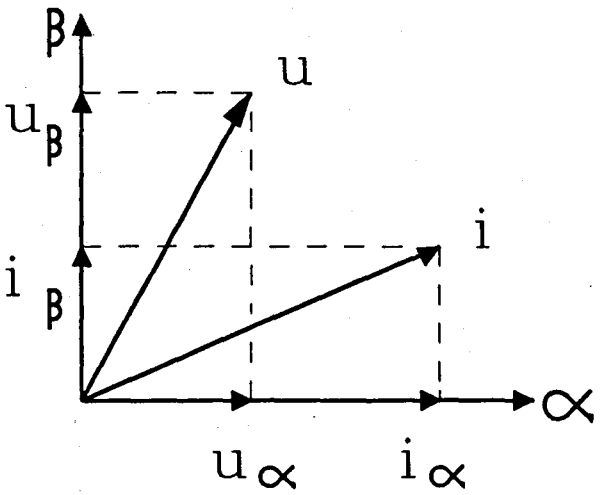

Fig. 6.10: Instantaneous Space Vectors

$$\begin{bmatrix} p \\ q \end{bmatrix} = \begin{bmatrix} u_\alpha & u_\beta \\ -u_\beta & u_\alpha \end{bmatrix} \cdot \begin{bmatrix} i_\alpha \\ i_\beta \end{bmatrix} \tag{6.11}$$

or

$$\begin{bmatrix} p \\ q \end{bmatrix} = \begin{bmatrix} i_\alpha & i_\beta \\ i_\beta & -i_\alpha \end{bmatrix} \cdot \begin{bmatrix} u_\alpha \\ u_\beta \end{bmatrix} \tag{6.12}$$

where p is instantaneous real power and q instantaneous imaginary power. For the definition of instantaneous reactive power the authors [A1,2], divided the load current into two kinds of instantaneous current components.

$$\begin{bmatrix} i_\alpha \\ i_\beta \end{bmatrix} = \begin{bmatrix} i_{\alpha p} \\ i_{\beta p} \end{bmatrix} + \begin{bmatrix} i_{\alpha q} \\ i_{\beta q} \end{bmatrix} \tag{6.13}$$

with

$$i_{\alpha p} = \frac{u_\alpha . p}{u_\alpha^2 + u_\beta^2} \qquad \alpha\text{-phase instantaneous active current}$$

$$i_{\alpha q} = \frac{-u_\beta . q}{u_\alpha^2 + u_\beta^2} \qquad \alpha\text{-phase instantaneous reactive current}$$

$$i_{\beta p} = \frac{u_\beta . p}{u_\alpha^2 + u_\beta^2} \qquad \beta\text{-phase instantaneous active current}$$

$$i_{\beta q} = \frac{u_\alpha . q}{u_\alpha^2 + u_\beta^2} \qquad \beta\text{-phase instantaneous reactive current} \tag{6.14}$$

From these components the different components of instantaneous power are derived.

$$p_{\alpha p} = \frac{u_\alpha^2 . p}{u_\alpha^2 + u_\beta^2} \qquad \alpha\text{-phase instantaneous active power}$$

$$p_{\alpha q} = \frac{-u_\alpha . u_\beta . q}{u_\alpha^2 + u_\beta^2} \qquad \alpha\text{-phase instantaneous reactive power}$$

$$p_{\alpha p} = \frac{u_\beta^2 . p}{u_\alpha^2 + u_\beta^2} \qquad \beta\text{-phase instantaneous active power}$$

$$p_{\alpha q} = \frac{u_\alpha . u_\beta . q}{u_\alpha^2 + u_\beta^2} \qquad \beta\text{-phase instantaneous active power} \qquad (6.15)$$

These components are used by Akagi et al to control a three phase DPF only capable of symmetrical compensation under steady state conditions with periodical waveforms for the current and sinusoidal voltages [A1,2]. Some amendments are made to the basic definition to accommodate zero-sequence components. This is done on the basis of defining a third orthogonal component into the 0-co-ordinated. The divisions shown in equations (6.9) - (6.15) are revised to accommodate this zero-phase sequence components in unbalanced three-phase loads [A2].

From the authors point of view, the instantaneous power components do have some advantages in the control of DPF's, this instantaneous power division is, however, not related to the load and does not describe the power phenomena in the power network. Furthermore this division does not make provision for the subdivision of fictitious power into other components. This implies that it can not be used in the proposed compensation philosophy derived in chapter 3.

6.5.3 Load Current Division According to Filipski

The load current division of Filipski [A60,61] is based on the time domain definition of power by Fryze [A69]. This division involves an orthogonal current divider which con-

sists of two multipliers, a summation circuit and a low-pass filter with high gain [A60,61]. Through the low-pass filter the orthogonality is obtained, which again puts the fundamental limitations on the dynamic bandwidth of the system. Figure 4.1 shows a functional block diagram of the orthogonal current divider. Mathematically the divider is evaluated in chapter 4, paragraph 4.2.2 [A60].

This current division system, described by Filipski, is incorporated in the control system of the experimental DPF system because of the simple design for fictitious current division. Controlling the DPF system with this current division approach encounters some problems which are summarized underneath:

The inherent nature of this division makes it impossible to obtain a real-time division of the orthogonal components. The low-pass filter in the orthogonal current divider has a time constant of typical 3 - 5 seconds, which has a negative effect on the dynamic response and is not practical for aperiodic waveforms and the subdivision of fictitious power into other components is problematic.

Similar Fryze based approaches of other authors, for example the Schwan implementation of the Depenbrock definition [A119], have similar limitations which are realized in more complicated hardware.

6.5.4 Orthogonal Current Division with Adaptive Techniques

As stated above the derivation of the reference current is based on the calculation of the instantaneous signals in real-time. The fundamental limitations remain that the power components can only be calculated after the measurement interval have elapsed. It is thus clear that a power averaging approach is a prerequisite for load current division to have adequate attributes in terms of the power phenomena in the network. In real-time applications the above mentioned prerequisite implies contradicting requirements. It has,

however, been found that typical power network loading shows statistical properties which can be utilized to implement an adaptive signal processing system, calculating the required reference signals in a real-time manner using calculated average power values (chapter 4,5).

The control of fictitious power compensation systems, is proposed to be more effective with time domain signal processing and adaptive filter techniques. This approach is realized in a 15 kVA three-phase DPF, which gave good results. As a trial run, the digital signal processing techniques are implemented within a personal computer. The personal computer, with associated control algorithm, is introduced into the control loop of the DPF.

The fundamental principle of this proposed generation of the reference current is based on the proposed correlation definition of electric power (chapter 3). The block diagram representation of the combination of digital and analogue signal processing techniques, proposed in the current division system, are shown in fig. 6.11.

The input to the system is the instantaneous values of the voltage and current, which is sampled at an appropriate frequency, sent through an analogue-to-digital converter and used in the correlation algorithm. A correlation algorithm, similar to the one used in the signal processing simulations shown in fig. 5.8, is proposed to calculate the network parameters. The predicted network parameters G and B are derived from the calculated active and reactive powers, in the estimation algorithm shown in chapter 5. Using these network parameters, the instantaneous signals of the different currents are derived by means of analogue signal processing techniques to optimize the speed of the current division. The instantaneous signals are calculated using eq. (6.16) [A52]:

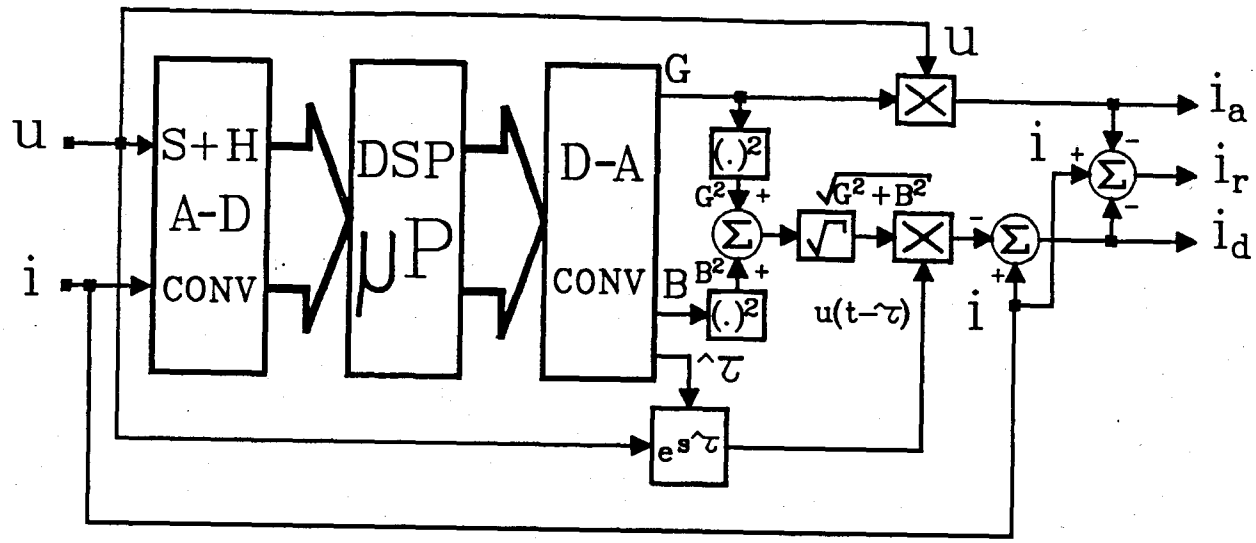

Fig. 6.11: Block Diagram Representation of Correlation Based Orthogonal Current Divider

$$
\begin{aligned}
i_a(t) &= G.u(t) \\
i_d(t) &= i(t) - \sqrt{[G^2 + B^2]}.u(t-\hat{\tau}) \\
i_r(t) &= i(t) - i_a(t) - i_d(t)
\end{aligned}
\qquad (6.16)
$$

with $u(t-\hat{\tau})$ the time delayed voltage. The time delay is equivalent to the time-shift associated with the point of maximum cross-correlation $\hat{R}_{ui}(\tau)$.

A fast dedicated DSP microprocessor, performing the correlation software algorithm, is proposed to be the basis of this approach. Calculation of the conductance G and susceptance B is time critical for real-time applications. In typical 50 Hz power networks the calculation time of the network parameters has to be smaller than 2 ms. (An order of magnitude smaller than the time interval.) This places a fundamental limitation on the DSP microprocessor. In chapter 4, fig. 4.8, the proposed signal processor is described. The analogue signal processing is obtained by means of operational amplifiers and precision analogue multiplying devices. This adaptive signal processing system is implemented in the generation of the reference current control input to the experimental 15 kVA dynamic power filter, described in the first part of this chapter.

6.6 BLOCK DIAGRAM REPRESENTATION OF TOTAL DPF CONTROL SYSTEM

The control system of the 15 kVA experimental DPF consists of a combination of the systems described in the previous paragraphs. The different control loops can be described as follows: the Active Filter Compensation loop (AFC) canceling the limit-cycle problems, as described in paragraph 6.3; the loss-compensation loop described in paragraph 6.4 and the reference current generation (RCG) loop described in paragraph 6.5. The reference current generation loop consists of two methods of orthogonal current division. The first is based on the Filipski current divider (paragraph 6.5.3), which is limited to fictitious power compensation, while the other is the proposed adaptive signal processing system described in paragraph 6.5.4.

To demonstrate the total compensation philosophy, only a DPF is used for all the different components of compensation because it is capable of compensating all the different fictitious power components. In a practical fictitious power compensation system all the different compensation systems, as described in chapter 5, or some of them may be utilized to realize a cost effective compensation system in total.

6.6.1 Control System Using the Filipski Current Divider

Full compensation of fictitious power, means the compensation of all the loading power, which does not contribute to net energy transfer from source to load. The Filipski load current division is one of the most simple approaches for deriving the fictitious current, as described in paragraph 6.5.3.

Figure 6.12 shows the total block diagram representation of the DPF with the Filipski orthogonal current divider implemented as reference current generator. This representation shows the non-linear load Y coupled to a power supply with a nearly sinusoidal voltage generating function u(t). On the power network, in parallel with the non-linear load, the passive DPF with isolation transformer IT and low-pass power

filter C_f and L_f is shown. The converter bridge is controlled by means of the duty cycle d, derived from the hysteresis controller. The current-fed converter is fed from the inductor L.

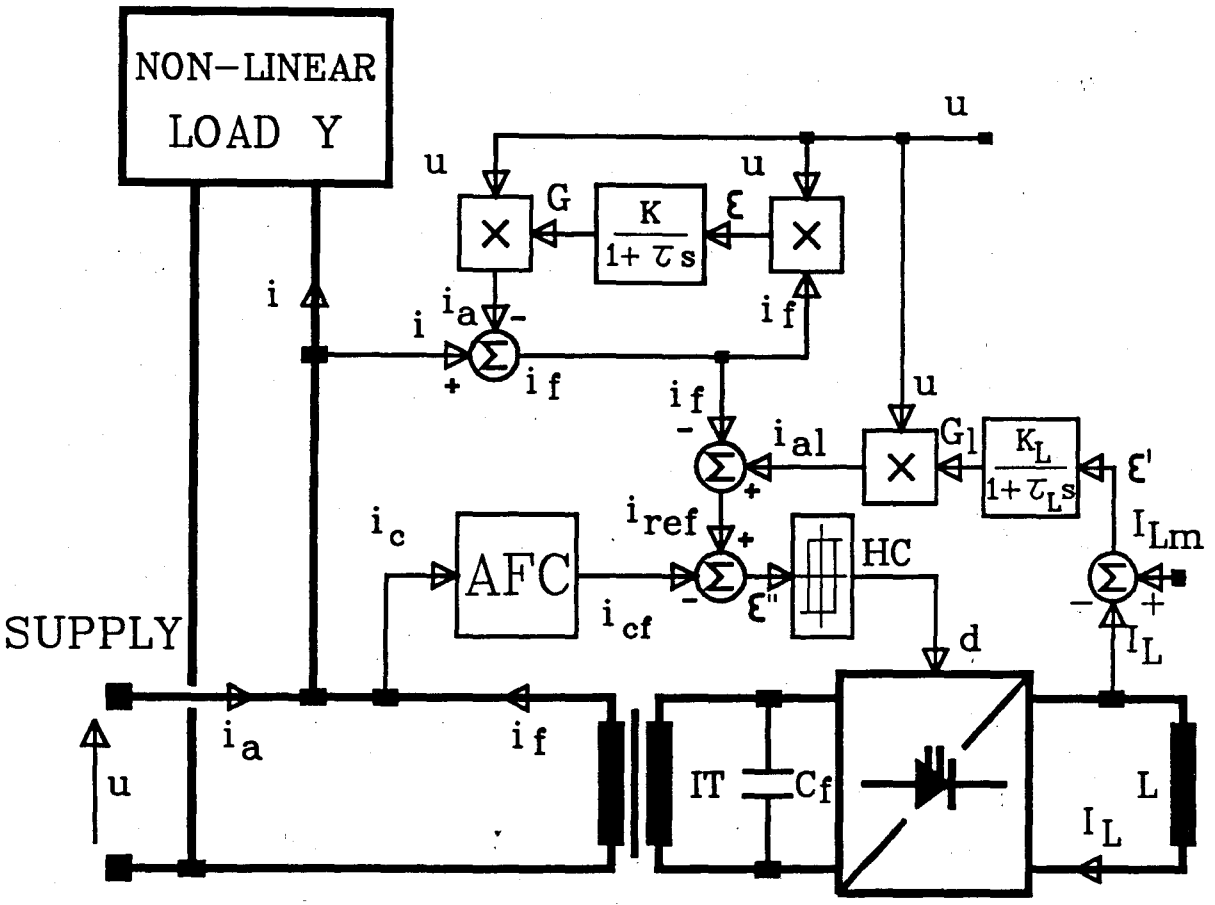

Fig. 6.12: Block Diagram Representation of DPF with Filipski Reference Current Divider (Single phase).

The load current i(t) and supply voltage u(t) is measured directly on-line. The Filipski current divider is used to obtain the fictitious current i_f, which is used to control the DPF. The loss-compensation and the Active Filter Compensation loops are clearly shown in fig. 6.12.

6.6.2 Control System Using the Proposed Adaptive Signal Processing Current Divider

The total control system of the 15 kVA DPF with the adaptive signal processing reference current generating system, is

shown in fig. 6.13. The diagram shows that only deactive power is drawn from the DPF, the reactive power is drawn from an equivalent reactive power compensation capacitor C.

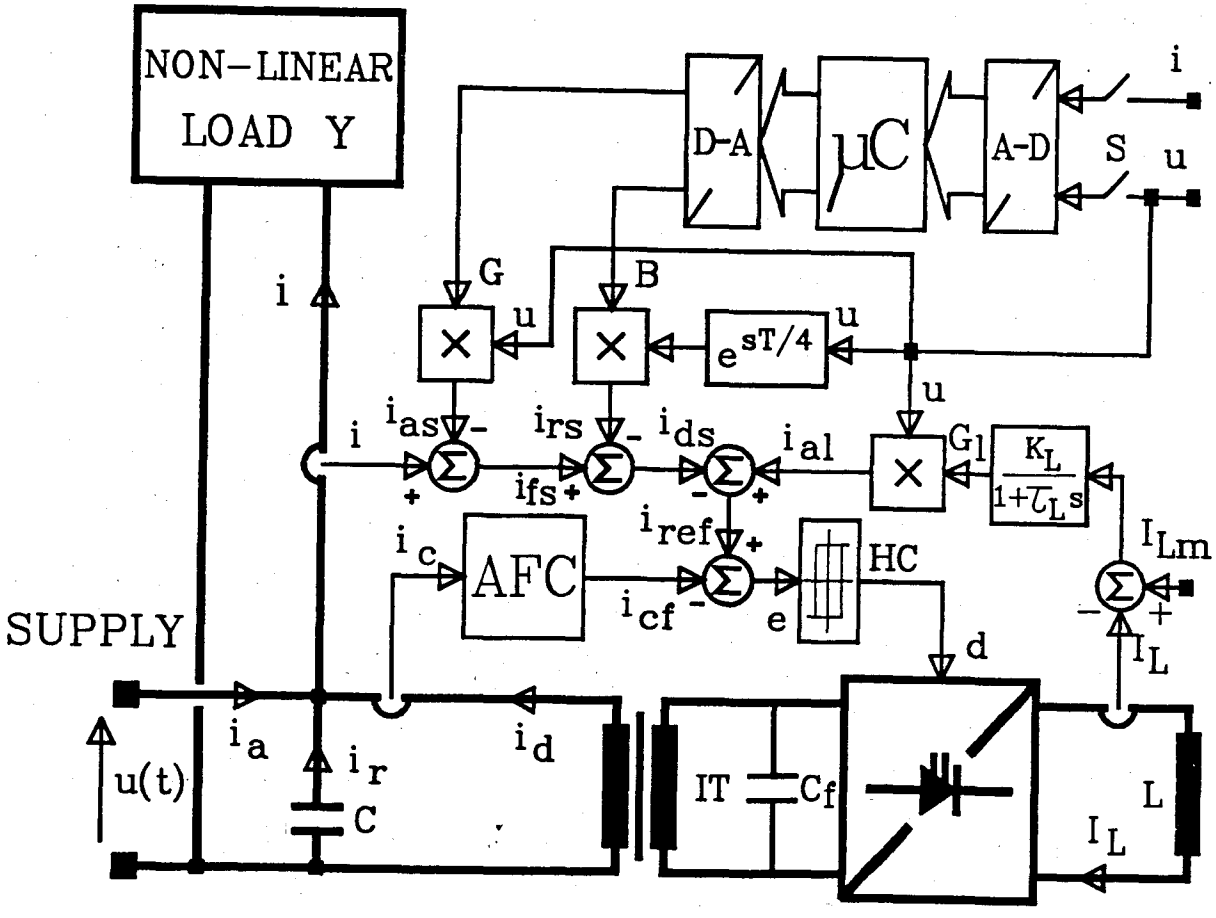

Fig. 6.13: Block Diagram Representation of DPF with Proposed Adaptive Signal Processing Reference Current Divider

To evaluate the fictitious power compensation philosophy, the proposed DSP microprocessor based digital controller is implemented with an AT compatible personal computer, using an appropriate A-D and D-A bus card. The reference current i_{ds} is obtained from the calculated estimated equivalent network parameters G and B. The voltage u and current i forms the input to the signal processing system. These two signals are sampled, fed through an analogue to digital converter card, into the personal computer μC (HP-VECTRA), where the signal processing algorithm is executed. The sample frequency obtained from the A-D card is 6,6 kHz at 12-bit resolution and the computer has a 8 MHz clock fre-

quency, using an Intel 80286 microprocessor with a 80287 numerical co-processor.

The software control algorithm is shown in fig. 6.14 with the Pascal source code shown in Appendix B2. The calculated values of B and G are sent through the 12-bit digital to analogue converter card.

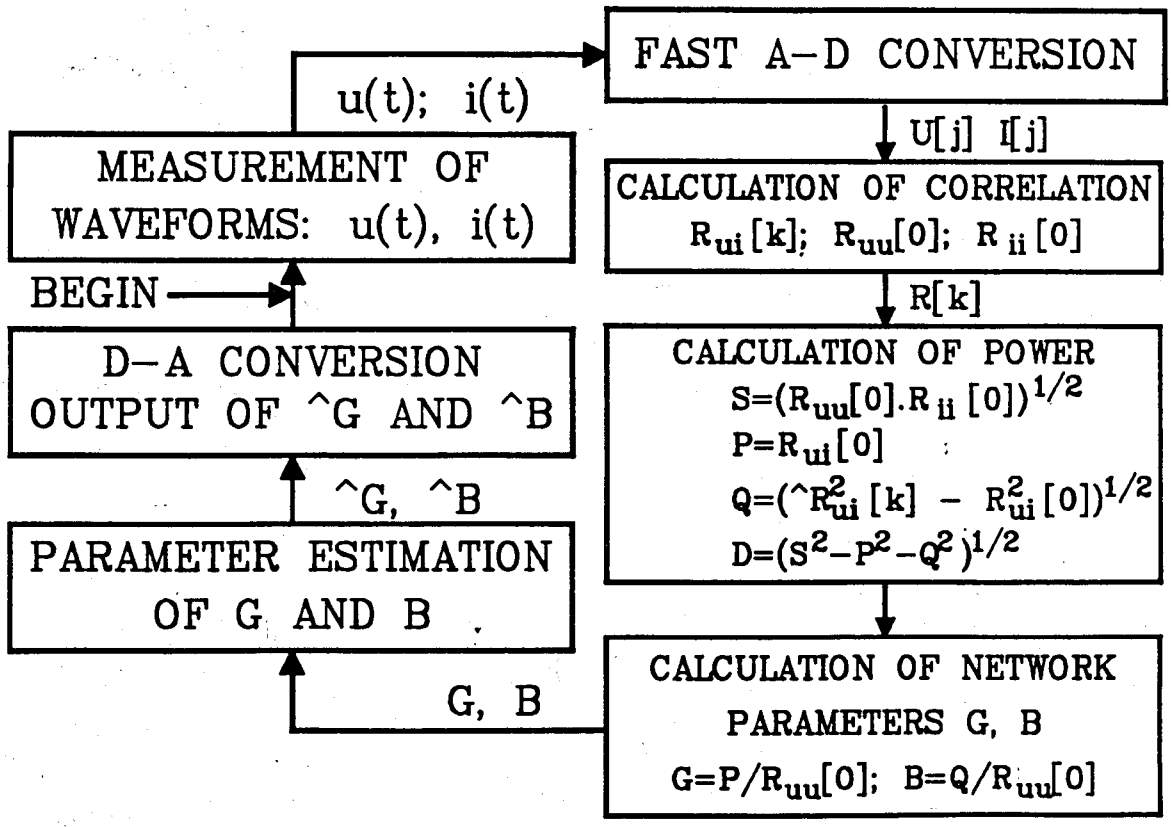

Fig. 6.14: Block Diagram Representation of DPF Software Control Algorithm

The generating function u(t) is nearly sinusoidal, which implies that the reactive current i_{rs} can easily be obtained from the equivalent network parameter B and a $\pi/2$ phase shift in the voltage waveform u(t). By taking the necessary analogue summations and multiplications the deactive current is derived.

6.7 SCHEMATIC DIAGRAM OF NON-LINEAR LOAD, DSP MEASUREMENT SYSTEM AND DPF FICTITIOUS POWER COMPENSATION SYSTEM

The total experimental system consists of a typical non-linear load which has to be compensated by means of the DPF. The compensation system is chosen to compensate all the components of fictitious power, which has to be a dynamic power filter in general. The proposed compensation philosophy implies that there is no need to compensate all the fictitious power components with a DPF, only the deactive power component has to be compensated by means of a fast responsive dynamic power filter. Figure 6.15 shows the schematic diagram of the non-linear load, a 10 kVA static Scherbius rotor cascade induction machine drive in parallel with a load resistance R_{load} and the DPF with the reference current generation system (RCG). The measurement system, based on the same proposed power definition, is necessary for the on-line measurement of the different power components to evaluate the compensation performance.

The 10 kVA induction machine, capable of over synchronous operation, is speed controlled by means of a static Scherbius rotor cascade configuration [A140, D2]. The rotor power is rectified by means of the rectifier (RC) and inverted to the 50 Hz supply, by means of a six-pulse supply commutated inverter (IC). The inverter is controlling the speed of the induction machine by changing the equivalent rotor resistance [A140, D2]. The inverter (IC), is a current-fed inverter, which generate characteristic reactive and deactive power. The current is the well known quasi square wave, based on phase control. Fundamental reactive power, associated with the phase angle control, and deactive power which results from the quasi square wave current waveform, are generated by the non-linear load. The digital oscilloscope and PC based measurement system is the same system used for the analysis of distortion in different power systems, as described in chapter 4.

The system shown in fig. 6.15 forms the experimental system from which all the results are obtained. The different control possibilities of the DPF, pointed out in the previous paragraph, are evaluated experimentally in the next paragraph.

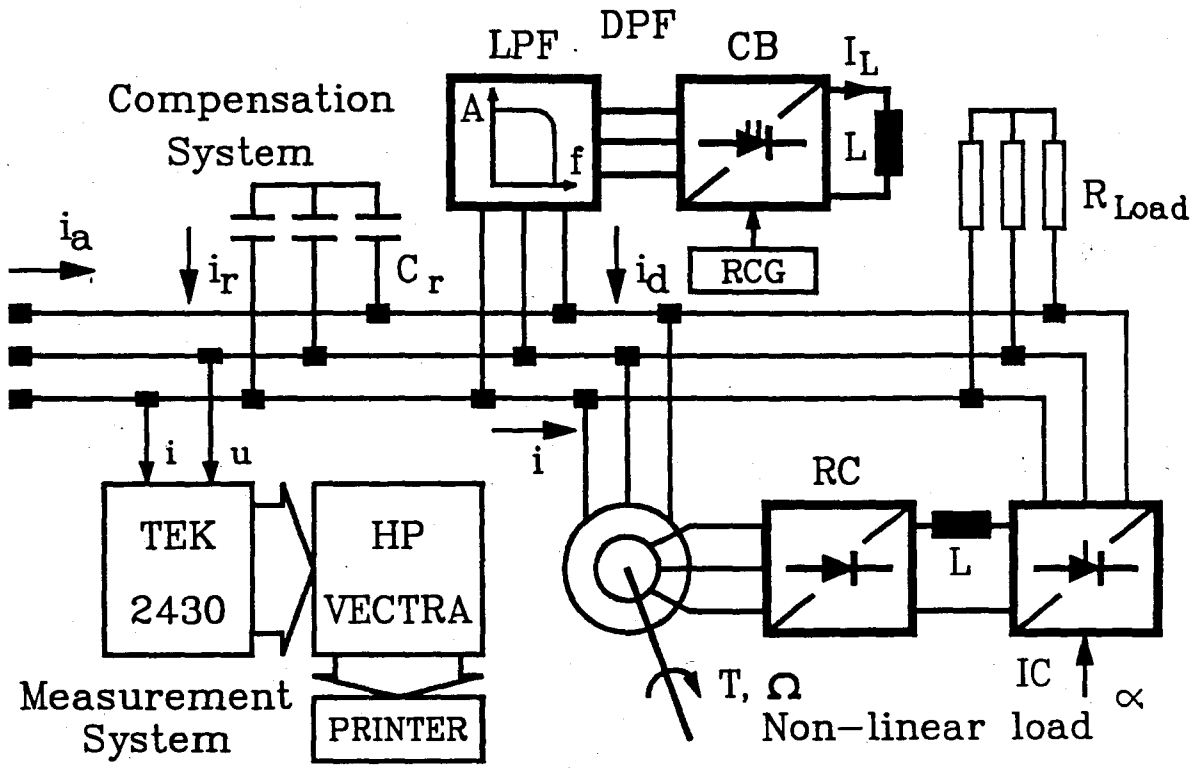

Fig. 6.15: Block Diagram Representation of Non-linear Load, DPF and Distortion Measurement System.

6.8 EXPERIMENTAL RESULTS OBTAINED FROM THE DYNAMIC POWER FILTER

The adaptive signal processing based reference current generation (RCG) system produced the current waveforms shown in fig. 6.16. The DPF is controlled by means of the fictitious current i_{fs} obtained from the simple Filipski current divider described in paragraph 6.6.1, or by means of the adaptive signal processing system described in paragraph 6.6.5. The same results were obtained under steady state conditions. The DPF is also controlled by means of the deactive current i_{ds}, which is generated by the adaptive signal processing system. Paragraph 6.8.3 describes the time scaled results under dynamic loading conditions.

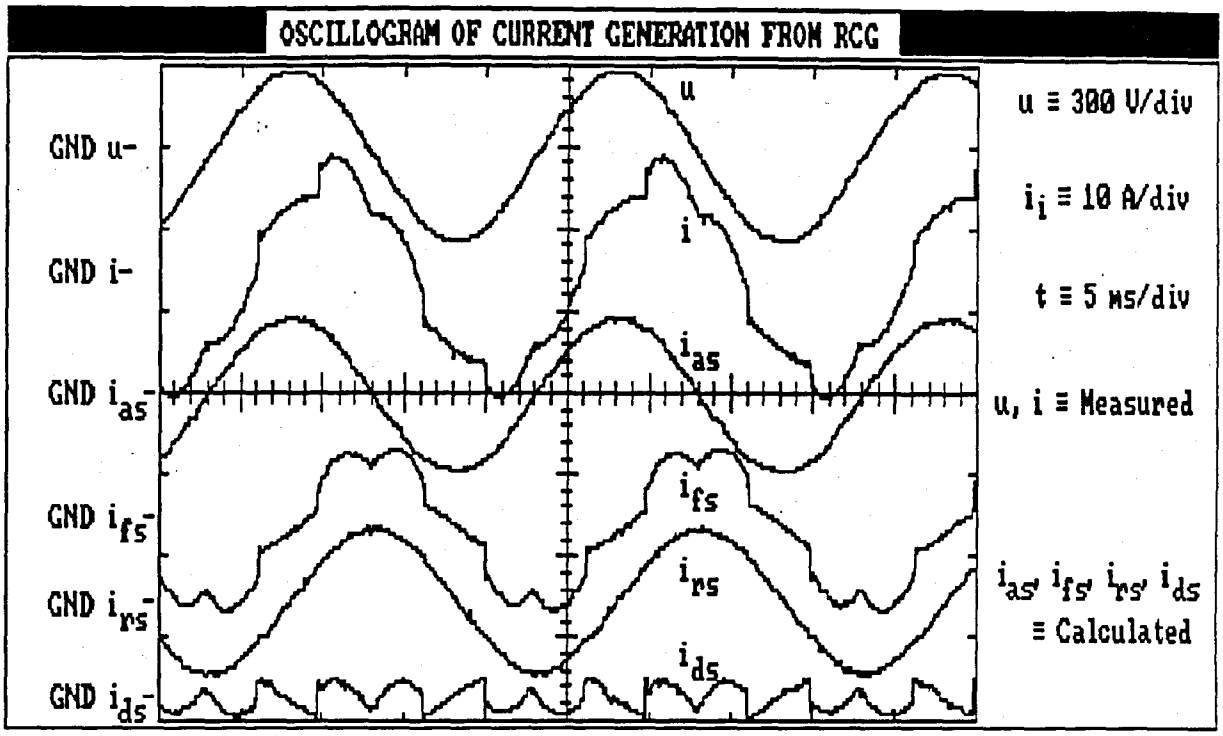

Fig. 6.16: Signal Processing Waveforms of Reference Current Generation System (RCG)

6.8.1 Full Fictitious Power Compensation Results

The oscillogram in fig. 6.17 shows the operation of the DPF controlled by means of the fictitious current i_f, under steady state conditions. The voltage waveform u is nearly sinusoidal with the load current i showing the characteristic waveform of a current-fed six-pulse supply commutated inverter.

The supply current waveform i_a, after compensation, is a sinusoidal with minimal distortion. The small spikes on the current waveform is the result of the dynamic limitations associated with the low-pass filter L_f and C_f, shown in fig. 6.5. The effect of the compensation is reflected in the results obtained from the measurement system, showing the measured per phase result before and after compensation, in fig. 6.18 and 6.19 respectively.

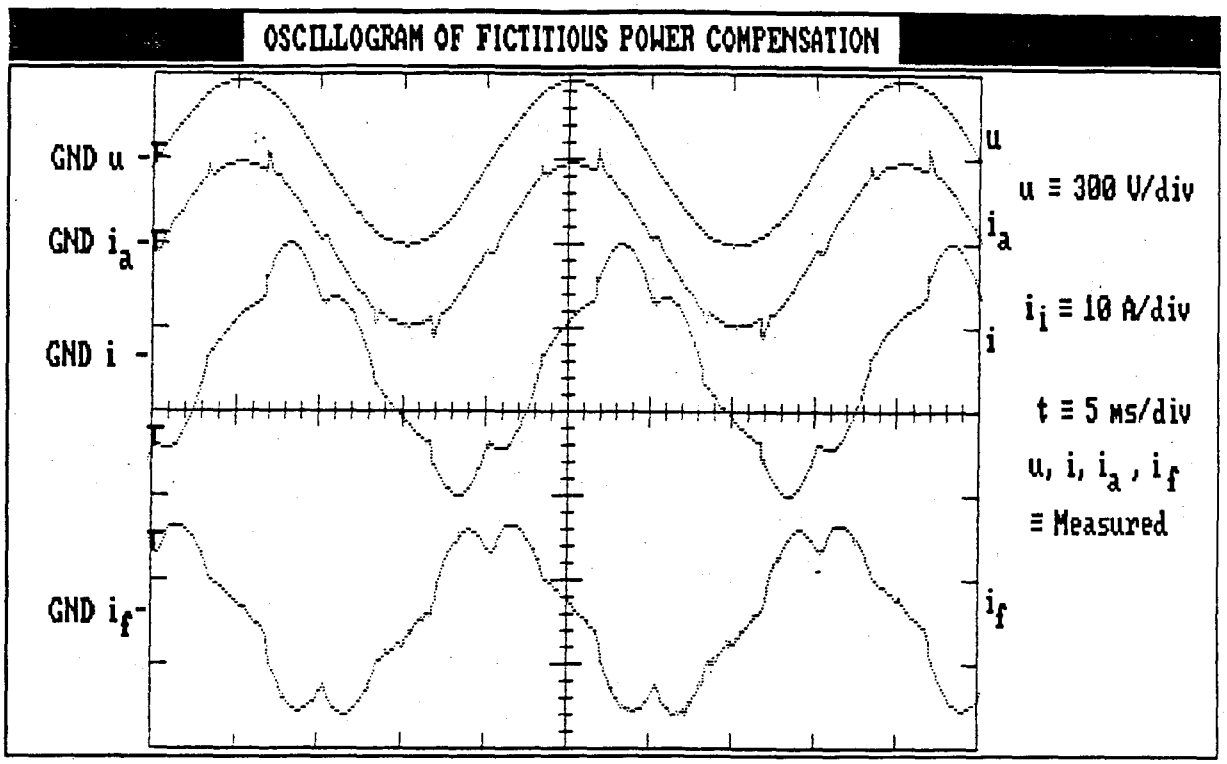

Fig. 6.17: Result of Full Fictitious Power Compensation

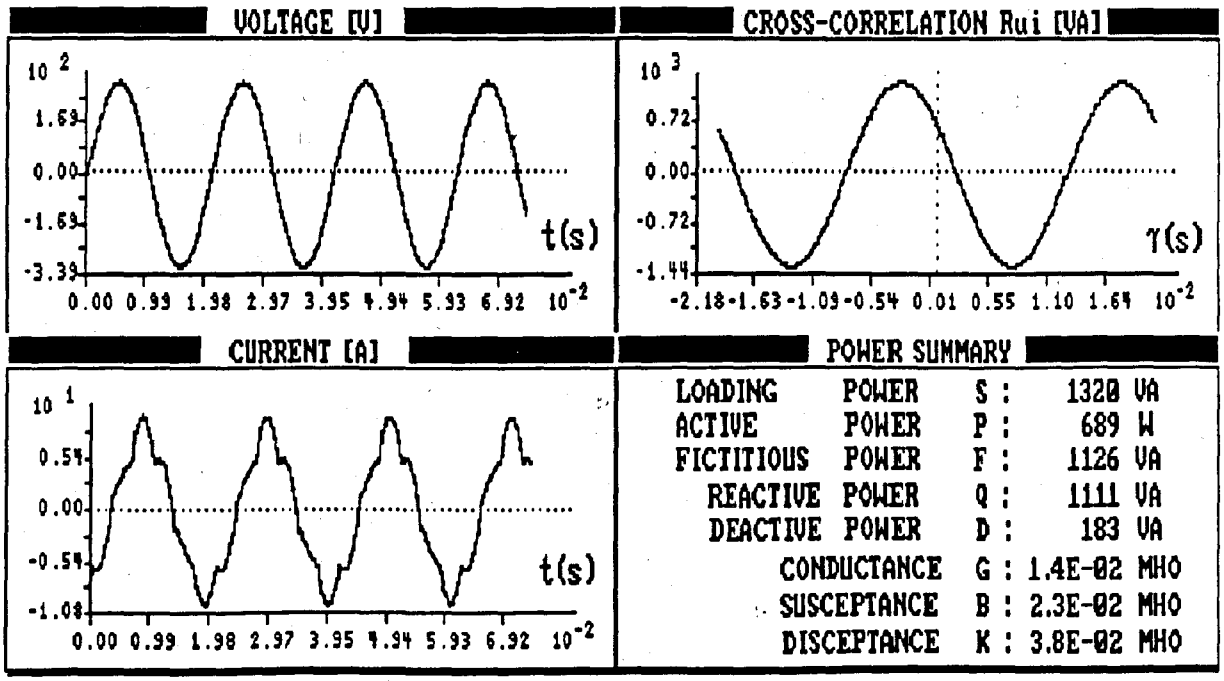

Fig. 6.18: Measurement of Power Components BEFORE Fictitious Power Compensation

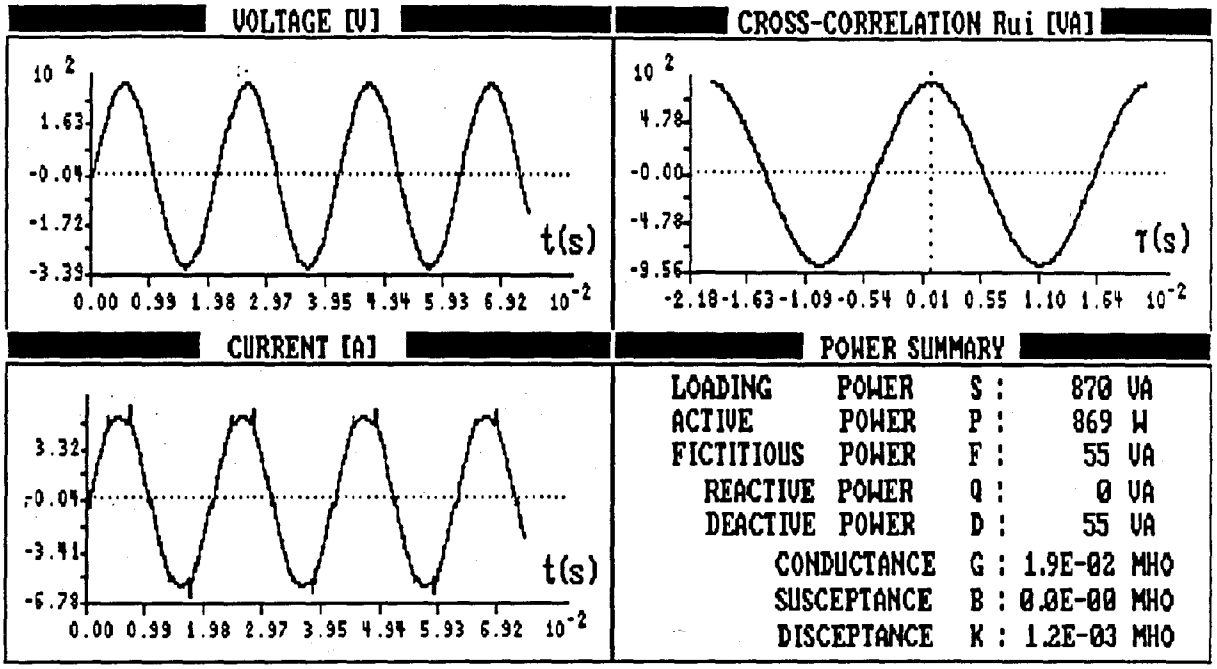

Fig. 6.19: Measurement of Power Components AFTER Fictitious Power Compensation

A decrease from 1320 VA to 870 VA in the loading power is obtained. From fig. 6.19 it is clear that practically all the fictitious power is compensated. The resultant 55 VA deactive power is the result of bandwidth limitations associated with the low-pass filter and the finite resolution of the 8-bit analogue to digital converter within the digital oscilloscope. The zero reactive power implies that the DPF did full fictitious power compensation, thus compensating both reactive and deactive power.

From the above results it is clear that the DPF has to generate a large effective value of fictitious current when utilized for full fictitious power compensation, while the deactive power is small compared to loading power (10-15%). It is therefore advantageous to compensate only the deactive power with the sophisticated DPF, while a simple capacitor can be used for compensation of the reactive power. This em-

phasizes one of the major advantages of subdividing the fictitious power into reactive and deactive powers. The extra amount of active power, visible in fig. 6.19 (869 W as opposed to 689 W) is appointed to the power losses in the passive dynamic power filter, which is a strong function of the effective value of the compensation current. This is yet another inherent reason to subdivide the fictitious power into reactive and deactive powers. In the next paragraph only deactive power is compensated by the dynamic power filter, reactive power can be compensated by a simple capacitor network, as shown in fig. 6.12.

6.8.2 Deactive Power Compensation Results

From the above mentioned results it is clear that it is advantageous to subdivide the fictitious power into other components. This is done by means of the DSP based reference current generation system, described in paragraph 6.5.4 and shown in fig. 6.13.

The total algorithm time of fig. 6.14, when implemented with the personal computer shown in fig. 6.13, is in the order of 3 to 4 seconds, performed on a measurement time window of 3 fundamental periods (60 ms). This is relatively slow because of the relative long cross-correlation algorithm time (2 - 3 seconds). This system can, however, demonstrate the compensation philosophy even under dynamic conditions if the time constant of the dynamic response is scaled down to the same order as the response time of the RCG system.

An oscillogram showing the operation of the interim personal computer based system is shown under steady state conditions in fig 6.20. Figure 6.16 shows the generation of the different current components from the signal processing system, while fig. 6.20 shows the measured currents during the process of compensation. It is clear that the three generated waveforms i_{rs}, i_{ds} and i_{as} are mutually orthogonal.

Only the deactive current is assumed to be generated by means of the dynamic power filter. The reactive current, shown in fig. 6.16, can be obtained from a passive capacitor. Figures 6.21 and 6.22 show the components of power before and after deactive power compensation. The shifted reactive power is still clearly visible after deactive power compensation. Deactive power is, however, reduced to a much lower value, again the bandwidth limitations caused by the low-pass filter and the resolution of the 8-bit A-D converter is responsible for the non-zero deactive power present in fig. 6.22. The losses of the DPF are much lower compared to full fictitious power compensation. In the results shown below the reactive power decreased from 1077 VA to 852 VA in the compensation of deactive power. This is the result of the decrease from 1108 VA to 900 VA in the loading power. This phenomena is yet another advantage of separate compensation of the fictitious power components.

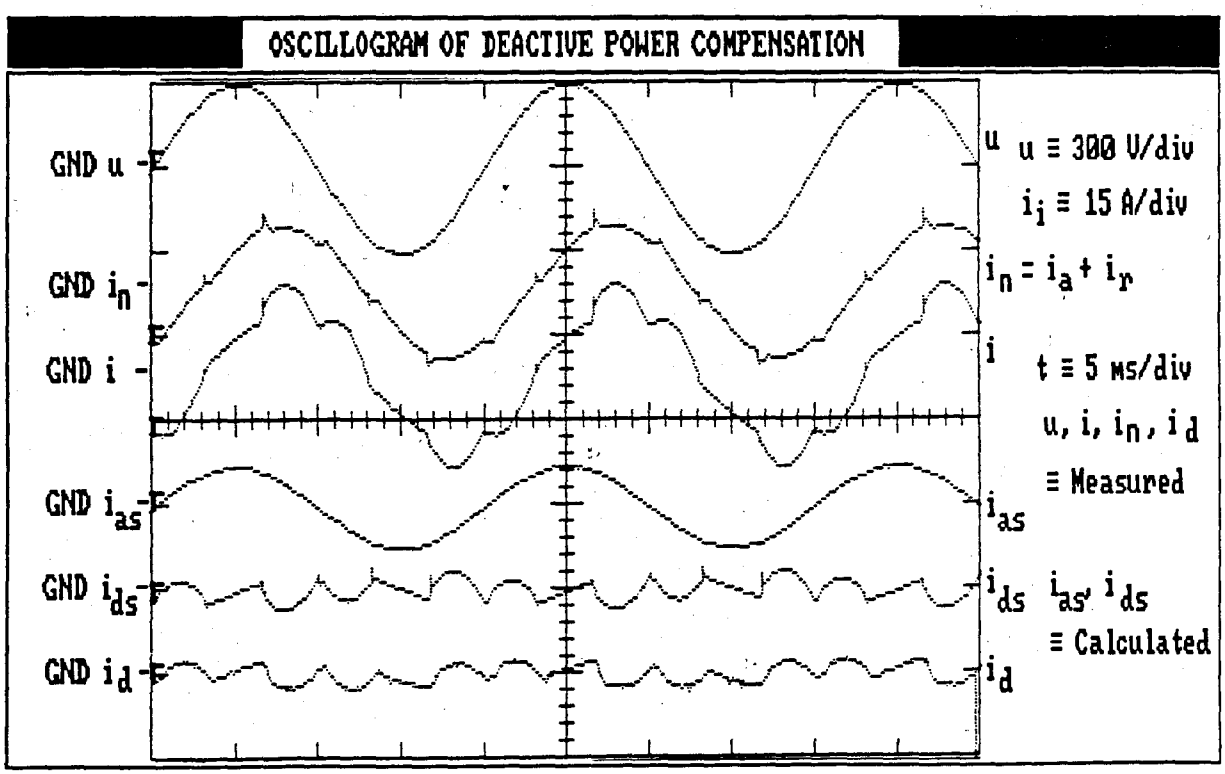

Fig. 6.20: Compensation of Deactive Power

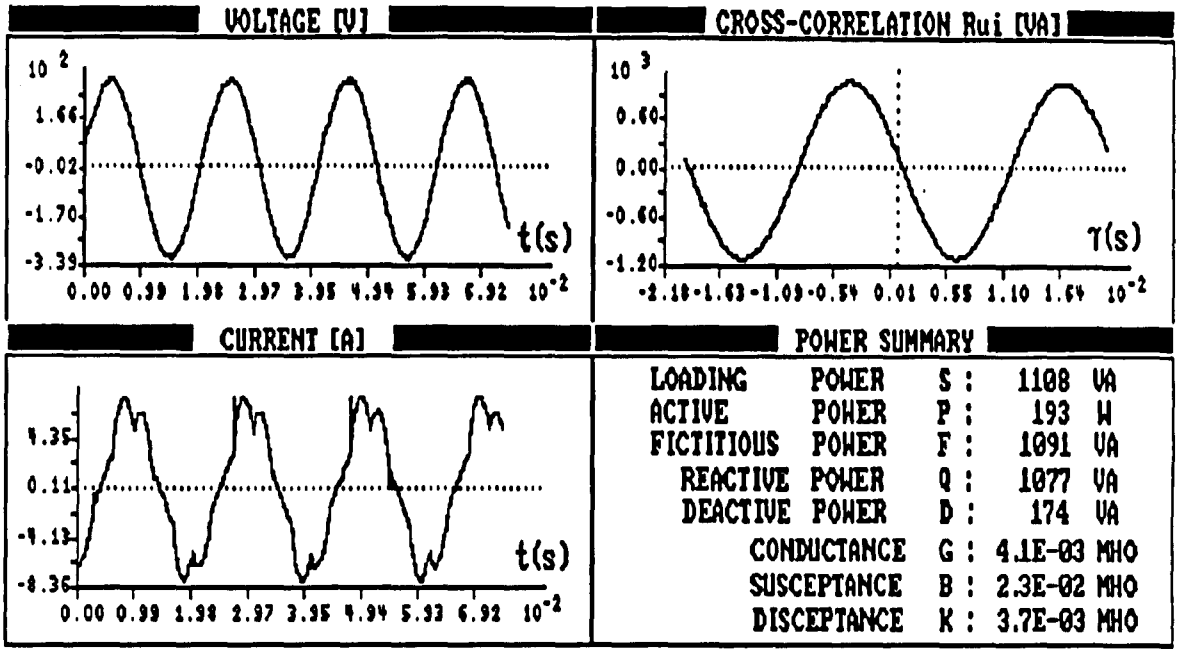

Fig. 6.21: Calculated Power Components from Measured Voltage and Current Waveforms, BEFORE Deactive Power Compensation.

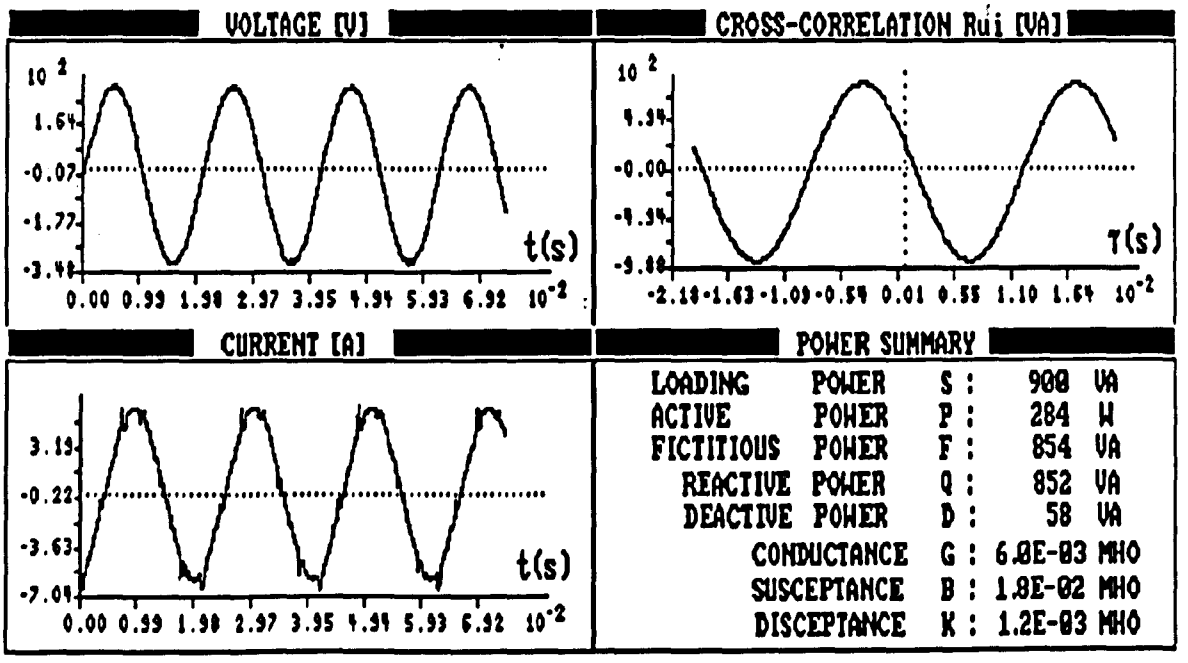

Fig. 6.22: Calculated Power Components from Measured Waveforms, AFTER Deactive Power Compensation.

6.8.3 Experimental Results Under Dynamic Operating Conditions

The DPF is evaluated under dynamic operating conditions using the adaptive signal processing reference current generation system. The estimation algorithm, described in chapter 5, is performed on the calculated equivalent conductance and susceptance. A non-linear load under dynamic operating conditions is compensated by means of the dynamic power filter. The reference current generation system used to obtain these results, is also based on a personal computer controller, performing a Pascal algorithm with relative slow computation time. To overcome this limitation and still evaluate the control algorithm, time scaling is performed on the dynamic loading of the non-linear load. The same induction machine drive, as shown in fig. 6.15, is used as a non-linear load. The fire angle α is, however, varied to represent dynamic loading.

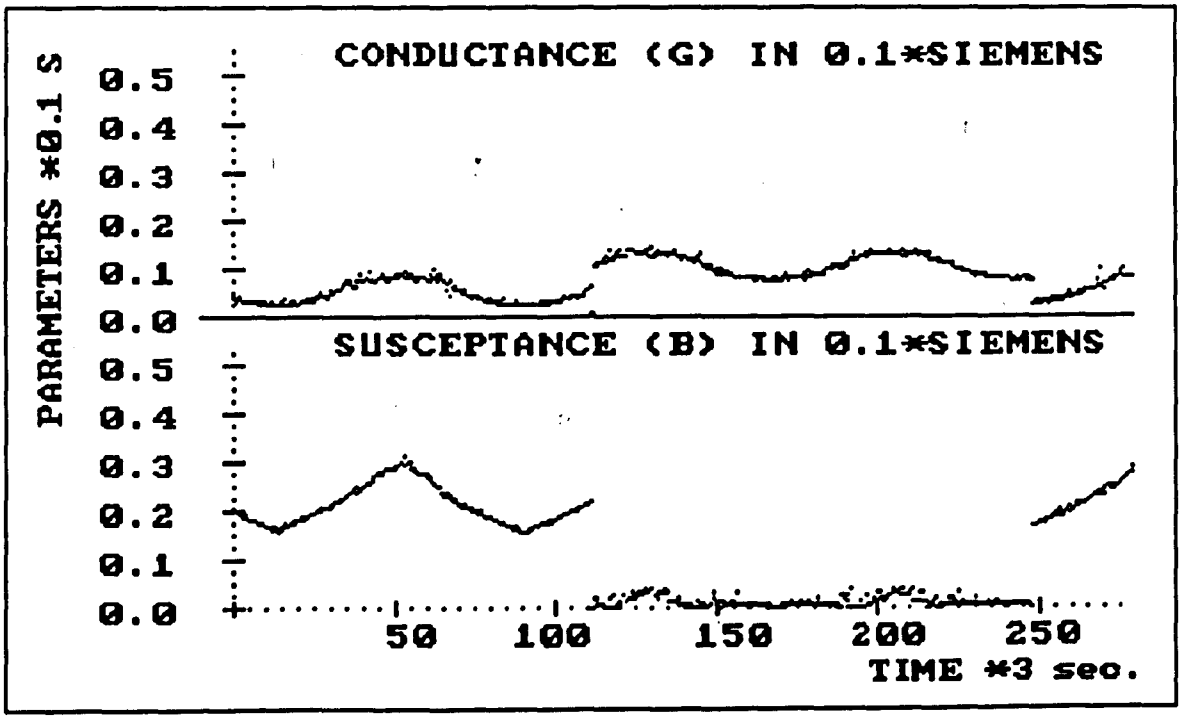

Fig. 6.23: Result of DPF under Dynamic Loading Conditions

Figure 6.23 shows the conductance G and susceptance B, calculated from the measured voltage and current and the predicted values of the conductance $\hat{G}$ and susceptance $\hat{B}$ plotted together. The DPF is switched off in the first and last portion of the plotted result. When the DPF is switched on, the decrease in the susceptance B is staggering. This decrease in the susceptance is obtained from the DPF under full fictitious power compensation control. The DPF is, however, too small to compensate for all the fictitious power through the total dynamic loading cycle which results in an increase of the susceptance. The conductance G shows an increase when the DPF is operative which is the result of the losses associated within the DPF. The predicted values of G and B follow the actual measured values reasonably well. There is, however, some inaccurate estimations when the network characteristics are changing haphazardly. In general the system responds well to dynamic loading conditions.

6.9 SUMMARY

The structure and specially the control scheme of the DPF, with associated internal control loops, are described in this chapter. The different possibilities to generate the reference control current are critically reviewed, with an adaptive signal processing system proposed in the compensation of fictitious power.

This chapter shows experimental results of the implementation of the fictitious power compensation philosophy based on the proposed definition of electric power. The derived DPF software control algorithm is shown in a block diagram. The control programs coded in Turbo Pascal, can be found in Appendix B2.

The reference current generating system, used to obtain the experimental results, is based on a AT compatible personal computer. The final controller should, however, be implemented by means of a fast dedicated DSP microprocessor, optimized for

real-time decomposition of load current (total network parameter calculation time less than 1-2 ms).

There are many advantages in the compensation of fictitious power with the proposed compensation philosophy which is evaluated experimentally in this chapter. These include higher power rated compensation systems capable of compensating all the fictitious power in the distorted supplies; good control strategy for fictitious power compensation systems; low power rated sophisticated DPF's with a control scheme optimized to compensate only deactive power; integral design of DPF's in power control apparatus etc. From these experimental results in this chapter it is clear that the dynamic power filter has a great future in the compensation of highly distorted power networks if they can be combined with other compensation systems, with a lesser degree of sophistication but rated for a much higher compensation power.

CHAPTER 7

SUMMARY OF THE CONCLUSIONS FROM THIS THESIS

7.1 INTRODUCTION

The determination and dynamic compensation of fictitious power in electric power systems seem to have far reaching consequences as emphasized throughout this study. The determination of electric power, especially fictitious power, is a broad concept which involves the definition, the physical interpretation and the measurement of these power concepts.

Fictitious power arises from the implementation of electrical apparatus in the power system. The state of the art in power control systems, is to design this electrical apparatus in such a way as to generate minimal distortion, which is of course the final solution. It is, however, not possible to eliminate all the distortion in electric power systems, especially under dynamic loading conditions. Furthermore the cost constraints are proportional to the power rating and complexity of the electrical apparatus. The technology, associated with higher performance and larger converters, is developing with rapid strides and is normally measured in terms of the power-frequency product. This product is a constant at a certain level of the technology. This implies that the generated distortion increases with the power rating of the power converters.

Compensation of this characteristic distortion in power systems is being investigated. The effective control, utilizing the fast system response of some of the compensation systems under dynamic loading conditions, is one of the major contributions of this work. The study is divided into four major categories, as described in chapter 1:

(i) the generalized definition of power under non-sinusoidal conditions;
(ii) the effective measurement of power in contaminated power networks;
(iii) the analysis and characterization of distortion in power networks;
(iv) the effective compensation of distortion in contaminated power networks.

7.2 THE GENERALIZED DEFINITION OF POWER

A definition of power, based on correlation techniques, is developed which contains attributes of the energy phenomena in the network. This definition is formulated in the time domain with reference to the Fryze, Depenbrock and Nowomiejski approaches. The definition is not formulated in the frequency domain, but is extended to the frequency domain for the purpose of frequency domain distortion analysis and characterization. From the generalized definition of electric power, the equivalent network parameters are derived and the loading function is decomposed into three mutually orthogonal components. The source, characterized by means of the generating function, is not divided into different components, as proposed by Depenbrock. The main reason for this is the complexity of the Depenbrock approach. The Nowomiejski approach is followed to a large extent, with a difference in the subdivision of fictitious power into other components.

Nowomiejski introduced the Hilbert transform to obtain the subdivision which, from the authors viewpoint, produces results that are not related to the energy phenomena in the power network. Furthermore the purpose of the Nowomiejski approach is to divide the load current into different components and then define the power components from these divided current components. This approach define the power components from averaging correlation techniques.

The orthogonality in the proposed correlation approach is assumed in the calculation of the different power components. Simulations of different waveforms of the decomposed loading function is successfully tested. The power components are to a limited extent mathematically described in terms of the quaternion theory to a limited extent. The results obtained from the quaternion theory correspond to the power components calculated from the correlation approach, which is a test for the mathematical representation.

The power definition is evaluated for a number of voltage and current waveforms. The results from the correlation approach correspond with the results of other definitions only when the generating function has a sinusoidal waveshape. Different results for reactive and deactive power have been obtained with non-sinusoidal generating functions. The advantages of this definition are pointed out and have far reaching consequences in the compensation of fictitious power. All the power components, network parameters and decomposed loading functions are derived from a single correlation function. The accuracy of the measurement is a function of the measurement time interval dT, when compared to other techniques, but are not incorrect as with the frequency domain approach, for example when the measurement interval is not an exact multiple of the fundamental period.

This definition was originally developed for application in electric power systems. Chemical, mechanical and thermal power systems have the same distortion constraints and therefore the identification of a generalized energy theory approach should be investigated further. In all the above mentioned systems a generating and loading function can be identified. A typical example is found in mechanical power systems where the generating function in a rotational system can be expressed in terms of the rotational speed Ω, while the loading function can be expressed as the torque T in the axle. All the proposed mechanical power components can be derived for this loading and generating function, characterizing the distortion in terms of the measured axle torque pulsations.

7.3 THE MEASUREMENT OF ELECTRIC POWER

The measurement of electric power utilizing digital and/or analogue measurement techniques based on the correlation between the loading and generating functions is believed to be effective with the proposed definition. Optics, acoustic waves, dedicated DSP microprocessors or hard wired based correlators are proposed in the measurement of the different power components. The measurement and calculation speeds of the correlation based measurements are of the utmost importance in certain applications. For example, in the control of fictitious power compensation systems, under dynamic loading conditions.

The definition of average power is based on averages which do present some fundamental problems in real-time measurement applications. The majority of power systems have some statistical properties which can be harnessed in the calculation of these power components, to result in a real-time type system. The approach adopted in this work is based on the adaptive signal processing theory. It is fundamentally impossible to derive power components without prior information concerning the characteristics of the power system under consideration.

The representation of instantaneous currents is still a controversial matter in the sense that it is possible to derive a multiple of instantaneous currents to describe the power flow through the power network, having the same effective values. The choice in this study is based on the correlation between the voltage and current which seems to give reasonable results for the waveforms simulated.

In power measurement applications where the measurements are not time critical, the measurements can be performed using a personal computer with analogue to digital interface capabilities and a correlation algorithm. Such a system is developed in this study and is used for the measurements of the different power components throughout this work. These measurement principles have recently been implemented in a DSP microprocessor based real-time

measurement system, in the application of fictitious power compensation.

7.4 ANALYSIS OF DISTORTION IN POWER SYSTEMS

Distortion analysis is an important aspect when characterizing distortion in contaminated power supplies. Without this analysis it is impossible to calculate the effects and compensate distortion in power networks effectively. The analysis of distortion with this correlation approach seems to have many advantages. The analysis of distortion is performed using an equivalent circuit of the distorted network, which is based on the known network parameters conductance and susceptance, and a newly introduced parameter disceptance, based on the non-linear and uncorrelated properties of the network.

Each network parameter has a different effect, based on the difference of their respective methods of generation. The conductance is associated with the energy transfer, the equivalent susceptance described in terms of the reciprocal energy flow between this equivalent susceptance and the power source. The disceptance is based on the power loading of the network associated with the uncorrelation between the generating and loading functions, normally associated with the non-linear properties of the load. It should be pointed out that the equivalent diagram should not be confused with the schematic circuit diagram of the network. These two diagrams can be totally different in general. The equivalent diagram does not have schematic symbols for components, but describe the power phenomena in the network. Analysis is proposed to be performed in the time domain using these above-mentioned equivalent parameters. Time domain analysis can be performed under dynamic loading conditions with aperiodic waveshapes for generating and loading functions.

In some analysis, especially the analysis of the effects of distortion and the design of compensation systems, the frequency domain should be used. The correlation approach is therefore extended to the frequency domain by implementing the power cross-

spectral density function, which implies that a frequency transform is performed on the cross-correlation function. From this frequency transform the correlated power components (active and reactive power) are decomposed in their harmonic components. This analysis can only be performed under steady state conditions with the cross-correlation a periodic function, which implies that the generating and loading functions should also be periodic.

7.5 THE COMPENSATION OF FICTITIOUS POWER

The cost effective compensation of fictitious power is high on the list of priorities for research in the field of producing a high quality power supply. Compensation systems have normally a high capital investment, resulting from the high power ratings of these systems. Typical power ratings can be 100 MVA or higher, for example in HVDC converter stations.

It is thus of primary importance to design these compensation systems in a cost effective way. Limited by the level of technology the power rating of the converters are inversely proportional to their sophistication, which results that high power converters are not effective in the compensation of distortion with high dynamic properties. For this reason it is necessary to implement a combination of high power and low power compensation systems collectively with a control philosophy that optimizes the advantages of these different compensation systems.

Cost effective fictitious power compensation is proposed to be obtained from the diversity of these different converter systems, compensating collectively the different fictitious power components. The compensation of fictitious power in power systems with a sinusoidal generating function is unambiguously referred to in literature. The principle of the compensation technique is to obtain a loading function with the same in phase sinusoidal waveform as the generating function. In these systems the loading function is decomposed into an active component and a fictitious component. The unwanted fictitious component is compensated by means of an appropriate compensation system. In these sinusoidal

generating function systems it is proposed to subdivide the fictitious component, and thus the loading function, into two other components on the basis of their power phenomena associated with the power network. The unwanted components can then be compensated by means of the inverse network parameter resulting in at least two compensation systems, each compensating a specific component of the fictitious power, viz. reactive and deactive power. For sinusoidal generating functions all the reactive power can be compensated by means of a simple reactive element, for example a capacitor or inductor of sufficient size. This leaves only the deactive power to be compensated by means of a sophisticated high dynamic response power filter.

In power systems where the generating function cannot be expressed as a simple sinusoidal, a somewhat different approach should be adopted. Again the compensation system should produce a loading function to have the same waveform as the generating function and eliminating in the process all the fictitious power components. Ensuing the same motivation to have different compensation systems for the different components of fictitious power, present problems when the generating function is non-sinusoidal. This results from the fact that the reactive loading component is also non-sinusoidal, which implies that it is impossible to compensate all the reactive power by means of a single reactive element. Depenbrock defined, for this reason, reactive power only in fundamentals of the generating and loading functions.

In the correlation approach the same principle is adopted to define the fundamental reactive power and residual reactive power which is the correlated fictitious power after the fundamental reactive power is subtracted. Thus in principle the reactive power, associated with the fundamentals of the loading and generating functions, can in all the cases be compensated by means of a simple reactive element. This fundamental reactive power can be derived by the same techniques as implemented by Depenbrock and Schwan. The distinct advantage of the correlated residual reactive power subdivision, is found in the fact that reactive power can be identified and compensated in one or more specific harmonics of the generating function. The compensation of a specific

reactive power harmonic can be obtained from a passively tuned harmonic power filter, which consists in general of an inductor and a capacitor. This principle implies that residual reactive power can also be compensated by means of passive elements. In these systems some uncompensated residual reactive power and deactive power should be compensated by means of a compensation system with adequate dynamic response time.

Low power compensation systems with a high dynamic response can be implemented within high power converters with characteristic distortion, to compensate the deactive power. This will result in cost effective, high power converters on a sinusoidal supply, because not all the power through the converter system has to be conditioned, only the deactive power portion.

7.6 SUMMARY

It may be some time before the ideas resulting from this work will find there pragmatic place in the generalized field of high quality power supply and utilization, but most of them will have a positive effect on the understanding, measurement, analysis, characterization and compensation of distortion in generalized energy systems.

"To believe your own thought, to believe that what is true for you in your private heart is true for all men, - that is genius." in Self-Reliance, Ralph Waldo Emerson, 1803 - 1882.

REFERENCES

(I) TEXTBOOKS

[H1] Arrillaga, J.; Bradley, D.A.; Bodger, P.S.: "Power system harmonics", chap.3,4,5,10, New York, John Wiley & Sons, 1985.

[H2] Bellanger, M.: "Digital processing of signals: Theory and practice", chap.1,6,7,9,11, New York, John Wiley & Sons, 1984.

[H3] Bozic, S.M.: "Digital and Kalman filtering", part 2, London, Edward Arnold (Publishers) Ltd., 1979.

[H4] Brand, L.: "Vector and tensor analysis", chap.X, New York, John Wiley & Sons, 1947.

[H5] Gibbs, W.J.: "Tensors in electrical machine theory", chap.I,II, London, Chapman & Hall, 1952.

[H6] Haykin, S.: "Adaptive filter theory", chap.3,6,8, New Jersey, Prentice-Hall, 1986.

[H7] Hayt, W.H.: "Engineering Electromagnetics", 4th edition, chap.10,11, Tokyo, McGraw-Hill, 1981.

[H8] Hoft, R.G.: "Semiconductor power electronics", chap.7-11, New York, Van Nostrand Reinhold Company Inc., 1986.

[H9] Heumann, K.: "Basic principles of power electronics", chap.7,8,11, Berlin, Springer-Verlag, 1986.

[H10] International Electrotechnical Commission (IEC), Tech. Committee No. 25, Working Group 7, Report: "Reactive power and distortion power", Doc.25(Secr.), no.113, Dec. 1980.

[H11] Kraus, J.D.; Craver, K.R.: "Electromagnetics", 2nd. edition, chap.9,10, Tokyo, McGraw-Hill, 1973.

[H12] Kron, G.: "The application of tensors to the analysis of rotating electrical machinery", 2nd edition, chap.I,II, XVI, Schenectady, N.Y., General Electric Review, 1942.

[H13] Lander, C.W.: "Power electronics", 2nd edition, chap.7, London, McGraw-Hill, 1987

[H14] Miller, T.J.E.: "Reactive power control in electric systems", chap.4,5,8, New York, John Wiley & Sons, 1982.

[H15] Papoulis, A.: "The Fourier integral and its applications", chap.8,10,12, New York, McGraw-Hill, 1962.

[H16] Rissik, H.: Mercury-arc current converters. chap.XIV, London, Pitman, 1935 and 1963.

[H17] Schwartz, M: "Information transmission, modulation, and noise", chap.1,2,7, New York, McGraw-Hill, 1959.

[H18] Sorenson, H.W. (Ed.): "Kalman filtering: Theory and Applications", IEEE Press, 1985.

[H19] Smith, W.R.: "Basics of the SAW interdigital transducer", in Computer-Aided Design of SAW Devices, Elsevier Scientific Publishing Co., New York, 1976.

[H20] Stanley, W.D.; Dougherty, G.R.; Dougherty, R.: "Digital signal processing", 2nd edition, chap.8,12,11,15, Reston, Prentice-Hall, 1984.

[H21] Static Power Committee of the IEEE-IAS: "IEEE guide for harmonic control and reactive compensation of static power converters", IEEE Std. 519-1981, 1981.

[H22] Texas Instruments: "Digital signal processing applications with the TMS320 family",chap.1,2,3,5,6,12,24, France, TI Press, 1986.

[H23] Widrow, B.; Stearns, S.D.: "Adaptive signal processing", New Jersey, Prentice-Hall, 1985.

[H24] Williamson, R.E.; Trotter, H.F.: "Multivariable Mathematics", chap.8, New York, Prentice-Hall, 1974.

[H25] Yuen, C.K.; Beauchamp, K.G.; Robinson, G.P.S.: "Microprocessor systems and their applications to signal processing", chap.7,8, London, Academic Press, 1982.

(II) ARTICLES IN TECHNICAL JOURNALS AND CONFERENCE PAPERS

[A1] Akagi, H.; Kanazawa, Y.; Nabae, A: "Instantaneous reactive power compensators comprising switching devices without energy storage components", in IEEE Trans. Ind. Appl., vol.IA-20, no.3, pp.625-465, May/June 1984.

[A2] Akagi, H.; Nabae, A.; Atoh, S.: "Control strategy of Active Power Filters using multiple voltage-source PWM converters", in IEEE Trans. Ind. Appl., vol.IA-22, no.3, pp.460-465, May/June 1986.

[A3] Alexandrovitz, A.; Epstein, E.; Yair, A.: "Analysis of a static VAR compensator with optimal energy storage element", in IEEE Trans. Ind. Electron., vol.IE-31, no.1, pp.28-33, Feb. 1984.

[A4] Arrillaga, J.; Acha, E.; Densen, T.J.; Bodger, P.S.: "Ineffectiveness of transmission line transpositions at harmonic frequencies", in Proc. IEE, pt.C, vol.133, no.2, pp.99-104, Mar. 1986.

[A5] Baghzouz, Y.; Tan, O.T.: "Harmonic analysis of induction watthour meter performance", in IEEE Trans. Power App. Syst., vol.PAS-104, no.2, pp.399-406, Feb. 1985.

[A6] Baghzouz, Y.; Tan, O.T.: "Probabilistic modeling of power system harmonics", in IEEE Trans. Ind. Appl., vol.IA-23, no.1, pp.173-180, Jan./Feb. 1987.

[A7] Becker, W.; Janssen, R.; Müller-Hellmann, A.; Skudelny, H.-Ch.: "Analysis and microcomputer-aided optimization of the reactive and psophometric current and characteristics of power converters for AC-fed traction drives", in Proc. of IEEE International Semiconductor Power Converter Conference (ISPCC-82), Orlando, USA, pp.122-136, 24-27 May 1982.

[A8] Bendien, J.Ch.; Fregien, G.; Van Wyk, J.D.: "High-efficiency on-board battery charger with transformer isolation, sinusoidal input current and maximal power factor", in Proc. IEE, pt.B, vol.133, no.4, pp.197-204, July 1986.

[A9] Blanchon, G.; Girard, N.; Logeay, Y.; Meslier, F.: "New developments in planning of reactive power compensation devices", in IEEE Trans. Power Syst., vol.PWRS-2, no.3, pp.764-771, Aug. 1987.

[A10] Bohmann, L.J.; Lasseter, R.H.: "Equivalent circuit for frequency response of a static VAR compensator", in IEEE Trans. Power Syst., vol.PWRS-1, no.4, pp.68-74, Nov. 1986.

[A11] Bowes, S.R.; Bullough, R.I.: "Harmonic minimisation in microprocessor controlled current fed PWM inverter drives", in Proc. IEE, pt.B, vol.134, no.1, Jan. 1987.

[A12] Buchholz, F.: "Untersuchung über die Dartstellung der Begriffe "Scheinleistung" und "Scheinarbeit" sowie ihrer Unterbegriffe bei Mehrphasenstrom", in Licht und Kraft, Org. Elektrotechn. Verein München, no.22, pp.1-6, 1921.

[A13] Budeanu, C.I.: "Reactive and fictitious powers", in Rumanian National Institute (Bucharest, Rumania), publication no.2, 1927.

[A14] Budeanu, C.I.: "The different options and conceptions regarding active power in non-sinusoidal systems", in Rumanian National Institute (Bucharest, Rumania), publication no.4, 1927.

[A15] Budeanu, C.I.: "Kapazitäten und Induktivitäten als verzerende Elemente", in Archiv für Elektrotechnik, vol.32, pp.251-259, 1938.

[A16] Choe, G.; Park, M.: "Analysis and control of Active Power Filter with optimized injection", in Proc. of 17th IEEE Power Electronics Specialists Conference (PESC-86), Vancouver, USA, pp.401-409, 23-27 June 1986.

[A17] Chatterjee, J.K.; Doshi, B.M.; Kumar, K.; Ray, K.K.: "A new concept for thyristor phase controlled VAR compensator", in Proc. IEEE 1987 Industrial Applications Annual Meeting (IAS-87), Atlanta, Georgia, USA, part I, pp.828-834, 18-23 Oct. 1987.

[A18] Cox, M.D.; Mirbod, A.: "A new static VAR compensator for an arc furnace", in IEEE Trans. Power Systems, vol.PWRS-1, no.3, pp.110-120, Aug. 1986.

[A19] Cummings, P.G.: "Estimating effects of system harmonics on losses and temperature rise of squirrel-cage motors", in IEEE Trans. Ind. Appl., vol.IA-22, no.6, pp.1121-1126, Nov./Dec. 1986.

[A20] Czarnecki, L.S.: "1-Ports with orthonormal properties," in Int. J. Circuit Theory Appl., vol.6, pp.65-73, 1978.

[A21] Czarnecki, L.S.: "Minimisation of distortion power of non-sinusoidal sources applied to linear loads", in Proc. IEE, pt.C, vol.128, no.4, pp.208-210, July 1981.

[A22] Czarnecki, L.S.: "Measurement of the individual harmonics reactive power in nonsinusoidal systems", in IEEE Trans. Instrum. Meas., vol.IM-32, no.2, pp.383-384, June 1983.

[A23] Czarnecki, L.S.: "An orthogonal decomposition of current of nonsinusoidal voltage sources applied to non-linear loads", in Int. J. Circuit Theory and Appl., vol.11, pp.235-239, 1983.

[A24] Czarnecki, L.S.: "Measurement principle of the reactive current rms value and the load susceptances for harmonic frequencies meter for nonsinusoidal systems", in IEEE Trans. Instrum. Meas., vol.IM-34, no.1, pp.14-17, March 1985.

[A25] Czarnecki, L.S.: "Considerations on reactive power in non-sinusoidal situations", in IEEE Trans. Instrum. Meas., vol.IM-34, no.3, pp.399-404, Sept. 1985.

[A26] Czarnecki, L.S.: "Minimisation of reactive power under nonsinusoidal conditions", in IEEE Trans. Instrum. Meas., vol.IM-36, no.1, pp.18-22, March 1987.

[A27] Czarnecki, L.S.: "What is wrong with the Budeanu concept of reactive power and why it should be abandoned", in IEEE Trans. Instrum. Meas., vol.IM-36, no.3, pp.834-837, Sept. 1987.

[A28] Dash, P.K.; Panda, P.C.; Hill, E.F.: "Adaptive controller for static reactive-power compensators in power systems", in Proc. IEE, pt.C, vol.134, no.3, pp.256-264, May 1987.

induction generators", in IEEE Trans. Power App. Syst., vol.PAS-104, no.7, pp.1825-1831, July 1985.

[A42] Emanuel, A.E.; Erlicki, M.S.: "New aspects of power factor improvement: Part II -Practical circuits", in IEEE Trans. Ind. Gen. Appl., vol.IGA-4, no.4, pp.447-455, July/Aug. 1968.

[A43] Emanuel, A.E.: "Suggested definition of reactive power in nonsinusoidal systems", in Proc. IEE, vol.121, no.7, pp.705-706, July 1974.

[A44] Emanuel, A.E.: "Energetical factors in Power Systems with Nonlinear loads", in Archiv für Electrotechnik, vol.59, pp.183-189, 1977.

[A45] Emanuel, A.E; Pileggi, D.J.; Orr, J.A.; Gulachenski, E.M.: "A non-contact technique for determining harmonic currents present in individual conductors of overhead lines", in IEEE Trans. Power App. Syst., vol.PAS-102, no.3, pp.596-603, March 1983.

[A46] Emanuel, A.E.; Sen, K.: "Unity power factor single phase power conditioning", in Proc. of 18th IEEE Power Electronics Specialists Conference (PESC-87), Blacksburg, USA, pp.516-524, 22-25 June 1987.

[A47] Emanuel, A.E.; Kaprielian, S.R.: "Contribution to the theory of stochastically periodic harmonics in power systems", in IEEE Trans. Power Del., vol.PWRD-1, no.3, pp.285-293, July 1986.

[A48] Enslin, J.H.R.; Van Wyk, J.D.: "Digital signal processing in power systems: Calculation of power under nonsinusoidal voltage and current conditions", in Proc. of 5th SA Digital Signal Processing Symposium, Grahamstown, RSA, pp. 1.5.1 - 1.5.6, 6 July 1987.

[A49] Enslin, J.H.R.; Van Wyk, J.D.; Van Rhyn, P.; Schoeman, J.J.: "Development and characteristics of battery-fed, high power, high-frequency converters in parallel operation", in Proc. of 2nd European Conference on Power Electronics and Applications (EPE-87), Grenoble, France, pp.141-146, 22-24 Sept. 1987.

[A50] Enslin, J.H.R.; Van Wyk, J.D.: "A new control philosophy for power electronic converters as fictitious power compensators", in Proc. of 19th IEEE Power Electronics Specialists Conference (PESC-88), Kyoto, Japan, pp.1188-1196, 11-14 April 1988.

[A51] Enslin, J.H.R.; Van Wyk, J.D.; Naudé, M.; Van der Lingen, S.E.: "Adaptive power estimation under nonsinusoidal voltage and current conditions", in Proc. of 5th IFAC/IFIP Symposium on Software For Computer Control (SOCOCO-88), Johannesburg, RSA, pp.17.1-17.15, 26-28 April 1988.

[A52] Enslin, J.H.R.; Van Wyk, J.D.: " 'n Nuwe benadering tot die definisie van elektriese drywing, onder toestande van vervormde spannings en strome", in "Suid-Afrikaanse Tydskrif vir Natuurwetenskap en Tegnologie, S.A. Akademie vir Wetenskap en Kuns", vol.7, no.2, pp.76-82, June 1988.

[A53] Enslin, J.H.R.; Van Wyk, J.D.: "Measurement and compensation of fictitious power under nonsinusoidal voltage and current conditions", in IEEE Trans. Instrum. Meas., vol.IM-37, no.3, Sept. 1988.

[A54] Enslin, J.H.R.; Van Wyk, J.D.: "Digital signal processing in power systems: Calculation of power under nonsinusoidal voltage and current conditions", in SAIEE Trans., vol.79, no.1, Aug. 1988.

[A55] Epstein, E.; Yair, A.; Alexandrovitz, A,: "Analysis of a reactive current source used to improve current drawn by static inverters", in IEEE Trans. Ind. Electron. Control Instrum., vol.IECI-26, no.3, pp.172-177, Aug. 1979.

[A56] Epstein, E.; Yair, A.; Alexandrovitz, A,: "Three-phase static VAR compensator with reduced energy storage", in ETZ Archiv, vol.8, no.6, pp.213-219, 1986.

[A57] Erlicki, M.S.; Emanuel, A.E.: "New aspects of power factor improvement: Part I -Theoretical basis", in IEEE Trans. Ind. Gen. Appl., vol.IGA-4, no.4, pp.441-446, July/Aug. 1968.

[A58] Evans, P.D.; Close, P.R.: "Harmonic distortion in PWM inverter output waveforms", in Proc. IEE, pt.B, vol.134, no.4, pp.224-232, July 1987.

[A59] Filicori, F.; Mirri, D.; Rinaldi, M.: "Error estimation in sampling digital wattmeters", in Proc. IEE, pt.A, vol.132, no.3, pp.122-128, May 1985.

[A60] Filipski, P.: "A new approach to reactive current and reactive power measurement in nonsinusoidal systems", in IEEE Trans. Instrum. Meas., vol.IM-29, no. 4, pp.423-426, Dec. 1980.

[A61] Filipski, P.: "The measurement of distortion current and distortion power", in IEEE Trans. Instrum. Meas. vol.IM-33, no.1, pp.36-40, March 1984.

[A62] Filipski, P.: "The systematic errors of a time-division power converter under sinusoidal and nonsinusoidal conditions", in IEEE Trans. Power Delivery, vol.PWRD-1, no.3, pp.61-67, July 1986.

[A63] Filipski, P.: "System for testing wattmeters under nonsinusoidal conditions", in IEEE Trans. Instrum. Meas., vol.IM-36, no.2, pp.347-353, June 1987.

[A64] Fischer, H.D.: "Bermerkungen zu Leistungsbergriffen bei Stromen und Spannungen mit Oberschwingungen", in Archiv für Elektrotechnik, vol.64, pp.289-295, 1982.

[A65] Fischer, H.D.: "Blindleistungskompensation bei nichtperiodischen Strömen und Spannungen", in ETZ Archiv, vol.4, no.4, pp.127-131, 1982.

[A66] Fischer, H.D.: "Leistungsbegriffe für Mehrphasensysteme. Teil 1: Die Leistungsbegriffe nach Buchholz und nach Quade", in Siemens Forsch.- u. Entwickl.-Ber., vol.14, no.5, pp.245-251, 1985.

[A67] Fischer, H.D.: "Leistungsbegriffe für Mehrphasensysteme. Teil 2: Vergleich der Leistungsbegriffe nach Buchholz und nach Quade", vol.14, no.6, pp.299-305, 1985.

[A68] Fisher, R.; Hoft, R.: "Three-phase power line conditioner for harmonic compensation and power factor correction", in Proc. IEEE 1987 Industrial Applications Annual Meeting (IAS-87), Atlanta, Georgia, USA, part I, pp.803-807, 18-23 Oct. 1987.

[A69] Fryze, S.: "Wirk-, Blind-, und Scheinleistung in Elektrisch Stromkreisen mit nichtsinusoidalformingen Verlauf von Strom und Spannung", in ETZ, vol.53, no.25, pp.596-599, 625-627, 700-702, 1932.

[A70] Fuchs, E.F.; Roesler, D.J.; Kovacs, K.P.: "Aging of electrical appliances due to harmonics of the power system's voltage", in IEEE Trans. Power Del., vol.PWRD-1, no.3, pp.301-307, July 1986.

[A71] Fuchs, E.F.; Roesler, D.J.; Kovacs, K.P.: "Sensitivity of electrical appliances to harmonic and fractional harmonics of the power system's voltage. Part II: Television sets, induction watthour meters and universal machines", in IEEE Trans. Power Del., vol.PWRD-2, no.2, pp.445-453, April 1987.

[A72] Galloway, J.H.: "Line current waveforms for a large multiphase thyristor converter system", in IEEE Trans. Ind. Appl. vol.IA-13, no.5, pp.394-399, Sept./Oct. 1977.

[A73] Grady, W.M.; Heydt, G.T.: "Prediction of power system harmonics due to gaseous discharge lightning", in IEEE Trans. Power App. Syst., vol.PAS-104, no.3, pp.554-651, March 1985.

[A74] Grady, W.M.; Heydt, G.T.: "Determination of harmonics in an AC power system caused by HVDC converters", in Electric Machines and Power Systems, Hemishere Publishing Corp., vol.10, no.1, pp.39-52, 1985.

[A75] Graham, J.H.; Schonholzer, E.T.: "Line harmonics of converters with DC-motor loads", in IEEE Trans. Ind. Appl. vol.IA-19, no.1, pp.84-93, Jan./Feb. 1983.

[A76] Gretsch, R.; Krost, G.: "Betrags- und winkelrichtige Messung von Spannungs- und Stromharmonischen", in ETZ Archiv vol.3, no.5, pp.149-152, 1981.

[A77] Grünberg, D.; Reiche, W.: "Effects of electric Arc-furnaces on power systems and methods of compensation", in Brown Boveri Review, vol.73, no.8, pp.471-480, Aug. 1986.

[A78] Guntersdorfer, M.: "At the crossroads of acoustics and electronics", in Siemens Review, vol.53, no.2, pp.36-39, Febr. 1986.

[A79] Gyugyi, L.: "Reactive power generation and control by thyristor circuits", in IEEE Trans. Ind. Appl. vol.IA-15, no.5, pp.521-532, Sept./Oct. 1979.

[A80] Gyugyi, L.; Taylor, E.R.: "Characteristics of static, thyristor-controlled shunt compensators for power transmission applications", in IEEE Trans. Power App. Syst., vol.PAS-99, no.5, pp.1795-1804, Sept./Oct. 1980.

[A81] Harashima, F.; Inaba, H.; Tsuboi, K.: "A closed-loop control system for the reduction of reactive power required by electronic converters", IEEE Trans. Ind. Electron. Control Instrum., vol.IECI-23, no.2, pp.162-166, May 1976.

[A82] Hosono, I.; Yano, M.; Takeda, M.; Yuya, S.; Sueda, S.: "Suppression and measurement of arc furnace flicker with a large static VAR compensator", in IEEE Trans. Power App. Syst., vol.PAS-98, no.6, pp.2276-2284, Nov./Dec. 1979.

[A83] Hsu, Y.Y.; Cheng, C.H.: "Design of a static VAR compensator using model reference adaptive control", in Journ. Electrical Power Systems Research, Elsevier Sequoia SA, vol.13, no.2, pp.129-138, Oct. 1987.

[A84] Kaiserslautern, C.T.: "Regelung von Blindleistungskompensatoren mit aktiven Filtern", in Automatiserungstechnik, vol.34, no.8, pp.302-310, 1986.

[A85] Kalman, R.E.: "A new approach to linear filtering and prediction problems", in Trans. ASME, J. of Basic Eng., series 82D, pp.35-45, March 1960.

[A86] Kawahira, H.; Nakamura, T.; Nakazawa, S.; Nomura, M: "Active power filter", in Proc., International Power Electronics Conference (IPEC-83), Tokyo, Japan, pp.981-992, 27-31 March 1983.

[A87] Kitai, R.: "On-line measurement of power system harmonic magnitude and phase angle", in IEEE Trans. Instrum. Meas., vol.IM-27, no.1, pp.79-81, March 1978.

[A88] Klaas, L.: "Einige Bemerkungen zur digitalen Leistungserfassung in nichtlinearen Wechselstromsystemen", in ETZ Archiv vol.3, no.3, pp.89-90, 1981.

[A89] Klinger, G.: "Wechselstromkomponentenspalter", in ETZ-B, vol.26, no.17, pp.433-434, 1974.

[A90] Komatsugi, K.; Imura, T.: "Harmonic current compensator composed of static power converter", in Proc. of 17th IEEE Power Electronics Specialists Conference (PESC-86), Vancouver, USA, pp.283-290, 23-27 June 1986.

[A91] Korvink, G.J.: "Minimisation of errors in the measurement of three-phase voltage and current", in Trans. SAIEE, vol.73, no.5, pp.178-182, Sept. 1982.

[A92] Kusic, G.L.; Whyte, I.A.: "Three phase steady-state static VAR-generator filter design for power systems", in IEEE Trans. on Power App. Syst., vol.PAS-103, no.4, pp.811-818, April 1981.

[A93] Kusters, N.L.; Moore, W.J.M.: "On the definition of reactive power under nonsinusoidal conditions", in IEEE Trans. Power App. Syst., vol.PAS-99, no.5, pp.1845-1854, Sept./Oct. 1980.

[A94] Lavers, J.D.; Danai, B.; Biringer, P.P.; Chee-Hing, D.J.: "A method of examining in detail electric arc furnace performance", in IEEE Trans. Ind. Appl., vol.IA-21, no.1, pp.137-146, Jan./Feb. 1985.

[A95] Lin, D.W.: "On digital implementation of the fast Kalman Algorithms", in IEEE Trans. Acous. Speech and Signal Processing, vol.ASSP-32, no.5, pp.998-1005, Oct. 1984.

[A96] Lin, K.S.; Frantz, G.A.; Simar, R.: "The TMS320 Family of digital signal processors", in IEEE Proc. vol.75, no.9, pp.1143-1159, Sept. 1987.

[A97] Linders, J.R.: "Electric wave distortion: Their hidden costs and containment", in IEEE Trans. Ind. Appl., vol.IA-15, no.5, pp.458-471, Sept./Oct. 1979.

[A98] Littler, G.E.: "The production of residual currents due to harmonic loading", in Proc. IEE, Pt.C, vol.132, no.6, pp.195-201, July 1985.

[A99] Liu, C.C.; Tomsovic, K.: "An expert system assisting decision-making of reactive power\voltage control", in IEEE Trans. Power Syst., vol.PWRS-1, no.3, pp.195-201, Aug. 1986.

[A100] Ljung, L.: "Analysis of a general recursive predictor error identification algorithm", in Automatica, vol.17, no.1, pp.89-99, 1981.

[A101] Malesani, L.; Rosetto, L.; Tenti, P.: "Active filters for reactive power and harmonics compensation", in Proc. of 17th IEEE Power Electronics Specialists Conference (PESC-86), Vancouver, USA, pp.321-330, 23-27 June 1986.

[A102] Matsui, M.; Fukao, T.: "A detection method for Active reactive negative-sequence power and application", in Proc. IEEE 1987 Industrial Applications Annual Meeting (IAS-87), Atlanta, Georgia, USA, part I, pp.821-827, 18-23 Oct. 1987.

[A103] Mc. Clellan, J.H.; Parks, T.W.; Rabiner, L.R.: "A computer program for designing FIR linear phase digital filters", in IEEE Trans. Audio Electroacoustics, vol.AU-21, no.6, pp.506-562, 1973.

[A104] McGranaghan, M.F.; Shaw, J.H.; Owen, R.E.: "Measuring voltage and current harmonics on distribution systems", in IEEE Trans. Power App. Syst., vol.PAS-100, no.7, pp.3599-3608, July 1981.

[A105] Miyairi, S.; Iida, S.; Nakata, K.; Masukawa, S.: "New method for reducing harmonics involved in input and output of rectifier with interphase transformer", in IEEE Trans. Ind. Appl., vol.IA-22, no.5, pp.790-797, Sept./Oct. 1986.

[A106] Müller-Hellmann, A.; Skudelny, H.-Ch.: "Average power factor for traction duty cycles", in Proc. IEEE 1980 Industrial Applications Annual Meeting (IAS-80), pp.790-797, Sept. 1980.

[A107] Naraine, P.; Cambell, C.K.; Ye, Y.: "A SAW step-type delay line for efficient high order harmonic mode excitation", in Proc. 1980 IEEE Ultrasonics Symposium, Boston, USA, IEEE Group on Sonics and Ultrasonics, pp.322-325, 5-7 Nov. 1980,

[A108] Nowomiejski, Z.: "Analyse elektrischer Kreise mit periodischen nichtsinusoidalförmigen Vorgängen", in Wissensch. Z. d. Elektrotechnik, vol.8, pp.244-254, 1967.

[A109] Nowomiejski, Z.: "Generalized theory of electric power", in Archiv für Electrotechnik, vol.63, pp.177-182, 1981.

[A110] Oberdorfer, G.: "Begriffserklärung und Erläuterung der Blindleistung", VDE-Verlag GmbH-Berlin, VDE-Buchreihe, Band 10, Blindleistung Vorträge, München, FRG, pp.12-34, 27-28 March 1963.

[A111] Odendal, E.J.; Harley, R.G.: "Interaction between power electronic converters and the supply network", in Journ. Electrical Power Systems Research, vol.10, no.1, pp.63-68, Jan. 1986.

[A112] Orr, J.A.; Emanuel, E.; Pileggi, D.J.: "Current harmonics, voltage distortion, and powers associated with electric vehicle battery chargers distributed on the residential power system", in IEEE Trans. Ind. Appl., vol.IA-20, no.4, pp.727-734, July/Aug. 1984.

[A113] Page, C.H.: "Reactive power in nonsinusoidal situations", in IEEE Trans. Instrum. Meas., vol.IM-29, no.4, pp.420-423, Dec. 1980.

[A114] Poynting, J.H.: "On the transfer of energy in the electromagnetic field", in Phil. Trans. of the Royal Society of London, part I, vol.174, pp.343-361, 1884.

[A115] Quade, W.: "Zusammensetzung der Wirk-, Blind- und Scheinleistung bei Wechselstromen beliebiger Kurvenform und neue Leistungsdefinition für unsymmetrische Mehrphasenströme beliebiger Kurvenform", in ETZ, vol.58, no.49, pp.1313-1316 and pp.1341-1344, 1937.

[A116] Quade, W.: "Neue Darstellung der Verzerrungsleistung eines Wechselstroms mit Hilfe des Funktionenraums", in Archiv für Electrotechnik vol.23, pp.277, 1939.

[A117] Rissik, H.: "The influence of mercury arc rectifiers upon the powerfactor of the supply system", in J. IEE, vol.72, pp.435-455, May 1935.

[A118] Schlecht, M.F.; Miwa, B.A.: "Active power factor correction for switching power supplies", in IEEE Trans. Power Electron., vol.PE-2, no.4, pp.273-281, Oct. 1987.

[A119] Schwan, U.: "A measuring instrument to split the line current into orthogonal components", in VDE-Verlag GmbH-Berlin, ETG-Fachberichte no.11, Vorträge der ETG/GMR Fachtagung, "Elektronik in der Energietechnik" and "Leittechnik in der Elektrischen Antriebstechnik", Braunschweig, FRG, pp.59-64, 12-14 October 1982.

[A120] Schwartz,F.C.; Klaassens, J.B.: "A controllable secondary multikilowatt DC current source with constant maximum power factor in its three phase supply line", in IEEE Trans. Ind. Electron. Contr., vol.IECI-23, no.2, pp.142-150, May 1976.

[A121] Sharon, D.: "Reactive-power definitions and power-factor improvement in nonlinear systems", in Proc. IEE, vol.120, no.6, pp.704-706, June 1973.

[A122] Shepherd, W.; Zakikhani, P.: "Suggested definition of reactive power in nonsinusoidal system", in Proc. IEE, vol.119, no.9, pp.1361-1362, Sept. 1972, and vol.120, no.7, pp.706-798, July 1973.

[A123] Shepherd, W.; Zakikhani, P.: "Power factor compensation of thyristor-controlled single-phase load", in Proc. IEE, vol.120, no.2, pp.245-246, Feb. 1973.

[A124] Shipp, D.D.: "Harmonic analysis and suppression for electrical systems supplying static power converters and other nonlinear loads", in IEEE Trans. Ind. Appl., vol.IA-15, no.5, pp.453-458, Sept./Oct. 1979.

[A125] Singer, S.: "Modeling and synthesis of harmonic-free power conversion and VAR compensation systems", in IEEE Trans. Ind. Electron., vol.IE-34, no.2, pp.257-262, May 1987.

[A126] Singer, S.: "Gyrators application in power processing circuits", in IEEE Trans. Ind. Electron., vol.IE-34, no.3, pp.313-318, Aug. 1987.

[A127] Skinner, J.W.: "The measurement basis of electrical supply metering", in Proc. IEE, Pt.A, vol.107, no.31, pp.75-84, Feb. 1960.

[A128] Smith, R.L.; Stratford, R.P.: "Power system harmonic effects from adjustable-speed drives", in IEEE Trans. Ind. Appl., vol.IA-20, no.4, pp.973-977, July/Aug. 1984.

[A129] Sorenson, H.W.: "Least-squares estimation from Gauss to Kalman", in IEEE Spectrum, vol.7, no.7, pp.63-68, July 1970.

[A130] Steeper, D.E.; Stratford, R.P.: "Reactive compensation and harmonic suppression for industrial power systems using thyristor converters", in IEEE Trans. Ind. Appl., vol.IA-12, no.3, pp.232-254, May/June 1976.

[A131] Stratford, R.P.: "Rectifier harmonics in power systems", in IEEE Trans. Ind. Appl., vol.IA-16, no.2, pp.271-275, Mar./April 1980.

[A132] Stratford, R.P.: "Harmonic pollution on power systems - a change in philosphy", in IEEE Trans. Ind. Appl., vol.IA-16, no.5, pp.617-623, Sept./Oct. 1980.

[A133] Stratford, R.P.: "Analysis and control of harmonic current in systems with static power converters", in IEEE Trans. Ind. Appl., vol.IA-17, no.1, pp.71-81, Jan./Feb. 1981.

[A134] Sumi, Y.; Harumoto, Y.; Hazegawa, T.; Yano, M.; Ikeda, K.; Matsura, T: "New static VAR control using force commutated inverters", in IEEE Trans. Power App. Syst., vol.PAS-100, no.9, pp.4216-4224, Sept. 1981.

[A135] Szabados, B.; Hill, E.F.: "On-line measurement of power system harmonics", in IEEE Trans. Instrum. Measurements, vol.IM-26, no.2, pp.170-175, June 1977.

[A136] Takeda, M.; Ikeda, K.; Tominaga, Y.: "Harmonic current compensation with active filter", in Proc. IEEE 1987 Industrial Applications Annual Meeting (IAS-87), Atlanta, Georgia, USA, part I, pp.808-815, 18-23 Oct. 1987.

[A137] Toth III, J.J.; Velazquez, D.J.: "Benefits of an automated on-line harmonic measurement system", in IEEE Trans. Ind. Appl., vol.IA-22, no.5, pp.952-963, Sept./Oct. 1986.

[A138] Tschappu, F.: "Problems of the exact measurement of electrical energy in networks having content in the current," in Landis and Gyr Review, vol.28, no.2, pp.8-15. 1981.

[A139] Van Schoor, G.; Van Wyk, J.D.: "A study of current fed converters as an active three phase filter", in Proc. of

18th IEEE Power Electronics Specialists Conference (PESC-87), Blacksburg, USA, pp.482-490, 22-25 June 1987.

[A140] Van Wyk, J.D.; Enslin, J.H.R.: "A study of a wind power converter with microcomputer based maximal power control utilising an oversynchronous electronic Scherbius cascade", in Proc. of International Power Electronics Conference (IPEC-83), Tokyo, Japan, pp.766-777, 27-31 March 1983.

[A141] Van Wyk, J.D.; Marshall, D.A.; Boshoff, S.: "Simulation and experimental study of a reactively loaded PWM converter as a fast source of reactive power", in IEEE Trans. Ind. Appl., vol.IA-22, no.6, pp.1082-1089, Nov./Dec. 1986.

[A142] Van Wyk, J.D.; Skudelny, H.-Ch.; Müller-Hellmann, A.: "Power electronics, control of the electro-mechanical energy conversion process and some applications",in Proc. IEE, vol.133, pt.B, no.6, pp.369-399, Nov. 1986.

[A143] Van Wyk, J.D.; Swart, P.L.; Olivier, D.N.; Van Niekerk, J.D.: "On-line harmonic analysis as a dianostic design and control tool for power systems feeding arc furnaces, thyristor-controlled mill drives, and power factor correction equipment", in IEEE Trans. Ind. Appl., vol.IA-19, no.6, pp.932-939, Nov./Dec. 1983.

[A144] Velayudhan, C.; Bundell, J.H.: "An electronic three-phase active and reactive power transducer", in Int. J. Electronics, vol.57, no.2, pp.267-276, 1984.

[A145] Walker, L.H.: "Forced-commutated reactive-power compensation", in IEEE Trans. Ind. Appl., vol.IA-22, no.6, pp.1091-1104, Nov.\Dec. 1986.

[A146] Weschta, A.: "Influence of thyristor-controlled reactors on harmonics and resonance effects in power supply systems", in Siemens Forsch.- u. Entwickl.-Ber., vol.14, no.2, pp.62-68, 1985.

[A147] Working Group on Power System Harmonics (IEEE): "Power system harmonics: An overview", in IEEE Trans. Power App. Syst., vol.PAS-102, no.8, pp.2455-2460, Aug. 1983.

[A148] Working Group on Power System Harmonics (IEEE): "Bibliography of power system harmonics; Part I and II", in IEEE Trans. Power App. Syst., vol.PAS-103, no.9, pp.2460-2479, Sept. 1984.

[A149] Yacamini, R.; De Oliveira, J.C.: "Harmonics in multiple converter systems: a generalized approach", in Proc. IEE, vol.127, pt.B, no.2, pp.96-106, March 1980.

[A150] Zuckerberger, A.; Alexandrovitz, A.: "Determination of commutation with a view to eliminating harmonics in microprocessor-controlled PWM voltage inverter", in IEEE Trans. Ind. Electron., vol.IE-33, no.3, pp.262-270, Aug. 1986.

(III) DISSERTATIONS AND TECHNICAL REPORTS

[D1] Depenbrock, M.: "Untersuchen über die Spannungs- und Leistungverhältnisse bei Umrichtern ohne Energiespeicher", Final D.Eng. dissertation, Technischen Hochshule Hannover, 1962.

[D2] Enslin, J.H.R.: "Struktuur, gedrag en beheer van stelsels vir die optimale benutting van elektriese energie opgewek uit die wind onder dinamiese toestande", Final M.Eng. dissertation, Dept. Electrical and Electronic Engineering, Faculty of Engineering, RAU, Johannesburg, Nov. 1983.

[D3] Enslin, J.H.R.: "Proposed definition and measurement of loading-, active- and nonactive power in power systems with nonsinusoidal currents and voltages", Internal Report, no. 86-VA-001, Dept. of Electrical Engineering, University of Pretoria, Pretoria, Feb. 1987.

[D4] Enslin, J.H.R.; Van Wyk, J.D.: "A method for measuring power by SAW correlators", Internal Report, no. END-67, Energy Laboratory, RAU, Johannesburg, March 1987.

[D5] Enslin, J.H.R.: "New control philosophy for fictitious power compensation systems", Internal Report, no.86-VA-006, Dept. Electrical Engineering, University of Pretoria, Pretoria, Sept. 1987.

[D6] Koch, K.: "Bestimmung von Wechselstromgrösen in Mehr-Leiter-Systemen", Final D.Eng. dissertation, Technischen Hochshule Bochum, 1984.

[D7] Naudé, M.; Enslin, J.H.R.; Van Der Lingen, S.E.: "Voorspelling van kragnetwerk-parameters deur middel van Kalman-filtertegnieke", Internal Report, no.86-VA-005, Dept. Electrical Engineering, University of Pretoria, Aug. 1987.

[D8] Schwan, U.: "Beitrag zur ein- und mehrphasigen On-Line Leistungsmessung im Zeitbereich bei Spannungen und Strömen mit beliebigem Zeitverlauf", Final D.Eng. dissertation, Rheinisch-Westfälischen Technischen Hochshule Aachen, 1983.

[D9] Van Der Lingen, S.E.: "The integrity of parameter adaptive control", PhD Thesis, Dept. Electrical Eng., University of Pretoria, Pretoria, To be submitted Sept. 1988.

[D10] Van Schoor, G.: "Analise, sintese en beheer van stroomgevoerde mutators met pulswydtemodulasie, as aktiewe filters in elektriese energienetwerke", Final M.Eng dissertation, Energy Laboratory, RAU, Johannesburg, 1987.

[D11] Vaupel, G.: "Netzspannungsstabilisierung bei grossen, schnell veränderlichen Lasten durch netzgeführte Stromrichter", Final D.Eng. dissertation, Technischen Hochshule Bochum, 1986.

APPENDICES

APPENDIX A: MATHEMATICAL ANALYSIS AND MANIPULATIONS

A1: MATHEMATICAL REPRESENTATION OF NON-SINUSOIDAL CURRENTS AND VOLTAGES

The well known phasor representation of voltage and current is generally used for power flow studies in electric power systems. The phasor theory is characteristic of a time-invariant mathematical representation of sinusoidal voltage and current waveforms, in terms of an effective magnitude and a phase angle. This time-invariant representation cannot be used when the waveforms of current and voltage are non-sinusoidal and is undefined when the voltages and currents are characterized as aperiodic waveforms.

In terms of phasors a sinusoidal voltage and phase shifted current is represented in eq. (A.1) as two exp-functions:

$$\mathbf{U} = \sqrt{2}.U\, e^{j(\omega t-\alpha)}; \qquad \mathbf{I} = \sqrt{2}.I\, e^{j(\omega t-\beta)} \qquad (A.1)$$

$$\theta = \beta - \alpha$$

where θ is the phase angle between **U** and **I** phasors, and U and I the effective values of the voltage and current sinusoidal waveforms respectively. These representations are normally written in the phasor short form:

$$\mathbf{U} = U\ \arg(\alpha); \qquad \mathbf{I} = I\ \arg(\beta) \qquad (A.2)$$

From these phasor representations the complex power **S** is derived (chap. 1), which is used to represent the apparent power S in the complex Re-Im plane. Two orthogonal power components, active power P and reactive power Q, are derived:

$$\mathbf{S} = P + jQ; \quad S = |\mathbf{S}| \tag{A.3}$$

$$P = U.I \cos\theta; \quad Q = U.I \sin\theta \tag{A.4}$$

which is the well known definition of the average active and reactive power.

In the seek for an orthogonal mathematical representation of non-sinusoidal quantities of voltages and currents, the quaternion theory [H4] seems to be appropriate because a quaternion consists of a vector and a scalar, with the vector defined in three orthogonal components. The vector space is described in terms of three orthogonal unit vectors, while the scalar describes the average value of the quaternion. In this theory a quaternion $\mathbf{q}$ is of the form

$$\mathbf{q} = a\mathbf{i} + b\mathbf{j} + c\mathbf{k} + d \tag{A.5}$$

where a,b,c,d are ordinary real numbers and $\mathbf{i},\mathbf{j},\mathbf{k}$ are the quaternion unit vectors, satisfying the algebraic rules, which are defined as orthogonal [H4]:

$$\mathbf{i}^2 = \mathbf{j}^2 = \mathbf{k}^2 = -1;$$

$$\mathbf{jk} = -\mathbf{kj} = \mathbf{i}; \quad \mathbf{ki} = -\mathbf{ik} = \mathbf{j}; \quad \mathbf{ij} = -\mathbf{jk} = \mathbf{k}. \tag{A.6}$$

The vector part $V\mathbf{q}$, scalar part $S\mathbf{q}$, conjugate part $\mathbf{q}^*$, norm $|\mathbf{q}|$, and reciprocal $\mathbf{q}^{-1}$ are defined in the following equations [H4]:

$$V\mathbf{q} = a\mathbf{i} + b\mathbf{j} + c\mathbf{k}; \quad S\mathbf{q} = d; \quad \mathbf{q} = V\mathbf{q} + S\mathbf{q}; \quad \mathbf{q}^* = -V\mathbf{q} + S\mathbf{q};$$

$$|\mathbf{q}| = \sqrt{[a^2 + b^2 + c^2 + d^2]}; \quad \mathbf{q}^{-1} = \mathbf{q}^*/|\mathbf{q}| \tag{A.7}$$

The product of two quaternions $\mathbf{q}_1$ and $\mathbf{q}_2$, is shown in eq. (A.8):

$$\mathbf{q}_1 \cdot \mathbf{q}_2 = S\mathbf{q}_1 . S\mathbf{q}_2 + S\mathbf{q}_1 . V\mathbf{q}_2 + S\mathbf{q}_2 . V\mathbf{q}_1 + V\mathbf{q}_1 . V\mathbf{q}_2 \tag{A.8}$$

Using the above-mentioned principles the voltage and the current can be expressed as quaternions, as shown in the following equations (A.9):

$$\mathbf{Uq} = U_i\mathbf{i} + U_j\mathbf{j} + U_k\mathbf{k} + U_{avg}$$
$$\mathbf{Iq} = I_i\mathbf{i} + I_j\mathbf{j} + I_k\mathbf{k} + I_{avg} \qquad (A.9)$$

where U_i, U_j and U_k are three orthogonal representations U_{avg} is the average value of the voltage signal. The same components can be derived for the current quaternion.

When these quaternions are time-variant, a second order tensor representation (matrix) [H4,5,12] should be used to characterize the mathematical representation of voltage and current as time-variant tensors, generally accepted in any time domain waveform of voltage and current.

The voltage and current time-variant quaternion representations can be used to represent quaternion power **Sq** in terms of the quaternion product, which can be seen as an extension of the complex power **S**, describing active, reactive and deactive power.

$$\mathbf{Sq} = \mathbf{Uq}\cdot\mathbf{Iq}^* = (P + Q\mathbf{k} + D\mathbf{j}) \qquad (A.10)$$

The loading power and effective values U and I can be derived from the quaternion voltage, current and power directly:

$$U = |\mathbf{Uq}|; \quad I = |\mathbf{Iq}|; \quad S = |\mathbf{Sq}| \qquad (A.11)$$

These power components are shown schematically in fig. A.1, while the voltage and current vector components are shown in a decomposed form in fig A.2. The power components are shown in a real component and two imaginary components **k** and **j**, representing the active power and two fictitious power components; the reactive and the deactive power.

The voltage and current quaternions are decomposed into three orthogonal vector components and one scalar component:

$$\mathbf{Uq} = U.\cos\alpha_u.\cos\beta_u\mathbf{i} + U.\cos\beta_u.\sin\alpha_u\mathbf{j} + U.\sin\beta_u\mathbf{k} + U_{avg}$$
$$\mathbf{Iq} = I.\cos\alpha_i.\cos\beta_i\mathbf{i} + I.\cos\beta_i.\sin\alpha_i\mathbf{j} + I.\sin\beta_i\mathbf{k} + I_{avg}$$
(A.12)

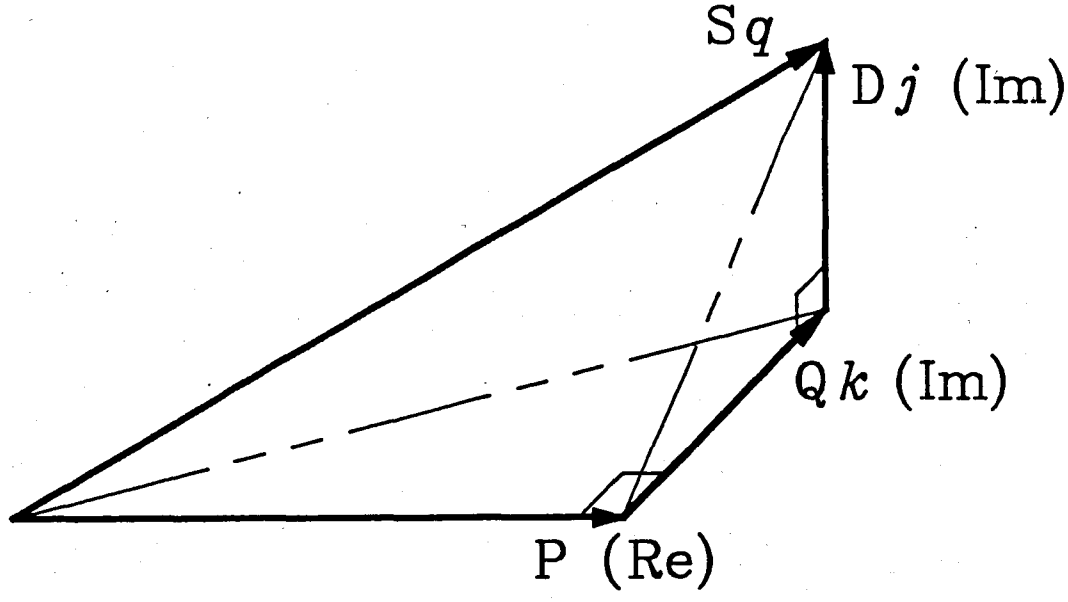

Fig. A.1: Quaternion Representation of Power Components

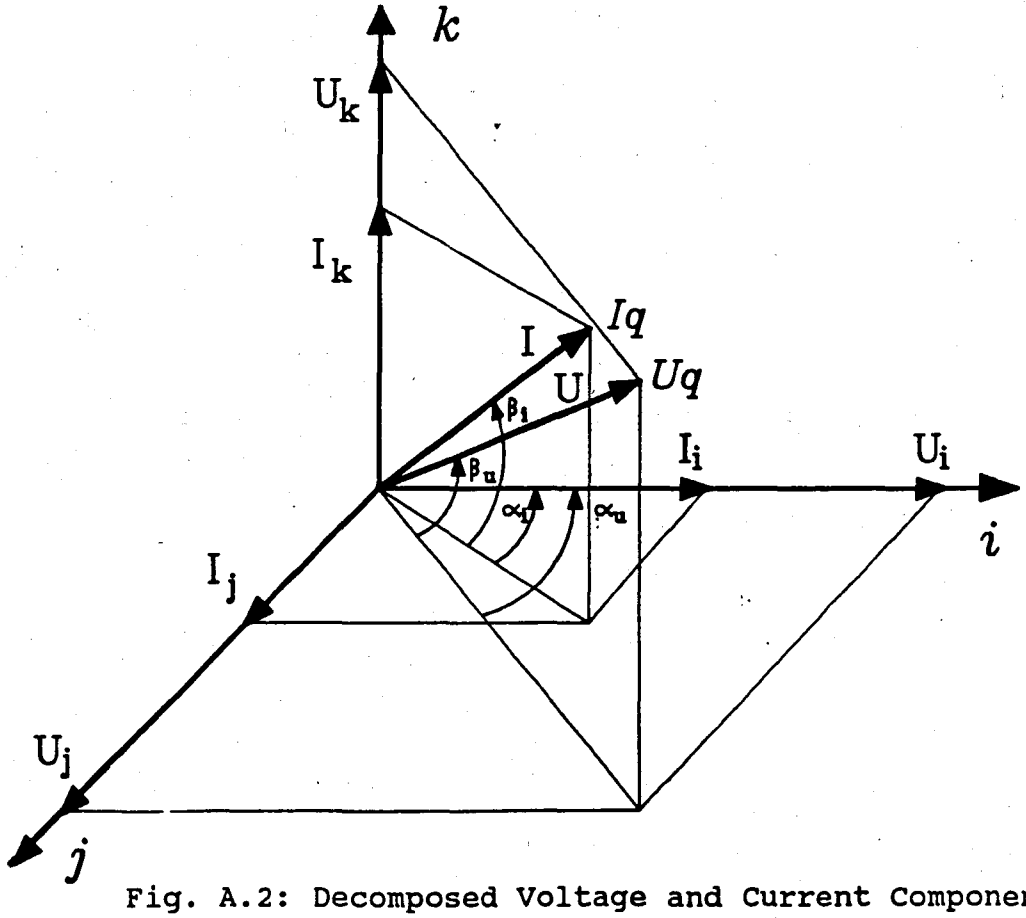

Fig. A.2: Decomposed Voltage and Current Components

Using the decomposed components of the voltage and the current, the quaternion power can be derived from the quaternion product as described in eq. (A.8) and (A.10). The result is shown in eq. (A.13):

$$\mathbf{Sq} = \mathbf{Uq} \cdot \mathbf{Iq}^*$$

$$\begin{aligned}\mathbf{Sq} = {} & U_{avg}.I_{avg} + UI\cos\alpha_u.\cos\beta_u.\cos\alpha_i.\cos\beta_i + UI\cos\beta_u.\sin\alpha_u.\cos\beta_i.\sin\alpha_i + UI\sin\beta_u.\sin\beta_i + \\ & (-U_{avg}.I\cos\alpha_i.\cos\beta_i + I_{avg}.U\cos\alpha_u.\cos\beta_u - UI\cos\beta_u.\sin\alpha_u.\sin\beta_i + UI\sin\beta_u.\cos\beta_i.\sin\alpha_i)\mathbf{i} + \\ & (-U_{avg}.I\sin\alpha_i.\cos\beta_i + I_{avg}.U\sin\alpha_u.\cos\beta_u + UI\sin\beta_i.\cos\beta_u.\cos\alpha_u - UI\sin\beta_u.\cos\beta_i.\cos\alpha_i)\mathbf{j} + \\ & (-U_{avg}.I\sin\beta_i + I_{avg}.U\sin\beta_u - UI\cos\beta_i.\cos\beta_u.\cos\alpha_u.\sin\alpha_i + UI\cos\beta_u.\cos\beta_i.\cos\alpha_i.\sin\alpha_u)\mathbf{k}\end{aligned} \qquad (A.13)$$

This quaternion power describes the loading, active, reactive and deactive power. This theory has been evaluated on a limited scale with two examples shown below:

Example 1: Using sinusoidals for the voltage and current waveforms:

$$\begin{aligned} u(t) &= \sqrt{2}.U\cos wt \\ i(t) &= \sqrt{2}.I\cos(wt-\alpha_i) \end{aligned} \qquad (A.14)$$

Using eq. (A.13) and implementing the above simplifications, the following results are obtained:

$$\mathbf{Uq} = (U\cos\alpha_u)\mathbf{i} + (U\sin\alpha_u)\mathbf{j} + 0\mathbf{k} + 0 \qquad (A.15)$$

$$\mathbf{Iq} = (I\cos\alpha_i)\mathbf{i} + (I\sin\alpha_i)\mathbf{j} + 0\mathbf{k} + 0 \qquad (A.16)$$

$$\mathbf{Sq} = \mathbf{Uq}\cdot\mathbf{Iq}^* = UI\cos\alpha_i - UI\sin\alpha_i\mathbf{k} \qquad (A.17)$$

Example 2: Using a sinusoidal for the voltage waveform and a block function for the current waveform, results in:

$$\begin{aligned} u(t) &= \sqrt{2}.U\cos wt \\ i(t) &= +\hat{}I \quad \text{for} \quad 0 < t \le T/2 \\ &= -\hat{}I \quad \text{for} \quad T/2 < t \le T \end{aligned} \qquad (A.18)$$

Using eq. (A.13) and implementing again the above simplifications, the following results are obtained:

$$\mathbf{Uq} = (U \cos \alpha_u)\mathbf{i} + (U \sin \alpha_u)\mathbf{j} \qquad (A.19)$$

$$\mathbf{Iq} = (I \cos \beta_i.\cos \alpha_i)\mathbf{i} + (I \cos \beta_i.\sin \alpha_i)\mathbf{j} + (I \sin \beta_i)\mathbf{k} \qquad (A.20)$$

$$\mathbf{Sq} = UI \cos \beta_i.\cos \alpha_i + UI \sin \beta_i\mathbf{j} - UI \cos \beta_i.\sin \alpha_i\mathbf{k} \qquad (A.21)$$

When the power in these two examples are calculated from basic principles the following results are obtained:

Example 1: $P = UI \cos \alpha_i$ and $Q = UI \sin \alpha_i$; (A.22)

which correspond with the real part and **k**-th component of the quaternion power shown in eq. (A.17) respectively.

Example 2: $P = \sqrt{8}/\pi.UI \cos \alpha_i$; $Q = \sqrt{8}/\pi.UI \sin \alpha_i$ and $D = \sqrt{[1-8/\pi^2]}.UI$; (A.23)

which correspond with the real part, **k**-th component and **j**-th component of the quaternion power shown in eq. (A.21) respectively. ($\cos \beta_i = \sqrt{8}/\pi$)

The signs in the quaternion power give information of the direction of the power flow. Active power is dissipated in the load and the load forms a conductance, therefore the positive signs. This formulation of the power components corresponds furthermore with the results from the cross-correlation calculation in chapter 3. This approach seems to have good prospects in the quest for a good mathematical representation of orthogonal power components in any generalized energy system, which can be used as powerful analysis and representation tools in power flow studies.

A2: MATHEMATICAL ANALYSIS OF AMPLITUDE MODULATED SURFACE ACOUSTIC WAVE (SAW) CORRELATOR

To realize ultra fast correlations on power systems with the aid of SAW devices, it is a fundamental requirement to do amplitude modulation on the voltage and current waveforms, before they are passed through the SAW-correlator. The carrier frequency should be in the range of 100 - 300 MHz to reduce the physical size of the SAW device. The realization of the correlator should be investigated by using two interdigital transducers (IDT) [H19]. Figure A.3 shows a basic SAW filter. The piezoelectric solid in the free surface has the ability to support a mode of mechanical wave propagation, confined to a region of the solid immediately below the free surface.

In the majority of SAW-designs, piezoelectric surfaces like normal quartz crystals or other substrates are used so that mechanical wave motion can simply be attained with the aid of an electric applied signal, shown in fig. A.3. The velocity of SAW propagation is in the range of 1000 - 6000 m/s and is independent of the signal frequency. For quartz crystals the SAW velocity is in the order of 3200 m/s. The metallisation ratio is in the order of 0,5 in most designs, while the bandwidth, of these devices is inversely proportional to the number of comb fingers. The efficiency of the mechanical to electrical coupling is given by the electro-mechanical coupling constant, which is a property of the piezoelectrical substrate incorporated in the design.

Some of the major disadvantages of SAW-devices is the temperature sensitivity and large dimensions at low frequency applications. A temperature change causes a SAW-plane velocity change and a thermal expansion of critical physical dimensions. This can, however, be compensated for by means of frequency adaption. A 1 MHz signal frequency SAW-device, used as a simple delay line, incorporating a quartz substrate, has a mechanical wavelength of 3 mm, so that the total structure can be of the order of 30 cm or longer. This is the basic limitation which has to be overcome in power signal processing.

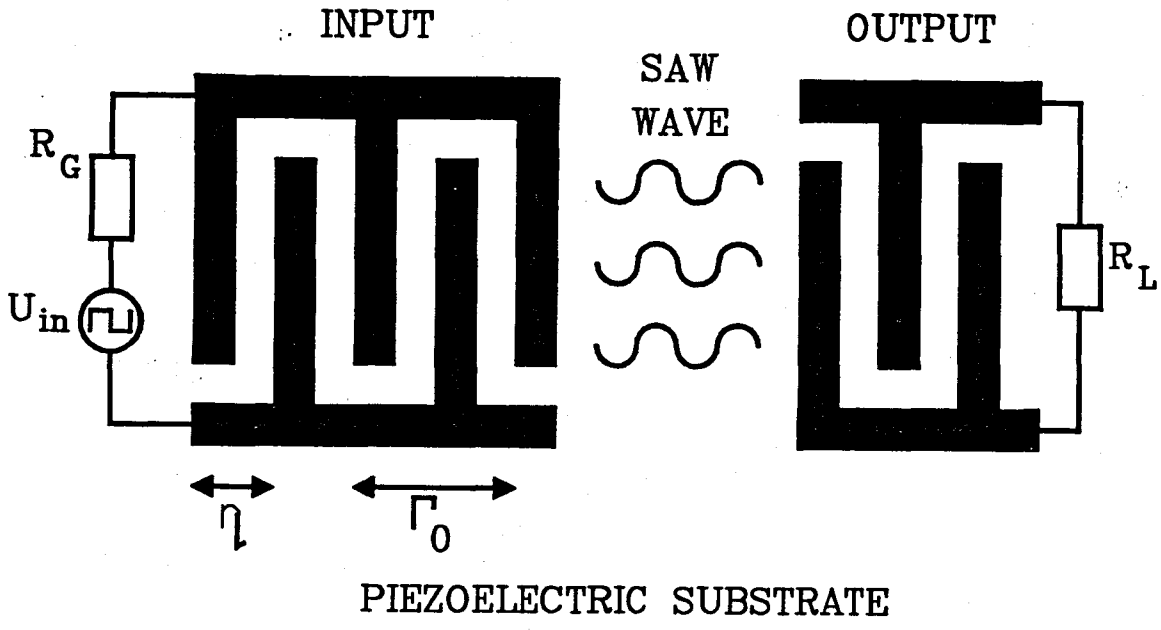

Fig. A.3: Basic Surface Acoustic Wave Structure in Signal Processing Applications.

However, if a carrier wave of between 100 and 300 MHz is superimposed onto the original current and voltage signals, a power correlator can be realized using acoustic wave technology. The basic advantage over digital techniques is that a correlator can be realized 100 times faster than the fastest digital processor correlator, operating at about 20 microseconds to do a full correlation, appose to 0.5 - 2 ms for digital processors.

The AM technique is illustrated below for two basic sinusoidals, describing the voltage and current waveforms. These two signals are displaced by θ degrees. Firstly the cross-correlation is calculated without the carrier frequency modulated onto the basic voltage and current waveforms. Secondly the cross-correlation is performed with the modulated carrier frequency. The correlated result should be the same for both, after the signal is passed through a low-pass filter. The final proposed correlator, based on an interdigital convolver is shown in chapter 4.

A2.1 Unmodulated Cross-correlation of Signals

The original voltage and current waveforms are shown in Eq. (A.24), with amplitudes $\hat{U}$ and $\hat{I}$ and θ the phase shift between these two quantities.

$$u(t) = \hat{U} \sin wt$$
$$i(t) = \hat{I} \sin (wt + \theta); \quad w = 2\pi/T \tag{A.24}$$

$$R_{ui}(\tau) = \frac{1}{T} \int_{-T/2}^{+T/2} u(t).i(t-\tau).dt \tag{A.25}$$

with R_{ui} the cross-correlation between u(t) and i(t).

$$= \frac{1}{T} \int_{-T/2}^{+T/2} \hat{U} \sin wt.\ \hat{I} \sin (wt+\theta-\tau).dt$$

$$= \frac{\hat{U}\hat{I}}{T} \int_{-T/2}^{+T/2} \sin wt.[\sin wt.\cos (\theta-\tau) + \cos wt.\sin (\theta-\tau)].dt$$

$$= \frac{\hat{U}\hat{I}}{T} \left[\int_{-T/2}^{+T/2} \sin^2 wt.\cos (\theta-\tau).dt \right.$$

$$\left. + \int_{-T/2}^{+T/2} \sin wt.\cos wt.\sin (\theta-\tau).dt \right]$$

$$= \frac{\hat{U}\hat{I}}{T} \left[\cos (\theta-\tau).(t/2 - \frac{1}{4w} \sin 2wt) \right.$$

$$\left. + \sin (\theta-\tau).(\frac{1}{2w} \sin^2 wt) \right]_{-T/2}^{+T/2}$$

$$R_{ui}(\tau) = \frac{\hat{U}\hat{I}}{T} \left[T/2 \cos (\theta-\tau)\right]$$

$$R_{ui}(\tau) = \tfrac{1}{2}\ \hat{U}\hat{I} \cos (\theta-\tau) = U.I \cos (\theta-\tau) \tag{A.26}$$

which represents mathematically the cross-correlation function R_{ui}.

$$R_{ui}(0) = U.I \cos\theta \equiv P \qquad (A.27)$$

which corresponds to active power in the two waveforms.

A2.2 Amplitude Modulated Cross-correlation.

For the second manipulation the voltage and current waveforms are modulated with a high frequency carrier, $\cos w_c t$.

$$u(t) = \hat{U} \cos w_c t.\sin wt \qquad (A.28)$$
$$i(t) = \hat{I} \cos w_c t.\sin (wt+\theta);\ w = 2\pi/T \qquad (A.29)$$

with w_c the carrier frequency
$w_c >> w$

$$R^*_{ui}(\tau) = \frac{1}{T}\int_{-T/2}^{+T/2} u(t).i(t-\tau).dt$$

$$R^*_{ui}(\tau) = \frac{1}{T}\int_{-T/2}^{+T/2} [\hat{U} \sin wt.\hat{I} \sin (wt-\tau+\theta).\cos^2 w_c t].dt$$

$$= \frac{\hat{U}\hat{I}}{T}\int_{-T/2}^{+T/2} \sin wt.[\sin wt.\cos(\theta-\tau) + \cos wt.\sin(\theta-\tau)].\cos^2 w_c t.dt$$

$$= \frac{\hat{U}\hat{I}}{T}\left[\int_{-T/2}^{+T/2} [\sin^2 wt.\cos^2 w_c t.\cos(\theta-\tau)].dt + \int_{-T/2}^{+T/2} [\sin wt.\cos wt.\cos^2 w_c t.\sin(\theta-\tau)].dt\right]$$

$$R^*_{ui}(\tau) = \frac{\hat{U}\hat{I}}{T}\left[\cos(\theta-\tau)\int_{-T/2}^{+T/2} [\sin^2 wt.\cos^2 w_c t].dt\right.$$

$$+ \sin(\theta-\tau) \int_{-T/2}^{+T/2} [\sin wt.\cos wt.\cos^2 w_c t].dt \Big]$$

$$= \frac{\hat{U}\hat{I}}{T} \Big[\cos(\theta-\tau) \int_{-T/2}^{+T/2} \tfrac{1}{4}.(1 - \cos 2wt).(1 + \cos 2w_c t).dt$$

$$+ \sin(\theta-\tau) \int_{-T/2}^{+T/2} \tfrac{1}{2}.\sin wt.\cos wt.(1 + \cos 2w_c t).dt \Big]$$

$$= \frac{\hat{U}\hat{I}}{T} \Big[\tfrac{1}{4}.\cos(\theta-\tau) \int_{-T/2}^{+T/2} [1 + \cos 2w_c t - \cos 2wt$$

$$- \cos 2wt.\cos 2w_c t].dt$$

$$+ \tfrac{1}{2}.\sin(\theta-\tau) \int_{-T/2}^{+T/2} \tfrac{1}{2}.[\sin 2wt - \sin 2wt.\cos 2w_c t].dt \Big]$$

$$= \frac{\hat{U}\hat{I}}{T} \Bigg[\tfrac{1}{4}.\cos(\theta-\tau) \Big[t + \frac{1}{2w_c}.\sin 2w_c t - \frac{1}{2w}.\sin 2wt$$

$$- \frac{1}{4(w-w_c)}.\sin 2(w-w_c)t - \frac{1}{4(w-w_c)}.\sin 2(w+w_c)t \Big]$$

$$+ \tfrac{1}{4}.\sin(\theta-\tau) \Big[- \frac{1}{2w}.\cos 2wt + \frac{1}{4(w-w_c)}.\cos 2(w-w_c)t$$

$$+ \frac{1}{4(w+w_c)}.\cos 2(w+w_c)t \Big] \Bigg]_{-T/2}^{+T/2}$$

$$R^*_{ui}(\tau) = \frac{\hat{U}\hat{I}}{T} \Big[\frac{T}{4}.\cos(\theta-\tau) \Big]$$

$$\Rightarrow R^*_{ui}(\tau) = \frac{\hat{U}\hat{I}}{4}.\cos(\theta-\tau)$$

$$= \tfrac{1}{2}.U.I \cos(\theta-\tau) \qquad (A.30)$$

which is proportional to eq. (A.27) with a constant 1/2. If the same manipulation is repeated for other waveforms of current and voltage, the same proportional constant is obtained.

In general it can be accepted that the modulated signals give a proportionally correlated output to the unmodulated cross-correlation of the signals.

A3: MATHEMATICAL ANALYSIS OF A DIODE-RESISTANCE CIRCUIT IN A TYPICAL SINUSOIDAL NETWORK

In this section a simple diode-resistance combination, fed from a sinusoidal voltage source, is analysed with different methods. The analysis is performed in both the frequency and time domain for comparison purposes. This analysis is also done using the proposed time domain correlation based definition. All the results can then be compared to show the validity of the different definitions. Figure A.4 shows the basic schematic diagram of a voltage source u(t), which feeds a diode and a pure resistance combination.

The current waveform i(t) is shown in figure A.4(b). This current waveform is orthogonally divided into two components $i_a(t)$ and $i_f(t)$ respectively, shown in figure A.4(c). The active current $i_a(t)$ has the same waveshape as the voltage u(t), while the $i_f(t)$ component is orthogonal and is calculated from instantaneous values of i(t) and $i_f(t)$. With the proposed definition of power, the different currents are defined in terms of the equivalent conductance, susceptance and disceptance network parameters. The power components are defined in terms of the cross-correlation, between voltage and current (chap. 3).

The different definitions described in chapter 1 and the proposed definition, derived in chapter 3, will be evaluated for this schematic diagram. The voltage and current waveforms and calculated power components are shown in eq. (A.31). It is clear that there is no reactive power present in this circuit because there

is not a passive reactive element, neither is there phase control incorporated in the circuit, resulting in no time shift and thus no equivalent susceptance.

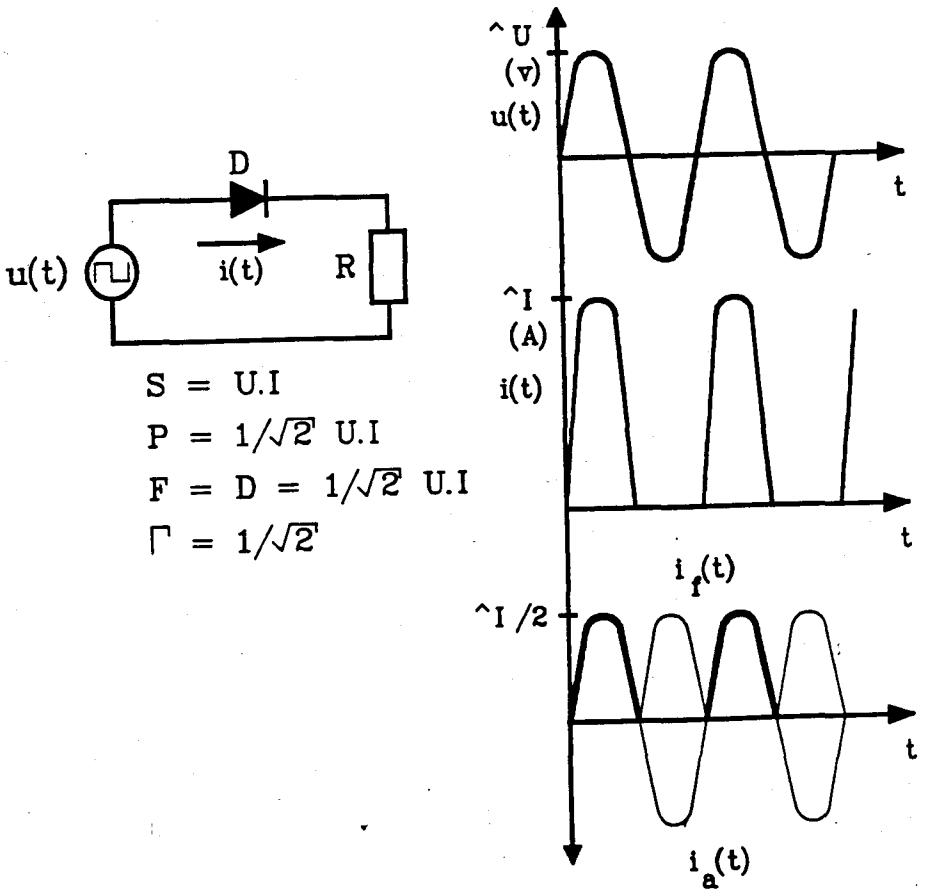

Fig. A.4: Analysis of a Diode-resistance Network.

$$
\begin{aligned}
&u(t) = \hat{U}.\sin\,(2\pi/T)t \\
&i(t) = \hat{I}.\sin\,(2\pi/T)t \quad \text{for } 0 < t \leq T/2 \\
&\quad\;\; = 0 \qquad\qquad\qquad\;\; \text{for } -T/2 < t \leq 0 \\
&i(t) = i_a(t) + i_f(t) \\
&i(t) = i_a(t) + i_r(t) + i_d(t) \\
&S = U.I; \qquad P = 1/\sqrt{2}\ U.I; \qquad F = 1/\sqrt{2}\ U.I; \\
&Q = 0; \qquad\;\; D = 1/\sqrt{2}\ U.I
\end{aligned}
\tag{A.31}
$$

A3.1 Calculation of Power Components from Basic Principles

From basic principles power components are calculated. Effective values U, and I are derived:

$$U = \hat{U}/\sqrt{2} \tag{A.32}$$

$$I^2 = \frac{1}{T}\int_{-T/2}^{+T/2} i^2(t).dt = \frac{\hat{I}^2}{T}\int_{0}^{+T/2} \sin^2 (2\pi/T)t.dt$$

$$I = \tfrac{1}{2}\hat{I} \tag{A.33}$$

$$P = \frac{1}{T}\int_{0}^{+T/2} u(t).i(t).dt$$

$$P = \frac{1}{T}\int_{0}^{+T/2} \hat{I}\hat{U} \sin (2\pi/T)t.\sin (2\pi/T)t.dt$$

$$P = \frac{\hat{U}\hat{I}}{T}\left[t/2 - T/8\pi \sin (4\pi/T)t \right]_{0}^{+T/2}$$

$$P = \frac{\hat{U}\hat{I}}{4} = 1/\sqrt{2}\ U.I \tag{A.34}$$

The loading power S, is calculated from effective values.

$$S = U.I \tag{A.35}$$

The fictitious power F, is calculated from the vector difference:

$$F = (S^2 - P^2)^{1/2}$$

$$F = 1/\sqrt{2}\ U.I \tag{A.36}$$

From Eq. (A.34) and (A.35) the power factor Γ, is derived as $1/\sqrt{2}$. The diode without phase angle control excludes the possibility of reactive power. As defined in chapter 3, the

total fictitious power is deactive power and the reactive power should be zero in this example.

A3.2 Calculation of Power Components from Correlation Techniques

This section uses the definition described in chapter 3. The cross-correlation is defined in eq. (A.37).

$$R_{ui}(\tau) = \frac{1}{T}\int_{-T/2}^{+T/2} u(t).i(t-\tau).dt \qquad (A.37)$$

$$R_{ui}(\tau) = \frac{\hat{U}\hat{I}}{T}\left[\int_{0}^{+T/2} \sin(2\pi/T)t.[\sin(2\pi/T)t.\cos\tau - \cos(2\pi/T)t.\sin\tau].dt\right]$$

$$R_{ui}(\tau) = \frac{\hat{U}\hat{I}}{T}\left[\cos\tau.[t/2 - T/8\pi \sin(4\pi/T)t] - \sin\tau.[T/4\pi \sin^2(2\pi/T)t]\right]_0^{+T/2}$$

$$= \frac{\hat{U}\hat{I}}{T}\left[\cos\tau.[T/4 - T/8\pi \sin 2\pi] - T/4\pi \sin\tau.\sin^2\pi\right]$$

$$= \frac{\hat{U}\hat{I}}{4}\cos\tau$$

$$R_{ui}(\tau) = 1/\sqrt{2}\ U.I\cos\tau \qquad (A.38)$$

$$\Rightarrow\ R_{ui}(0) = P = 1/\sqrt{2}\ U.I \qquad (A.39)$$

which corresponds with eq. (A.31).

$$S = \left[R_{uu}(0)\right]^{\frac{1}{2}}.\left[R_{ii}(0)\right]^{\frac{1}{2}} \qquad (A.40)$$

$$R_{uu}(\tau) = \frac{1}{T}\int_{-T/2}^{+T/2} u(t).u(t-\tau).dt$$

$$R_{ii}(\tau) = \frac{1}{2}\int_{-T/2}^{+T/2} i(t).i(t-\tau).dt$$

$$\Rightarrow \quad S = \left[\frac{1}{T}\int_{-T/2}^{+T/2} u^2(t).dt\right]^{\frac{1}{2}}.\left[\frac{1}{T}\int_{-T/2}^{+T/2} i^2(t).dt\right]^{\frac{1}{2}}$$

$$S = U.I \tag{A.41}$$

The fictitious power is calculated from the orthogonality principle in eq. (A.42):

$$F = \sqrt{[S^2 - P^2]} = 1/\sqrt{2}\ U.I \tag{A.42}$$

which gives the same result as eq. (A.42). The subdivision of the fictitious power into reactive and deactive power, is also obtained from the cross-correlation. By calculating the maximum value of the cross-correlation, shown in eq. (A.38), the following results:

$$\hat{R}_{ui}(\tau) = \max[1/\sqrt{2}\ U.I \cos\tau]$$
$$\Rightarrow \quad \text{where} \quad \cos\tau = 1$$
$$\text{with } \tau = 0° \tag{A.43}$$

This implies that $R_{ui}(0) = \hat{R}_{ui}(\tau)$.

Using the proposed way of calculation (chapter 3), implies:

$$Q = [\hat{R}^2_{ui}(\tau) - R^2_{ui}(0)]^{1/2}$$
$$\Rightarrow Q = 0 \tag{A.44}$$

Therefore deactive power

$$D = [S^2 - P^2 - Q^2]^{1/2}$$

$$= [U^2.I^2 - \tfrac{1}{2}U^2.I^2 - 0]^{1/2}$$

$$\Rightarrow \quad D = 1/\sqrt{2}\ U.I \tag{A.45}$$

In this circuit there is no reactive power Q, only deactive power D. The fundamental and residual reactive power is also zero.

The different current waveforms are defined in terms of the equivalent network parameters G, B, K and instantaneous values of u(t) and $R_{ui}(\tau)$. Instantaneous active current is defined in terms of conductance G, and instantaneous voltage u(t).

$$i_a(t) = G.u(t) \tag{A.46}$$

Instantaneous fictitious current is shown as the difference between $i_a(t)$ and i(t).

$$i_f(t) = i(t) - i_a(t) \tag{A.47}$$

The second orthogonal division relates to the reactive and deactive currents. Deactive current $i_d(t)$ is defined in terms of the cross-correlation time shift at maximum correlation $\hat{\tau}$.

$$i_d(t) = i(t) - \sqrt{[G^2 + B^2]}.u(t-\hat{\tau}) \tag{A.48}$$

The reactive current is then the difference between fictitious current and deactive current.

$$i_r(t) = i_f(t) - i_d(t) \tag{A.49}$$

For the diode-resistance case, this resolves to

$$\begin{aligned} G = P/U^2 &= R_{ui}(0)/R_{uu}(0) \\ &= (1/\sqrt{2}\ U.I)/U^2 \\ &= I/(\sqrt{2}\ U) \end{aligned} \tag{A.50}$$

$$\Rightarrow \quad i_a = I/(\sqrt{2}\ U).u(t) \tag{A.51}$$

$$B = Q/U^2 = 0; \qquad \hat{\tau} = 0$$

$$\Rightarrow \quad i_d = i(t) - I/(\sqrt{2}\,U).u(t) \tag{A.52}$$

$$\Rightarrow \quad i_r = i(t) - I/(\sqrt{2}\,U).u(t) - [i(t) - I/(\sqrt{2}\,U).u(t)]$$
$$= 0 \tag{A.53}$$

These instantaneous values are shown in figure A.3.

A3.3 Calculation of Power Components from Orthogonal Current Division According to Nowomiejski

The two components are divided into $i_a(t)$ and $i_f(t)$, which are shown in figure A.4(c) [A60,61].

$$i_a(t) = G.u(t); \qquad i_f(t) = i(t) - i_a(t) \tag{A.54}$$

$$S = I.U; \quad P = I_a.U; \quad F = I_f.U \tag{A.55}$$

Filipski [A61] used these orthogonal divided current components and a Hilbert transform [H15] to derive the decomposed current components and calculate the power components, as defined by Nowomiejski [A109].

$$\overline{i_a.i_f} = 0 \qquad \text{with } i_a + i_f = i \tag{A.56}$$

$$\overline{i_a.(i-i_a)} = 0$$

$$\overline{G.u(t).[i(t) - G\,u(t)]} = 0$$

$$\overline{G.u(t).i(t)} = \overline{G^2.u^2(t)}$$

$$\overline{u(t).i(t)} = G.U^2 = \frac{1}{T}\int_{-T/2}^{+T/2} u(t).i(t).dt$$

$$\Rightarrow \quad P = G.U^2 \tag{A.57}$$

and from Nowomiejski

$$Q = \overline{u(t).H\{i\}} = -\overline{i(t).H\{u(t)\}} \tag{A.58}$$

The active and fictitious currents are shown below for the diode-resistance case:

$$i_a(t) = G.u(t) \qquad = P/U^2.u(t) \tag{A.59}$$

$$i_f(t) = i(t) - i_a(t) \tag{A.60}$$

$$I_a^2 = \frac{1}{T}\int_{-T/2}^{+T/2} i_a^2(t).dt \qquad = \frac{\hat{I}^2}{4T}\int_{-T/2}^{+T/2} \sin^2 (2\pi/T)t.dt$$

$$I_a = 1/\sqrt{2}.I \tag{A.61}$$

$$\Rightarrow \quad P = U.I_a = 1/\sqrt{2}\ U.I \tag{A.62}$$

which is again equivalent to eq. (A.34). Loading and active power, S and F can again be derived as shown in eq. (A.35) and (A.36). Calculation of the reactive power according to Filipski [A61] and Nowomiejski [A109] implies the calculation of the Hilbert transform (appendix A4):

$$H\{u\} = \frac{1}{\pi}\int_{-\infty}^{+\infty} \frac{u(\tau).d\tau}{\tau - t} \tag{A.63}$$

$$= \frac{\hat{U}}{\pi}\int_{-\infty}^{+\infty} \frac{\sin (2\pi/T)\tau.d\tau}{\tau - t}$$

The voltage is a sinusoidal which implies that H{u} is also a sinusoidal but shifted by 90° [H15].

$$H\{u\} = \hat{U} \cos (2\pi/T)t \tag{A.64}$$

$$Q = \overline{u(t).H\{u\}} = 0 \quad \text{and} \quad D = F \tag{A.65}$$

equivalent to the result obtained from the proposed definition. This is the result of the fact that the generating function, the voltage signal, is assumed to be sinusoidal. When the generating function is non-sinusoidal, as shown in chapter 3, the different time domain definitions does not give the same results.

A3.4 Frequency Domain Analysis of Diode-resistance Circuit

In performing the frequency transform on the voltages and currents, valuable information concerning the harmonic power can be obtained, if the limitations of the frequency transform is taken into account (chapter 1). Furthermore it is proposed to use power cross-spectral densities to calculate harmonic power components from the cross-correlation function, described in paragraph 3.11. The frequency transform is performed on the diode-resistance network. The basic assumption holds that the signals must be periodic. This implies the following:

$$\begin{aligned} i(t+T) &= i(t) \\ u(t+T) &= u(t) \end{aligned} \qquad \text{(A.66)}$$

For periodic signals the Fourier series has physical meaning and can be expressed for the voltage and current signals as follows:

$$\begin{aligned} u(t) &= \hat{U} \sin wt \\ i(t) &= \hat{I} \sin wt \qquad 0 < wt < \pi \\ i(t) &= 0 \qquad\qquad\quad \pi < wt < 2\pi \end{aligned}$$

$$i(t) = a_0 + \sum_{n=1}^{\infty} \left[a_k.\cos\,(2\pi n/T)t + b_k.\sin\,(2\pi n/T)t \right] \qquad \text{(A.67)}$$

which constitutes a frequency domain representation of the periodic current waveform. In eq. (A.67) a_0 represent the average value of i(t), whilst a_k and b_k, the coefficients of the series, are rectangular components of the k-th harmonic. The corresponding k-th harmonic vector is

$$A_k = a_k + jb_k \qquad \text{(A.68)}$$

$$A_k.\arg(\theta_k) = a_k + jb_k$$

with $A_k = \sqrt{[a_k^2 + b_k^2]}$ and $\theta_k = \tan^{-1}(b_k/a_k)$

The components a_0, a_k and b_k can be derived from the periodic signals using eq.(A.69).

$$a_0 = \frac{1}{2\pi} \int_{-\pi}^{+\pi} x(wt).d(wt)$$

$$a_k = \frac{1}{\pi} \int_{-\pi}^{+\pi} x(wt).\cos(nwt).d(wt)$$

$$b_k = \frac{1}{\pi} \int_{-\pi}^{+\pi} x(wt).\sin(nwt).d(wt) \qquad \text{(A.69)}$$

The Fourier analysis of the diode-resistance combination gives the following results:

$$a_0 = \frac{1}{2\pi} \int_{0}^{+\pi} \hat{I} \sin wt.d(wt) = \frac{\hat{I}}{2\pi} \int_{0}^{+T/2} \sin(2\pi/T)t.dt$$

$$a_0 = \hat{I}/\pi \qquad \text{(A.70)}$$

$$a_1 = \frac{\hat{I}}{T\pi} \int_{0}^{+T/2} \sin(2\pi/T)t.\cos(2\pi/T)t.dt$$

$$= \hat{I}/2\pi \sin^2 \pi = 0 \qquad \text{(A.71)}$$

$$b_1 = \frac{\hat{I}}{T\pi} \int_{0}^{+T/2} \sin^2(2\pi/T).dt = \hat{I}/2 \qquad \text{(A.72)}$$

$$\Rightarrow \quad \hat{I}_1 = \hat{I}/2 \text{ and } \phi_1 = \tan^{-1}(\infty) = 90°$$

The corresponding first harmonic is shown in effective values:

$$I_1 = \hat{I}/(2.\sqrt{2}) \arg(90°) \qquad \text{(A.73)}$$

The voltage is a sinusoidal; from the coefficients result:

$$U = U \arg(\theta) = \hat{U}/\sqrt{2} \arg(90°)$$

There is no fundamental time shift, which implies that there is not Budeanu reactive power present, this result corresponds to all the other definitions, again because the voltage is a simple sinusoidal waveform. The calculations of the power components are shown below:

$$P = U_1.I_1 \cos \phi_1$$

$$= \frac{\hat{U}}{\sqrt{2}} \cdot \frac{\hat{I}}{2\sqrt{2}} = 1/\sqrt{2}\ U.I \qquad (A.74)$$

$$Q_B = U_1.I_1 \sin \phi_1 = 0; \qquad (A.75)$$

$$D_B = \sqrt{[S^2 - P^2 - Q_B^2]} = 1/\sqrt{2}\ U.I \qquad (A.76)$$

$$S = U.I \qquad (A.77)$$

This implies that the total amount of fictitious power F, is described by the Budeanu distortion power D_B and no Budeanu reactive power result Q_B. All the definitions seem to give consistent results for periodic, sinusoidal voltage waveforms, under steady state loading conditions. When the waveform of voltage is non-sinusoidal and the load are changing dynamically, total different results are obtained.

Using the power cross-spectral density $S_{ui}(f)$, frequency domain analysis can be performed using the proposed correlation definition as described in chapter 3. By implementing the magnitude and phase frequency transform on the cross-correlation function R_{ui}, the different correlated power components, active power and reactive power, can be decomposed in terms of their harmonic components. Deactive power is, however, uncorrelated which implies that it cannot decompose in different harmonic components. The power cross-spectral density function is shown in eq. (A.78):

$$S_{ui}(f) = \int_{-\infty}^{+\infty} R_{ui}(\tau).e^{-j2\pi f\tau}.d\tau \qquad (A.78)$$

The k-th correlated harmonic power component can be derived from the power cross-spectral density, as shown in eq. (3.43) and (3.44) chapter 3. In the diode-resistance circuit the cross-correlation function is shown in fig. 3.16(a), which is a sinusoidal with $\hat{\tau} = 0$ (fig. 3.16(a)). This implies that there is only fundamental correlated power components, furthermore $\hat{\tau}$ is zero which implies the following:

$$P_1 = |S_{ui}(1)| \cos 0 = R_{ui}(0) = 1/\sqrt{2}\ U.I \qquad (A.79)$$

$$Q_1 = |S_{ui}(1)| \sin 0 = 0 \qquad (A.80)$$

which correspond to the results obtained above

A4: MATHEMATICAL INTERPRETATION OF AUTOCORRELATION, CROSS-CORRELATION, POWER CROSS-SPECTRAL DENSITY AND THE HILBERT TRANSFORM, IN THE CALCULATION OF ELECTRIC POWER COMPONENTS

To get a better physical interpretation of the auto- and cross-correlation in the time domain, it can be shown that the autocorrelation in the time domain is equivalent to a multiplication of the signal by itself in the frequency domain. On the other hand the cross-correlation in the time domain is equivalent to multiplication of the two signals in the frequency domain, which forms the basis of any effective and average value measurement. The cross-spectral density can be interpreted as the decomposition of the cross-correlation function in the frequency domain. The Hilbert transform is interpreted in the frequency domain as a rotation of the signal by 90° over an infinite bandwidth, without any change in the effective value of the argument signal.

A4.1 Correlation of Power Signals

The definition of power components in voltage and current signals with a random nature is of interest. Chapter 3 showed the possibility of using correlation techniques in the measurement and analysis of these power components. In cases where the signals of voltage and current are of a random nature the instantaneous power function p(t) may be either a continuous or discontinuous signal. The first case is known as an infinite energy signal while the second is normally characterized as a finite energy signal. Normally in power systems a continuous instantaneous power signal is used to transfer energy from the source to the load. Thus the energy is infinite, hence the integrals

$$\int_{-\infty}^{+\infty} u(t).e^{jwt}.dt \approx \infty; \qquad \int_{-\infty}^{+\infty} i(t).e^{jwt}.dt \approx \infty \qquad \text{(A.81)}$$

do not converge and therefore the Fourier transform of u(t) or i(t) is meaningless [H15]. However, the time averages of the signal u(t) and i(t) do exist and therefore the averaging functions in the sense of the autocorrelation of u(t) and i(t) and the cross-correlation between u(t) and i(t) are meaningful [H15].

$$R_{uu}(\tau) = \lim_{dT\to\infty} \frac{1}{2dT} \int_{-dT}^{+dT} u(t).u(\tau+t).dt \qquad \text{(A.82)}$$

$$R_{ii}(\tau) = \lim_{dT\to\infty} \frac{1}{2dT} \int_{-dT}^{+dT} i(t).i(\tau+t).dt \qquad \text{(A.83)}$$

$$R_{ui}(\tau) = \lim_{dT\to\infty} \frac{1}{2dT} \int_{-dT}^{+dT} u(t).i(\tau+t).dt \qquad \text{(A.84)}$$

where R_{uu} and R_{ii} are the voltage and current autocorrelations respectively, R_{ui} the cross-correlation between

voltage and current, τ the time shift correlation variable and dT the integration limit.

Using equations (A.82-84) the following conditions are of interest:

$$\tau = 0 \Rightarrow \quad R_{uu}(0) = \overline{u^2(t)} \equiv U^2 \tag{A.85}$$

$$R_{ii}(0) = \overline{i^2(t)} \equiv I^2 \tag{A.86}$$

$$R_{ui}(0) = \overline{u(t).i(t)} \equiv P \tag{A.87}$$

$\hat{R}_{ui}(\tau) \equiv$ the point on the cross-correlation function where the two signals u(t) and i(t) have maximum correlation.

The Cauchy-Schwarz inequality for integrals results in:

$$R_{ui}(0) \leq \hat{R}_{ui}(\tau) \tag{A.88}$$

These correlation functions do not have to be defined from minus infinity to plus infinity if the average values are only of interest over a specific time interval dT, with eq. (A.82-84) simplifying to the following:

$$R_{uu}(\tau) = \frac{1}{dT} \int_{t-dT}^{t} u(t).u(t-\tau).dt \tag{A.89}$$

$$R_{ii}(\tau) = \frac{1}{dT} \int_{t-dT}^{t} i(t).i(t-\tau).dt \tag{A.90}$$

$$R_{ui}(\tau) = \frac{1}{dT} \int_{t-dT}^{t} u(t).i(t-\tau).dt \tag{A.91}$$

These integrals can be calculated at any instant t, over the past time interval dT. In general t can be ignored and the correlations is thus a function of the time interval dT at any time instant t. A frequency domain interpretation of

correlation functions is of interest when the voltage and current signals are transformable into the frequency domain. The correlation in the time domain is equivalent to multiplication in the frequency domain [H15]. This implies that the frequency transform of the cross-correlation, results in the power cross-spectral density. This phenomena can be used to calculate power components over the total bandwidth of the measurement equipment in the frequency domain. The power cross-spectral density is shown in eq. (A.92) [H15]:

$$S_{ui}(f) = \int_{-\infty}^{+\infty} R_{ui}(\tau).e^{-j2\pi f\tau}.d\tau \qquad (A.92)$$

The zero-value of the power cross-spectral density function $S_{ui}(0)$ represent the DC active power component, while the correlated power k-th harmonic component can be derived from the power cross-spectral density as shown in eq. (A.93) and (A.94). The k-th active power harmonic component expressed as P_k and the k-th reactive power harmonic component expressed as Q_k.

$$P_k = |S_{ui}(k)| \cos \phi_k \qquad (A.93)$$

$$Q_k = |S_{ui}(k)| \sin \phi_k \qquad (A.94)$$

where $|S_{ui}(k)|$ is the magnitude of the k-th power cross-spectral point and ϕ_k the phase shift associated with the k-th power cross-spectral point.

Normally these correlation functions are implemented with a digital computer, therefore the correlations should be expressed in terms of their digital equivalents [H2,20].

$$R_{ui}[j] = 1/N \sum_{k=0}^{N-1} U[k].I[k-j] \qquad (A.95)$$

$$R_{uu}[j] = 1/N \sum_{k=0}^{N-1} U[k].U[k-j] \qquad (A.96)$$

$$R_{ii}[j] = 1/N \sum_{k=0}^{N-1} I[k].I[k-j] \qquad (A.97)$$

$j = -N+1 \ldots N-1$

where U[k] and I[k] are the N-sampled arrays of the voltage and current signals respectively.

A4.2 Hilbert Transform Utilized as an Orthogonal Transform by Nowomiejski and Filipski

The Hilbert transform is used by Nowomiejski [A109] to derive the reactive power Q_N, while Filipski [A61] developed a current measuring apparatus utilizing this Hilbert transform. A method to separate signals based on the 90 degrees phase selectivity, can be performed by means of this Hilbert transform [H2,15,20]. Consider a voltage signal u(t), the Hilbert transform of this voltage signal is shown in eq. (A.98).

$$H\{u(t)\} = PV \frac{1}{\pi} \int_{-\infty}^{+\infty} \frac{u(\tau).d\tau}{t - \tau} \qquad (A.98)$$

where PV is the Cauchy's principle value resulting at the discontinues point $\tau = t$. This value is chosen unity for notational simplicity [H2,15]. The Hilbert transform of u(t) is a linear operation. Thus the inverse Hilbert transform results in the original signal u(t).

It can be noted that the Hilbert transform of the voltage H{u(t)} may be interpreted as the convolution of u(t) with the time function $1/(\pi t)$ [H15, A109]. The frequency transform of $1/(\pi t)$ is equal to $-j$ sgn (f), where sgn (f) is the signum function defined in eq. (A.99):

$$sgn(f) = \begin{cases} 1, & f > 0 \\ 0, & f = 0 \\ -1, & f < 0 \end{cases} \qquad (A.99)$$

Equation (A.99) states that the Hilbert transform can be obtained by passing the signal u(t) through a linear two-port device with transfer function equal to -j.sgn(f) [H15, A20,23,109]. This device may be considered as one that produces a phase shift of -90° for all positive frequencies of the input signal and 90° for all negative frequencies as shown in fig. A.5:

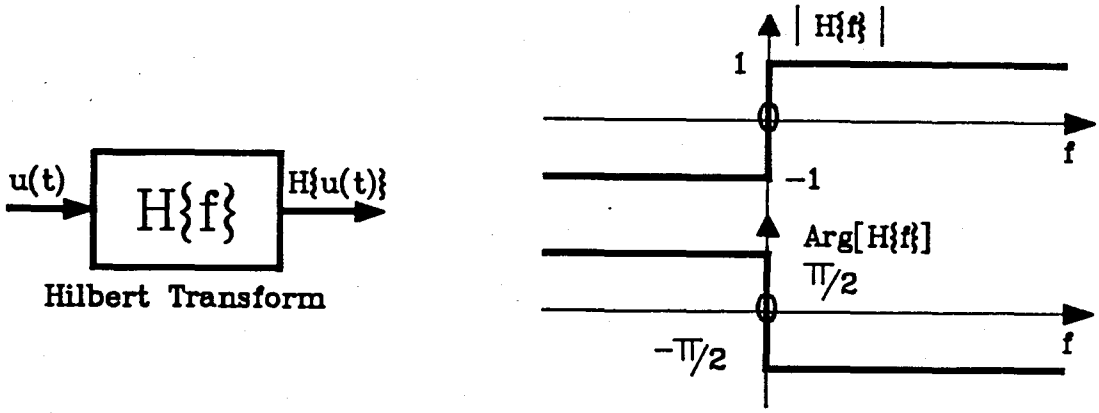

Fig. A.5: Phase and Magnitude Characteristics of the Hilbert Transform

The amplitude of all frequency components in the signal u(t) are, however, unaffected by the Hilbert transformer shown in fig. A.5. The use of this transform is equivalent to a rotation of u(t) by $-\pi/2$ to obtain the Nowomiejski reactive current without any change to the effective value of the voltage. The amplitude of the Nowomiejski reactive current signal is obtained from the equivalent susceptance of the network.

The Hilbert transform can also be expressed in terms of a digital equivalent [H2]:

$$H\{U[j]\} = \frac{2}{\pi} \sum_{k=-\infty}^{\infty} U[j-k].\frac{\sin^2[\pi(k/2)]}{k} \qquad (A.100)$$

A band limited digital Hilbert transform can be realized by means of a FIR (Finite Impulse Response) filter with a quadrature transfer function [H2, A103, D8]. Figure A.6 shows a

realization of a real-time band limited Hilbert transform used to calculate reactive power in the Nowomiejski definition [A109, D8]. The digital Hilbert transform is experimentally investigated by means of digital simulations, using eq. (A.100) and with the tuned analogue Hilbert transform of Filipski [A61]. The results are shown in fig. 3.13(c) and fig. 4.3(a) respectively.

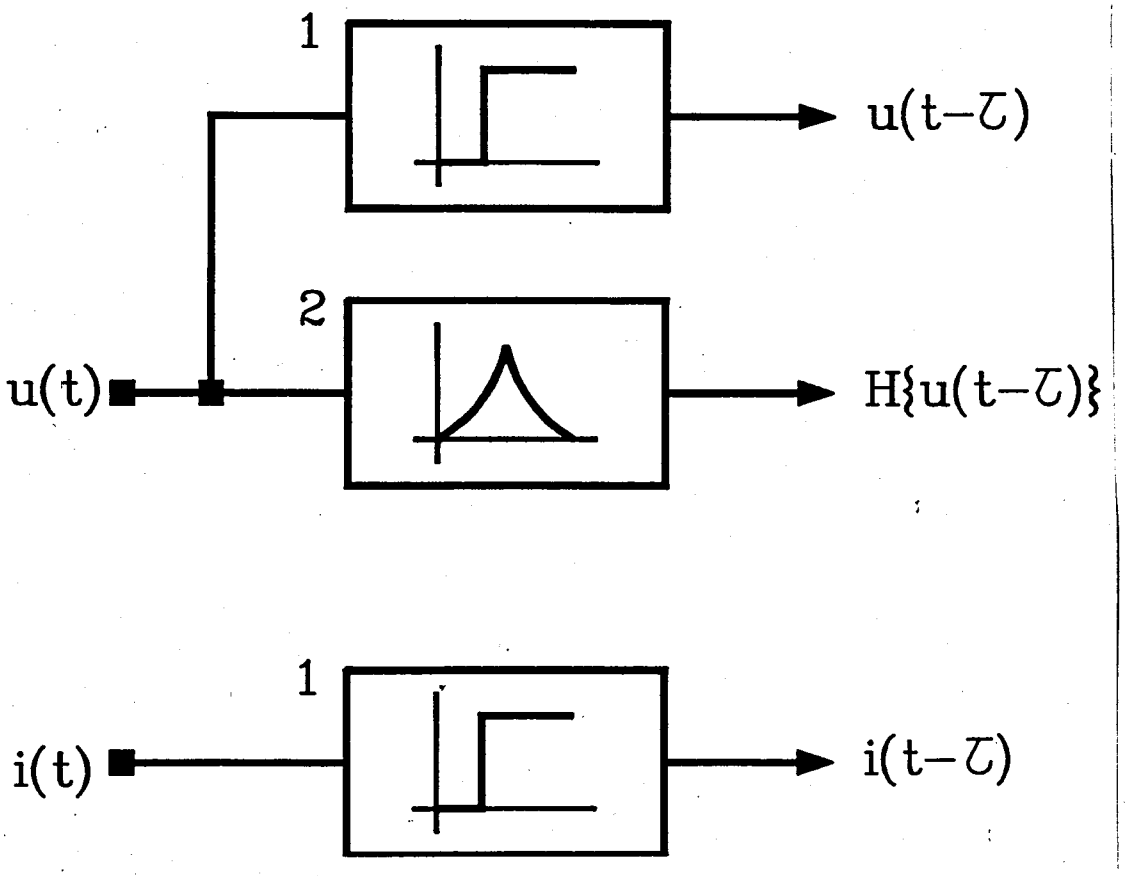

Fig. A.6: Block Diagram Representation of Hilbert Transform used to Calculate Nowomiejski Reactive Power

with 1 the FIR filter realization of the digital Hilbert transform and 2, two dead-time filters corresponding to half of the impulse response time of the FIR filter, necessary to compare the different time functions [D8].

In cases where the voltage waveform is a simple sinusoidal, the Hilbert transform can simply be realized by means of a simple $-\pi/2$ phase shift circuit with transfer function $\exp(sT/4)$, where T is the period of the voltage sinusoidal.

APPENDIX B: TURBO PASCAL III CODED COMPUTER PROGRAMS

B1: TURBO PASCAL PROGRAMS TO SIMULATE THE DIFFERENT POWER WAVEFORMS AND CALCULATE THE DIFFERENT POWER COMPONENTS

This program (POWER) calculates the power components from either simulated or actual measured data. The measured data is obtained from a separate program (TRANSFER) which transfers data from a Tektronix 2430 digital sample oscilloscope via the National Instruments IEEE-488 interface bus. The simulated waveforms are generated with a separate program (INPUT). In continuous operation, a BATCH program is written to combine the different programs in the appropriate structure and obtains the desired results. Results are plotted with the aid of the Turbo Graphics Toolbox. All the global variables are defined in the include program POWERDEF.

PROGRAM POWER

```
(*************************************************)
(* THIS PROGRAM COMPUTES THE DIFFERENT COMPONENTS*)
(*   OF POWER, USING ONLY THE TIME FUNCTIONS OF  *)
(* VOLTAGE AND CURRENT. THIS IS DONE BY MEANS OF *)
(*        A DIGITAL CORRELATION ALGORITHM.       *)
(* DESIGNED BY JHR ENSLIN THROUGH 1986 AND 1987  *)
(*************************************************)
(* Waveforms are either generated by means of a  *)
(*   function generator INPUT or by means of     *)
(*   measured waveforms, through a measurement   *)
(*   system and stored in a data file on disk.   *)
(*************************************************)

Program POWER3(input,output);

{$I POWERDEF.JHE}
{$I kernel.sys}
{$I windows.sys}
{$I findwrld.hgh}
{$I axis.hgh}
{$I polygon.hgh}
{$I INPUT.JHE}
{$U+}
(*****************SUBROETINES*********************)
(*--------------SEEK POWER WINDOW--------------*)

Procedure SeekWindow(Mat:dim);
  {This procedure seeks the appropriate power
   window with a digital filter algorithm}
var
    j,l:integer;
const
    Alpha = 0.9;
begin
    For j:=1 to N-1 do  {Digital Filter}
       Filter[j] := Alpha*Filter[j-1]
                  + (1-Alpha)*Mat[j-1];
    l:=0;
    For j:=0 to 1 do begin
       Repeat l:=l+1; until Filter[l]>0; First:=l;
       l:=l+1;
       Repeat l:=l+1; until Filter[l]<0;
       l:=l+1;
       Repeat l:=l+1; until Filter[l]>0;
       Last:=l;
    end;  {for}
    Max:=Last-First;
    First:=Last; Last:=Last+Max;
    If First > 300 then begin
        First := 220;
        If Max > 220 then Max:=220;
        Last := First + Max;
```

```
    end;   { If }
end;   {SeekWindow}

(*----------AUTOCORRELATION Rxx[0]--------------*)

Procedure AutoKor(Mat:dim; var Awgk:real);
  {This procedure implements a discrete
   autocorrelation of the voltage or current
   waveforms to form a rms value of current and
   voltage.  The autocorrelation is calculated as
   follows Awgk = SQRT(1/N*(sum A(j)*A(j))), with N
   the total data points.}
var   j:integer; Tydelik:dim;
begin
    Tydelik[-1]:=0;
    For j:=0 to Max-1 do
       Tydelik[j]:= Mat[First+j]*Mat[First+j]
                              + Tydelik[j-1];
    Awgk:= SQRT(Tydelik[Max-1]/(Max));
end; {AutoKor}

(*----------CROSS-CORRELATION Rvi[tau]----------*)

Procedure KruisKor(St,Vn:dim; var Rvi:dim2);
  {This procedure implements a discrete power
   cross-correlation of the voltage and current
   waveforms to form a time correlated power
   function. The correlation is as follows
   Rvi(k):=1/N*(sum Un(j)*In(j-k)), with N the
   total data points between the limits 0 and N.}
var   j,k:integer; Tydelik:dim;
begin
    For k:=-Max to Max do Rvi[k]:=0;
    For k:=-Max to Max do begin
        For j:= 0 to Max-1 do begin
            Tydelik[j]:= Vn[First+j]*St[First+j-k];
            Rvi[k]:= Rvi[k] + Tydelik[j];
        end; {For}
        Rvi[k]:=Rvi[k]/(Max);
    end; {For}
end; {KruisKor}

(*----GET THE PEAK IN THE CROSS-CORRELATION------*)

Procedure KorPiek(var Rpiek:real);
  {This routine calculates the peak value of the
   cross-correlation function Rui[k].}
var  Maks:integer;
begin
     Maks:=Round(Max/3);
     Rpiek:=ABS(Rvi[-Maks+3]);
     For i:=-(Maks-3) to (Maks-3) do
     If Rpiek<=ABS(Rvi[i]) then Rpiek:=ABS(Rvi[i]);
end;     { KorPiek }

(*-------------TO MAKE A PLOTARRAY--------------*)

Procedure PlotMatrix;
  {This procedure generate a PlotArray of the
   Cross-correlation, Voltage and Current Arrays,
   which can be plotted on the defined windows.}
begin
    For  i:=1 to 2*Max-2 do begin
       PlotRui[i,2]:= Rvi[i-(Max-1)];
       PlotRui[i,1]:= (i-(Max-1))*DeltaV;
    end; {For}
    For i:=1 to N do begin
       PlotU[i,2]:= Vn[i-1];
       PlotU[i,1]:= (i-1)*DeltaV;
    end; {For}
    For i:= 1 to N do begin
       PlotI[i,2]:=  St[i-1];
       PlotI[i,1]:= (i-1)*DeltaI;
    end; {For}
end;   {PlotMatrix}

(*----------DEFINE THE PLOT WINDOWS------------*)

Procedure PlotDef;
  {This routine define the windows.}
var
    Temp1,Temp2:Integer;
begin
    If GraphI = 'EGA' then begin
       Temp1:=174; Temp2:=349;
    end   {then}
    else begin
       Temp1:=99; Temp2:=199;
    end;   {else}
    SetBackground(0);
    DefineWindow(1,40,0,XMaxGlb,Temp1);
    DefineWindow(2,0,0,39,Temp1);
    DefineWindow(3,0,Temp1,39,Temp2);
    DefineWindow(4,40,Temp1,XMaxGlb,Temp2);
end; {PlotDef}
(*----------PLOT THE DIFFERENT ARRAYS----------*)
Procedure MatPlot(PlotMat:PlotArray;
                  WindowNr,Max:Integer;
                  Opskrif:KarString);
  {This routine plot the different functions.}
var  Y1,Y2,temp:real;
begin
    DefineHeader(WindowNr,Opskrif);
    FindWorld(WindowNr,PlotMat,Max,1.1,1.1);
                {Do all the graphs scaling}
    with World[WindowNr] do
       begin
           temp:=Y1; Y1:=Y2; Y2:=temp;
       end; {with World}
    SelectWorld(WindowNr);
    SelectWindow(WindowNr);
    SetHeaderOn;
    DrawBorder;
    DrawAxis(9,8,1,4,1,4,1,1,false);
    DrawPolygon(PlotMat,1,Max,0,1,0);
end; {MatPlot}

(*---CALCULATE AND PLOT THE POWER COMPONENTS-----*)

Procedure PowerCalc;
  { The power components are calculated }
var
    Drywing,Belading,Vervorming,Qdrywing,Ddrywing,
                                  Y,G,B,K:WrkString;
    Tydelik,Tyd1,Tyd2,Konduktansie,Susseptansie,
                  Admitansie,Disseptansie:real;
begin
    DefineHeader(4,'POWER SUMMARY');
    DefineWorld(4,0,1000,1000,0);
    SelectWorld(4); SelectWindow(4);
    SetHeaderOn; DrawBorder;
       Pakt:=Round(Rvi[0]);
       Rpiek:=(SQR(Rpiek)-SQR(Rvi[0]));
       Skyn:=Round(Vwgk*Iwgk);
          Tydelik:=ABS(Vwgk*Iwgk*Vwgk*Iwgk
                                - Rvi[0]*Rvi[0]);
       Dver:=Round(SQRT(Tydelik));  Tyd1:=Dver;
    ReaktVerv:=Round(SQRT(ABS(Rpiek)));
Tyd2:=ReaktVerv;
    Tydelik:=ABS(Tyd1*Tyd1 - Tyd2*Tyd2);
    DeaktVerv:=Round(SQRT(Tydelik));
    Admitansie:=Skyn/(Vwgk*Vwgk);
    Konduktansie:=Pakt/(Vwgk*Vwgk);
    Susseptansie:=ReaktVerv/(Vwgk*Vwgk);
    Disseptansie:=DeaktVerv/(Vwgk*Vwgk);
    Str(Pakt:4,Drywing);
    Str(Skyn:4,Belading);
    Str(Dver:4,Vervorming);
    Str(ReaktVerv:4,Qdrywing);
    Str(DeaktVerv:4,Ddrywing);
    Str(Admitansie:3,Y);
    Str(Konduktansie:3,G);
    Str(Susseptansie:3,B);
    Str(Disseptansie:3,K);
    If GraphI = 'EGA' then begin
      DrawTextW(90.0,90.0,1,'LOADING POWER S: '
```

```
            +Belading + ' VA');
      DrawTextW(90.0,190.0,1,'ACTIVE POWER P: '
            +Drywing + ' W');
      DrawTextW(90.0,290.0,1,'FICTITIOUS POWER F: '
            +Vervorming + ' VA');
      DrawTextW(130.0,410.0,1,'REACTIVE POWER Q: '
            +Qdrywing + ' VA');
      DrawTextW(130.0,510.0,1,'DEACTIVE POWER D: '
            +Ddrywing + ' VA');
      DrawTextW(170.0,630.0,1,'ADMITTANCE  Y: '
            +Y + ' MHO');
      DrawTextW(170.0,730.0,1,'CONDUCTANCE G: '
            +G + ' MHO');
      DrawTextW(170.0,830.0,1,'SUSCEPTANCE B: '
            +B + ' MHO');
      DrawTextW(170.0,930.0,1,'DISCEPTANCE K: '
            +K + ' MHO');
    end   {then}
    else begin
      DrawTextW(100.0,90.0,1,'LOADING   POWER S: '
            +Belading + ' VA');
      DrawTextW(100.0,200.0,1,'ACTIVE    POWER P: '
            +Drywing + ' W');
      DrawTextW(100.0,310.0,1,'FICTITIOUS POWER F:'
            +Vervorming + ' VA');
      DrawTextW(170.0,450.0,1,'REACTIVE POWER Q: '
            +Qdrywing + ' VA');
      DrawTextW(170.0,560.0,1,'DEACTIVE POWER D: '
            +Ddrywing + ' VA');
      DrawTextW(220.0,700.0,1,'CONDUCTANCE G: '
            +G + ' MHO');
      DrawTextW(220.0,810.0,1,'SUSCEPTANCE B: '
            +B + ' MHO');
      DrawTextW(220.0,920.0,1,'DISCEPTANCE K: '
            +K + ' MHO');
    end;    {else}
end;                    { PowerCalc }

(*----------SCREEN SAVED ON DISK IS READ---------*)

Procedure ScreenRead;
var
    ScreenNo,ScreenFile : WrkString;
begin
    ClrScr; Writeln; Writeln;
    Writeln(' What is the name of the screen?');
    Writeln('          (C:\TURBO\DATA\XXXXX.SCR)');
    readln(ScreenNo);
    ScreenFile:=Concat('C:\TURBO\DATA\'
                ,ScreenNo,'.SCR');
    repeat
       Writeln(' Is HardCopy required? (Y or N)');
       readln(key);
    until (key='Y') or (key='N');
    InitGraphic;
    LoadScreen(ScreenFile);
    Wait;
    If (key='Y') then HardCopy(false,6);
    Wait;
    LeaveGraphic;
end;       {ScreenRead}

(*-----------SCREEN IS SAVED ON DISK ----------*)
Procedure ScreenSave;
var
    ScreenNo,ScreenFile : WrkString;
begin
    Writeln; Writeln;
    Writeln('What name should be used?');
    Writeln('          (C:\TURBO\DATA\XXXXX.SCR)');
    readln(ScreenNo);
    ScreenFile:=Concat('C:\TURBO\DATA\'
                              ,ScreenNo,'.SCR');
    repeat
       Writeln(' Is HardCopy required? (Y or N)');
       readln(key);
    until (key='Y') or (key='N');
    InitGraphic;
    LoadScreen('C:\TURBO\DATA\STORE.SCR');
    SaveScreen(ScreenFile);
    If (key='Y') then HardCopy(false,6);
    LeaveGraphic;
end;       {ScreenSave}

(*******************MAIN PROGRAM*****************)
begin
    ClrScr; Writeln; N:=Samples;
Writeln('****************************************');
    Writeln('THIS PROGRAM COMPUTES THE DIFFERENT
                          COMPONENTS OF POWER, ');
Writeln('****************************************');
    Writeln('** Voltage and current waveforms are
                       either generated      **');
    Writeln('** internally, or a data file is read
                        with the waveform data**');
    Writeln('** There is also the possibility to
                      read old generated data **');
    Writeln('** from a SCR file. Press any key to
                        continue.             **');
Writeln('****************************************');
    Writeln; Writeln; Writeln; Wait;
    repeat
      Writeln('  Where should the data be found?');
      Writeln('Old Correlated screen? (O)');
      Writeln('New Data or Mathematical
                         simulations? (N)');
      Writeln('          Give input (O,N)');
      readln(ch);
    until (ch='O') or (ch='N');
    If (ch='N') then begin
      Input; {Get the input from INPUT.JHE}
      SeekWindow(Vn); {Get the measurement window}
      AutoKor(Vn,Vwgk); {Autocorrelation Vn Values}
      AutoKor(St,Iwgk); {Autocorrelation St Values}
      KruisKor(St,Vn,Rvi); {Cross-correlation}
      KorPiek(Rpiek); {Peak from Rui[k]}
      PlotMatrix; {Make plot matrixes}
      repeat  {The output is stored as a data
                                  screen XXXX.SCR}
        Writeln('  Should the generated screen be
                           saved on disk? (Y,N)');
        readln(ch);
      until (ch='Y') or (ch='N');
      InitGraphic;
      PlotDef;   {Define the windows for plotting}
      Opskrif:='       VOLTAGE [V]        ';
      MatPlot(PlotU,2,N,Opskrif); {Plot voltage Vn}
      Opskrif:='       CURRENT [A]        ';
      MatPlot(PlotI,3,N,Opskrif); {Plot current St}
      Opskrif:='CROSS-CORRELATION Rui [VA]';
      MatPlot(PlotRui,1,2*Max-2,Opskrif);
                    {Plot correlation function Rui}
      PowerCalc; {Calculate the power components}
      SaveScreen('C:\TURBO\DATA\STORE.SCR');
      Wait;
      LeaveGraphic;
      If (ch='Y') then ScreenSave;
    end       {If}
    else ScreenRead;
    Wait;
end.          {Power3}
```

PROGRAM INSTANT

```
(***********************************************)
(*THIS PROGRAM DERIVES THE INSTANTANEOUS SIGNALS *)
(* OF ORTHOGONAL CURRENT COMPONENTS Ia, Ir, Id.  *)
(*  DESIGNED BY JHR ENSLIN IN APRIL 1988        *)
(***********************************************)
Program InstantCurrents;
(********** VARIABLE DEFINITION PART ***********)
const
    Samples=500; MaxWorldsGlb=4; MaxWindowsGlb=16;
    MaxPiesGlb=10; MaxPlotGlb=Samples;
```

```
    StringSizeGlb=80; HeaderSizeGlb=10;
    RamScreenGlb:boolean=true;
    CharFile:string[StringSizeGlb]='4x6.fon';
    MaxProcsGlb=27; MaxErrsGlb=7;
    Pi =3.14159265358979;      {Pi}
    Pi2=6.28318530717959;      { 2*Pi }
    FileName='TEMP.DAT'; GraphI='IBM';
type
    wrkstring=string[StringSizeGlb];
    WorldType=record x1,y1,x2,y2:real; end;
    WindowType=record x1,y1,x2,y2:integer;
               header:wrkstring; drawn,top:boolean;
               size:integer; end;
    worlds=array [1..MaxWorldsGlb] of WorldType;
    windows=array [1..MaxWindowsGlb] of WindowType;
    PlotArray=array [1..MaxPlotGlb,1..2] of real;
    character=array [1..3] of byte;
    CharArray=array [32..126] of character;
    PieType=record
            area:real; text:wrkstring; end;
    PieArray=array [1..MaxPiesGlb] of PieType;
    BackgroundArray=array [0..7] of byte;
    LineStyleArray=array [0..7] of boolean;
    KarString = packed array[1..42] of char;
    Ibstring = string[50];
var
    X1WldGlb,X2WldGlb,Y1WldGlb,Y2WldGlb:real;
    AxGlb,AyGlb,BxGlb,ByGlb:real;
    X1RefGlb,X2RefGlb,Y1RefGlb,Y2RefGlb,
                              LinestyleGlb:integer;
    MaxWorldGlb,MaxWindowGlb,WindowNdxGlb:integer;
    X1Glb,X2Glb,Y1Glb,Y2Glb:integer;
    XTextGlb,YTextGlb,VStepGlb:integer;
    PieGlb,DirectModeGlb,TopGlb,AxisGlb,
                                  HatchGlb:boolean;
    MessageGlb,BrkGlb,HeaderGlb:boolean;
    ClippingGlb,GrafModeGlb:boolean;
    CntGlb,ColorGlb:byte;
    ErrCodeGlb:byte;
    LineStyleArrayGlb:LineStyleArray;
    ErrorProc:array [0..MaxProcsGlb] of ^WrkString;
    ErrorCode:array [0..MaxErrsGlb] of ^WrkString;
    PcGlb:string[40]; AspectGlb:real;
    GrafBase:integer; world:worlds; window:windows;
    CharSet:CharArray;  Opskrif:KarString;
    CH1,CH2,CH3,CH4,CH5,CH6:PlotArray;
    ch,key:char; Max,Punte,Aantal,N,i:integer;

(************ GRAPHICS INCLUDE FILES *************)
{$I graphix.IBM}
{$I kernel.sys}
{$I windows.sys}
{$I findwrld.hgh}
{$I axis.hgh}
{$I polygon.hgh}
{$U+}
(*******************SUBROETINES*********************)
(*********************WAIT**************************)
Procedure Wait;
begin
    repeat until(KeyPressed);
end;                { Wait }
(*********************INPUT*************************)
Procedure Input;
const
    FileName='C:\TURBO\DATA\TEMP.DAT';
type dim=Array[1..MaxPlotGlb] of Real;
var  Vn : dim;
     DeltaV,VensterV,CorAdm,Sus,Con,Degrees : Real;
     Phase : Integer;

(*---------MATHEMATICAL GENERATION ROUTINES------*)
Procedure MathGen;
    procedure MathFunction (var DataMat:dim;
              var Venster, Delta:real; N:integer);
    label KiesReg;
    var
        S,T,Fr,F,G:real; tel,i:integer; ch1:char;

(*--------- DIFFERENT FUNCTIONS ------------*)
    procedure Sinus (var DataMat:dim);
    var
        Fase,Theta,Alpha:real; tel,k:integer;
    begin
        Writeln; Writeln;
        Writeln(' What is the CONTROL angle?');
        Readln(Alpha);
        Alpha:=(Pi2*Alpha)/360; k:=1;
        Fase:=(Pi2*F)/360;  {Phase in radials}
        For tel:=0 to N-1 do begin
            DataMat[tel]:=0;
            Theta:=((Pi2*tel*Venster)/(N-1)
                                        - Fase);
            DataMat[tel]:= G + S*sin(Theta);
            If (Theta > k*Pi) then begin
                Alpha:=Alpha+Pi; k:=k+1;
            end;      {If}
            If (Theta < Alpha) and (Alpha > 0)
                        then DataMat[tel]:=0;
        end;     {For}
    end;      {Sinus}
(*----------------------------------------*)
procedure Block (var DataMat:dim);
var
    Fase,Theta,Alpha:real; tel,k:integer;
begin
    Writeln; Writeln;
    Alpha:=0;
    Alpha:=(Pi2*Alpha)/360; k:=1;
    Fase:=(Pi2*F)/360;  {Fase in radiale}
    For tel:=0 to N-1 do begin
        DataMat[tel]:=0;
        Theta:=((Pi2*tel*Venster)/(N-1)
                                        - Fase);
        DataMat[tel]:= sin(Theta);
        If (Theta > k*Pi) then begin
            Alpha:=Alpha+Pi; k:=k+1;
        end;      {If}
        If (Theta < Alpha) and (Alpha>0)
                        then DataMat[tel]:=0;
        If DataMat[tel] > 0
                        then DataMat[tel]:=G+S;
        If DataMat[tel] < 0
                        then DataMat[tel]:=G-S;
    end;      {For}
end; {Block}

(*----------------------------------------*)
procedure TrapBlok (var DataMat:dim);
var
    Fase,Theta,Alpha:real; tel,k:integer;
begin
    Alpha:=(Pi2*60)/360; k:=1;
    Fase:=(Pi2*(F-30)/360);  {Phase in radials}
    For tel:=0 to N-1 do begin
        DataMat[tel]:=0;
        Theta:=((Pi2*tel*Venster)/(N-1)
                                        - Fase);
        DataMat[tel]:= sin(Theta);
        If (Theta > k*Pi) then begin
            Alpha:=Alpha+Pi; k:=k+1;
        end;      {If}
        If (Fase<Theta) and (Theta<Alpha)
            and (Alpha>0) then DataMat[tel]:=0;
        If DataMat[tel] > 0
                        then DataMat[tel]:=G+S;
        If DataMat[tel] < 0
                        then DataMat[tel]:=G-S;
    end;      {For}
end;     {TrapBlok}
(*----------------------------------------*)
procedure Driehoek (var DataMat:dim);
var
    Fase,Theta,Alpha,m,Temp:real;
    Phase,tel,k,p:integer; Tydelik:dim;
begin
```

```
        Writeln(' What is the CONTROL angle?  ');
        Readln(Alpha);
        m:=4*S*Venster/N;
        Alpha:=(Pi2*(Alpha-90))/360; k:=1; p:=0;
        Fase:=(Pi2*(F+90))/360;  {Fase in radiale}
        Temp:=G+S;
        For tel:=0 to N-1 do begin
            DataMat[tel]:=0;
            Theta:=(Pi2*tel*Venster)/(N-1);
            DataMat[tel]:= sin(Theta);
            If (Theta > k*Pi) then begin
                Alpha:=Alpha+Pi; k:=k+1;
            end;     {If}
            If DataMat[tel] > 0
                          then DataMat[tel]:=G+S;
            If DataMat[tel] < 0
                          then DataMat[tel]:=G-S;
            If (Temp<>DataMat[tel]) then begin
                 p:=0; m:=-m; Temp:=DataMat[tel];
            end;   {If}
            DataMat[tel]:=DataMat[tel]-m*p; p:=p+1;
            If (Theta < Alpha) and (Alpha>0)
                              then DataMat[tel]:=0;
        end; {For}
        If F<0 then F:=F+360;
        Phase:= round(F*N/(Venster*360));
        If Phase >=1 then begin
            For i:=0 to N-1 do begin
                If (i+Phase)>N-1 then
                Tydelik[i]:= DataMat[i+Phase-N+1]
                else Tydelik[i]:= DataMat[i+Phase];
            end; {For}
            For i:=0 to N-1 do
                          DataMat[i]:=Tydelik[i];
        end; {If}
        For i:=0 to N-1 do
                        DataMat[i]:= -DataMat[i];
    end;       {Driehoek}
    (*-----------------------------------------*)
    procedure HalfGolfGelykrigBeheer
                                  (var DataMat:dim);
    var
        Fase,Theta,Alpha:real; tel,k:integer;
    begin
        Writeln(' What is the CONTROL angle?  ');
        Readln(Alpha);
        Fase:=(Pi2*F)/360;  {Phase in radials}
        Alpha:=(Pi2*Alpha)/360; k:=1;
        For tel:=0 to N-1 do begin
            DataMat[tel]:=0;
            Theta:=((Pi2*tel*Venster)/(N-1)
                                        - Fase);
            DataMat[tel]:= G + S*sin(Theta);
            If (Theta > k*Pi2) then begin
                Alpha:=Alpha+Pi2; k:=k+1;
            end;     {If}
            If (Theta<Alpha) and (Alpha>0)
                              then DataMat[tel]:=0
                 else If DataMat[tel]<=0
                              then DataMat[tel]:=0;
        end;    {For}
    end;     {HalfGolfGelykrigBeheer}

(*-----------------------------------------*)
begin
    KiesReg: Writeln('Choose again');
    repeat
        Writeln;
        Writeln('THIS FUNCTIONS ARE POSSIBLE.');
        Writeln;
        Writeln(' Sinuswave                :"S" ');
        Writeln(' Blockwave                :"B" ');
        Writeln(' Staircase Block          :"C" ');
        Writeln(' Controlled rectified     :"D" ');
        Writeln(' Triangle wave            :"T" ');
        Writeln('      Which one? (S,B,C,T,D) ');
        Writeln;  readln(ch1);
    until (ch1='S') or (ch1='B') or (ch1='C')
                  or (ch1='D') or (ch1='T');
    Writeln; Writeln;
    If (ch1='S')or (ch1='B') or (ch1='C')
    or (ch1='D') or (ch1='T')  then begin
        Writeln('   What is the Amplitude (V/A),');
        Writeln('      the Frequency (Hz),');
        Writeln('      the Phaseshift (degrees)');
        Writeln('      and DC offset (V/A).');
        Writeln('   Give input (Ampl Fr Ph DC)');
        Readln(S,Fr,F,G);
        T:=1/Fr; Writeln;
        Venster:=3;
        Delta:=((Venster*T)/N);
        Case ch1 of
            'S' : Sinus(DataMat);
            'B' : Block(DataMat);
            'C' : TrapBlok(DataMat);
            'T' : Driehoek(DataMat);
            'D' : HalfGolfGelykrigBeheer(DataMat);
        end;     {case}
    end {Then}
    else goto KiesReg;
end;      {MathFunction}

(*-----------------------------------------*)
begin
    ClrScr; Writeln; Writeln;
    Writeln('    VOLTAGE MATHEMATICAL EQUATION ');
    MathFunction(Vn,VensterV,DeltaV,Max);
    For i:=1 to Max-1 do begin
        CH1[i,2]:=Vn[i];  CH1[i,1]:=i;
    end;  {For}
    Writeln; Writeln;
    Writeln('    CURRENT MATHEMATICAL EQUATION ');
    MathFunction(Vn,VensterV,DeltaV,Max); ClrScr;
    For i:=1 to Max-1 do begin
        CH2[i,2]:=Vn[i]; CH2[i,1]:=i;
    end;  {For}
    Writeln; Writeln;
    Writeln('    ACTIVE CURRENT GENERATION ');
    Writeln('What is the Conductance G?');
    ReadLn(Con);
    For i:=1 to Max-1 do begin
        CH3[i,2]:=Con*CH1[i,2]; CH3[i,1]:=i;
    end;  {For}
    Writeln('    FICTITIOUS CURRENT GENERATION ');
    For i:=1 to Max-1 do begin
        CH4[i,2] := CH2[i,2] - CH3[i,2];
        CH4[i,1]:=i;
    end;  {For}
    Writeln; Writeln;
    Writeln('    DEACTIVE CURRENT GENERATION ');
    Writeln('What is the Susceptance B?');
    ReadLn(Sus);
    CorAdm:=Sqrt(Sqr(Con) + Sqr(Sus));
    Writeln; Writeln;
    Writeln('What is the Correlation Shift ?');
    ReadLn(Degrees);
    Phase := Round(Degrees/2.1557);
    Max:=333;
    For i:=84-Phase to 418+Phase do begin
        CH6[i,2] := - CorAdm*CH1[i-Phase,2]
                    + CH2[i,2]; CH6[i,1]:=i;
    end;  {For}
    Writeln('    REACTIVE CURRENT GENERATION ');
    For i:=84 to 418 do begin
        CH5[i,2]:= CH2[i,2] - CH3[i,2] - CH6[i,2];
        CH6[i,1]:=i;
    end;  {For}
    Writeln; Writeln;
end;       {MathGen}

(*********************************************)
Procedure Plaas;
begin
    For i:=1 to Max do begin
        CH1[i,2]:=0.3*CH1[i+84,2] + 70;
        CH1[i,1]:=i;
```

```
        CH2[i,2]:=0.3*CH2[i+84,2] + 30;
        CH2[i,1]:=i;
        CH3[i,2]:=0.3*CH3[i+84,2]; CH3[i,1]:=i;
        CH4[i,2]:=0.3*CH4[i+84,2] - 35;
        CH4[i,1]:=i;
        CH5[i,2]:=0.3*CH5[i+84,2] - 55;
        CH5[i,1]:=i;
        CH6[i,2]:=0.3*CH6[i+84,2] - 85;
        CH6[i,1]:=i;
    end;
end;

(*-------------------------------------------*)
begin
    ClrScr; Writeln; MathGen; Plaas;
end;      {Input}

(*********** DEFINE THE PLOT WINDOWS ***********)
Procedure PlotDef;
  {This routine define the windows.}
var
    Temp:Integer;
begin
    SetBackground(0);
    Temp:=Round(0.8*XMaxGlb);
    DefineWindow(1,10,12,Temp,YMaxGlb-2);
    DefineWindow(2,0,0,XMaxGlb,YMaxGlb);
end; {PlotDef}

(*********PLOT THE DIFFERENT ARRAYS*************)
Procedure Plot (Opskrif:KarString);
  {This routine plot the oscilograms.}
var l:integer;

(*-------------------------------------------*)
procedure TeksMerk;
begin
    DrawTextW(4,71,1,'Gnd CH1 --');
    DrawTextW(4,31,1,'Gnd CH2 --');
    DrawTextW(4,1,1,'Gnd CH3 --');
    DrawTextW(4,-34,1,'Gnd CH4 --');
    DrawTextW(4,-54,1,'Gnd CH5 --');
    DrawTextW(4,-84,1,'Gnd CH6 --');
    DrawTextW(85,70,2,Chr(27)+'3'+'  u(t)');
    DrawTextW(85,40,2,Chr(27)+'4'+'  i(t)');
    DrawTextW(85,10,2,Chr(27)+'5'+'  i (t)');
    DrawTextW(92,5,1,'a');
    DrawTextW(85,-20,2,Chr(27)+'1'+'  i (t)');
    DrawTextW(92,-25,1,'f');
    DrawTextW(85,-50,2,Chr(27)+'2'+'  i (t)');
    DrawTextW(92,-55,1,'r');
    DrawTextW(85,-80,2,Chr(27)+'7'+'  i (t)');
    DrawTextW(92,-85,1,'d');
end;  {TeksMerk}

(*-------------------------------------------*)
procedure Merk;

var LengteHL, LengteHK : Real;
begin
    LengteHL := Max/10; LengteHK := Max/50;
    DrawLine(0,0,Max,0);
    DrawLine(Max/2,100,Max/2,-100);
    For i:=-4 to 4 do begin
      DrawLine((Max/2)-2,25*i,(Max/2)+2,25*i);
      DrawLine(0,25*i,+3,25*i);
      DrawLine(Max-2,25*i,Max,25*i);
    end;  {For}
    For i:=-20 to 20 do
      DrawLine((Max/2)-1,5*i,(Max/2)+1,5*i);
    For i:=1 to 10 do begin
      DrawLine(i*LengteHL,-3,i*LengteHL,3);
      DrawLine(i*LengteHL,100,i*LengteHL,97);
      DrawLine(i*LengteHL,-100,i*LengteHL,-95);
    end;   {For}
    For i:= 1 to 49 do
      DrawLine(i*LengteHK,-2,i*LengteHK,2);
end;  {merk}

(*-------------------------------------------*)
begin
    DefineWorld(2,1,-100,100,100);
    SelectWorld(2);
    SelectWindow(2);
    DefineHeader(2,Opskrif);
    SetHeaderOn;
    DrawBorder;
    TeksMerk;
    DefineWorld(1,1,100,Max,-100);
    SelectWorld(1);
    SelectWindow(1);
    DrawBorder;
    Merk;
        DrawPolygon(CH1,1,Max,0,1,0);
        DrawTextW(Max-10,-85,2,Chr(27)+'3');
        DrawPolygon(CH2,1,Max,0,1,0);
        DrawTextW(Max-10,-35,2,Chr(27)+'4');
        DrawPolygon(CH3,1,Max,0,1,0);
        DrawTextW(Max-10,5,2,Chr(27)+'5');
        DrawPolygon(CH4,1,Max,0,1,0);
        DrawTextW(Max-10,35,2,Chr(27)+'1');
        DrawPolygon(CH5,1,Max,0,1,0);
        DrawTextW(Max-10,60,2,Chr(27)+'2');
        DrawPolygon(CH6,1,Max,0,1,0);
        DrawTextW(Max-10,90,2,Chr(27)+'7');
end;   {Plot}

(*********SCREEN SAVED ON DISK IS READ***********)
Procedure ScreenRead;
var
    ScreenNo,ScreenFile : WrkString;
begin
    ClrScr; Writeln; Writeln;
    Writeln('What is the Data screen name ?');
    Writeln('          (C:\TURBO\DATA\XXXXX.SCR)');
    readln(ScreenNo);
    ScreenFile:=Concat('C:\TURBO\DATA\',
                                  ScreenNo,'.SCR');
    repeat
        Writeln('Is HardCopy required? (Y or N)');
        readln(key);
    until (key='Y') or (key='N');
    InitGraphic;
    LoadScreen(ScreenFile);
    Wait;
    If (key='Y') then HardCopy(false,6);
    Wait;
    LeaveGraphic;
end;       {ScreenRead}

(********** SCREEN IS SAVED ON DISK **************)
Procedure ScreenSave;
var
    ScreenNo,ScreenFile : WrkString;
begin
    Writeln; Writeln;
    Writeln('  What name for the Data screen?');
    Writeln('          (C:\TURBO\DATA\XXXXX.SCR)');
    readln(ScreenNo);
    ScreenFile:=Concat('C:\TURBO\DATA\
                                  ',ScreenNo,'.SCR');
    repeat
        Writeln('Is HardCopy required? (Y or N)');
        readln(key);
    until (key='Y') or (key='N');
    InitGraphic;
    LoadScreen('C:\TURBO\DATA\STORE.SCR');
    SaveScreen(ScreenFile);
    If (key='Y') then HardCopy(false,6);
    LeaveGraphic;
end;       {ScreenSave}

(******************MAIN PROGRAM*****************)
begin
   ClrScr; Writeln; Max:=Samples;
```

```
    Writeln('************************************');
    Writeln('*THIS PROGRAM PLOT INSTANTANEOUS   *');
    Writeln('**              CURRENTS           **');
    Writeln('************************************');
     Writeln('*   Old data can also be read     *');
     Writeln('**   Press any key to continue.  **');
     Writeln('************************************');
     Writeln; Writeln; Writeln; Wait;
     repeat
       Writeln('  Where should the data be found?');
       Writeln('  Old screen saved on disk? (O)');
       Writeln('  New Data? (N)');
       Writeln('          Give input (O,N)');
       readln(ch);
     until (ch='O') or (ch='N');
     If (ch='N') then begin
       Input;
       Max:=333;
       repeat  {The output stored as a data screen}
         Writeln('Should screen be saved? (Y,N)');
         readln(ch);
       until (ch='Y') or (ch='N');
       InitGraphic;
       PlotDef;   {Define the windows for plotting}
       Opskrif:=' REPRESENTATION OF
                          INSTANTANEOUS CURRENTS ';
       Plot(Opskrif);
       SaveScreen('C:\TURBO\DATA\STORE.SCR');
       Wait;
       LeaveGraphic;
       If (ch='Y') then ScreenSave;
     end        {If}
     else ScreenRead;
     Wait;
end.            {InstantCurrents}
```

PROGRAM INPUT

```
(************************************************)
(*                                              *)
(*   The input program for the power program.   *)
(*Different possibilities, which include function*)
(*generation, measured input data or previously  *)
(*saved data, can be used.                       *)
(* Written during 1986 and 1987 by J.H.R. Enslin *)
(************************************************)

(**********************WAIT**********************)

Procedure Wait;
begin
    repeat until(KeyPressed);
end;                { Wait }

(**********************INPUT*********************)

Procedure Input;
Const   FileName='C:\TURBO\DATA\TEMP.DAT';

(*--------MATHEMATICAL GENERATION ROUTINES-------*)

Procedure MathGen;

    Procedure MathFunction (var DataMat:dim;
                            var Venster,
                            Delta:real; N:integer);
    label KiesReg;
    var
        S,T,Fr,F,G:real; tel,i:integer; ch1:char;

    (*************DIFFERENT FUNCTIONS************)

        Procedure Sinus (var DataMat:dim);
        var
            Fase,Theta,Alpha:real; tel,k:integer;
        begin
            Writeln; Writeln;
            Writeln(' What is the CONTROL angle?');
            Readln(Alpha);
            Alpha:=(Pi2*Alpha)/360; k:=1;
            Fase:=(Pi2*F)/360;  {Phase in radials}
            For tel:=0 to N-1 do begin
                DataMat[tel]:=0;
                Theta:=((Pi2*tel*Venster)/(N-1)
                                          - Fase);
                DataMat[tel]:= G + S*sin(Theta);
                If (Theta > k*Pi) then begin
                    Alpha:=Alpha+Pi; k:=k+1;
                end;     {If}
                If (Theta<Alpha) and (Alpha>0)
                            then  DataMat[tel]:=0;
            end;    {For}
        end;     {Sinus}
(*-----------------------------------------*)
    Procedure Block (var DataMat:dim);
    var
        Fase,Theta,Alpha:real; tel,k:integer;
    begin
        Writeln; Writeln;
        Writeln(' What is the CONTROL angle?  ');
        Readln(Alpha);
        Alpha:=(Pi2*Alpha)/360; k:=1;
        Fase:=(Pi2*F)/360;  {Fase in radiale}
        For tel:=0 to N-1 do begin
            DataMat[tel]:=0;
            Theta:=((Pi2*tel*Venster)/(N-1)
                                          - Fase);
            DataMat[tel]:= sin(Theta);
            If (Theta > k*Pi) then begin
                Alpha:=Alpha+Pi; k:=k+1;
            end;     {If}
            If (Theta < Alpha) and (Alpha>0) then
                                  DataMat[tel]:=0;
            If DataMat[tel] > 0 then
                                  DataMat[tel]:=G+S;
            If DataMat[tel] < 0 then
                                  DataMat[tel]:=G-S;
        end;     {For}
    end; {Block}

(*-----------------------------------------*)

    Procedure TrapBlok (var DataMat:dim);
    var
        Fase,Theta,Alpha:real; tel,k:integer;
    begin
        Alpha:=(Pi2*60)/360; k:=1;
        Fase:=(Pi2*(F-30)/360);  {Phase in radials}
        For tel:=0 to N-1 do begin
            DataMat[tel]:=0;
            Theta:=((Pi2*tel*Venster)/(N-1)
                                          - Fase);
            DataMat[tel]:= sin(Theta);
            If (Theta > k*Pi) then begin
                Alpha:=Alpha+Pi; k:=k+1;
            end;     {If}
            If (Fase<Theta) and (Theta<Alpha) and
               (Alpha > 0) then DataMat[tel]:=0;
            If DataMat[tel] > 0 then
                                  DataMat[tel]:=G+S;
            If DataMat[tel] < 0 then
                                  DataMat[tel]:=G-S;
        end;     {For}
    end;     {TrapBlok}

(*-----------------------------------------*)
    Procedure Driehoek (var DataMat:dim);
    var
        Fase,Theta,Alpha,m,Temp:real;
        Phase,tel,k,p:integer; Tydelik:dim;
    begin
        Writeln(' What is the CONTROL angle?  ');
        Readln(Alpha);
        m:=4*S*Venster/N;
```

```
        Alpha:=(Pi2*(Alpha-90))/360; k:=1; p:=0;
        Fase:=(Pi2*(F+90))/360;  {Fase in radiale}
        Temp:=G+S;
        For tel:=0 to N-1 do begin
            DataMat[tel]:=0;
            Theta:=(Pi2*tel*Venster)/(N-1);
            DataMat[tel]:= sin(Theta);
            If (Theta > k*Pi) then begin
                Alpha:=Alpha+Pi; k:=k+1;
            end;     {If}
            If DataMat[tel] > 0 then
                                DataMat[tel]:=G+S;
            If DataMat[tel] < 0 then
                                DataMat[tel]:=G-S;
            If (Temp<>DataMat[tel]) then begin
                 p:=0; m:=-m; Temp:=DataMat[tel];
            end;   {If}
            DataMat[tel]:=DataMat[tel] - m*p;
            p:=p+1;
            If (Theta<Alpha) and (Alpha>0) then
                                  DataMat[tel]:=0;
        end; {For}
        If F<0 then F:=F+360;
        Phase:= round(F*N/(Venster*360));
        If Phase >=1 then begin
            For i:=0 to N-1 do begin
                If (i+Phase)>N-1 then
                Tydelik[i]:= DataMat[i+Phase-N+1]
                else Tydelik[i]:= DataMat[i+Phase];
            end; {For}
            For i:=0 to N-1 do
                          DataMat[i]:= Tydelik[i];
        end; {If}
        For i:=0 to N-1 do
                         DataMat[i]:= -DataMat[i];
    end;       {Driehoek}

(*-----------------------------------------------*)

    Procedure HalfGolfGelykrigBeheer
                                (var DataMat:dim);
    var
        Fase,Theta,Alpha:real; tel,k:integer;
    begin
        Writeln(' What is the CONTROL angle?  ');
        Readln(Alpha);
        Fase:=(Pi2*F)/360;  {Phase in radials}
        Alpha:=(Pi2*Alpha)/360; k:=1;
        For tel:=0 to N-1 do begin
            DataMat[tel]:=0;
            Theta:=((Pi2*tel*Venster)/(N-1)
                                          - Fase);
            DataMat[tel]:= G + S*sin(Theta);
            If (Theta > k*Pi2) then begin
                Alpha:=Alpha+Pi2; k:=k+1;
            end;     {If}
            If (Theta<Alpha) and (Alpha>0) then
                                DataMat[tel]:=0
            else
            If DataMat[tel]<=0 then
                                DataMat[tel]:=0;
        end;    {For}
    end;     {HalfGolfGelykrigBeheer}

(*************************************************)
begin
    ClrScr;  KiesReg: ClrScr;
    repeat
        Writeln;
        Writeln(' THE FOLLOWING FUNCTIONS ARE
                  POSSIBLE.'); Writeln;
        Writeln('     Sinuswave             :"S" ');
        Writeln('     Blockwave             :"B" ');
        Writeln('     Staircase Block       :"C" ');
        Writeln('     Controlled rectified :"D" ');
        Writeln('     Triangle wave         :"T" ');
        Writeln('        Which one? (S,B,C,T,D) ');
        Writeln;  readln(ch1);
    until (ch1='S') or (ch1='B') or (ch1='C') or
                    (ch1='D') or (ch1='T');
    Writeln; Writeln;
    If (ch1='S')or (ch1='B') or (ch1='C')
    or (ch1='D') or (ch1='T')  then begin
        Writeln('   What is the Amplitude (V/A),');
        Writeln('      the Frequency (Hz),');
        Writeln('      the Phaseshift (degrees)');
        Writeln('      and DC offset (V/A).');
        Writeln('   Give input (Ampl Fr Ph DC)');
        Readln(S,Fr,F,G);  T:=1/Fr; Writeln;
        Writeln(' What is the Window width?
                    (Portion of period d*T)');
        Readln(Venster);
        Delta:=((Venster*T)/N);
        Case ch1 of
            'S' : Sinus(DataMat);
            'B' : Block(DataMat);
            'C' : TrapBlok(DataMat);
            'T' : Driehoek(DataMat);
            'D' : HalfGolfGelykrigBeheer(DataMat);
        end;     {case}
    end {Then}
    else goto KiesReg;
end;      {MathFunction}

begin
    ClrScr; Writeln; Writeln;
    Writeln('  VOLTAGE MATHEMATICAL EQUATION
                    (Press any key)');
    Wait;
    MathFunction(Vn,VensterV,DeltaV,N);
    ClrScr; Writeln; Writeln;
    Writeln('CURRENT MATHEMATICAL
                   EQUATION (Press any key)');
    Wait;
    MathFunction(St,VensterI,DeltaI,N);
end;       {MathGen}

(********ROUTINE TO READ DATA FROM DISK***********)

Procedure DataStored (var N:integer;
                      var Vn,St:dim);
var
    ch1,ch2:char;
    ScreenNo,ScreenFile : WrkString;

    (*----------PROCEDURE RECORDFILE READ--------*)

    Procedure RecordFileRead(FileName:ibstring;
                          var Y1,Y2,X:dim);
    {This procedure reads a record file from disk.}
    var
        Karakter:string[1]; XTime,CH1,CH2:real;
        k:integer;
    begin
        Assign(RecordMat, FileName);
        Reset(RecordMat);
        i:=-3;
        repeat
            with DataRec do begin
               time:=XTime; channel1:=CH1;
               channel2:=CH2;
               read(RecordMat,DataRec);
               X[i]:=Time;  Y1[i]:=Channel1;
               Y2[i]:=Channel2;
            end;    {with}
            i:=i+1;
        until (eof(RecordMat)) or (i=N+2);
        close(RecordMat);
    end;              {RecordFileRead}

(*-----------------------------------------------*)
begin
    Writeln; Writeln;
    Writeln('The data is a Record of t,U,I');
    Writeln; Writeln;
    Writeln('What is the Data file name?');
```

```
    Writeln('          (C:\TURBO\DATA\XXXXX.DAT)');
    readln(ScreenNo);
    ScreenFile:=Concat('C:\TURBO\DATA\',ScreenNo,
                                        '.DAT');
    Writeln; Writeln;
    RecordFileRead(ScreenFile,Vn,St,time);
    DeltaV:=(time[10]-time[4])/6; DeltaI:=DeltaV;
end; {DataStored}

(*-----READ PREVIOUSLY STORED DATA FROM DISK-----*)

Procedure InputRead (var DeltaV,DeltaI:real;
                     var CHAN1,CHAN2:dim);
    {This procedure reads a record file from disk.}
begin
    Assign(RecordMat2, FileName);
    Reset(RecordMat2);
    i:=0;
    with DataRec2 do begin
        read(RecordMat2,DataRec2);
        DeltaV:=Channel1; DeltaI:=Channel2;
    end;    {with}
    repeat
        with DataRec2 do begin
            read(RecordMat2,DataRec2);
            CHAN1[i]:=Channel1; CHAN2[i]:=Channel2;
        end;    {with}
        N:=i+1; i:=i+1;
    until (eof(RecordMat2));
    close(RecordMat2);
end;     {InputRead}

(*----ROUTINE TO WRITE DATA GENERATED TO DISK----*)

Procedure InputStored (CHAN1,CHAN2:dim);
    {This procedure write data to disk. }
var
    CH1,CH2:real; k:integer;
begin
    Assign(RecordMat2, FileName);
    Rewrite(RecordMat2);
    with DataRec2 do begin
        Channel1:=DeltaV; Channel2:=DeltaI;
        write(RecordMat2,DataRec2);
    end;    {with}
    For i:=0 to N-1 do begin
        with DataRec2 do begin
            Channel1:=CHAN1[i]; Channel2:=CHAN2[i];
            write(RecordMat2,DataRec2);
        end;    {with}
    end;   {For}
    close(RecordMat2);
end;     {InputRead}


(*******************MAIN PROGRAM*******************)

begin
    ClrScr; Writeln;

Writeln('************************************');
    Writeln('*THIS PROGRAM GENERATES THE INPUT *');
    Writeln('*THERE IS SEVERAL POSSIBILITIES   *');
    Writeln('*MATHEMATICAL GENERATED WAVEFORMS *');
    Writeln('*ACTUAL DATA READ FROM DISK FILE. *');
    Writeln('*THE INPUT IS STORED ON DATA FILE *');
Writeln('************************************');
    Writeln;
    Repeat
      Writeln('Change setup? (Y,N)');
         Readln(ch);
    until Upcase(ch) in ['Y','N'];
    If ch='Y' then begin
      Writeln; Writeln; Writeln;
      repeat
    Writeln('************************************');
    Writeln('*THE POSSIBILITIES ARE THE
                                    FOLLOWING: *');
    Writeln('* Different Mathematical Generated
                          Waveforms:-    "A" *');
    Writeln('* Data Generated From Actual
                          Measurements:-       "B" *');
    Writeln('** Data Stored Previously:-  "C" *');
    Writeln('* GIVE INPUT "A","B" OR "C"   *');
    Writeln('************************************');
      readln(ch);
      until (ch='A') or (ch='B') or (ch='C');
      Case ch of
       'A': begin MathGen; InputStored(Vn,St); end;
          {Generates input from function generator}
       'B' : begin DataStored(N,Vn,St);
                   InputStored(Vn,St); end;
          {Generates input from data file}
       'C' : InputRead(DeltaV,DeltaI,Vn,St);
          {Retrieves data stored previous on disk}
      end;    {case}
    end;    {If}
end;      {Input}
```

PROGRAM SCOPE TRANSFER

```
Program ScopeTransfer;
{This program transfer waveform data from the TEK
2430 oscilloscope to ASCII files. }

{tpdecl.pas} {Include file from National Instrum}
Const
     ERR  = $8000;      (* Error detected        *)
     TIMO = $4000;      (* Timeout               *)
     SRQI = $1000;      (* SRQ detected          *)
     RQS =  $800;       (* Device needs service *)
     DataFile1 = 'C:\TURBO\DATA\REF1.DAT';
                        (* Data file 1           *)
     DataFile2 = 'C:\TURBO\DATA\REF2.DAT';
                        (* Data file 2           *)
     DataFile3 = 'C:\TURBO\DATA\REF3.DAT';
                        (* Data file 3           *)
     DataFile4 = 'C:\TURBO\DATA\REF4.DAT';
                        (* Data file 4           *)
     DataFile5 = 'C:\TURBO\DATA\CH1.DAT';
                        (* Data file 3           *)
     DataFile6 = 'C:\TURBO\DATA\CH2.DAT';
                        (* Data file 4           *)
Var
     control,i,k,max : integer;
     scope : integer;
     cmd : iobuf;
     ScopeCntr : ibstring;
     WaveForm : file of byte;

(*************************************************)

(*------------------FUNCTIONS------------------*)

     function itohex (i:integer):str4;
          (* Convert integer to hex string. *)
     var  k,nib:integer; s:string[4];
     begin
       k := 12;  s := '';
       while (k >= 0) do begin
          nib := (i shr k) and $f;
          if ($A <= nib) and (nib <= $F)
             then nib := nib + $37
             else nib := nib + $30;
          s := s + chr(nib);
          k := k - 4;
       end;      {while}
       itohex := s;
     end;              {itohex}

(*----------------PROCEDURES-------------------*)

(*--------------WAIT PROCEDURE-----------------*)
     procedure Wait;
```

```
    (*this procedure put a wait in the program*)
    begin
        Repeat until KeyPressed;
    end;                {Wait}
(*--------ERROR DECODING PROCEDURES------------*)

    procedure prvars (ibsta:integer;iberr:integer;
                      ibcnt:integer);
    var  stas : string[4];
    begin
        stas := itohex(ibsta);
        writeln('ibsta=0x',stas,'iberr=0x',
                iberr,'ibcnt=0x',ibcnt);
    end;                {prvars}

    procedure finderr;
      (* This routine would notify you that the
         ibfind call failed and refer you to the
         driver software configuration
         procedures.                          *)
     begin
        writeln (' Find error');
     end;               {finderr}

    procedure error;
    (* This routine would, among other things,
       check iberr to determine the exact cause of
       the error condition and then take action
       appropriate to the application. For errors
       during data transfers, ibcnt may be
       examined to determine the actual number of
       bytes transferred.                       *)

    begin
        writeln (' Error');
        prvars (ibsta,iberr,ibcnt);
    end;                {error}

   (*---PROCEDURE TO INITIALIZE SCOPE TRANSFER--*)
    procedure Init;
    (* This procedure initialize the scope and
                                  gpib interface *)
    begin
    (* Assign a unique identifier to the interface
       board "GPIB0" and to the device "SCOPE24"*)
       control := ibfind ('GPIB0');
       scope   := ibfind ('SCOPE24');
       if (control < 0) then finderr;
       if (scope < 0) then finderr;
       (* Send the Interface Clear message *)
       ibsic (control);
       ibclr (scope);
       (* Check for an error on each GPIB call  *)
       if ((ibsta AND ERR) <> 0) then error;
     end;               {Init}

   (*---PROCEDURE TO CONVERT CONTROL STRING----*)

    procedure ControlScope (CntrStr : ibstring);
    (*This procedure generate the control
      buffer array cns from the control string
      CntrStr and write the command to the scope*)
    var cns : iobuf;
        max : integer;
    begin
        max:=Length(CntrStr);
        for i:=1 to max do
        cns[i]:=Copy(CntrStr,i,1);
        ibwrt(scope,cns,max);
        if ((ibsta AND ERR) <> 0) then error;
    end;                { ControlScope}

    (*----------DATA INPUT FROM SCOPE----------*)

    procedure ScopeRead(FileName:ibstring);
    (*This procedure read data from scope and
      store it on file        *)
    begin
        ibrdf(scope,FileName);
    end;                {ScopeRead}

    (*----------PROCEDURE FILE READ-----------*)

    procedure FileRead(FileName:ibstring);
    (*This procedure read a data file from disk*)
    var  Greep:byte;
         Karakter:string[1];
         k:integer;
    begin
         Assign(WaveForm, FileName);
         Reset(Waveform);
         repeat
           read(WaveForm,Greep);
           Karakter:= chr(Greep);
           write(Karakter);
           until karakter = ';';
         close(Waveform);
         Wait;
    end;                {FileRead}


    (*-------PROCEDURE READ ALL SIGNALS--------*)
    procedure ReadAll;

    begin
        ScopeCntr:=('WAV?; DAT ENC:ASC,SOU:REF1');
        ControlScope(ScopeCntr);
        ScopeRead(DataFile6);
        ScopeCntr:=('WAV?; DAT ENC:ASC,SOU:REF2');
        ControlScope(ScopeCntr);
        ScopeRead(DataFile1);
        ScopeCntr:=('WAV?; DAT ENC:ASC,SOU:REF3');
        ControlScope(ScopeCntr);
        ScopeRead(DataFile2);
        ScopeCntr:=('WAV?; DAT ENC:ASC,SOU:REF4');
        ControlScope(ScopeCntr);
        ScopeRead(DataFile3);
        ScopeCntr:=('WAV?; DAT ENC:ASC,SOU:CH1');
        ControlScope(ScopeCntr);
        ScopeRead(DataFile4);
        ScopeCntr:=('WAV?; DAT ENC:ASC,SOU:CH2');
        ControlScope(ScopeCntr);
        ScopeRead(DataFile5);
        ScopeCntr:=('WAV?; DAT ENC:ASC,SOU:REF1');
        ControlScope(ScopeCntr);
        ScopeRead(DataFile6);
    end;                {ReadAll}

(*****************MAIN PROGRAM*********************)

 begin
     Init;
     ReadAll;
     FileRead(DataFile1);
     FileRead(DataFile2);
     FileRead(DataFile3);
     FileRead(DataFile4);
     FileRead(DataFile5);
     FileRead(DataFile6);
end.                    {ScopeTransfer}
```

PROGRAM ASCII TRANSFER

```
PROGRAM TRANSFER (input,output);
{This program transfer ASCII data to a record file}
Const
   File1 = 'C:\TURBO\DATA\CH1.DAT'; (*Data file 1*)
   File2 = 'C:\TURBO\DATA\CH2.DAT'; (*Data file 2*)
   File3 = 'C:\TURBO\DATA\DATA4.DAT';
                              (*Record data file 1*)
   Chan1Scale = 300; (* Scale chan 1 to V/div    *)
   Chan2Scale = 50;  (* Scale chan 2 to A/div    *)
   TimeBase = 5.0E-3; (*Time base set at 5ms/div *)
Type
```

```
    DataRecord = record
                   time,channel1,channel2:real;
                 end;       {DataRecord}
    DataFile = file of DataRecord;
    IbString = String[50];
Var
    Waveform : file of byte;
    Y1Chan, Y2Chan : array [1..1024] of real;
    i,k,max : integer;
    Ch,Ch1 : char;
    RecordMat : DataFile;
    DataRec : DataRecord;
    DataFile1 : IbString; (* Data file 1      *)
    DataFile2 : IbString; (* Data file 2      *)
    DataFile3 : IbString; (* Record file 1    *)
    VoltageScale : Real; (* Scale ch 1 V/div  *)
    CurrentScale : Real; (* Scale ch 2 A/div  *)
    XINCR : Real; (* Time base set at ms/div  *)

(*************************************************)
(*-----------------PROCEDURES--------------------*)
(*----------------WAIT PROCEDURE-----------------*)

Procedure Wait;
(* This procedure put a wait in the program. *)
begin
   Repeat until KeyPressed;
end;              {Wait}

(*--------PROCEDURE FOR INPUT OF ASCII FILES-----*)

 Procedure Input;
 (*This procedure assign data files to be converted
                          to a typedef file     *)
 var  k:integer;
      procedure ShowSetup;
      begin
          For k:=0 to 3 do Writeln;
          Writeln('  THE SETUP IS AS FOLLOWS');
          For k:=0 to 2 do Writeln;
          Writeln(' 1. Voltage File : ',Datafile1);
          Writeln(' 2. Current File : ',Datafile2);
          Writeln(' 3. Record File : ',DataFile3);
          Writeln(' 4. Voltage Scale :
                        ',VoltageScale,' V/div');
          Writeln(' 5. Current Scale :
                        ',CurrentScale,' A/div');
          Writeln(' 6. Time : ',XINCR*50,' sec');
          Writeln; Writeln;
      end; { ShowSetup }

(*-----------------------------------------------*)
 begin
    ClrScr;
    Writeln('*************************************');
    Writeln('*THIS PROGRAM READ A VOLTAGE AND
                              CURRENT ASCII FILE*');
    Writeln('* AND CONVERT THEM TOGETHER WITH TIME
                                 INCREMENTS   *');
    Writeln('*INTO A t,u,i RECORD FILE FOR USE IN
                               OTHER PROGRAMS*');
    Writeln('*************************************');
    For k:=0 to 3 do Writeln;
    repeat
        Writeln('SHOULD SETUP BE READ? (Y,N)');
        readln(ch);
    until Upcase(ch) in ['Y','N'];
    ClrScr;
    If ((ch = 'Y') or (ch = 'y')) then begin
        DataFile1 := File1; DataFile2 := File2;
        DataFile3 := File3;
        VoltageScale := Chan1Scale;
        CurrentScale := Chan2Scale;
        XINCR := TimeBase/50;
        ShowSetup;
    end; { If }
    Writeln; Writeln; Ch1 := 'Y'; ch := 'N';
    repeat
        repeat
            Writeln('SHOULD ANY PARAMETER 1-6 BE
                                  CHANGED? (Y,N)');
            readln(ch);
        until Upcase(ch) in ['N','Y'];
        If ((ch = 'Y') or (ch = 'y')) then begin
           Writeln; Writeln;
           repeat
              Writeln('WHICH PARAMETER SHOULD
                              BE CHANGED? (1-6)');
              readln(ch);
           until ch in ['1','2','3','4','5','6'];
           Case ch of
             '1' : begin
                     Writeln('New Voltage File');
                     Writeln('C:\TURBO\DATA\
                                    XXXXX.DAT');
                     readln(DataFile1);
                     DataFile1:=Concat('C:\TURBO\
                         DATA\',DataFile1,'.DAT');
                   end;  { Case 1 }
             '2' : begin
                     Writeln('New Current File');
                     Writeln('C:\TURBO\DATA\
                                     XXXXX.DAT');
                     readln(DataFile2);
                     DataFile2:=Concat('C:\TURBO\
                          DATA\',DataFile2,'.DAT');
                   end;  { Case 2 }
             '3' : begin
                     Writeln('New Record File');
                     Writeln('C:\TURBO\DATA\
                                    XXXXX.DAT');
                     readln(DataFile3);
                     DataFile3:=Concat('C:\TURBO\
                          DATA\',DataFile3,'.DAT');
                   end;  { Case 3 }
             '4' : begin
                     Writeln('New Voltage Scale
                            ( ',VoltageScale,' )');
                     readln(VoltageScale);
                   end;  { Case 4 }
             '5' : begin
                     Writeln('New Current Scale
                            ( ',CurrentScale,' )');
                     readln(CurrentScale);
                   end;  { Case 5 }
             '6' : begin
                     Writeln('New Time Base
                              ( ',Xincr*50,' )');
                     readln(Xincr);
                        Xincr := Xincr/50;
                   end;  { Case 6 }
           end;  { Case }
           ShowSetup;
           repeat
             Writeln('SHOULD ANOTHER PARAMETER
                          1-6 BE CHANGED? (Y,N)');
             readln(ch1);
           until Upcase(ch1) in ['N','Y'];
        end  { If }
        else begin
           ch1 := 'N';
           ClrScr;
           ShowSetup;
        end;  { else }
    until Upcase(ch1) in ['N'];
end; { Input }

(*------------PROCEDURE FILE READ---------------*)

    procedure FileRead(FileName:IbString);
    (*This procedure read a data file from disk.*)
        var  Greep:byte;
             Karakter:string[1];
             k:integer;
        begin
             Assign(Waveform, FileName);
```

```
            Reset(Waveform);
            repeat
               read(Waveform,Greep);
               Karakter:= chr(Greep);
               write(Karakter);
            until eof(Waveform);
            close(Waveform);
         end;          {FileRead}

(*----------PROCEDURE TO ORGINIZE DATA----------*)

    procedure DataOrg;
    (*This procedure read the ASCI data files from
      disk and organize it in real calibrated
      arrays Y1Chan and Y2Chan, callibrated     *)
    type
       DataArrayI = array [1..1024] of integer;
       DataArrayC = array [1..4500] of char;
       CharByte = String[4];
    var
       Y1Data, Y2Data : DataArrayI;
    procedure IntegerTransfer(FileName:ibstring;
              var YData:DataArrayI);

    var  Greep:byte;
         Char1:CharByte;
         Result,Value,i,j,k,
         Points:integer;
         Data:DataArrayC;

    begin
        writeln(FileName);
        Assign(Waveform, FileName);
        Reset(Waveform);
        repeat
          read(Waveform,Greep);
          Char1:= chr(Greep);
        until (Char1 = ';') or (eof(Waveform));
        for i:=1 to 5 do read (Waveform,Greep);
        k:=1;
        repeat
          read(Waveform,Greep);
          Data[k]:= chr(Greep);
          k:=k+1;
        until eof(Waveform);
        close(Waveform);
        Points:=k;
        j:=0;  i:=1;
        While i<=Points do begin
            k:=0; Char1:='';
            while (Data[i+k]<> ',')  do begin
               Char1:= Concat(Char1,Data[i+k]);
               k:=k+1;
            end;     {while}
            i:=i+k;
            val(Char1,Value,Result);
            YData[j]:=Value;
            j:=j+1; i:=i+1;
        end;      {while}
        end;              {IntegerTransfer}

        (*-----------------------------------*)
         procedure ScaleData;

            var Y1Scale,Y2Scale:real;

            begin
                Y1Scale:=VoltageScale/25;
                Y2Scale:=CurrentScale/25;
                for i:=1 to 1022 do begin
                    Y1Chan[i]:=Y1Data[i]*Y1Scale;
                    Y2Chan[i]:=Y2Data[i]*Y2Scale;
                end;   {for}
            end;              {ScaleData}

         (*-----------------------------------*)

         begin
            IntegerTransfer(DataFile1,Y1Data);
            IntegerTransfer(DataFile2,Y2Data);
            ScaleData;
        end;              {DataOrg}


(*------------PROCEDURE RECORDFILE-------------*)

    procedure RecordFile;
    (* This procedure write the data to a record
       file and store it on disk                *)
    begin
        Assign(RecordMat,DataFile3);
        Rewrite(RecordMat);
        for i:=1 to 1022 do begin
          with DataRec do begin
             time := (i-1)*XINCR;
             channel1 := Y1Chan[i];
             channel2 := Y2Chan[i];
             write(RecordMat,DataRec);
          end;    {with}
        end;     {for}
        close(RecordMat);
        Writeln(DataFile3);
    end;       {RecordFile}

(*---------PROCEDURE RECORDFILE READ------------*)

    procedure RecordFileRead(FileName:ibstring);
    (*This procedure read a record file.        *)
    var
        X,Y1,Y2:array [1..1024] of real;
        Karakter:string[1];
        XTime,CH1,CH2:real; k:integer;
    begin
        Assign(RecordMat, FileName);
        Reset(RecordMat); i:=1;
        repeat
          with DataRec do begin
             time:=XTime;
             channel1:=CH1; channel2:=CH2;
             read(RecordMat,DataRec);
             X[i]:=Time;
             Y1[i]:=Channel1; Y2[i]:=Channel2;
          end;    {with}
          i:=i+1;
        until eof(RecordMat);
        close(RecordMat);
    end;              {RecordFileRead}

(*******************MAIN PROGRAM*******************)
begin
    Input;
    DataOrg;
    RecordFile;
end.                  {ScopeControl}
```

B2: TURBO PASCAL PROGRAMS TO CONTROL THE DYNAMIC POWER FILTER

This program (CONTROL) takes measurements of the voltage and current signals, sample them at 6,6 kHz and read the data in the computer with a 12-bit A-D PC-card. After the correlation algorithm is performed, the power components are calculated and the network parameters are derived, a Kalman based estimation algorithm (KALMAN) is performed on the equivalent network parameters G,B. These estimated values form the output after a 12-bit D-A conversion. These estimated parameters are then used to derive the instantaneous value of the reference current i_{fs} or i_{ds}.

PROGRAM CONTROL

```
{************************************************}
{*   PROGRAM TO CALCULATE G AND B OF A GIVEN    *}
{*   WAVEFORM. THIS PROGRAM IS USED TO CONTROL  *}
{*   THE DPF. IT USES A PC-30 A/D AND D/A CARD. *}
{*   The base address of the PC-30 card must be *}
{*   selected 700 H.                            *}
{*   created  by J.H.R. ENSLIN July 1987        *}
{*   The A-D and D-A is done in the include file.*}
{************************************************}
PROGRAM CorrelationControl;

{$C-}
{$I PC30JHE.INC}  { The A-D and D-A include file }
Const
      Pi =3.14159265358979;            {Pi}
      Pi2=6.28318530717959;            { 2*Pi }
      VoltageScale = 34;
      CurrentScale = 2;
Type
      String_20 = String[20];
      Dim = Array[-2..200] of Real;
      Dim2 = Array[-200..200] of Real;
      DataRecord = record
                     Cnt,Ho,Mi,Se,Fr:Integer;
                     Unn,Inn,Lp,Pa,Fp,Rp,Dp,Yn,
                     Gn,Bn,Dn,Gnp,Bnp:Real;
                   end;       {DataRecord}
      DataFile = file of DataRecord;
Var
      RecordMat : DataFile;
      DataRec : DataRecord;
      Ch:Char;
      Irms,Urms,Rpeak:Real;
      Pactive,Preactive,Pload,
      Pnonactive,Pdeactive:Real;
      Conductance,PredCond,
      Susceptance,PredSus:Real;
      Disceptance,PredDis,PrevPreDis:Real;
      PrevPreCond,PrevPreSus,Gscale,Bscale:Real;
      First,Last,Max,PlotCount,
      GraphCount,Count:Integer;
      Rui:Dim2;
      VoltageArray,CurrentArray:DataArray;
      DataFileName,ScreenName:StringType;

{$I KALMAN.MND} { The estimation include file }

{************************************************}
{*----------------ANALOG-DIGITAL---------------*}

Procedure Analog_Digital; {Calls the A-D procedure}
Begin
    HighSpeedSample(VoltageArray, CurrentArray);
    PlotPoints(VoltageArray,CurrentArray);
End;   {Analog_Digital}

{*------------------SEEKWINDOW-----------------*}

Procedure SeekWindow(Mat:DataArray);
{Derive the appropriate measurement window}

var
    i,j,l:integer;
    Tydelik:dim;
begin
    l:=0;
    While Mat[l]<0 do l:=l+1;   l:=l+1;
    For i:=1 to 3 do begin
       While Mat[l]<0 do l:=l+1;
       While Mat[l]>=0 do l:=l+1;  l:=l+1;
    end;
    First:=l;   l:=l+1;
    For i:=1 to 1 do begin
       While Mat[l]<0 do l:=l+1;
       While Mat[l]>=0 do l:=l+1;  l:=l+1;
    end;
    Last:=l;
    Max:=Last-First;
end;     {SeekWindow}

{*------------AUTOCORRELATION Rxx[0]-----------*}

Procedure AutoCor(MatPoints:DataArray;
                  var Awgk:real);
{This procedure implements a discrete auto-
 correlation of the voltage or current waveforms to
 form a rms value of current and voltage. The auto-
 correlation is as follows:
 Awgk = SQRT(1/N*(sum A(j)*A(j))), with N the
 total data points between the limits 0 and N.}
var
    j:integer;
    Temp:dim;
begin
    Temp[-1]:=0;
    For j:=0 to Max-1 do
    Temp[j]:= MatPoints[First+j]*MatPoints[First+j]
                                    + Temp[j-1];
    Awgk:= SQRT(Temp[Max-1]/(Max-0.5));
```

```
end; {AutoCor}

{*------------CROSS-CORRELATION Rui[tau]--------*}

Procedure CrossCor(Voltage,Current:DataArray);
{This procedure implements a discrete power
 correlation of the voltage and current waveforms
 to form a time correlated power function.  The
 correlation is as follows:
 Rui(k):=1/N*(sum Un(j)*In(j-k)), with N the total
 data points between the limits 0 and N.}
var
    i,j,k:integer;
    Temp:dim;
begin
    For k:=-Max to Max do Rui[k]:=0;
    For k:=-Max to Max do begin
      For j:= 0 to Max-1 do begin
        Temp[j]:= Voltage[First+j]
                                *Current[First+j-k];
         Rui[k]:= Rui[k] + Temp[j];
      end; {For}
      Rui[k]:=Rui[k]/(Max-0.6);
    end; {For}
end; {CrossCor}

{*------GET THE PEAK IN THE CROSS-CORRELATION----*}
Function CorPeak:Real;
Var Temp:Real; i:Integer;
begin
     Temp:=ABS(Rui[-Max+10]);
     For i:=-(Max-11) to (Max-11) do
     If Temp<=ABS(Rui[i]) then Temp:=ABS(Rui[i]);
     CorPeak:=Temp;
end;           { CorPeak }

{*-------PROCEDURE TO PLOT POWER RESULTS---------*}

Procedure PrintPower;
Var  Unn,Inn,S,P,F,Q,D,Y,G,B,K,pG,ppG,pB,
     ppB,pK:Real; i:Integer;
Begin
     TextMode;
     Unn:=Urms*VoltageScale;
     Inn:=Irms*CurrentScale;
     S:=Pload*CurrentScale*VoltageScale;
     F:=Pnonactive*CurrentScale*VoltageScale;
     P:=Pactive*CurrentScale*VoltageScale;
     Q:=Preactive*CurrentScale*VoltageScale;
     D:=Pdeactive*CurrentScale*VoltageScale;
     G:=Conductance*CurrentScale/VoltageScale;
     B:=Susceptance*CurrentScale/VoltageScale;
     Y:=S/(SQR(Urms*VoltageScale));
     K:=SQRT(ABS(SQR(Y)-SQR(G)-SQR(B)));
     pG:=PrevPreCond*CurrentScale/VoltageScale;
     pB:=PrevPreSus*CurrentScale/VoltageScale;
     ppG:=PredCond*CurrentScale/VoltageScale;
     ppB:=PredSus*CurrentScale/VoltageScale;
     ClrScr;
     Puts(25,5,'POWER AND NETWORK PARAMETERS');
     writeln;
     Writeln('     ','Effective Voltage Urms  =
                                  ',Unn:4:0,' V');
     Writeln('     ','Effective Current Irms  =
                                  ',Inn:4:2,' A');
     Writeln;
     Writeln('     ','Loading Power    S  =
                                   ',S:5:0,' VA');
     Writeln('     ','Active Power     P  =
                                   ',P:5:0,' W');
     Writeln('     ','Fictitious Power F  =
                                  ',F:5:0,' VA');
     Writeln;
     Writeln('     ','    Reactive Power Q =
                                  ',Q:5:0,' VA');
     Writeln('     ','    Deactive Power D =
                                  ',D:5:0,' VA');
     Writeln;
     Writeln('     ','       Admittance  Y =
                                    ',Y*1000:5:1,' mS');
     Writeln('     ','       Conductance G =
                                    ',G*1000:5:1,' mS');
     Writeln('     ','       Susceptance B =
                                    ',B*1000:5:1,' mS');
     Writeln('     ','       Disceptance K =
                                    ',K*1000:5:1,' mS');
     Writeln;
     Writeln('     ','     Previous Predictions');
     Writeln('     ','     Conductance 'G =
                                    ',pG*1000:5:1,' mS');
     Writeln('     ','     Susceptance 'B =
                                    ',pB*1000:5:1,' mS');
     Writeln;
     Writeln('     ','     Present Predictions');
     Writeln('     ','     Conductance 'Gn =
                                    ',ppG*1000:5:1,' mS');
     Writeln('     ','      Susceptance 'Bn =
                                    ',ppB*1000:5:1,' mS');
     Writeln;
end;    {PrintPower}

{*----------POWER COMPONENTS CALCULATION---------*}

Procedure PowerComp;
Var
    Temp1,Temp2:Real;
begin
     Pload:=Urms*Irms;
     Pactive:=Rui[0];
     Temp1:=SQR(Pload) - SQR(Pactive);
     Pnonactive:=SQRT(ABS(Temp1));
     Temp2:=SQR(Rpeak) - SQR(Pactive);
     Preactive:=SQRT(ABS(Temp2));
     Pdeactive:=SQRT(ABS(Temp1 - Temp2));
     Conductance:=Pactive/(Urms*Urms);
     Susceptance:=Preactive/(Urms*Urms);
     Disceptance:=Pdeactive/(Urms*Urms);
     If count >= 1 then begin
        PrevPreCond:=PredCond; PrevPreSus:=PredSus;
        KALMAN(Conductance,Susceptance,
               PredCond,PredSus,Count);
        { PrintPower;}
     end   {then}
     else begin
          PrevPreCond:=Conductance;
          PrevPreSus:=Susceptance;
          Gscale:=381*(Conductance*CurrentScale)
                                  /(2*VoltageScale);
          Bscale:=345*(Susceptance*CurrentScale)
                                  /(2*VoltageScale);
     end;    {else}
     If count>= 3 then begin
        If ((ABS(ABS(PredCond)
           -ABS(Conductance))>10.0E-02) or
           (ABS(ABS(PredSus)
           -ABS(Susceptance))>10.0E-02)) then begin
             PredCond:=Conductance;
             PredSus:=Susceptance;
        end;   {if}
        Gscale:=381*(Conductance*CurrentScale)
                                  /(2*VoltageScale);
        Bscale:=345*(Susceptance*CurrentScale)
                                  /(2*VoltageScale);
     end  {then}
     else begin
          Gscale:=381*(Conductance*CurrentScale)
                                  /(2*VoltageScale);
          Bscale:=345*(Susceptance*CurrentScale)
                                  /(2*VoltageScale);
     end;  {else}
 end;        { PowerComp }

{*--------------INITIALIZE GRAPHICS------------*}

Procedure PlotInit;
begin
```

```
    GraphColorMode;
    Palette(2); Xaxis(319,40,186,50,3,0,50);
    Yaxis(40,186,16,3,0,100,0.1);
    Draw(30,90,639,90,3);
    Yaxis(40,90,16,3,0,0,0.1);
    Draw(55,12,65,12,1); Puts(10,2,'G');
    Draw(90,12,100,12,2); Puts(14,2,'^G');
    Draw(55,108,65,108,1); Puts(10,14,'B');
    Draw(90,108,100,108,2); Puts(14,14,'^B');
    Puts(10,1,'CONDUCTANCE (G) IN 0.1*SIEMENS');
    Puts(10,13,'SUSCEPTANCE (B) IN 0.1*SIEMENS');
end;    {PlotInit}

{*----------PLOT OF NETWORK PARAMETERS----------*}

Procedure PlotGB;
Var  Temp1,Temp2:Integer;
begin
     GraphWindow(40,10,639,90);
     Temp1:=Round((80 - (Conductance*CurrentScale
                         *1600/VoltageScale)));
     Temp2:=Round((80 - (PrevPreCond*CurrentScale
                         *1600/VoltageScale)));
     Plot(PlotCount,Temp2,2);
     Plot(PlotCount,Temp1,1);
     GraphWindow(40,106,639,186);
     Temp1:=Round((80 - (Susceptance*CurrentScale
                         *1600/VoltageScale)));
     Temp2:=Round((80 - (PrevPreSus*CurrentScale
                         *1600/VoltageScale)));
     Plot(PlotCount,Temp2,2);
     Plot(PlotCount,Temp1,1);
     PlotCount:=PlotCount+1
 end;        { PlotGB }

{*-------SAVE THE LAST SCREEN ON DISK-----------*}

Procedure ScreenSave;
   Var Temp:Char;

   begin
       Temp:=Char(GraphCount+47);
       ScreenName:=Concat('C:\TURBO\DATA\
                           CONTR_',Temp,'.SCR');
       GraphCount:=GraphCount + 1;
   end;        { ScreenSave }

{*----------PROCEDURE RECORDFILE OPEN----------*}

Procedure RecordFileOpen;
{ This procedure opens a record file to store the
  data on disk.      }
var  Temp:Char;
begin
     Temp:=Char(GraphCount+47);
     DataFileName:=Concat('C:\TURBO\DATA\
                           CONTR_',Temp,'.DAT');
     Assign(RecordMat,DataFileName);
     Rewrite(RecordMat);
end;       {RecordFileOpen}

{*-------PROCEDURE READ TIME FROM MS-DOS---------*}

Procedure Timer(var Hour,Min,Sec,Frac:Integer);
type
    RegPack = Record
                AX,BX,CX,DX,BP,SI,DI,
                DS,ES,Flags:Integer;
              end;  {record}
var
   Regs:Regpack;
begin
     with Regs do begin
          AX := $2C00;
          MsDos(Regs);
          Hour := Hi(CX);
          Min := Lo(CX);
          Sec := Hi(DX);
          Frac := Lo(DX);
       end;   {with}
end;   {Timer}

{*-----------PROCEDURE RECORDFILE--------------*}

Procedure StoreRecord;
{ This procedure write a record of data to the
  record file  }
var
   hour,min,sec,frac,i:integer;
begin
    Timer(hour,min,sec,frac);
    with DataRec do begin
      Cnt := Count;
      Ho := hour; Mi := min; Se := sec; Fr := Frac;
      Unn:=Urms*VoltageScale;
      Inn:=Irms*CurrentScale;
      Lp := Pload*CurrentScale*VoltageScale;
      Pa := Pactive*CurrentScale*VoltageScale;
      Fp := Pnonactive*CurrentScale*VoltageScale;
      Rp := Preactive*CurrentScale*VoltageScale;
      Dp := Pdeactive*CurrentScale*VoltageScale;
      Yn := Lp/(SQR(Urms*VoltageScale));
      Gn := Conductance*CurrentScale/VoltageScale;
      Bn := Susceptance*CurrentScale/VoltageScale;
      Dn := SQRT(ABS(SQR(Yn)-SQR(Gn)-SQR(Bn)));
      Gnp := PredCond*CurrentScale/VoltageScale;
      Bnp := PredSus*CurrentScale/VoltageScale;
      write(RecordMat,DataRec);
    end;    {with}
end;       {StoreRecord}

{*----------PROCEDURE RECORDFILE READ----------*}

Procedure RecordFileRead(FileName:StringType);
{ This procedure read a record file from disk. }
var
  temp1,temp2,temp3,temp4,temp5,
  count,hour,min,sec,frac,i:integer;
  temp6,temp7,temp8,temp9,temp10,temp11,temp12,
  temp13,temp14,temp15,temp16,temp17,temp18,
  Une,Ine,S,P,F,Q,D,Y,G,B,K,Gp,Bp:real;
begin
     Assign(RecordMat, FileName);
     Reset(RecordMat);
     repeat
       with DataRec do begin
          Cnt:=temp1;
          Ho:=temp2; Mi:=temp3; Se:=temp4;
          Fr:=temp5; Unn:=temp6; Inn:=temp7;
          Lp:=temp8; Pa:=temp9; Fp:=temp10;
          Rp:=temp11; Dp:=temp12;
          Yn:=temp13; Gn:=temp14; Bn:=temp15;
          Dn:=temp16; Gnp:=temp17; Bnp:=temp18;
          read(RecordMat,DataRec);
          count:=Cnt; hour:=Ho; min:=Mi; sec:=Se;
          frac:=Fr; Une:=Unn; Ine:=Inn; S:=Lp;
          P:=Pa; F:=Fp; Q:=Rp; D:=Dp; Y:=Yn; G:=Gn;
          B:=Bn; K:=Dn; Gp:=Gnp; Bp:=Bnp;
          ClrScr;
          Puts(25,5,'POWER AND NETWORK
                                  PARAMETERS');
          For i:=0 to 1 do writeln;
          Writeln(' ','Data point: ',Count,
                  '  Time: ',hour,':',min,':',
                                  sec,':',Frac);
          Writeln;
          Writeln('     ','Effective Voltage Urms
                                  = ',Une:4:0,' V');
          Writeln('     ','Effective Current Irms
                                  = ',Ine:4:2,' A');
          Writeln;
          Writeln('     ','Loading Power    S  =
                                  ',S:5:0,' VA');
          Writeln('     ','Active Power     P  =
                                  ',P:5:0,' W');
          Writeln('     ','Fictitious Power F  =
```

```
                                    ',F:5:0,' VA');
          Writeln;
          Writeln('     ',' Reactive Power Q =
                                    ',Q:5:0,' VA');
          Writeln('     ',' Deactive Power D =
                                    ',D:5:0,' VA');
          Writeln;
          Writeln('     ','   Admittance  Y =
                                  ',Y*1000:5:1,' mS');
          Writeln('     ','    Conductance G =
                                  ',G*1000:5:1,' mS');
          Writeln('     ','    Susceptance B =
                                  ',B*1000:5:1,' mS');
          Writeln('     ','    Disceptance K =
                                  ',K*1000:5:1,' mS');
          Writeln;
          Writeln('     ',' Prediction of
                                 Network parameters');
          Writeln;
          Writeln('     ','      Conductance ^G =
                                  ',Gp*1000:5:1,' mS');
          Writeln('     ','      Susceptance ^B =
                                  ',Bp*1000:5:1,' mS');
          Wait;
        end;    {with}
      until (eof(RecordMat));
      close(RecordMat);
end;        {RecordFileRead}
{************************************************}
{            M A I N     P R O G R A M           }
{************************************************}

BEGIN
   PORT[$703] := $92;  {Initialization of A/D  PPI}
   PORT[$70B] := $9B;  {Initialization Port A,B,C }
   ClrScr;
   Digital_Analog(3.0,0);
   Analog_Digital;
   CH := ' ';
   PlotCount:=0; Count:=0; GraphCount:=1;
   REPEAT
     PlotInit;
     RecordFileOpen;
     Repeat
       HighSpeedSample(VoltageArray,CurrentArray);
       SeekWindow(VoltageArray);
       AutoCor(VoltageArray,Urms);
       AutoCor(CurrentArray,Irms);
       CrossCor(VoltageArray,CurrentArray);
       Rpeak:=CorPeak;
       PowerComp;
       StoreRecord;
       Count:=Count+1;
       Digital_Analog(Gscale,Bscale);
       If count>=3 then PlotGB;
       If KeyPressed then Read(kbd,ch);
     until ((Plotcount>=280)or(ch='e')or(ch='E'));
     ScreenSave;
     close(RecordMat);
     PlotCount:=0; Count:=2;
   UNTIL ((ch = 'E') or (ch = 'e'));
   RecordFileRead(DataFileName); wait1;
   GraphColorMode; Palette(2);  {HiRes;}
   LoadScreen(ScreenName);
   Wait1;
END.
```

PROGRAM PC30JHE

```
{************************************************}
{*   INCLUDE PROCEDURE TO PLOT, DO A-D AND D-A   *}
{*   FOR THE CONTROL PROGRAM, CONTROLLING THE    *}
{*   DYNAMIC POWER FILTER.                       *}
{*   created  by J.H.R. ENSLIN July 1987.        *}
{************************************************}

Const
    Xmax         = 700;
    BoardAddress = $700;
    GrafBase = $8800;
Type
    DataArray = Array[0..Xmax] of Real;
    StringType = String[80];
    ScreenType=array [0..8400] of integer;
    ScreenPointer=^ScreenType;
{************************************************}
Procedure Wait1; {Wait Procedure}
  Var Ch1:Char;
  Begin
      Repeat Read(Ch1) until ch1 = ' ';
  End;    {Wait1}
{************************************************}
Procedure Wait;
  Begin
      Repeat until (KeyPressed);
  End;    {Wait}
{************************************************}
Procedure Puts (x,y:Integer;  Str:StringType);
  Begin      {Puts string on screen}
      GOTOXY (x,y);
      Write(Str);
  End;    {Puts}
{************************************************}
Procedure SaveScreen(FileName:StringType);
{ Save screen on disk }
  type PicFile=file of ScreenType;
  var picture:ScreenPointer;
      PictureFile:PicFile;
  begin
    picture:=ptr(GrafBase,0);
    assign(PictureFile,FileName);
    {$I-} rewrite(PictureFile); {$I+}
    {$I-} write(PictureFile,picture^); {$I+}
    {$I-} close(PictureFile); {$I+}
  end; { SaveScreen }
{************************************************}
Procedure LoadScreen(FileName:StringType);
{ Load screen from file }
  type PicFile=file of ScreenType;
  var picture:ScreenPointer;
      PictureFile:PicFile;
  begin
    picture:=ptr(GrafBase,0);
    assign(PictureFile,FileName);
    {$I-} reset(PictureFile); {$I+}
    read(PictureFile,picture^);
    close(PictureFile);
  end;  { LoadScreen }
{************************************************}
Procedure Beep;  { Make beep sound }
  Begin
      Sound(500); Delay(150); Nosound;
  End;    {Beep}
{************************************************}
Procedure YAXIS (xposition,yposition,
                 incrDisplacement,color:INTEGER;
                 yzero,ymax,increment:REAL);
{PROCEDURE YAXIS draws a yaxis on the 640 x 200
screen. Xposition and yposition are the zero points
of the graph; incrDisplacement is the displacement
per given increment in points on the screen. Yzero
is the y-value at point zero of the graph; ymax is
the max y value increment is the increment of num-
bering of the yaxis.  0,199 is bottom left corner}
VAR
   x,xplot,yplot:INTEGER; y,z:REAL;
BEGIN
   z:=incrDisplacement/4; x:= xposition;
   y:= yposition;
   REPEAT
     yplot := ROUND (y);
     PLOT (x,yplot,color); y:= y - z;
   UNTIL y <= ymax ;
   x:= xposition; yplot:= yposition;
```

```
    REPEAT
      DRAW (x-3,yplot,x+3,yplot,color);
      yplot:= yplot - incrDisplacement;
    UNTIL yplot <= ymax;
    yplot := ROUND (yposition/8);
    y := yplot; z:= incrDisplacement/8;
    REPEAT
      GotoXY (1,yplot+1); Write (yzero:3:1);
      yzero := (yzero + increment); y := y - z;
      yplot := ROUND(y);
    UNTIL ((yplot < 1) or (yplot<= ymax/8));
  END;  { YAXIS }
{***********************************************}
Procedure XAXIS (Pixels,xposition,yposition,
                 incrDisplacement, color:INTEGER;
                 xzero,increment:REAL);
{ XAXIS draws a yaxis on the 640 x 200 screen.
Xposition and yposition are the zero points of the
graph; incrDisplacement is the displacement per
given increment in points on the screen. Xzero is
the x-value at point zero of the graph; increment
is the increment of numbering of the yaxis. }
VAR
   xplot,yplot:INTEGER; x,y,z:REAL;
BEGIN
   z := incrDisplacement/10;
   x := xposition;
   REPEAT
     xplot := ROUND (x);
     PLOT (xplot,yposition,color); x := x+z;
   UNTIL xplot> Pixels;
   xplot := xposition;
   REPEAT
     DRAW(xplot,yposition+2,xplot,
                              yposition-2,color);
     xplot := xplot + incrDisplacement;
   UNTIL xplot > Pixels;
   xposition := xposition +incrDisplacement;
   xplot := ROUND (xposition/8);
   x := xplot; z := incrDisplacement/8;
   yplot := ROUND (yposition/8) + 2;
   xzero := xzero + increment;
   REPEAT
     GotoXY (xplot,yplot); Write (xzero:3:0);
     xzero := xzero + increment;
     x := x + z; xplot := ROUND (x);
   UNTIL xplot > Pixels/8;
END;  {XAXIS}
{***********************************************}
Procedure PlotPoints (Y1,Y2:DataArray);
Type
   DataPoints = Array[0..640] of Integer;
Var
   i:Integer; Plot1,Plot2:DataPoints;
Begin
    For i:=0 to 20 do
                writeln(Y1[i]:5:3,'  ',Y2[i]:5:3);
    Wait;
    For i:=0 to 639 do begin
      Plot1[i]:=-Round(10*Y1[i] - 100);
      Plot2[i]:=-Round(10*Y2[i] - 100);
    End;    {for}
    HiRes;
    XAXIS(639,40,100,100,1,0,100.0);
    YAXIS(40,199,16,1,-10,0,1.6667);
    For i:=40 to 639 do begin
      Plot(i,Plot1[i],5);
      Plot(i,Plot2[i],5);
    End;     {For}
    Wait1;
    TextMode;
End;    {PlotPoints}
{***********************************************}
Procedure HighSpeedSample (Var Ch1,Ch2:DataArray);
{Sampling of channels 1 and 2 at highspeed}
Var
  i,j:Integer;
  ByteCh1,ByteCh2:Array[0..Xmax] of Byte;
  function ADSample (Channel:Integer):Byte;
  Var j:Integer;
  Begin
      PORT [$702]:=(Channel SHL 4) + 02;
      PORT [$702]:=(Channel SHL 4) + 03;
      For j:=0 to 6 do begin end;
        ADSample:=((((PORT[$701] and $0F)*256)
                              + PORT[$700]) div 25);
  End;    {ADSample}
Begin
    For i:=0 to Xmax do begin
      ByteCh1[i]:=ADSample(1);
      ByteCh2[i]:=ADSample(2);
    End;   {For}
    For i:=0 to Xmax do begin
      Ch1[i]:=(ByteCh1[i]-81)/8.22;
      Ch2[i]:=(ByteCh2[i]-81)/8.22;
    End;   {For}
End;   {HighSpeedSample}
{***********************************************}
Procedure Digital_Analog (OutputVoltage1,
                          OutputVoltage2:Real);
{ This procedure does a 12-bit D-A conversion. }
Var
    DA_msb1,DA_lsb1,DA_msb2,DA_lsb2,
    Temp1,Temp2,Channel:Integer;
Begin
    Temp1 := Round((1.02*OutputVoltage1
                                *(2048/-10))+2048);
    Temp2 := Round((1.02*OutputVoltage2
                                *(2048/-10))+2048);
    If Temp1>4095 then Temp1:=4095;
    If Temp2>4095 then Temp2:=4095;
    DA_msb1 := Temp1 SHR 4; DA_msb2 := Temp2 SHR 4;
    DA_lsb1 := (Temp1 SHL 4) AND $F0;
    DA_lsb2 := (Temp2 SHL 4) AND $F0;
    PORT[$714] := DA_msb1;      {set D/A-8 1 }
    PORT[$715] := DA_msb2;      {set D/A-8 2 }
    PORT[$70D] := DA_msb1;  {set msb D/A-12 1}
    PORT[$70C] := DA_lsb1;  {set 4 lsb's D/A-12 1}
    PORT[$711] := DA_msb2;  {set   msb   D/A-12 2}
    PORT[$710] := DA_lsb2;  {set 4 lsb's D/A-12 2}
  End;     {Digital_Analog}
{***********************************************}
```

PROGRAM KALMAN

```
{***********************************************}
{*   INCLUDE PROCEDURE TO ESTIMATE THE NETWORK   *}
{*   PARAMETERS, USING THE KALMAN ALGORITHM      *}
{*   created  by M. NAUDé during 1987 adapted by *}
{*              J.H.R. Enslin                    *}
{***********************************************}
{*The procedure call has the following structure:*}
{* KALMAN(yg,yb,xyg,xyb,count);                 *}
{* with yg,yb the present input values of the   *}
{* network parameters conductance and susceptance*}
{* and xyg,xyb the output values of the Kalman  *}
{* predictions of conductance and susceptance.  *}
{* The parameter count is an integer count      *}
{* which should be 1 before the procedure can be.*}
{***********************************************}

var
    mm,nn,kk,ll,oo,pp,rr,ss,tt:integer;
    KG,KB,KX,KD,a,ab,xk1,xk,Pak1,Pak,Pakg,
    Pakb,Pakd,Pk1,Pk,Pkg,Pkb,Pkd,G,B:real;
    y,sv,sw,ak,ak1,akb,akg,akd,ag,ad:real;
    aa,cc,ee:real;

Procedure KALMAN(yg,yb:real;
                 var xkg,xkb:real; tel:integer);
{***********************************************}
procedure KalmanVoorspeller;
{This procedure implement the estimation equation}
begin
    B := KX*(a*Pk*(1/(Pk + sv)));
```

```
    xk1 := KX*(a*xk + B*(y - xk));
    Pk1 := a*a*Pk - a*B*Pk + sw;
end;        { KalmanVoorspeller }
{***********************************************}
procedure SkatParameter;
{This procedure does parameter estimation       }
begin
    G := KX*(Pak*xk*(1/(xk*xk*Pak + sw)));
    ak1 := (ak + G*(y - xk*ak));
       Pak1 := Pak - (G*xk*Pak) + (xk*sw*xk);
 end; { SkatParameter }
{***********************************************}
procedure SkatG;
{ This procedure first predicts the dynamics of the
system and then the conductance for (k+1), given
the k data. }
begin
    If (tel=1) then begin
       xkg := yg; akg := 1; Pakg := 1; Pkg := 1;
    end;  {If}
    xk := xkg; y := yg; sw := sqr(xk - yg);
    If (sw=0) then sw:=1;
    sv := sqr(0.01 * yg); ak := akg;
    Pak := Pakg; KX := KG;
    SkatParameter;
    If (ak1 < 0.00001) then begin
       ak1 := 1; Pak1 := 1;
    end; {If}
    ag := ak1; akg := ak1; Pakg := Pak1;
    a := ag; Pk := Pkg;
    KalmanVoorspeller;
    If ( xk1 <= 0) then xk1 := xk1 + 0.00001;
    xkg := xk1; Pkg := Pk1;
end;  { SkatG }
{***********************************************}
procedure SkatB;
{ This procedure first predicts the dynamics of the
system and then the susceptance for (k+1), given
the k data. }
begin
    If (tel = 1 ) then begin
       xkb := yb; akb := 1; Pakb := 1; Pkb := 1;
    end;   {If}
    xk := xkb; y := yb; sw := sqr(xk - yb);
    if (sw=0) then sw:=1;
    sv := sqr (0.01 * yb); ak := akb;
    Pak := Pakb; KX := KB;
    SkatParameter;
    If ( ak1 < 0.00001) then begin
       ak1 := 1; Pak1 := 1;
    end;  {If}
    ab := ak1; Pakb := Pak1; akb := ak1;
    a := ab; Pk  := Pkb;
    KalmanVoorspeller;
    If ( xk1 <= 0 ) then xk1 := xk1 + 0.00001;
    xkb := xk1; Pkb := Pk1;
end;   { SkatB }

{***********************************************}

procedure Korreksie;

{ This procedure is used to do the main prediction.
Previous procedures are called from this procedure.
The present conductance and susceptance are needed.
xkg is the prediction of the conductance given the
present value yg. xkb is the prediction of the sus-
ceptance given the present value yb. }
begin
    If (tel=1) then begin
       mm:=0; pp:=0; nn:=0; ll:=0; kk:=0; oo:=0;
       KG := 1; KB := 1;
    end  {then}
    else begin
       If (yg > aa) then begin
          If (kk=0) then begin
             If (aa=0) then KG := 1
             else KG := 1.0*(yg/aa);
             kk:=kk+1; mm:=0; ll:=0;
          end  {then}
          else begin
             if aa=0 then KG := 1
             else KG := (yg/aa);
          end;  {else}
       end; {if}
       If (yg = aa) then begin
          If (mm=0) then begin
             KG := 1.0; mm:=mm+1; kk:=0; ll:=0;
          end  {then}
          else KG := 1;
       end;   {if}
       If (yg<aa) then begin
          If (ll=0) then begin
             If aa=0 then KG := 1
             else KG := 1.0*(yg/aa);
             mm:=0; ll:=ll+1; kk:=0;
          end
          else begin
             If aa=0 then KG := 1
             else KG := (yg/aa);
          end; {else}
       end;     {if}
       If (yb > cc) then begin
          If (oo=0) then begin
             If cc=0 then KB := 1
             else B := 1.0 * (yb / cc);
             nn:=0; pp:=0; oo:=oo+1;
          end   {then}
          else begin
             If cc=0 then KB := 1
             else KB := (yb / cc);
          end;  {else}
       end;      {if}
       If (yb = cc) then begin
          If (nn=0) then begin
             KB := 1.0; nn:=nn+1; oo:=0; pp:=0;
          end  {then}
          else KB := 1;
       end;      {if}
       If (yb < cc) then begin
          If (pp=0) then begin
             If cc=0 then KB := 1
             else KB := 1.0*(yb/cc);
             oo:=0; pp:=pp+1; nn:=0;
          end   {then}
          else begin
             if cc=0 then KB := 1
             else KB := (yb/cc);
          end;  {else}
       end;   {if}
    end;  {else}
    aa := yg; cc := yb;
    SkatG; SkatB;
    xkd:=yd;
end; { Korreksie }

{***********************************************}

begin
    Korreksie;
end;  { Kalman }

{***********************************************}
```

UITGEBREIDE OPSOMMING

BEPALING EN DINAMIESE KOMPENSASIE VAN FIKTIEWE DRYWING IN ELEKTRIESE DRYWINGSNETWERKE

I. INLEIDING

Die toename in die gebruik van elektroniese drywingsbeheerstelsels, boogoonde, gelykstroom-transmissiestelsels, fluoresseerlampe, batterylaaiers en ander elektriese apparaat wat die golfvorms van stroom of spanning vervorm, asook die alomteenwoordige magnetiese versadiging in elektriese apparaat, het 'n wesenlike probleem in elektriese drywingstelsels ontketen. Veral die injeksie en verspreiding van gekarakteriseerde en ongekarakteriseerde harmonieke van die vervormde stroom- en spanningsgolfvorms in elektriese energienetwerke, skep probleme vir ander elektriese apparaat en energieverbruikers wat op hierdie vervormde toevoer verbind word. Hoëfrekwensie harmonieke veroorsaak sekondêre effekte op kommunikasie- en beheerstelsels, wat elektromagnetiese interferensie in sensitiewe stelsels insluit.

Geïnjekteerde harmonieke in drywingstelsels het 'n vernietigende uitwerking op die meeste toerusting wat aan hierdie vervormde toevoer verbind word, soos byvoorbeeld roterende elektriese masjinerie, kapasitorbanke vir kompensasie van 'n nalopende arbeidsfaktor en sensitiewe rekenaarstelsels. Die elektriese voorsieningsnetwerke word verder teen 'n verhoogde belading bedryf, sonder dat daar 'n verhoging in netto elektriese energie is. Dit gaan gepaard met 'n verhoging in kapitale investering en lopende uitgawes van elektrisiteitsvoorsieningsorganisasies, wat weer 'n negatiewe effek op die prys van elektriese energie het.

Hieruit blyk dit dus noodsaaklik te wees om hierdie vervorming in elektriese stelsels noukeurig te meet en te karakteriseer.

Sodoende kan die effekte van 'n vervormde toevoer op komponente so effektief as moontlik geanaliseer word.

Om die effekte van bogenoemde vervorming in stelsels te minimeer, moet 'n vorm van vervormingskompensasie ingesluit word in aanwendings waar komplekse nie-lineêre lasse aan die energienetwerk gekoppel word. Dit geld veral indien die kortsluitvermoë van die toevoer relatief laag is. Die beheerfilosofie van hierdie kompensasiestelsels is tans nog 'n belangrike onopgeloste probleem. Die probleme geassosieer met die beheerfilosofie moet eers ondersoek en opgelos word, voordat effektiewe vervormingskompensasie in elektriese energiestelsels kan geskied.

Daar word voorgestel dat vir die definisie van elektriese drywing onder vervormde toestande, geen periodiese eienskappe en daarom ook geen harmoniekanalises van die golfvorms van stroom en/of spanning as basis vir die definisie gebruik moet word nie. Die definisie moet slegs die werklike tydsverlope van stroom en spanning gebruik om drywing te definieer. Die gevalle van periodiese golfvorms van stroom en spanning en gelykstroomdrywing moet beskou word as spesiale gevalle van die meer algemene definisie van elektriese drywing. 'n Tyddomein-definisie van elektriese drywing, wat gebaseer word op korrelasietegnieke, word voorgestel as 'n algemene definisie van elektriese drywing.

II. PROBLEME MET BESTAANDE DEFINISIES EN NIE-SINUSVORMIGE GROOTHEDE VAN ELEKTRIESE DRYWING

Hoofstuk 1 bespreek die algemene probleme wat ondervind word in die verbetering van die kwaliteit van elektriese energietoevoer. Die bestaande definisies van elektriese drywing het baie tekortkominge ten opsigte van die fundamentele probleme met die frekwensie-domein en die feit dat die definisies nie die drywing of energie einskappe van die las in ag neem nie. Die bekendste definisies word in hoofstuk 1 geëvalueer, om so die tekortkominge uit te wys. Die tegnieke wat van toepassing is op die analise van vervorming in elektriese drywingstoevoere is gewoonlik beperk tot die frekwensie-domein, met bepaalde tekortkominge en beperkings.

Die probleme met die analisetegnieke word in hoofstuk 1 en 2 bespreek. Effekte van 'n vervormde toevoer op ander stelsels is moelik bepaalbaar en nog moeiliker rekenbaar in geldwaarde, maar speel 'n baie groot rol in die prys van elektriese energieverskaffing en -benutting. Effekte en oorsake van vervorming op en deur verskeie elektriese apparatuur word ook kortliks in hoofstuk 2 beskryf.

III. VOORGESTELDE DEFINISIE VAN ELEKTRIESE DRYWING

Die voorgestelde definisie van elektriese drywing word in hoofstuk 3 volledig beskryf. Die definisie kan kortliks soos volg saamgevat word. Elektriese drywing word slegs in twee ortogonale komponente verdeel, **aktiewe drywing** P en **fiktiewe drywing** F. In toepassings van die karakterisering en beheer van fiktiewe drywing, word 'n verdere verdeling van fiktiewe drywing voorgestel, nl. **reaktiewe drywing** Q en **deaktiewe drywing** D. Die verdeling word volledig deur middel van korrelasietegnieke en ekwivalente netwerkparameters gerugsteun. Die elektriese netwerk word gekarakteriseer deur middel van die opwekfunksie en die beladingsfunksie, wat deur die stroom of die spanning in elektriese netwerke beskryf word. In die meeste gevalle word die opwekfunksie deur die spanning voorgestel, terwyl die stroom die beladingsfunksie beskryf. In die algemeen kan die stroom sowel as die spanning die beladingsfunksie of die opwekfunksie beskryf.

Definisie van Beladingsdrywing

Beladingsdrywing S is ekwivalent aan skyndrywing en word in verband met die belading van die elektriese netwerk gebring. Dit word bereken uit die effektiewe waardes van stroom en spanning oor 'n meettydsinterval dT. Die beladingsdrywing word uitgedruk in terme van die ekwivalente netwerkadmitansie Y oor die meettydsinterval dT.

$$S = U.I = U^2.Y \qquad (1)$$

Vir die meet van die effektiewe waardes van spanning u(t) en stroom i(t) oor die tydsinterval dT word 'n tyddomein-

outokorrelasie voorgestel. Die gebruik van 'n outokorrelasie is lewer dieselfde resultate as die definisie van die gemiddeld-kwadraatwaarde, geformuleer oor die fundamentele periode. Die outokorrelasie oor die tydsinterval dT word in vergelyking 2 getoon.

$$R_{uu}(\tau) = \frac{1}{dT}\int_{t-dT}^{t} u(t).u(t-\tau)dt \qquad (2)$$

Dit impliseer dat effektiewe waardes van enige golfvorm bereken kan word deur van 'n outokorrelasie gebruik te maak:

$$U = [R_{uu}(0)]^{1/2}\,|_{dT} \qquad (3)$$

$$I = [R_{ii}(0)]^{1/2}\,|_{dT} \qquad (4)$$

Die beladingsdrywing van die netwerk word met die ekwivalente admitansie Y van die netwerk geassosieer. Die effektiewe stroom I is verantwoordelik vir die beladingsdrywing S in die netwerk met effektiewe spanning U.

Definisie van Aktiewe Drywing

Aktiewe drywing P het slegs fisiese interpretasie indien dit oor 'n tydsinterval dT gedefineer word. Aktiewe drywing is 'n aanduiding van die gemiddelde tempo van energie-oordrag tussen bron en las oor die tydsinterval dT. Aktiewe drywing, geneem oor 'n tydsinterval dT, word bereken uit die kruiskorrelasie tussen stroom en spanning, soos getoon in vergelyking 5.

$$R_{ui}(\tau) = \frac{1}{dT}\int_{t-dT}^{t} u(t).i(t-\tau).dt \qquad (5)$$

Dit impliseer dat aktiewe drywing deur middel van 'n kruiskorrelasie tussen stroom en spanning oor enige tydsinterval dT bereken kan word. Die resultaat word in vergelyking 6 geton:

$$P = R_{ui}(0)\,|_{dT} \qquad (6)$$

Die aktiewe drywing word met die las geassosieer in terme van die ekwivalente konduktansie G. Die **aktiewe stroom** i_a is verantwoordelik vir die netto oordrag van energie vanaf die bron na die ekwivalente konduktasie G in die las.

$$P = U^2.G = U.I_a, \tag{7}$$

waar I_a die effektiewe waarde van die aktiewe stroom $i_a(t)$ is. Die aktiewe stroom $i_a(t)$ het dieselfde golfvorm as die spanning u(t), met die amplitude bepaal deur die konduktansie G:

$$i_a(t) = G.u(t) \tag{8}$$

Definisie van Fiktiewe Drywing

Fiktiewe drywing F word bereken uit die ortogonaliteit wat aanvaar word tussen die onderskeie drywingskomponente. Die fiktiewe stroom $i_f(t)$ is verantwoordelik vir die fiktiewe drywing wat in die netwerk bestaan.

$$F = \sqrt{[S^2 - P^2]} = U.I_f, \tag{9}$$

waar I_f die effektiewe waarde van die fiktiewe stroom $i_f(t)$ is. Vir doeleindes van die karakterisering en beheer van fiktiewe drywing word 'n verdere verdeling van fiktiewe drywing voorgestel. Fiktiewe drywing word in twee onderling ortogonale komponente verdeel: **reaktiewe drywing** Q en **deaktiewe drywing** D. Die verdeling word regstreeks uit die kruiskorrelasie tussen stroom en spanning bepaal.

(a) **Reaktiewe drywing** Q. Reaktiewe drywing word geassosieer met die ossillatoriese energievloei, sonder netto oordrag van energie tussen bron en las oor die meettydsinterval dT. Reaktiewe drywing word gekarakteriseer deur middel van 'n ekwivalente netwerkparameter, susseptansie B. Die ossillatoriese energievloei en dus ook omkeerbaarheid kan uitgedruk word in terme van 'n tydsverskuiwing tussen die golfvorms van stroom en spanning, terwyl daar steeds 'n mate van korrelasie tussen die onderlinge golfvorms mag wees. Dit is juis die gekorreleerdheid tussen die stroom en spanning wat 'n bydrae tot die reaktiewe drywing lewer,

terwyl die ongekorreleerdheid tussen die golfvorms die deaktiewe drywing daarstel.

Die maksimum waarde van die kruiskorrelasie tussen stroom en spanning $\hat{R}_{ui}(\tau)$ verkry oor die tydsinterval dT, stel die punt voor waar daar maksimum ooreenkoms tussen die stroom en spanningsgolfvorms bestaan. Die punt op die kruiskorrelasiefunksie stel die aktiewe drywing voor wat sou voorgekom het, indien die tydverskuiwing van die stroom ten opsigte van die spanning weggelaat sou word, en is daarom 'n aanduiding van die gekorreleerde fiktiewe drywing of kortweg die reaktiewe drywing. Die reaktiewe drywing word in vergelyking 10 uit die kruiskorrelasie geformuleer.

$$Q = \sqrt{[\hat{R}^2_{ui}(\tau) - R^2_{ui}(0)]}. \qquad (10)$$

Die ekwivalente netwerksusseptansie B word geassosieer met die reaktiewe drywing Q, terwyl die **reaktiewe stroom** I_r verantwoordelik is vir die reaktiewe drywing en energie ossillerend tussen die bron en susseptansie slinger.

Die golfvorm van die reaktiewe stroom moet ortogonaal wees op die ander komponente van die stroom, geneem oor die meettydsinterval, en om dié rede word die reaktiewe stroom regstreeks uit die kruiskorrelasie en ander stroom komponente bepaal. Aangesien dit die maklikste is om eers die deaktiewe stroom te bepaal, toon vergelyking 13 slegs die oomblikswaarde verskil. Die effektiewe waarde van die stroom word direk uit die susseptansie en effektiewe spanning bereken, soos getoon in vergelyking 11.

$$Q = U^2.B = U.I_r \qquad (11)$$

$$B = Q/U^2 = \frac{\sqrt{[\hat{R}^2_{ui}(\tau) - R^2_{ui}(0)]}}{[R_{uu}(0)]}, \qquad (12)$$

$$\text{met } \overline{i_a.i_r} = 0 \quad \text{en} \quad i_r = i - i_a - i_d \qquad (13)$$

Vir periodiese golfvorms kan die reaktiewe drywing verder verdeel word in die kapasitiewe of induktiewe reaktiewe drywing, of soos voorgestel fundamentele reaktiewe drywing Q_f en die resgedeelte

reaktiewe drywing Q_r. Dit het die voordeel dat die reaktiewe drywing in die grondkomponent deur middel van 'n kapasitor of induktor gekompenseer kan word.

(b) **Deaktiewe Drywing D.** Die tweede ortogonale komponent van fiktiewe drywing word geassosieer met die ongekorreleerdheid tussen die golfvorms van stroom en spanning. Met die verdeling van fiktiewe drywing, vergelyking 10, in reaktiewe en deaktiewe drywing, is daar juis die feit uitgewys dat die reaktiewe drywing gedefinieer word as die gekorreleerde fiktiewe drywing, terwyl die oorblywende drywing nl. deaktiewe drywing, juis dan die ongekorreleerde fiktiewe drywing behels. Uit die korrelasie tussen stroom en spanning is dit duidelik dat 'n sekere komponent van die beladingsdrywing veroorsaak word deur die ongekorreleerdheid van die stroomgolfvorm ten opsigte van die spanningsgolfvorm.

Die deaktiewe drywingskomponent word uit die ortogonaliteitsbeginsel van al die ander komponente van drywing bepaal.

$$D = \sqrt{[S^2 - P^2 - Q^2]} \tag{14}$$

'n Nuut-gedefinieerde netwerkparameter disseptansie K word geassosieer met die ongekorreleerde en nie-lineêre eienskappe van die las. Die admitansie Y geassosieer met die totale nie-lineêre las, word uitgedruk in terme van die drie ekwivalente netwerkparameters G, B en K.

$$Y^2 = G^2 + B^2 + K^2 \tag{15}$$

Deaktiewe stroom I_d is verantwoordelik vir die deaktiewe drywing D geassosieer met die disseptansie van die las. Die deaktiewe stroom oomblikswaarde kan bepaal word uit die korrelasie funksie deur al die stroom komponente wat wel korreleer af te trek van die lasstroom se oomblikswaarde.

$$D = U^2.K = U.I_d, \tag{16}$$

met $\overline{i_r.i_d} = 0$;

$i_d(t) = i(t) - \sqrt{[G^2 + B^2]}.u(t-\hat{}\tau)$;

I_d die effektiewe waarde van die deaktiewe stroom i_d.
$\hat{}\tau$ die tydsverskuiwing van die maksimumwaarde van die kruiskorrelasie $\hat{}R_{ui}(\tau)$.

Die bostaande opsomming van die voorgestelde drywingsdefinisie word volledig in hoofstuk 3 bespreek.

IV. ANALISE EN KARAKTERISERING VAN VERVORMING IN ELEKTRIESE DRYWINGSNETWERKE

In elektriese energiestelsels met vervormde stroom- en spanningsgolfvorms skep die karakterisering van die netwerk en die meet van die vervorming geweldige probleme. Die bostaande definisie van elektriese drywing word voorgestel in die analise van vervorming in elektriese energienetwerke. Die analise berus op die opstel van die ekwivalent netwerkdiagram, met ekwivalente netwerkparameters nl. konduktansie, susseptansie en disseptansie. Elke parameter beskryf eenduidig die eienskappe van die netwerk, dit wil sê die mate van omkeerbaarheid van die netwerk, die nielineêre eienskappe en die benutting van die netwerk. Berekening van die ekwivalente parameters toon dan die karakteristieke van die vervorming in die drywingsnetwerk. Die basiese tyddomein analisetegniek is ook uitgebrei na die frekwensie-domein deur gebruik te maak van die drywingspektraal-digtheidsfunksie $S_{ui}(f)$. Die funksie word verkry deur 'n Fourier-transform op die kruiskorrelasiefunksie $R_{ui}(\tau)$ uit te voer. Deur die hele proefskrif, veral in hoofstukke 3 en 4, word na die analise van vervorming in elektriese drywingstelsels verwys.

V. MEETTEGNIEK VAN TOEPASSING OP NETWERKE MET NIE-SINUSVORMIGE OPWEK- EN BELADINGSFUNKSIES

Die meet van stroom en spanning in elektriese netwerke skep baie probleme indien die stroom en spanningsverlope nie-sinusvormig is nie. Die akkurate meting van hierdie funksies is egter 'n fundamentele voorvereiste vir die analise, karakterisering en kompensasie van fiktiewe drywing. Tyddomein-meettegniek word voor-

gestel in die meting van drywing onder toestande van nie-sinusvormige stroom en spanningsverlope. Die tyddomein-tegnieke is gebaseer op die berekening van die korrelasie tussen die stroom en die spanning. Optiese, oppervlakgolf (SAW) en mikro-rekenaarstelsels, geskik vir seinverwerking, word voorgestel in die in-tydse meting van drywingskomponente, direk uit die tydsvelope van stroom en spanning. Statistiese eienskappe van die elektriese netwerk word gebruik om aanpassende seinverwerkingsalgoritmes te implementeer. Die meettegniek kan egter met 'n eenvoudige persoonlike rekenaarstelsel geïmplementeer word, indien die metings nie tydkritiek is nie. Algemene metings van drywing in aanlegte is nie tydkritiek nie en daarom is 'n persoonlike rekenaar ideaal vir sodanige metings. In hierdie studie is sodanige persoonlike rekenaar-meetstelsel ontwikkel en gebruik om al die resultate te verkry. Resultate verkry uit hierdie stelsel word getoon in hoofstukke 4 en 6.

VI. KOMPENSASIE VAN FIKTIEWE DRYWING IN ENERGIENETWERKE

Die kompensasie van fiktiewe drywing is een van die belangrikste uitvloeisels van die voorgestelde tyddomeindefinisie. Elkeen van die drywingskomponente, aktiewe, reaktiewe en deaktiewe drywing, word geassosieer met 'n unieke ekwivalent netwerkparameter. Dit impliseer dat die kompensasie van sodanige nie-lineêre netwerk bewerkstellig kan word deur die effektiewe kanselasie van sodanige ongewenste netwerkparameters, om die las in die ideale geval suiwer resistief te laat. Sinchrone masjiene, arbeidsfaktorkompensasie-kapasitorbanke, harmoniese drywingsfilters, tiristorbeheerde-reaktiewe-drywingsbronne en dinamiese drywingsfilters, elkeen met sy eie inherente voordele, kan gesamentlik of apart aangewend word om een of meer van die ongewenste netwerkparameters te kanselleer.

Die beheerfilosofie van hierdie kompensasie-apparatuur is daarom een van die belangrikste uitvloeisels van die voorgestelde definisie van elektriese drywing. Die totale kompensasiestelsel moet in die algemeen uit 'n susseptansie- en disseptansiegedeelte bestaan. Die reaktiewe drywing in die netwerk word gekompenseer

deur middel van 'n susseptansie, terwyl die deaktiewe drywing gekompenseer word deur middel van 'n ekwivalente disseptansie, sodat die totale ekwivalent netwerk slegs uit 'n konduktansie G bestaan. Die stelsel verantwoordelik vir reaktiewe drywingskompensasie, genereer die stroom $i_r(t)$ terwyl die stelsel verantwoordelik vir deaktiewe drywingskompensasie, die stroom $i_d(t)$ genereer en slegs die aktiewe stroom $i_a(t)$ word van die toevoerbron geneem.

Die onderverdeling van fiktiewe drywing in reaktiewe en deaktiewe komponente, hou baie voordele in by die kompensasie van fiktiewe drywing. Ondermeer kan kleiner drywingsfilters met hoë dimamiese stelselresponsie geïnkorporeer word in die kompensasie van slegs die deaktiewe drywing. Die reaktiewe drywing kan met lae dinamiese responsie kapasitornetwerke of toevoergekommuteerde drywingsfilters gekompenseer word. Dit het 'n positiewe effek op die koste van fiktiewe drywingskompensasie in elektriese energienetwerke. Verder kan lae-drywing, hoë-dinamiese responsie drywingsfilters gesamentlik met hoë-drywingsbeheerstelsels gebruik word. Die voordeel hiervan is dat slegs die deaktiewe drywing deur 'n hoë-dinamiese responsie stelsel gestuur word en nie die totale drywing wat beheer word nie.

VII. SAMEVATTING

Die proefskrif het die algemene probleme, geassosieer met netwerkvervorming, opsommenderwys bespreek. 'n Algemeen aanvaarbare drywingsdefinisie, wat berus op korrelasietegnieke, is ontplooi. Dit stel 'n nuwe benadering in die analise, meting en kompensasie van vervorming in elektriese netwerke daar. Die definisie is van toepassing in die algemeen, maar meer spesifiek waar die golfvorms van die opwek- en beladingsfunksies vervorm is vanaf die normale sinusvormige funksies. Die tegnieke word voorgestel om aangewend te word wyer as net in elektriese energiestelsels, maar is ook van toepassing op meganiese, chemiese en termiese energiestelsels, waar 'n opwek- en beladingfunksie geïdentifiseer kan word.